INTERNATIONAL
COOPERATION

Timothy R. Carter, Mike Hulme, Jennifer F. Crossley,
Sergey Malyshev, Mark G. New, Michael E. Schlesinger,
Heikki Tuomenvirta

Climate Change in the 21st Century - Interim Characterizations based on the New IPCC Emissions Scenarios
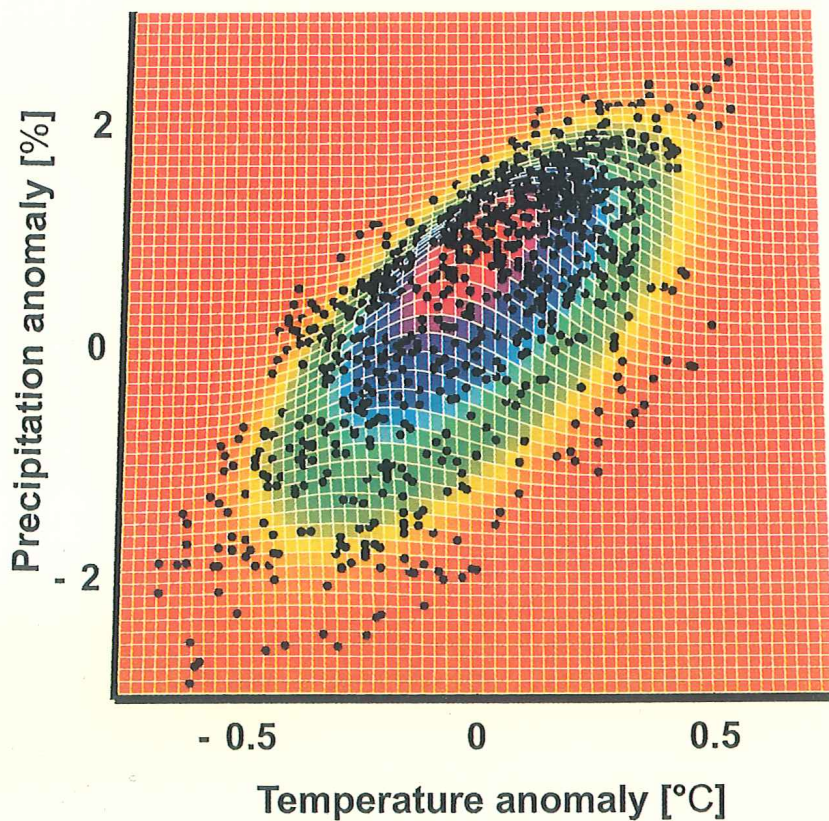
Timothy R. Carter, Mike Hulme, Jennifer F. Crossley,
Sergey Malyshev, Mark G. New, Michael E. Schlesinger,
Heikki Tuomenvirta

Climate Change in the 21st Century - Interim Characterizations based on the New IPCC Emissions Scenarios

Timothy R. Carter[1], Mike Hulme[2], Jennifer F. Crossley[3],Sergey Malyshev[4], Mark G. New[5],
Michael E. Schlesinger[4], Heikki Tuomenvirta[6]
[1]Finnish Environment Institute, Box 140, FIN-00251 Helsinki, Finland
[2]Tyndall Centre for Climate Research, University of East Anglia, Norwich NR4 7TJ, UK
[3]Climatic Research Unit, University of University of East Anglia, Norwich NR4 7TJ, UK
[4]Climate Research Group, Department of Atmospheric Sciences, University of Illinois at
Urbana-Champaign, Urbana, IL, 61801, USA
[5]School of Geography and the Environment, University of Oxford, Mansfield Road, Oxford, OX1 3TB, UK
[6]Finnish Meteorological Institute, Box 503, FIN-00101 Helsinki, Finland

HELSINKI 2000

Preface

In recent decades there have been numerous studies examining the possible impacts of future anthropogenically-induced climate change on the natural world and on human society. Since it it not yet possible to predict future climate, due both to incomplete knowledge about the processes of climate change and to uncertainties in the future composition of the atmosphere, most impact studies have considered a range of plausible future climates known as *climate scenarios*. These are usually constructed based on the results of simulations from general circulation models (GCMs). However, owing to the diversity of information available to impact assessors and to the lack of uniform criteria for selecting climate model outputs, there has been little consistency in the scenarios adopted in different impact studies. Furthermore, it is evident that the scenarios selected in most studies fail to sample systematically across the wide range of uncertainties that are known to exist in estimates of future climate. These include uncertainties concerning emissions of greenhouse gases and aerosols into the atmosphere, their concentrations in the atmosphere and consequent radiative forcing of climate, the global and regional climate response to radiative forcing, and the sea-level implications of these climate changes.

This report has been prepared to consider the implications of a new set of emissions scenarios developed for the Intergovernmental Panel on Climate Change (IPCC) Special Report on Emissions Scenarios (SRES). These scenarios[1] span a range of emissions arising from different assumptions of socio-economic development during the 21st century. The effects of these emissions scenarios on climate are currently being estimated using a number of fully coupled atmosphere-ocean general circulation models (AOGCMs). However, this work is still in progress, and results will take some time to be analysed and evaluated. In the meantime, interim characterizations of the climatic implications of the SRES scenarios can be obtained by using a combination of simple climate models and existing results from AOGCM simulations. It is results of this kind that are presented here.

Changes in mean seasonal temperature and precipitation are portrayed in a consistent manner for all major inhabited regions of the world, and the report seeks to identify regions where there is apparent agreement between models in the direction of future climate change, as well as regions where future changes are more uncertain. Moreover, each of the SRES scenarios is characterized by a level of demographic and economic development which are themselves important for determining future vunerability to a changing climate.

A major objective of the report is to provide quantitative guidance on the range of uncertainty in future regional climate changes. It is hoped that this may assist researchers wishing to select climate scenarios for new impact assessments. In addition, it provides background information that may be of use in evaluating the scenarios applied in published impact studies, especially with regard to the IPCC Third Assessment Report. In this latter role, a draft version of this document has already received extensive comment from several IPCC authors, whom

---

[1] The SRES scenarios quantified in this report are the four preliminary "marker" scenarios released for use by climate modellers in 1998. A final set of scenarios was approved by the IPCC in April 2000 (Nakićenović *et al.*, 2000). Revised versions of the four marker scenarios used here are included among the six "illustrative" scenarios presented in detail in that report.

Contents

Introduction

1.1 Purpose of this document

This report presents a set of mutually consistent characterizations of future states of the world during the 21st century. These characterizations are designed to paint alternative pictures of the future, both climatic and non-climatic, that are important for evaluating vulnerability to future climate change. The characterizations include:

- demographic and economic development
- atmospheric composition
- changes in average climate (seasonal temperature and precipitation)
- sea-level rise induced by climate change

They attempt to portray information about the magnitude and range of possible future changes on the basis of available knowledge. They offer a common reference for assessing the possible impacts of, and adaptability to, future climate change and are summarized in Table 1.

1.2 Sources of information for the characterizations

The quantitative characterizations presented here are based on three main sources of information:

1. A new set of emissions scenarios to the year 2100 developed for the IPCC Special Report on Emissions Scenarios (SRES - Nakićenović *et al.*, 2000)
2. A framework of simple models used in the IPCC Second Assessment Report to convert projected emissions into global mean values of atmospheric greenhouse gas concentration, radiative forcing of the climate, temperature change and sea-level rise
3. Information on the patterns of regional temperature and precipitation change simulated by coupled atmosphere-ocean general circulation models (AOGCMs) and available from the IPCC Data Distribution Centre[2]. Mapped information about the possible regional effects of SRES-based sulphate aerosol concentrations on temperature patterns climate is also provided.

A number of other important issues are treated qualitatively. These include:

4. Caveats relating to the depiction of future climate, including the averaging and scaling of AOGCM outputs, the superficial treatment of sulphate aerosol effects and the representation of uncertainties in descriptions of future climate.
5. Scenarios that posit a stabilization of CO_2 and greenhouse gas concentrations in the atmosphere.

---

[2] The IPCC Data Distribution Centre can be accessed at website:
http://ipcc-ddc.cru.uea.ac.uk/

Table 1. Attributes and regions for which characterizations are provided.

Attribute	Global	4 economic regions	14 continental-scale regions	32 sub-continental regions
Socio-economic/land cover				
Population	*	*		
Gross National Product (GNP)	*	*		
GNP/capita	*	*		
Energy Intensity	*	*		
Forest area	*	*		
Atmospheric composition				
Carbon dioxide (CO_2) emissions	*			
Sulphur emissions	*			
CO_2 concentration	*			
Climatic/sea-level				
Mean annual temperature change	*		*	
Seasonal temperature change			*	*
Seasonal precipitation change			*	*
Aerosol-induced change	*			
Sea-level change	*			

In the following sections we describe:
- The SRES scenarios: socio-economic characterizations (section 2)
- Global scale characterizations of atmospheric concentrations, temperature and sea-level forced by the SRES emissions scenarios (section 3)
- SRES-based interim regional climate change characterizations (sections 4-6)
- Important caveats relating to the characterizations (section 7)
- Stabilization scenarios (section 8)

The Preliminary SRES Marker Scenarios: Socio-Economic Driving Factors

2

The Special Report on Emissions Scenarios (SRES) was formally approved by the IPCC in April 2000 (Nakićenović *et al.*, 2000). However, a preliminary set of four "marker" emissions scenarios and their associated socio-economic driving forces were already in circulation in 1998, to provide inputs for GCM simulations. It is these scenarios (labelled SRES98), which in most respects differ little from the final versions, that have been used in this report. The SRES scenarios were constructed quite differently from the previous emissions scenarios developed by the IPCC (the IS92 scenarios - Leggett *et al.*, 1992). They are reference scenarios that seek specifically to exclude the effects of climate change and climate policies on society and the economy ("non-intervention"). They are based on a set of narrative storylines which are subsequently quantified using different modelling approaches. Each marker scenario represents a family of scenarios with a similar storyline. Jointly, the four markers capture most of the emissions and driving forces spanned by the full set of scenarios. In simple terms, the four marker scenarios combine two sets of divergent tendencies: one set varying between strong economic values and strong environmental values, the other set between increasing globalization and increasing regionalization (Nakićenović *et al.*, 2000). The storylines are summarized as follows:

- A1: A future world of very rapid economic growth, low population growth and rapid introduction of new and more efficient technology. Major underlying themes are economic and cultural convergence and capacity building, with a substantial reduction in regional differences in per capita income. In this world, people pursue personal wealth rather than environmental quality.
- A2: A differentiated world. The underlying theme is that of strengthening regional cultural identities, with an emphasis on family values and local traditions, high population growth, and less concern for rapid economic development.
- B1: A convergent world with rapid change in economic structures, "dematerialization" and introduction of clean technologies. The emphasis is on global solutions to environmental and social sustainability, including concerted efforts for rapid technology development, dematerialization of the economy, and improving equity.
- B2: A world in which the emphasis is on local solutions to economic, social, and environmental sustainability. It is a heterogeneous world with less rapid, and more diverse technological change but a strong emphasis on community initiative and social innovation to find local, rather than global solutions.

Although these are all non-intervention scenarios, it can be difficult to distinguish between scenarios that envisage stringent environmental policies (e.g. B1) and scenarios that include direct climate policies, such as the stabilization scenarios described in Section 8.

Quantifications of these storylines are presented in Tables 2-5.

Table 2. SRES98 preliminary AI marker scenario: quantification of population, GNP, GNP/capita, energy intensity and forest cover globally and for four world economic regions in 1990 and projected for 2020, 2050 and 2100. Source: Nakićenović et al. (2000).

Region	Year	Population (millions)	GNP (trillions 1990$)	GNP/Capita (thousands $)	Energy Intensity (MJ/$)	Forests (million ha)
OECD	1990	859	16.4	19.1	7.4	1056
	2020	1002	31.0	30.9	5.8	1105
	2050	1081	54.1	50.0	4.0	1243
	2100	1110	121.1	109.1	2.7	1370
EFSU	1990	413	1.1	2.7	51.5	960
	2020	430	2.9	6.7	17.5	970
	2050	423	12.4	29.3	6.8	973
	2100	339	34.2	100.9	3.3	1114
ASIA P	1990	2798	1.5	0.5	21.8	527
	2020	3851	12.3	3.2	11.1	411
	2050	4220	62.7	14.9	5.3	405
	2100	2882	207.3	71.9	3.2	472
ROW	1990	1192	1.9	1.6	13.7	1706
	2020	2211	10.3	4.7	12.6	1326
	2050	2980	52.0	17.4	7.1	1253
	2100	2727	165.9	60.8	3.9	1371
GLOBAL	1990	5262	20.9	4.0	11.3	4249
	2020	7493	56.5	7.5	8.8	3811
	2050	8704	181.3	20.8	5.5	3874
	2100	7056	528.5	74.9	3.3	4326

OECD - Organization of Economic Co-operation and Development; EFSU - Eastern Europe and the Former Soviet Union; ASIA P - Asian Pacific region; ROW - Rest of the World

Table 3. SRES98 preliminary A2 marker scenario: quantification of population, GNP, GNP/capita and energy intensity globally and for four world economic regions in 1990 and projected for 2020, 2050 and 2100. Source: Nakićenović et al. (2000).

Region	Year	Population (millions)	GNP (trillions 1990$)	GNP/Capita (thousands $)	Energy Intensity (MJ/$)	Forests (million ha)
OECD	1990	848	15.7	18.5	8.5	NA
	2020	1030	26.0	25.2	7.2	NA
	2050	1151	39.9	34.7	5.5	NA
	2100	1496	87.6	58.6	3.8	NA
EFSU	1990	420	1.0	2.4	61.6	NA
	2020	455	1.4	3.1	38.4	NA
	2050	519	3.7	7.1	21.7	NA
	2100	706	14.2	20.1	8.9	NA
ASIA P	1990	2779	1.7	0.6	30.1	NA
	2020	4308	5.3	1.2	27.8	NA
	2050	5764	15.0	2.6	18.4	NA
	2100	7340	57.1	7.8	8.3	NA
ROW	1990	1217	2.6	2.1	12.8	NA
	2020	2398	7.8	3.3	14.6	NA
	2050	3862	23.0	6.0	10.5	NA
	2100	5526	83.8	15.2	5.3	NA
GLOBAL	1990	5263	20.9	4.0	12.8	NA
	2020	8191	40.5	4.9	12.4	NA
	2050	11296	81.6	7.2	10.0	NA
	2100	15068	242.8	16.1	5.7	NA

OECD - Organization of Economic Co-operation and Development; EFSU - Eastern Europe and the Former Soviet Union; ASIA P - Asian Pacific region; ROW - Rest of the World

Table 4. SRES98 preliminary BI marker scenario: quantification of population, GNP, GNP/capita and forest cover globally and for four world economic regions in 1990 and projected for 2020, 2050 and 2100. Source: Nakićenović et al. (2000).

Region	Year	Population (millions)	GNP (trillions 1990$)	GNP/Capita (thousands $)	Energy Intensity (MJ/$)	Forests (million ha)
OECD	1990	801	16.51	20.6	NA	1114.8
	2020	950	32.22	33.9	NA	1160.2
	2050	1023	52.32	51.1	NA	1198.7
	2100	1055	78.19	74.1	NA	1199.8
EFSU	1990	413	0.97	2.3	NA	1147.0
	2020	442	1.78	4.0	NA	1326.2
	2050	437	5.12	11.7	NA	1414.9
	2100	352	15.4	43.8	NA	1450.9
ASIA P	1990	2790	1.42	0.5	NA	487.7
	2020	3924	6.57	1.7	NA	375.6
	2050	4209	29.92	7.1	NA	318.5
	2100	2875	119.36	41.5	NA	571.6
ROW	1990	1293	2.10	1.6	NA	1527.6
	2020	2450	7.64	3.1	NA	1232.9
	2050	3265	26.58	8.1	NA	1275.6
	2100	2958	125.07	42.3	NA	1853.2
GLOBAL	1990	5297	21.0	4.0	NA	4277.0
	2020	7767	48.2	6.2	NA	4095.0
	2050	8933	113.9	12.8	NA	4207.7
	2100	7239	338.3	46.7	NA	5075.5

OECD - Organization of Economic Co-operation and Development; EFSU - Eastern Europe and the Former Soviet Union; ASIA P - Asian Pacific region; ROW - Rest of the World

Table 5. SRES98 preliminary B2 marker scenario: quantification of population, GNP, GNP/capita, energy intensity and forest cover globally and for four world economic regions in 1990 and projected for 2020, 2050 and 2100. Source: Nakićenović et al. (2000).

Region	Year	Population (millions)	GNP (trillions 1990$)	GNP/Capita (thousands $)	Energy Intensity (MJ/$)	Forests (million ha)
OECD	1990	859	16.4	19.1	7.5	1056.3
	2020	982	30.3	30.9	5.3	1107.3
	2050	976	38.3	39.2	NA	1181.0
	2100	928	56.6	61.0	3.2	1290.3
EFSU	1990	413	1.1	2.7	45.8	960.0
	2020	418	1.8	4.3	27.1	940.3
	2050	406	6.6	16.3	10.3	967.2
	2100	379	14.5	38.3	5.4	1004.4
ASIA P	1990	2798	1.5	0.5	41.0	527.1
	2020	4008	13.2	3.3	10.9	411.7
	2050	4696	41.8	8.9	6.0	439.5
	2100	4968	97.1	19.5	4.0	482.7
ROW	1990	1192	1.9	1.6	20.7	1706.0
	2020	2263	5.5	2.4	13.5	1316.6
	2050	3289	22.8	6.9	6.7	1319.0
	2100	4139	66.8	16.1	4.6	1344.3
GLOBAL	1990	5262	20.9	4.0	12.9	4249.5
	2020	7672	50.7	6.6	8.5	3775.9
	2050	9367	109.5	11.7	6.0	3906.7
	2100	1041	4234.9	22.6	4.0	4121.7

OECD - Organization of Economic Co-operation and Development; EFSU - Eastern Europe and the Former Soviet Union; ASIA P - Asian Pacific region; ROW - Rest of the World

3 The Preliminary SRES Marker Scenarios: Global Characterizations

3.1 Estimating the climatic and sea-level responses to different emissions scenarios

The driving forces described and quantified in Section 2 give rise to a range of scenarios of greenhouse gas and sulphur emissions into the atmosphere. These were quantified for the SRES using different energy models, and the emissions profiles selected as the four preliminary marker scenarios are used here (Table 6). The implications of these emissions for atmospheric concentrations and subsequently for climate can be studied using two generic types of models: complex models or simple models (Figure 1).

| SIMPLE MODELS (GLOBAL-AVERAGE) | SCENARIOS | COMPLEX MODELS (REGIONALIZED) |

SOCIO-ECONOMIC AND TECHNOLOGICAL TRENDS

EMISSION SCENARIOS
e.g. IS92; SRES98

Simple gas models:
C, CH₄, N₂O, Halocarbons
Aerosols

ATMOSPHERIC CONCENTRATION

3-D atmospheric chemistry models

Radiative transfer model

RADIATIVE FORCING

Simple climate model

CLIMATE CHANGE

Coupled ocean-atmosphere GCMs

Thermal expansion model
Ice melt models

SEA-LEVEL CHANGE

Figure 1. Alternative pathways for obtaining projections of atmospheric composition, radiative forcing, climate and sea-level.

Complex models refer to numerical models that describe the dynamics of chemical and/or physical processes operating in the atmosphere. General circulation models are examples of such models. These models are capable of providing regional estimates of changes in atmospheric composition or of climate for a given emissions scenario (right hand side of Figure 1). However, they tend to be highly resource intensive, demanding large computing capacity, and this precludes rapid and/or multiple simulations for a range of different emissions scenarios. An alternative, is to use simple models (often referred to as simple climate models), usually operating over large regions or globally, that apply simplified representations of major processes operating in the atmosphere, enabling them to mimic the aggregate outputs from complex models but at a fraction of the computational cost. These models are useful tools for exploring rapidly the broad-scale implications of large numbers of emissions scenarios (left hand side of Figure 1).

Few estimates of atmospheric composition or of climate change have yet been reported from complex models based on the SRES98 emissions scenarios, although this work is in progress at several modelling centres around the world. In the absence of regional model outputs, alternative methods need to be sought to provide estimates of the possible atmospheric implications of the SRES emissions scenarios. For this exercise, we make use of existing information from both simple global models and GCMs. We first describe the use of simple climate models and then in Section 4 we illustrate an approach for combining information from these with GCM outputs.

3.2 Accounting for emissions uncertainties

We have used the same set of simple models (MAGICC - Wigley, 1995; Wigley and Raper, 1995; Wigley et al., 1997) that were applied in the IPCC Second Assessment Report to convert the SRES98 emissions scenarios into atmospheric concentrations, radiative forcing (i.e. the aggregate effect of concentrations on the Earth's radiation balance), mean annual temperature change and mean sea-level rise. Table 6 compares the global outcomes of the four SRES98 marker scenarios by the 2050s assuming a climate sensitivity[3] of 2.5°C and no aerosol forcing. The possible effects of aerosols are discussed in Section 7. The global mean annual temperature change by this time varies from 1.39°C under scenario B1 to 1.81°C under scenario A2. Table 6 also shows the IS92a scenario for comparison. An approximation of this IS92a emissions scenario, assuming a 1% growth in greenhouse gas concentrations per annum, has been widely applied in projecting future climate using GCMs (see Section 4).

---

[3] The climate sensitivity is the long term (equilibrium) change in global mean surface temperature following a doubling of atmospheric equivalent CO_2 concentration. Its likely range is estimated to be 1.5 to 4.5°C (IPCC, 1996).

Table 6. The SRES98 preliminary marker scenarios compared with IS92a and with estimates for year 2000. All calculations apply to the 2050s period (i.e., 2055). C is annual carbon emissions from fossil energy sources, S is annual sulphur emissions and pCO_2 is the atmospheric carbon dioxide concentration. Temperature (ΔT) and sea-level (ΔSL) changes assume no aerosol effect and a 2.5°C climate sensitivity and are calculated from a 1961-90 baseline using MAGICC (IPCC SAR version - Wigley, 1995; Wigley and Raper, 1995; Wigley et al., 1997).

	Population	C emissions from energy	Total S emissions	pCO2	Global ΔT	Global ΔSL
	(billions)	(GtC)	(TgS)	(ppmv)	(°C)	(cm)
2000	6.00	7.0	~75	~370	~0.30*	N/a
2050s						
IS92a	9.57	14.2	152	528	1.68	38
SRES98 B1	8.76	9.7	51	479	1.39	35
SRES98 B2	9.53	11.3	55	492	1.49	36
SRES98 A1	8.54	16.1	58	555	1.76	39
SRES98 A2	11.67	17.3	96	559	1.81	39

* Observed global warming of the 1990s relative to 1961-90 [Source: Hadley Centre and University of East Anglia]

It should be noted that somewhat different results from those presented in Table 6 would be obtained with the final SRES emissions scenarios, with more recent versions of the MAGICC models or with alternative models.

3.3 Accounting for uncertainties in the climate sensitivity

The estimates of temperature and sea-level change in Table 6 covered the range of SRES98 emissions scenarios but assumed a fixed, mid-range sensitivity of the climate to a given radiative forcing (2.5°C climate sensitivity). In order to account for a wider range of uncertainties, combinations of emissions scenarios and values of the climate sensitivity have been selected, as follows:

- B1-low, combining the B1 emissions with a 1.5°C climate sensitivity
- B2-mid (B2 emissions and 2.5°C sensitivity)
- A1-mid (A1 emissions and 2.5°C sensitivity)
- A2-high (A2 emissions and 4.5°C sensitivity)

We chose the two middle cases deliberately because even though the global warming is similar, the worlds which underlie the B2 and A1 emissions scenarios are quite different. The impacts of what may be rather similar global and regional climate changes could be quite different in these two cases. For example, world population is lower in the A1 world than in the B2 world, but GNP, carbon and sulphur emissions and CO_2 concentrations are higher (Tables 2, 5 and 6).

Outcomes of these four scenario combinations are shown in Table 7. Thus, the inclusion of the climate sensitivity uncertainty range has widened the range of global warming by the 2050s to 0.93-2.61°C compared to 1.39-1.81°C shown in Table 6.

3.4 Global sea-level changes

Global warming is expected to result in a worldwide rise in sea-level. The above global temperature change scenarios can be interpreted in terms of their effects on global-mean sea-level using simple models (Table 7). These calculations include estimates due to thermal expansion, glacier ice-melt and changes in ice-sheet mass balances, but do not account for regional differences in sea-level rise due to ocean and atmosphere circulation effects. Furthermore, Table 7 makes no allowances for natural vertical land movements due to geological causes: some land areas of the world are subsiding; others are emerging out of the ocean. Consideration of the impacts of sea-level rise also requires some assessment of the changing storm environment and the ways in which mean sea-level rise, storm regimes and offshore topography may combine to alter the return periods of high tide-levels.

Table 7. The four SRES98-based scenarios and their implications for CO_2 concentration, global mean annual temperature and sea-level by 2025, 2055, 2085 and 2100. C is annual carbon emissions from fossil energy sources, S is annual sulphur emissions. Temperature and sea-level changes assume no sulphate aerosol effect and are calculated from a 1961-90 baseline using MAGICC (IPCC SAR version - Wigley, 1995; Wigley and Raper, 1995; Wigley et al., 1997).

	2025	2055	2085	2100
C emissions from energy (GtC)				
B1	8.35	9.72	8.20	6.50
B2	9.45	11.30	12.74	13.70
A1	13.20	16.05	14.55	13.20
A2	12.10	17.30	24.15	28.80
Total S emissions (TgS)				
B1	54.9	51.3	38.0	28.6
B2	62.5	55.4	48.5	47.3
A1	96.1	57.7	29.9	27.4
A2	105.7	95.8	63.1	60.3
CO_2 concentration (ppmv)				
B1	421	479	532	547
B2	429	492	561	601
A1	448	555	646	680
A2	440	559	721	834
Global temperature change (°C)				
B1-low	0.60	0.93	1.21	1.28
B2-mid	0.93	1.49	1.96	2.18
A1-mid	1.02	1.76	2.25	2.41
A2-high	1.40	2.61	3.94	4.65
Global sea-level change (cm)				
B1-low	7	13	19	22
B2-mid	20	36	53	61
A1-mid	21	39	58	67
A2-high	38	68	104	124

4 Regional Climate Characterizations: Maps

Having defined four global climate scenarios, we need next to consider the range of climate changes at a regional level that may result from each of these possibilities. This section introduces a set of interim regional climatic characterizations based on the SRES98 marker emissions scenarios. They are interim because they will be superseded by a set of new simulations with AOGCMs forced by SRES98 emissions, which will start to become available during 2000. However, until these appear, we have employed existing GCM results in combination with simple global models to help us to define the range of regional climates to be expected for a given global warming.

We have made use of a set of regional (gridded) patterns of climate change from seven GCMs which were available from the IPCC Data Distribution Centre (DDC) as of June 1999[4]:

- CGCM1   Canadian GCM #1
  Boer *et al.* (2000)
- CSIRO-Mk2b Commonwealth Scientific and Industrial Research Organisation, Model #2b
  Hirst *et al.* (2000)
- ECHAM4   European Centre/Hamburg Model #4
  Roeckner *et al.* (1996); Zhang *et al.* (1998)
- GFDL-R15   Geophysical Fluid Dynamics Laboratory, R-15 resolution model
  Manabe and Stouffer (1996)
- HadCM2   Hadley Centre Coupled Model #2
  Mitchell and Johns (1997)
- NCAR1   National Centre for Atmospheric Research, Model #1
  Meehl and Washington (1995); Washington and Meehl (1996)
- CCSR-98   Centre for Climate Research Studies 1998 Model
  Emori *et al.* (1999)

All of these represent the simulated climate response to emissions that approximate the IS92a scenario (1% per annum growth in CO_2-equivalent greenhouse gas concentration). Some discussion about the validity of results from GCM experiments is provided in Box 1.

In this section we present global maps showing seasonal mean temperature and precipitation changes for the 2020s, 2050s and 2080s. The detailed construction of the global maps is described in Box 2, and the full set of maps is displayed in Appendix A (Figures A1 - A40). For each scenario, season, variable and time-slice we present two maps. One map shows the *median* change from our sample

---

[4] These experiments are documented at website: http://ipcc-ddc.cru.uea.ac.uk/cru_data/examine/ddc_GCMexperi.html

of ten standardized and scaled GCM responses and the other map shows the absolute *range* of these ten responses. We also introduce the idea of signal:noise ratios by comparing the median scaled GCM change against an estimate of natural multi-decadal variability also based on a GCM simulation (see Section 5.3). In the maps showing the median change we only plot these values where they *exceed* the 1 standard deviation estimate extracted from the 1400-year unforced simulation of HadCM2 (Tett *et al.* 1997). We recognise that by adopting this 1 SD limit we may be excluding regions in which important changes are estimated to occur, even if these are not statistically significant according to this criterion. Therefore, we advise readers to use the mapped information in conjunction with the regional scatter plots described in Section 6 and presented in Appendix B.

To summarize, the maps inform at a number of levels:

- Regional estimates of mean seasonal climate change (mean temperature and precipitation) for the full range of scenarios are presented;
- Estimates are derived from a sample (a pseudo-ensemble) of ten different GCM simulations, rather than being dependent on any single GCM or GCM experiment;
- Only median changes that exceed what may reasonably be expected to occur due to natural climate variability are plotted;
- The extent of inter-model agreement is depicted through the range maps.

BOX 1 *The validity of general circulation models*

Many impact assessment studies have used GCMs as the basis for creating climate scenarios. The major advantage of using GCMs for this purpose is that they are the only tool that estimates changes in climate due to increased greenhouse gases for a large number of climate variables in a physically consistent manner. A major disadvantage of using GCMs, however, is that, although they quite accurately represent global climate, their simulations of current regional climate can often be inaccurate. Although the variables within a GCM are all determined using physical laws, or empirical relationships based on physical laws, validation studies show that the internal relationships between these model variables may not necessarily be the same as the relationships observed in the real world. In many regions, GCMs may significantly underestimate or overestimate current temperatures and precipitation. Another disadvantage of GCMs is that they do not produce output on a geographic and temporal scale fine enough for many regional or national impact assessments. GCMs estimate uniform climate changes in grid boxes several hundred kilometres across, and although they estimate climate on a daily or even twice daily basis, results are generally archived and reported only as monthly averages or monthly time series.

Therefore, although GCMs have clear limitations for the purposes of climate scenario construction, they do provide the best information available on how global and regional climate may change as a result of increasing atmospheric concentrations of greenhouse gases.

BOX 2 *Constructing the global mapped climate change characterizations*

There are two approaches to identifying the range of possible regional responses. We can examine ensembles of simulations from the same model and generated by the same forcing (e.g. the HadCM2 experiment which generated ensembles with four members), or we can examine the full sample of results from all the GCM experiments. In this latter approach, the results are not directly comparable because although they are based on the same forcing (1% increase per annum) they *do* have different climate sensitivities (a factor we have already accounted for in our four global scenarios in Table 7). We therefore need some way to standardize the results from the GCMs to ensure that the different patterns of response are not biased by different model sensitivities and that the patterns are consistent with the four global warming scenarios we have adopted.

The simplest way to achieve such standardization is to normalize the GCM responses according to the global-mean temperature change of each respective GCM and then to scale these standardized patterns according to our global warming scenarios (following Santer *et al.*, 1990). This method, which is discussed further in Section 7, assumes that the regional *pattern* of climate change due to greenhouse gas forcing (the greenhouse "signal") remains invariant both over time and for different levels of forcing, and that this greenhouse signal can be adequately extracted from GCM experiments. In this way, the regional pattern of climate change by the 2050s from a GCM with a large global warming by the 2050s (i.e., a high model climate sensitivity) would be reduced in proportion to the ratio of the model's global warming to that computed for the four SRES98-based scenarios.

These characterizations use the 30-year mean GCM change patterns for the 2080s (i.e., 2070-2099 minus 1961-90 for each respective GCM simulation) to re-create all earlier timeslices (except for the GFDL-R15 and NCAR1 simulations where only the 2020s pattern was available and so we use this pattern to re-create later timeslices). The four HadCM2 ensemble members are scaled, and presented, separately. Our IPCC DDC "pseudo-ensemble" therefore comprises ten members.

The scaling is performed using the numbers given in Table 8. This shows the global-mean annual warming (°C) for the 30-year time-slices, expressed with respect to the 1961-90 means, computed using MAGICC (upper four rows in Table) and by GCMs (remaining rows). No aerosol effects are included in the MAGICC calculations (i.e., all aerosol forcing is switched off from 1765). This is to achieve consistency with the GCM simulations which are all forced with greenhouse gas concentration changes only. Thus to calculate the B1-low characterization for the 2050s for the HadCM2 GGa2 simulation, the GGa2 2080s change fields (seasonal mean temperature and precipitation; absolute changes) are multiplied by (0.93/3.03); and to calculate the A1-mid characterization for the 2080s for the GFDL-R15 simulation, the GFDL 2020s change fields (seasonal mean temperature and precipitation changes) are multiplied by (2.25/1.71).

Table 8. Global-mean warming (°C) for the four scenarios (cf. Table 7) and for the ten GCM simulations used. All warmings are shown for 30-year timeslices with respect to the 1961-90 mean. N/a indicates that data were not available.

	2020s	2050s	2080s
SRES98-based scenarios			
B1-low	0.60	0.93	1.21
B2-mid	0.93	1.49	1.96
A1-mid	1.02	1.76	2.25
A2-high	1.40	2.61	3.94
GCM outputs			
HadCM2 GGa1	1.21	2.10	3.17
HadCM2 GGa2	1.20	2.02	3.03
HadCM2 GGa3	1.16	2.06	3.07
HadCM2 GGa4	1.19	2.03	3.01
CGCM1	1.47	3.01	4.93
ECHAM4	1.22	2.13	3.02
CCSR-98	1.12	2.07	3.00
NCAR1	2.80	N/a	N/a
CSIRO-Mk2	1.21	2.05	3.06
GFDL-R15	1.71	N/a	N/a

All GCM fields were interpolated onto a common grid (the HadCM2 grid). Note that this re-gridding was *not* performed for the regional graphs depicted in Appendix B. Once all the respective GCM fields have been standardized and re-scaled to the three timeslices, we calculate the median change of the ten "pseudo-ensemble" members. For the precipitation plots and to ease interpretation, the re-scaled absolute changes (in mm/day) are converted into per cent changes from the respective 1961-90 model means. The median value is plotted as the left panel of the maps in Appendix A, *but only* where this value exceeds the 1 standard deviation estimate of natural climate variability derived from the 1400-year HadCM2 unforced simulation. The right-hand panel shows the range of scaled GCM changes for each gridbox, i.e., the maximum of the ten changes minus the minimum. This therefore provides a measure of inter-model and intra-ensemble agreement.

5 Regional Climate Characterizations: Summary Information

5.1 Projected rates of temperature change up to 2100

In order to summarise some of the regional changes displayed on the maps, we have estimated rates of mean annual temperature change under the two extreme scenarios, B1-low and A2-high, for each continent and for a number of oceanic regions (Table 9). The two values represent the spatial range of the median changes (left hand maps in Figures A1 and A31). The uncertainty attributable to inter-model differences is not shown, but can be read off the right hand maps (Figures A1 and A31). It should be stressed that the numbers contained in Table 9 are *visual estimates* and are highly approximate. They are provided to offer a quick summary of regional differences in climate projections, as a complement to the more detailed regional scatter plots presented in Appendix B.

Two further features of regional climate are also presented in Table 9 and in other supporting material:
1. Estimates of observed trends in regional climate during the 20th century
2. Model estimates of the range of multi-decadal "natural" variability in the climate.

5.2 Trends in observed climate since 1901

Trends in mean annual climate during the period 1901-1998 for each continent and for a number of ocean regions have been computed as anomalies relative to the 1961-1990 mean using four global gridded climatological databases. Anomalies of annual temperature are shown in Figure 2 and of annual precipitation in Figure 3. Smooth curves have also been fitted to the annual data to accentuate long term trends. In addition, least squares linear regression lines were computed for each of the temperature time series in order to evaluate long term trends in °C per century (Table 9).

Twentieth century trends in global climate are also depicted in map form for 5 x 5° latitude/ longitude grid boxes in Figures 4 (annual temperature) and 5 (annual precipitation). These are updated versions of maps that were first prepared for the IPCC Special Report on *The Regional Impacts of Climate Change* (Karl, 1998).

Table 9. Comparison of rates of mean annual temperature change projected for the 21st century (median changes) under a range of emissions and climate sensitivities with rates observed during the 20th century and with modelled multi-decadal natural variability (±1 standard deviations) for 14 world regions and globally. Note that the 2080s characterizations are based on visual estimates from maps in Appendix A.

| Region | Latitude/ longitude domain[a] | Mean annual air temperature | | Characterizations to 2080s (median - °C/century)[d] | |
		Land surface trends, 1901-98 (°C/century)[b]	±1 SD GCM multi-decadal variability (°C)[c]	B1-low	A2-high
Global	90°N - 90°S 180°W - 180°E	0.3-0.7°C[e]	0.061	1.2[f]	3.9[f]
Africa	35°N - 35°S; 20°W - 50°E	0.39	0.080	1 - 3	3.5 – 7
Asia	80°N - 10°S; 50°E - 170°W	0.50	0.096	1 - 3	3 – 9
Australasia	10°N - 50°S; 110°E - 180°E	0.45	0.100	1 - 2	3 – 5.5
Europe	70°N - 35°N; 30°W - 50°E	0.64	0.144	0.5 - 2	2 – 6
Latin America	25°N - 55°S; 110°W - 30°W	0.67	0.094	0.5 - 2	2 – 6
North America	70°N - 25°N; 170°W - 50°W	0.70	0.099	1 - 3	3.5 - 7.5
Antarctic	65°S - 90°S; 180°W - 180°E	1.91[g]	0.118	0 - 2	1 - 5.5
Arctic	90°N - 60°N; 180°W - 180°E	0.46	0.129	0.5 - 4	2 – 10
Caribbean	25°N - 10°N; 90°W - 60°W	0.76	0.109	1 - 1.5	3 – 4
Indian Ocean	0°N - 60°S; 50°E - 100°E	1.09[h]	0.072	0 - 1.5	1 - 4
Mediteranean	45°N - 30°N; 0°E - 40°E	0.60	0.121	1 - 1.5	3 – 5
Northern Pacific	40°N - 0°N; 140°E - 120°W	0.55[h]	0.069	0.5 - 1.5	2 – 4
Southern Pacific	0°N - 60°S; 150°E - 80°W	0.39[h]	0.048	0 - 1.5	1 – 4
Tropical NE. Atlantic	40°N - 0°N; 20°W - 40°W	-0.28[h]	0.057	0.5 - 1.5	2.5 – 4

[a] Some domains differ from those shown for similar regions in Section 6 (Figure 6); [b] Based on linear regression of annual time series in Figure 2; [c] From the HadCM2 1400-year unforced control simulation; [d] median of 10 scaled GCM outputs (visual estimates from Figures A1 and A31); [e] Based on the Jones et al. (1999); [f] Estimate from MAGICC (IPCC SAR version - Wigley, 1995; Wigley and Raper, 1995; Wigley et al., 1997); [g] Data for 1957-1998; [h] Combined land and ocean temperatures.
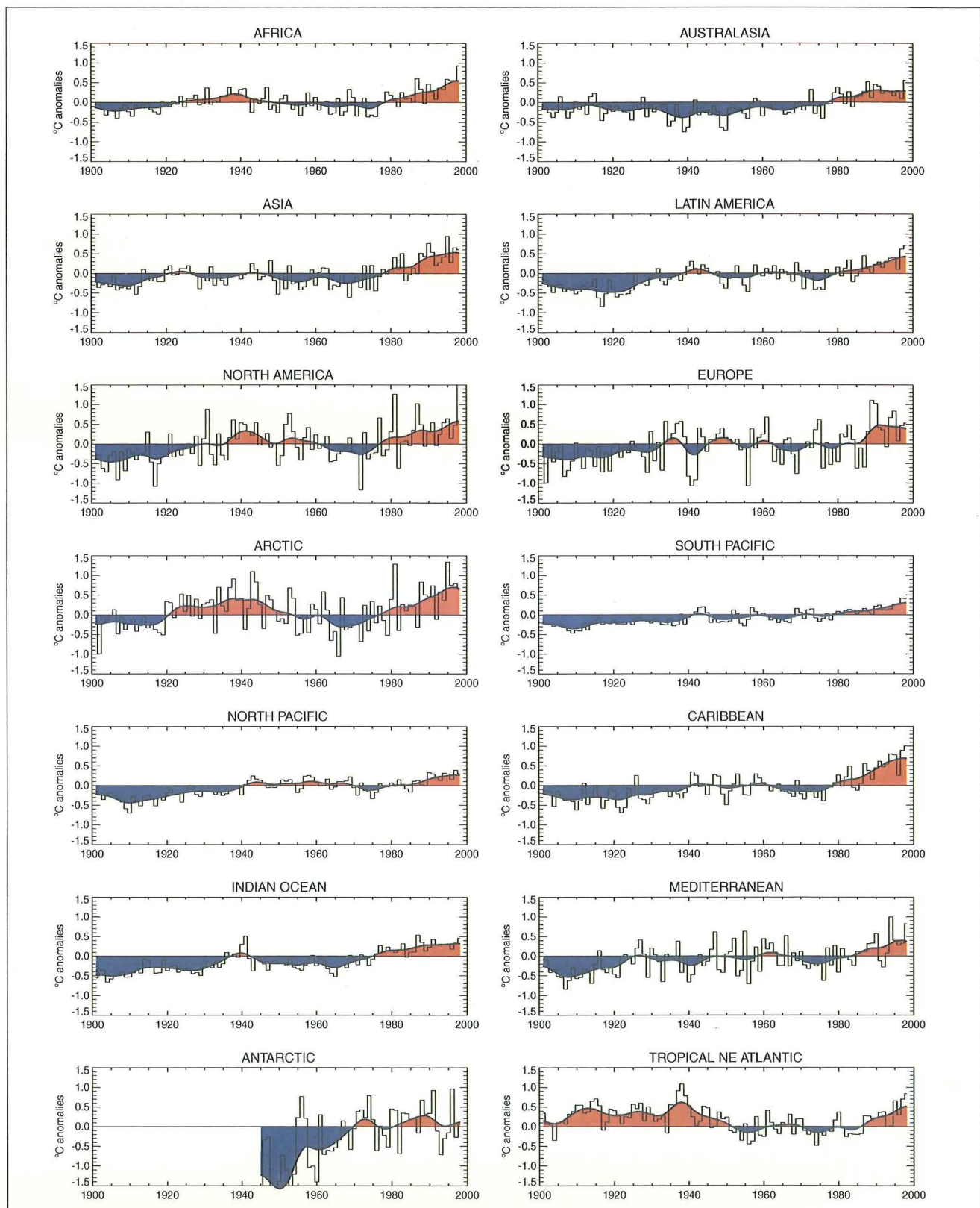
Figure 2. Anomalies of annual temperature for the period 1901-1998 relative to the 1961-1990 mean for 14 world regions (cf. Table 9). Curved lines represent a 15 point Gaussian filter fitted to the annual time series. Temperatures above and below the 1961-1990 mean are indicated in red and blue shading, respectively. Data for the Antarctic are for land areas during 1957-1998 (from Jones, 1995, updated). Data for the Pacific, Tropical NE Atlantic and Indian Oceans are combined land plus marine data (from Parker et al., 1994, updated). Both of these databases are gridded at 5° x 5° latitude/longitude resolution. Data for all other regions are from the 0.5° x 0.5° resolution global terrestrial data set of New et al. (1999, 2000).
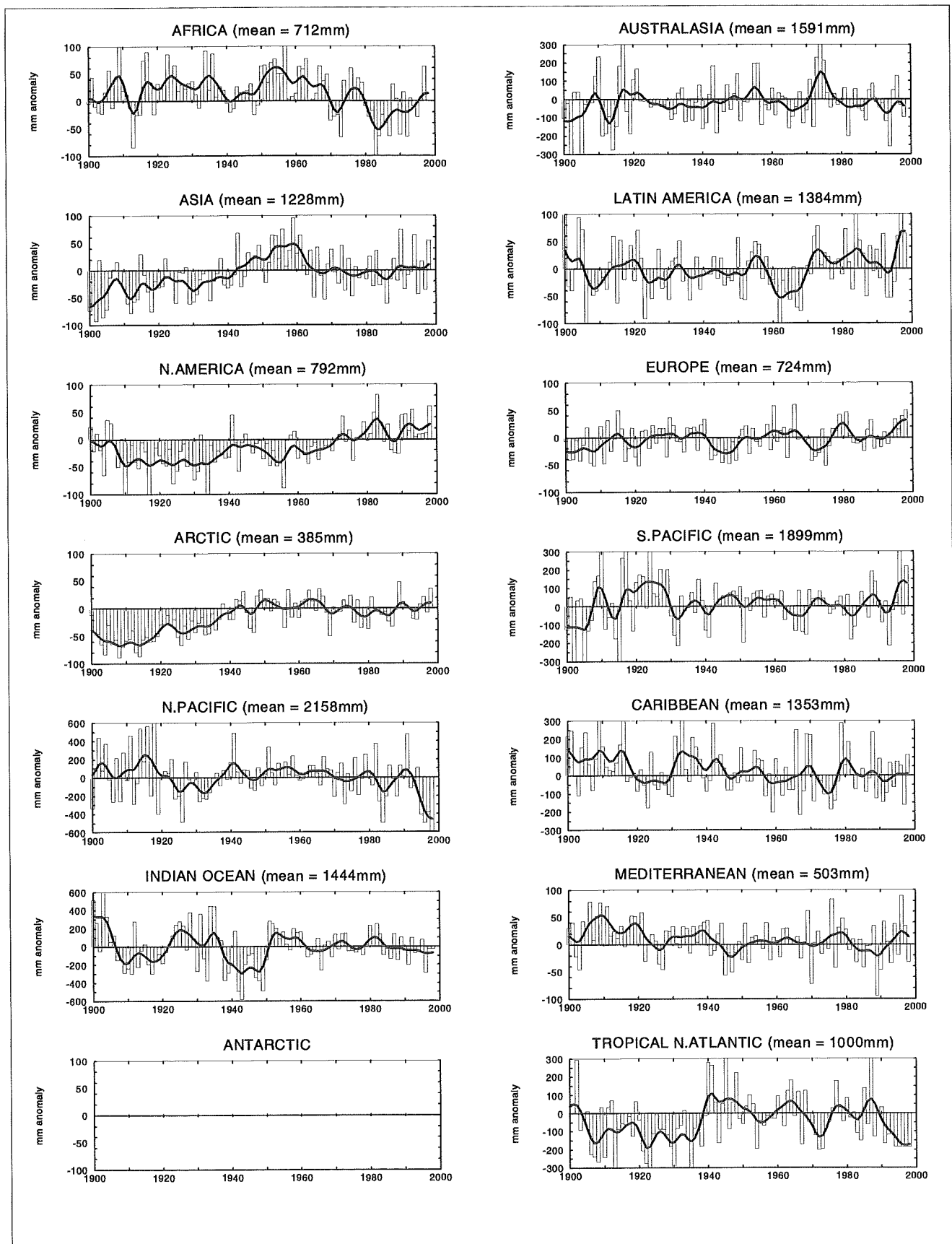
Figure 3. Anomalies of annual precipitation over land areas only for the period 1901-1998 relative to the 1961-1990 mean for 14 world regions (cf. Table 9). Curved lines represent a 10 point Gaussian filter fitted to the annual time series. Data are from the gridded terrestrial database of Hulme (1994, updated). There are no data for the Antarctic due to insufficient observations.

Trends (degC/century) in ANNUAL Temp
1901 - 1998

| -5C | -4C | -3C | -2C | -1C | 0C | 1C | 2C | 3C | 4C | 5C |
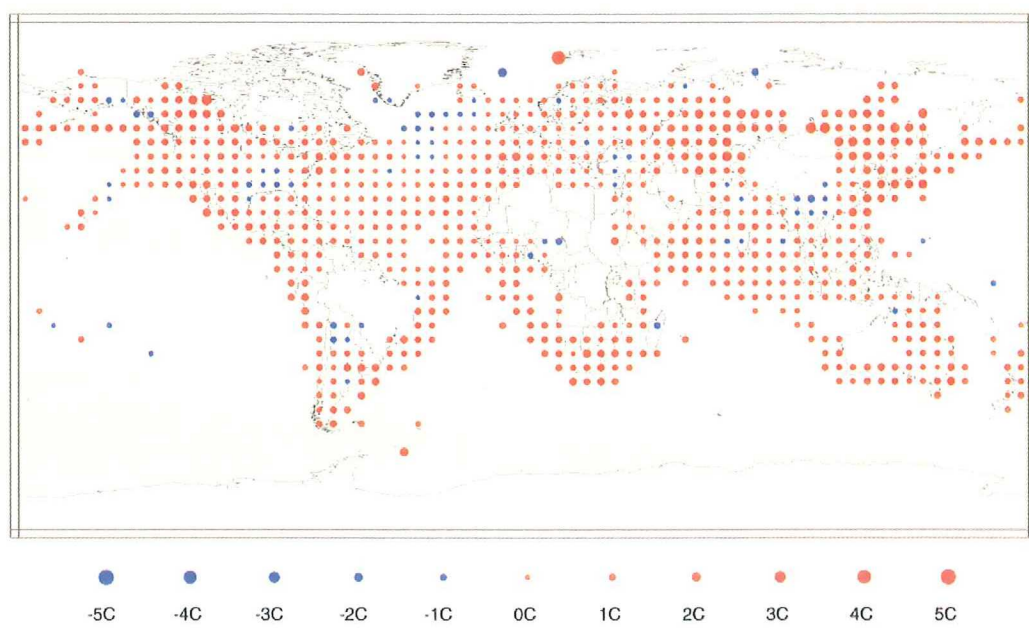
Figure 4. Mean annual near-surface temperature trends, 1901-1998, by 5° x 5° latitude/longitude grid box. The area of a circle represents the magnitude of the trend (°C/century): red circles indicate increasing trends; blue circles decreasing trends. Source: T. Karl (personal communication, 1999).

Trends (%/century) in Annual Precipitation
1900 - 1998

| -200% | -100% | -50% | -20% | -10% | 0% | 10% | 20% | 50% | 100% | 200% |
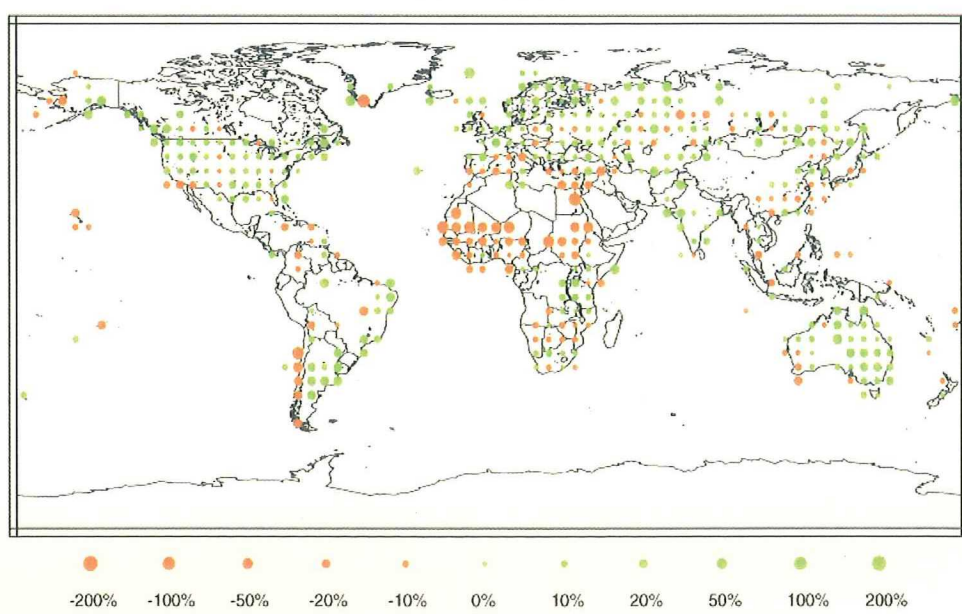
Figure 5. Mean annual land surface precipitation trends, 1900-1998, by 5° x 5° latitude/longitude grid box. The area of a circle represents the magnitude of the trend (%/century): green circles indicate increasing trends; brown circles decreasing trends. Stations with more than 1/6 of their data missing during the normal period or more than one season or year without any measurable precipitation were excluded from consideration. Trends were not calculated if less than 66% of the years were missing during the period cited. Source: T. Karl (personal communication, 1999).

5.3 Multi-decadal natural variability

Global and regional climate will vary naturally over future decades, with or without substantial human influence on climate. Therefore, it is useful to consider what range of naturally occurring future climates resource managers may have to adapt to in the absence of climate change. There are two ways to estimate this range: use long instrumental records of climate, or use long unforced GCM simulations. Using instrumental records has the disadvantage that they are at most 100-200 years in length and may already be contaminated by greenhouse warming (and are not therefore describing *natural* variability). Using model simulations has the disadvantage that models may not accurately simulate natural climate variability. Given that model simulations give us longer and more comprehensive estimates of natural variability, and that at least for some regions and on some time-scales these models yield estimates of natural variability quite similar both to observations (Tett *et al.*, 1997) and to climatic fluctuations reconstructed from proxy records over the past millennium (Jones *et al.*, 1998; Hulme *et al.*, 1999), we have chosen to use model simulations to quantify the range of natural climate variability.

We have adopted 30-year time-mean climates for this exercise (following the World Meteorological Organization convention adopted in this assessment). The distributions of 30-year climatic means allow us to estimate the probability of a "different" climate occurring in the future (say the 2050s), irrespective of human influence. We have chosen a change in 30-year mean climate of more than ±1 standard deviations relative to the long-term mean as our threshold for displaying median changes in temperature and precipitation in Figures A1-A40. Assuming a normally distributed set of 30-year mean climates, there is only a 16% probability that a change in climate exceeding this threshold could have occurred "naturally", in the absence of external forcing.

The ±1 SD limits for mean annual temperature from the unforced Hadley Centre simulation are summarised in Table 9 as a spatial range for each region. These values can be compared with the observed and projected trends in temperature also presented in Table 9. One of the key challenges for climatologists studying the instrumental record is to identify patterns in observed climate change that are abnormal with respect to natural variability (climate change detection) and to match them to GCM projections of future change under anthropogenic forcing (climate change attribution).

Errata

Page 24, Figure 5, Title:
Trends (mm/century) in Annual Precipitation
Page 24, Figure 5, Caption, 2nd sentence:
The area of a circle represents the magnitude of the trend (mm/century): green circles indicate increasing trends; brown circles decreasing trends.

6 Regional Climate Characterizations: Scatter Plots

To condense the scenario information further, we have constructed summary scatter plots for 32 world regions (Appendix B, Figures B1-B32). The regions are subdivisions of the continental-scale regions adopted by IPCC Working Group II in successive assessments. As such, they cover all global land areas as well as ocean areas in which the most numerous small island states are located (Table 10 and Figure 6). Their size, encompassing several model grid boxes, is small enough to distinguish important differences in climate changes between regions but large enough to reflect the types of broad scale changes that can be simulated with some confidence by GCMs.
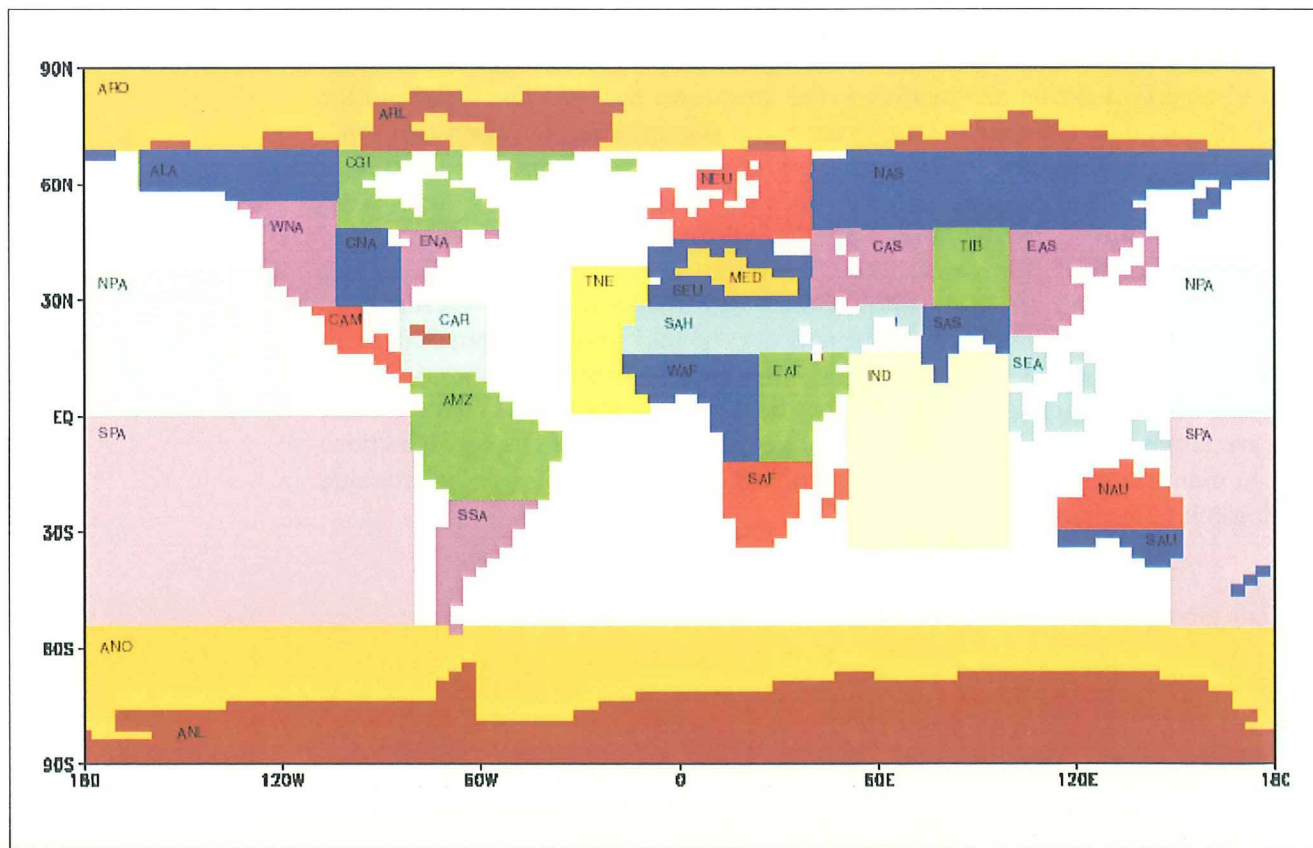
Figure 6. Map showing the 32 regions described in Table 10 as defined on the HadCM2 GCM grid. Regional domains are slightly different for each of the other GCMs.

Table 10. Subdivisions of the IPCC Working Group II regions used for characterizing possible future climate. Regions marked in italics are characterized by climate model ocean grid boxes. All other regions are represented as land grid boxes.

WG II Region	No.	Sub-region	Code	Latitude (°N)		Longitude (°E)	
Polar	1	Arctic/land	ARL	90.0	67.5	-180.0	180.0
	2	*Arctic/ocean*	ARO	90.0	67.5	-180.0	180.0
	3	Antarctic/land	ANL	-55.0	-90.0	-180.0	180.0
	4	*Antarctic/ocean*	ANO	-55.0	-90.0	-180.0	180.0
North America	5	Alaska/NW Canada	ALA	67.5	57.5	-170.0	-105.0
	6	NE Canada/S Greenland/Iceland	CGI	67.5	50.0	-105.0	-10.0
	7	Western North America	WNA	57.5	30.0	-135.0	-105.0
	8	Central North America	CNA	50.0	30.0	-105.0	-85.0
	9	Eastern North America	ENA	50.0	25.0	-85.0	-50.0
Latin America	10	Central America	CAM	30.0	10.0	-115.0	-85.0
	11	Amazonia	AMZ	10.0	-20.0	-80.0	-35.0
	12	Southern South America	SSA	-20.0	-55.0	-75.0	-40.0
Europe	13	Northern Europe	NEU	67.5	47.5	-10.0	40.0
	14	Southern Europe/North Africa	SEU	47.5	30.0	-10.0	40.0
Africa	15	Sahara	SAH	30.0	17.5	-20.0	65.0
	16	West Africa	WAF	17.5	-10.0	-20.0	25.0
	17	East Africa	EAF	17.5	-10.0	25.0	55.0
	18	Southern Africa	SAF	-10.0	-35.0	10.0	50.0
Asia	19	Northern Asia	NAS	67.5	50.0	40.0	-170.0
	20	Central Asia	CAS	50.0	30.0	40.0	75.0
	21	Tibetan Plateau	TIB	50.0	30.0	75.0	100.0
	22	East Asia	EAS	50.0	20.0	100.0	150.0
	23	South Asia	SAS	30.0	5.0	65.0	100.0
	24	Southeast Asia	SEA	20.0	-10.0	100.0	150.0
Australasia	25	Northern Australia	NAU	-10.0	-30.0	110.0	155.0
	26	Southern Australia/New Zealand	SAU	-30.0	-47.5	110.0	180.0
Small Islands	27	*Mediterranean*	MED	45.0	30.0	-5.0	35.0
	28	*Caribbean*[a]	CAR	25.0	10.0	-85.0	-60.0
	29	*Tropical NE Atlantic*	TNE	40.0	0.0	-30.0	-10.0
	30	*North Pacific*	NPA	40.0	0.0	150.0	-120.0
	31	*Indian Ocean*	IND	17.5	-35.0	50.0	100.0
	32	*South Pacific*[a]	SPA	0.0	-55.0	150.0	-80.0

[a] Also includes land grid boxes where these coincide with small islands

Each scatter plot shows, for each of the four seasons and for either the 2020s, 2050s or 2080s, the distribution of the modelled changes in mean temperature and precipitation for each GCM simulation and for each SRES98-based scenario. Appendix B provides a full description of the construction method. As with the maps, these changes are compared with the multi-decadal variability (MDV) of temperature and precipitation extracted from the HadCM2 1400-year unforced simulation. In addition, temperature and precipitation estimates of MDV taken from the GFDL 1000-year unforced simulation are also shown for comparison with the HadCM2 estimates.

These scatter plots provide a quick assessment at a regional-scale of the likely range and significance of future climate change and show the extent to which different GCMs agree in their regional response to a given magnitude of global warming.

7

Major Caveats

· ·

It is important to appreciate that the methods used to construct the climatic characterizations presented in the previous sections exhibit a number of important potential weaknesses. These concern:

1. sulphate aerosol effects;
2. the scaling method;
3. representation of uncertainties; and
4. post-2100 changes.

In this section we consider the first three of these. The fourth is discussed in the next section on stabilization scenarios. Clearly, as new information becomes available from GCM simulations conducted for a new set of emissions scenarios, it will be possible to compare those with the interim estimates presented in this document.

7.1 Sulphate aerosol effects

Climate can also be affected by a number of other agents in addition to greenhouse gases, and important amongst these are small particles (aerosols). These aerosols are suspended in the atmosphere and some types (e.g. sulphate aerosols derived from sulphur dioxide) reflect back solar radiation, having a cooling effect on climate. Although there are no measurements to show how these aerosol concentrations have changed over the past 150 years, there *are* estimates of how sulphur dioxide emissions (one of the main precursors for aerosol particles) have risen and there are projections of such emissions into the future. A number of such projections have been used in a sulphur cycle model as part of the MAGICC model framework (Wigley *et al.*, 1997) to calculate the accompanying rise in sulphate aerosol concentrations. When the IS92a sulphur dioxide emissions scenario is used, along with greenhouse gas increases, as input to GCMs, the global temperature rise to 2100 is reduced by between a quarter and a third.

These are very uncertain calculations, however, due to a number of factors. First, the IPCC emissions scenario on which it was based (IS92a) contains large rises in sulphur dioxide emissions for most regions over the next century. Three of the four preliminary SRES marker emissions scenarios, however, foresee only a small rise in global sulphur dioxide emissions over the next couple of decades followed by reductions to levels lower than today's by 2100 (cf. Table 7). The inclusion of these sulphur dioxide emissions scenarios into transient GCM experiments would actually produce a small temperature *rise* by 2100 relative to model experiments that excluded the aerosol effect (Schlesinger *et al.*, 2000). Results from such transient GCM experiments are not available yet. Second, more recent sulphur cycle models generate a lower sulphate burden per tonne of sulphur dioxide emissions and the radiative effect of the sulphate particles in more sophisticated radiation models is smaller than previously calculated. Third, in addition to their direct effect, sulphate aerosols can also cool climate by chang-

ing the reflectivity and longevity of clouds. These indirect effects are now realised as being as at least as important as the direct effect, but have not yet been included in GCM climate change simulations from which results are available for impacts work. Fourth, there are other types of aerosols (e.g. carbon or soot) which may also have increased due to human activity, but which act to warm the atmosphere. Above all, the short lifetime of sulphate particles in the atmosphere means that they should be seen as a temporary masking effect on the underlying warming trend due to greenhouse gases. For all these reasons, model simulations of future climate change using *both* greenhouse gases and sulphate aerosols were *not* used to develop the main climate scenario characterizations presented here.

However, it is recognised that in certain regions, especially over parts of southern and eastern Asia, the sulphur emissions in at least some of the preliminary SRES scenarios increase rapidly during the next few decades before falling equally rapidly during the middle decades of the century. These changes could potentially have a significant effect on the climate during the next half century, both locally and possibly in other regions too. Such regional effects on future climate are not accounted for in the main characterizations presented above.

Nonetheless, it is possible to use a set of recently (1997) completed equilibrium GCM simulations to characterize the regional effects of the preliminary SRES sulphur emissions scenarios using the scaling method proposed by Schlesinger *et al.* (2000). This method utilises a series of model equilibrium simulations completed using the University of Illinois at Urbana-Champaign (UIUC) 11-layer atmospheric GCM (AGCM), together with results from a simple climate model which simulates the global-mean temperature response to the SRES98 marker emissions scenarios. The simple climate model is run using the values of the climate sensitivity assumed for the SRES-based scenarios (see section 3.3). The global geographical response to aerosol forcing is deconstructed into six regional responses, each of which is then re-combined on the basis of the unique pattern of aerosol forcing in a given anthropogenic emissions scenario. Full details of the method are described in Schlesinger *et al.* (2000).

Figures C1 and C2 in Appendix C show the annual mean temperature change induced by the SRES98-derived sulphate aerosol concentrations alone for the four SRES98-based scenarios and for the 2020s, 2050s and 2080s. Aerosol-induced changes in annual-mean temperature relative to 1961-90 climate are generally in the range ±1°C, and for most scenarios and regions the changes end up being positive (i.e., warming). Figures C1 and C2 indicate annual cooling due to sulphate aerosol concentrations up to about 2050 over all regions of the world under the A2-high scenario, followed by an aerosol-induced warming up to 2100 as the sulphate burden is reduced. A similar, but weaker, pattern of cooling in all regions up to about 2020 for the A1-mid scenario is followed by warming (though lagged in the southern hemisphere and northern Africa), with all regions becoming warmer than present by 2100 due to aerosol effects. The B1-low and B2-mid sulphur scenarios produce relative warming from 2000 onwards in all regions except the southern hemisphere, reflecting the markedly reduced sulphate burden in all regions (Schlesinger *et al.*, 2000).

The same regional scaling method can be applied in the case of precipitation. Results are not shown here because of the generally much smaller signal-to-noise ratio of the estimated aerosol-induced regional precipitation changes. For most emissions scenarios, time-slices and regions these changes in annual mean precipitation are less than ±5 per cent which is well within the range of natural multi-decadal natural precipitation variability. Some localised aerosol-induced precipitation changes reach ±10 per cent, but the significance of these changes is

unclear. Reductions in sulphate aerosol forcing, as implied in the SRES98 emissions scenarios, do not automatically translate into a sign reversal of the estimated local/regional aerosol-induced precipitation change.

A number of things should be pointed out about the sulphate-aerosol induced climate changes estimated and discussed here:

- The changes shown in Figures C1 and C2 can be added to the greenhouse gas-induced temperature changes shown in Figures A1, A11, A21 and A31 to obtain a full, composite characterization of the preliminary SRES marker scenarios. It should also be noted that the colours in the legends of these two sets of maps represent *different temperature scales.*

- Until such time as results from fully coupled AOGCM climate change experiments forced with comprehensive SRES-derived forcings become available (during 2000), this composite method is the best interim approach for characterizing the climate implications of the SRES scenarios.

- It is important to realise that under most of the SRES98 emissions scenarios, and for most world regions, the effect of including suphate aerosol concentrations in climate scenarios is to *warm* regional climate with respect to 1961-90 and *not* to cool it. This is a different conclusion from that reached in the IPCC SAR and from that implied in the greenhouse gas and aerosol forced AOGCM experiments posted on the IPCC DDC, all of which use the (high) IS92a sulphur dioxide emissions projections.

7.2 Scaling climate model response patterns

The scaling technique we have employed to represent a wider range of possible future forcings than are available from GCM simulations alone (cf. Box 2) has been widely employed in impact studies. The approach was first suggested by Santer *et al.* (1990) and employed in the IPCC First Assessment Report to generate climate scenarios for the year 2030 (Mitchell *et al.*, 1990) using patterns from 2 x CO_2 GCM experiments. Fundamental assumptions in this technique are that the patterns of the climate response to anthropogenic forcing can be adequately defined from GCM experiments and that they are stable through time and across a representative range of possible anthropogenic forcings.

Saltzman and Ogelsby (1992) demonstrated that the patterns of equilibrium temperature response to increasing greenhouse gas forcing are fairly uniform over a wide range of concentrations, scaling approximately with CO_2 concentration or linearly with global-mean temperature. The main exception occurs in the regions of enhanced response near sea ice and snow margins. Mitchell *et al.* (1999) conclude that the uncertainties introduced by scaling decadal-mean temperature patterns are smaller than those due to the model's internal variability, although this conclusion probably does not hold for variables such as precipitation.

Uncertainties due to scaling climate response patterns increase for scenarios that include substantial regionally differentiated aerosol forcings. The problem here is that aerosol forcing can induce large changes in some regional climate responses to anthropogenic forcing without greatly altering the response in other regions or indeed without greatly affecting the global-mean temperature. This characteristic weakens the basis for scaling methods that are based on the assumption of a constant climate change pattern for a given global warming. Similar global-mean warmings can be associated with quite different regional patterns depending on the magnitude and pattern of the aerosol forcing. This

concern has been tackled by Schlesinger *et al.* (2000) in the approach described in Section 7.1 (above).

The above discussion demonstrates that the scaling of climate change response patterns across a range of greenhouse gas forcing scenarios may be an appropriate technique to apply to climate change scenario construction in circumstances such as the present application, when it is important to capture the effect of emissions or climate sensitivity uncertainties on future climate. However, it must be remembered that the pattern scaling method as a means of handling one type of uncertainty, introduces its own uncertainty that has not been thoroughly explored. The technique is likely to be less reliable in dealing with sulphate aerosol induced patterns of change, and may well be inappropriate in the case of stabilization forcing scenarios, where the forcing and response can be strongly non linear. Of the variables examined, the technique performs best in the case of surface air temperature and, as done here, when the response pattern to be scaled is averaged over a decade or longer and defined from an ensemble of model simulations.

7.3 Representation of uncertainties

The SRES-based characterizations were constructed to represent three important sources of uncertainty in climate projections:
- uncertainties in future emissions
- uncertainties in the global climate response to emissions (climate sensitivity)
- uncertainties in the regional climate response from different GCM simulations

It should be emphasised that the characterizations do not capture the full range of uncertainty in descriptions of future climate. The range of uncertainty for each of the three sources listed is wider than that applied in this exercise. Moreover, there are plausible instabilities in the earth-atmosphere system that could trigger abrupt responses to anthropogenic forcing, for example cooling over the north Atlantic due to a breakdown in the thermohaline circulation of the deep ocean (Rahmstorf and Ganopolski, 1997), or a rise of sea-level of several metres due to the break up of the West Antarctic Ice Sheet (Oppenheimer, 1998).

Finally, we have tried to characterize possible future changes in annual or seasonal mean climate. No information has been provided on possible changes in climatic variability or on changes in the frequency of extreme weather events. There is still considerable uncertainty surrounding estimates of future climatic variability at different time scales, and a comprehensive analysis of GCM results has yet to be completed and is well beyond the scope of this document. However, it is recognised that some of the most important impacts of future climate change will be due to the altered frequency and magnitude of extreme weather events rather than through slow changes in mean conditions.

8

Stabilization Scenarios

Work to develop storylines for a set of stabilization scenarios is currently being co-ordinated by IPCC Working Group III. However, as yet there is no agreed set of scenarios. Furthermore, although a number of climate model simulations of the effects of CO_2 stabilization (at different concentrations) on climate have been carried out, these have not been co-ordinated and differ in their underlying assumptions about the timing and level of stabilization. Finally, there have been few studies to assess the impacts of and adaptation to the climate changes resulting from a stabilization of greenhouse gas concentrations. For these reasons, we can offer only qualitative information about the possible implications of stabilization for climate and sea-level rise, comparing these to the range of SRES scenario outcomes.

8.1 Some features of stabilization scenarios

Some of the issues facing scientists treating the stabilization question include:

- *CO_2-only or CO_2-equivalent?* One key question concerns whether studies of stabilization should focus on CO_2 concentration alone, or on a basket of greenhouse gases together, which are commonly expressed in terms of equivalent CO_2 concentration. The effects of greenhouse gases are additive, so stabilization of CO_2 concentration at any level above about 500 ppmv is likely to lead to at least a doubling of pre-industrial CO_2 concentration in equivalent concentration terms, approximately 560 ppmv (Schimel *et al.*, 1997). Hence, stabilization of CO_2 at 550 ppmv is likely to be a less demanding target than stabilization at 550 ppmv CO_2-equivalent over the same time frame.

- *Interpreting stabilization storylines.* A given emissions profile leading to stabilization might be explained by many alternative storylines describing the driving factors and policies required to obtain stabilization. Some plausible storylines leading to stabilization might require very little, if any, direct policy intervention (e.g. the SRES98 B1 scenario - see Section 2). Moreover, it is important to recognise that alternative storylines will have different socio-economic assumptions that will affect the vulnerability of communities to climate change.

- *The timing of stabilization.* Emissions profiles leading to stabilization at concentrations ranging from 350 ppmv to 1000 ppmv have been evaluated by Schimel *et al.* (1997). Stabilization of concentrations is achieved by 2100 only for the most stringent targets, below about 550 ppmv. Otherwise, it is achieved during the 22nd or 23rd centuries for levels of up to 1000 ppmv.

- *The climate response to stabilization pre- and post-2100.* Simple global models, including the MAGICC models used in this exercise, have been used to explore the global temperature and sea-level implications up to 2100 of different stabilization profiles (Schimel *et al.*, 1997). Due to lags in the response of the climate system to forcing, the climate will continue to warm

for many decades following stabilization. Only for stabilization at 350 ppmv, in about 2040, do temperatures reach equilibrium before 2100. However, sea-level continues to rise strongly under all scenarios. Furthermore, results from stabilization experiments simulated by GCMs suggest that important non-linearities or reversals in the climate response could occur several centuries after stabilization (e.g. Walsh *et al.*, 1999). These are important results to consider, because the major focus of climate change impact assessment in recent years has been on the period up to 2100, whereas large and possibly non-linear climate changes may occur after this time.

8.2 Comparison of stabilization scenarios and SRES-based scenarios

Global mean temperature changes computed by MAGICC have been reported in Schimel *et al.* (1997) for the 450 and 650 ppmv cases across the same range of climate sensitivies as expressed in the SRES-based B1-low and A2-high scenarios (see Table 7). The 650 ppmv case with a 1.5°C climate sensitivity produces slightly less warming by 2100 than the B1-low scenario; for higher sensitivities, the 650 ppmv scenarios fall within the range of temperature changes estimated for the SRES-based scenarios. In contrast, the temperature response to 450 ppmv stabilization only achieves a warming as high as the SRES-based range with a 4.5°C climate sensitivity.

Researchers at the Hadley Centre have conducted 550 and 750 ppmv (CO_2-equivalent) stabilization runs with the HadCM2 AOGCM (see Web site at: http://www.cru.uea.ac.uk:80/link/res_scens/HadCM2_time.html). The global mean annual temperature reaches equilibrium by about 2150 under the 550 ppmv run, with warming by 2100 of about 1.7°C relative to 1961-1990, placing this within the SRES-based range (Table 7). Visual inspection of mean annual temperature changes relative to 1961-1990 on global maps for both simulations by the 2080s places regional temperature changes within the range of SRES-based estimates displayed in Table 7. Similar results have also been reported for a 550 ppmv stabilization run with the Climate System Model of the National Center of Atmospheric Research, USA (see Web site at: http://www.cgd.ucar.edu/~tls/CSM/tables.html#tbl2)

More GCM stabilization runs for a wider range of scenarios will be conducted during the next few years, but these initial investigations suggest that only the strictest emissions reductions, resulting in CO_2-equivalent stabilization below about 500 ppmv by the end of the 21st century, will result in global warming by 2100 that is lower than under the B1-low scenario.

References

Boer, G.J., G. Flato, and D. Ramsden, 2000: A transient climate change simulation with greenhouse gas and aerosol forcing: projected climate to the twenty-first century. *Climate Dynamics*, 16, 427-450.

Emori, S., T. Nozawa, A. Abe-Ouchi, A. Numaguti, M. Kimoto, and T. Nakajima, 1999: Coupled ocean- atmosphere model experiments of future climate change with an explicit representation of sulfate aerosol scattering. *J. Met. Soc. Ja*p., 77, 1299-1307.

Hirst, A.C., S.P. O'Farrell, and H.B. Gordon, 2000: Comparison of a coupled ocean-atmosphere model with and without oceanic eddy-induced advection. Part I: Ocean spinup and control integrations. *J. Climate*, 13, 139-163.

Hulme, M., 1994: Validation of large-scale precipitation fields in General Circulation Models. In: *Global Precipitations and Climate Change* [Desbois, M. and F. Désalmand (eds.)]. Springer-Verlag, Berlin, pp. 387-405.

Hulme, M., T.J.Osborn, J. Jones, K.R. Briffa and P.D. Jones, 1999: *Climate observations and GCM validation* Final report to the UK DETR, May, Climatic Research Unit, Norwich, 65 pp.

IPCC, 1996: Climate Change 1995. The Science of Climate Change. Contribution of Working Group I to the Second Assessment Report of the Intergovernmental Panel on Climate Change. [Houghton, J.T., L.G.M. Filho, B.A. Callander, N. Harris, A. Kattenberg, and K. Maskell (eds.)]. Cambridge University Press, Cambridge, 572 pp.

Jones, P.D., 1995: Recent variations in mean temperature and the diurnal temperature range in the Antarctic. *Geophysical Research Letters*, 22, 1345-1348.

Jones, P.D., K.R. Briffa, T.P. Barnett, and S.F.B. Tett, 1998: High-resolution palaeoclimatic records for the last millennium: interpretation, integration and comparison with GCM control-run temperatures. *The Holocene*, 8, 455-471.

Karl, T.R., 1998: Regional trends and variations of temperature and precipitation. In: *The Regional Impacts of Climate Change: An Assessment of Vulnerability. A Special Report of IPCC Working Group II.* [Watson, R.T., M.C. Zinyowera, and R.H. Moss (eds.)]. Cambridge University Press, Cambridge, pp. 411-425.

Manabe, S. and R.J. Stouffer, 1996: Low frequency variability of surface air temperature in a 1,000-Year integration of a coupled atmosphere-ocean-land surface model. *Journal of Climate*, 9, 376-393.

Meehl,G.A. and W.M. Washington, 1995: Cloud albedo feedback and the super greenhouse effect in a global coupled GCM. *Climate Dynamics*, 11, 399-411.

Mitchell, J.F.B. and T.C. Johns, 1997: On the modification of global warming by sulphate aerosols *J.Climate*, 10, 245-267.

Mitchell, J.F.B., S. Manabe, V. Meleshko, and T. Tokioka, 1990: Equilibrium climate change - and its implications for the future. In: *Climate Change: the IPCC Scientific Assessment* [Houghton, J.T., G.J. Jenkins, and J.J. Ephraums (eds.)]. Cambridge University Press, Cambridge, pp. 137-164.

Mitchell, J.F.B., T.C. Johns, M. Eagles, W.J. Ingram, and R.A. Davis, 1999: Towards the construction of climate change scenarios. *Climatic Change*, 41, 547-581.

Nakićenović, N., J. Alcamo, G. Davis, B. de Vries, J. Fenhann, S. Gaffin, K. Gregory, A. Grübler, T.Y. Jung, T. Kram, E.L. La Rovere, L. Michaelis, S. Mori, T. Morita, W. Pepper, H. Pitcher, L. Price, K. Raihi, A. Roehrl, H.-H. Rogner, A. Sankovski, M. Schlesinger, P. Shukla, S. Smith, R. Swart, S. van Rooijen, N. Victor, and Z. Dadi, 2000: *Emissions Scenarios. A Special Report of Working Group III of the Intergovernmental Panel on Climate Change.* Cambridge University Press, Cambridge, United Kingdom and New York, NY, USA, 599 pp.

New, M., M. Hulme, and P.D. Jones, 1999: Representing twentieth-century space-time climate variability. Part 1: development of a 1961-90 mean monthly terrestrial climatology. *J.Climate*, 12, 829-856.

New, M. G., M. Hulme and P. D. Jones, 2000: Representing twentieth-century space-time climate variability. Part II: development of 1901-1996 monthly grids of terrestrial surface climate. *J. Climate*, 13, 2217-2238.

Oppenheimer, M., 1998: Global warming and the stability of the West Antarctic Ice Sheet. *Nature*, 393, 325-332.

Rahmstorf, S, and A. Ganopolski, 1999: Simple theoretical model may explain apparent climate instability. *J. Climate*, 12, 1349–1352.

Roeckner,E., K. Arpe, L. Bengtsson, M. Christoph, M. Claussen, L. Dümenil, M. Esch, M. Giorgetta, U. Schlese, and U. Schulzweida, 1996: The atmospheric general circulation model ECHAM-4: model description and simulation of present-day climate. *Max-Planck Institute for Meteorology, Report No.218*, Hamburg, Germany, 90pp.

Saltzman, B. and R.J. Oglesby, 1992: Equilibrium climate statistics of a general circulation model as function of atmospheric carbon dioxide. Part I: Geographic distributions of primary variables. *J. Climate*, 5, 66-92.

Santer, B.D., T.M.L. Wigley, T.P. Barnett, and E. Anyamba, 1996: Detection of climate change and attribution of causes. In: *Climate Change 1995. The Science of Climate Change. Contribution of Working Group I to the Second Assessment Report of the Intergovernmental Panel on Climate Change*. [Houghton, J.T., L.G.M. Filho, B.A. Callander, N. Harris, A. Kattenberg, and K. Maskell (eds.)]. Cambridge University Press, Cambridge, pp. 407-443.

Schimel, D., M. Grubb, F. Joos, R. Kaufmann, R. Moss, W. Ogana, R. Richels, T. Wigley, R. Cannon, J. Edmonds, E. Haites, D. Harvey, A. Jain, R. Leemans, K. Miller, R. Parkin, E. Sulzman, R. Tol, J. de Wolde and M. Bruno, 1997: *Stabilization of atmospheric greenhouse gases: physical, biological and socio-economic implications*. Intergovernmental Panel on Climate Change, IPCC Technical Paper III,Geneva, 50 pp.

Schlesinger, M.E., S. Malyshev, E.V. Rozanov, F. Yang, N.G. Andronova, B. de Vries, A. Grübler, K. Jiang, T. Masui, T. Morita, J. Penner, W. Pepper, A. Sankovski and Y. Zhang, 2000: Geographical distributions of temperature change for scenarios of greenhouse gas and sulfur dioxide emissions. *Technological Forecasting and Social Change* (in press).

Tett, S.F.B., T.C. Johns, and J.F.B. Mitchell, 1997: Global and regional variability in a coupled AOGCM. *Climate Dynamics*, 13, 303-323.

Walsh, K., R. Allan, R. Jones, B. Pittock, R. Suppiah, and P. Whetton, 1999: *Climate Change in Queensland under Enhanced Greenhouse Conditions*. First Annual Report, 1997-1998. CSIRO Atmospheric Research, Aspendale, Australia, 84 pp.

Washington, W.M. and G.A. Meehl, 1996: High-latitude climate change in a global coupled ocean-atmosphere-sea ice model with increased atmospheric CO_2. *Journal of Geophysical Research*, 101, 12795-12801.

Wigley, T.M.L. and S.C.B. Raper, 1995: An heuristic model for sea-level rise due to the melting of small glaciers. *Geophys. Res. Letts.*, 22, 2749-2752.

Wigley, T.M.L., 1995: Global-mean temperature and sea level consequences of greenhouse gas concentration stabilization. *Geophys. Res. Letts.*, 22, 45-48.

Wigley,T.M.L., S.C.B. Raper, M. Salmon, and M. Hulme, 1997: *MAGICC: Model for the Assessment of Greenhouse-gas Induced Climate Change: Version 2.3*, Climatic Research Unit, Norwich, UK

Zhang, X-H., J.M. Oberhuber, A. Bacher, and E. Roeckner, 1998: Interpretation of interbasin exchange in an isopycnal ocean. *Climate Dynamics*, 14, 725-740.

Appendix A: Global Maps Of Annual And Seasonal Temperature And Precipitation Change Under The Four SRES-Based Scenarios

Figures A1-A10. The B1-low characterization of temperature and precipitation change relative to 1961-1990. Each figure shows maps for the 2020s (top), 2050s (middle) and 2080s (bottom). The left hand panel shows median changes from 10 GCM simulations. The right hand panel shows the range of GCM results. Temperature changes (°C) are shown in Figures A1-A5; precipitation changes (percent) in Figures A6-A10. Consecutive figures show annual and seasonal (December-February, March-May, June-August and September-November) mean changes.

B1-low, Annual Temperature
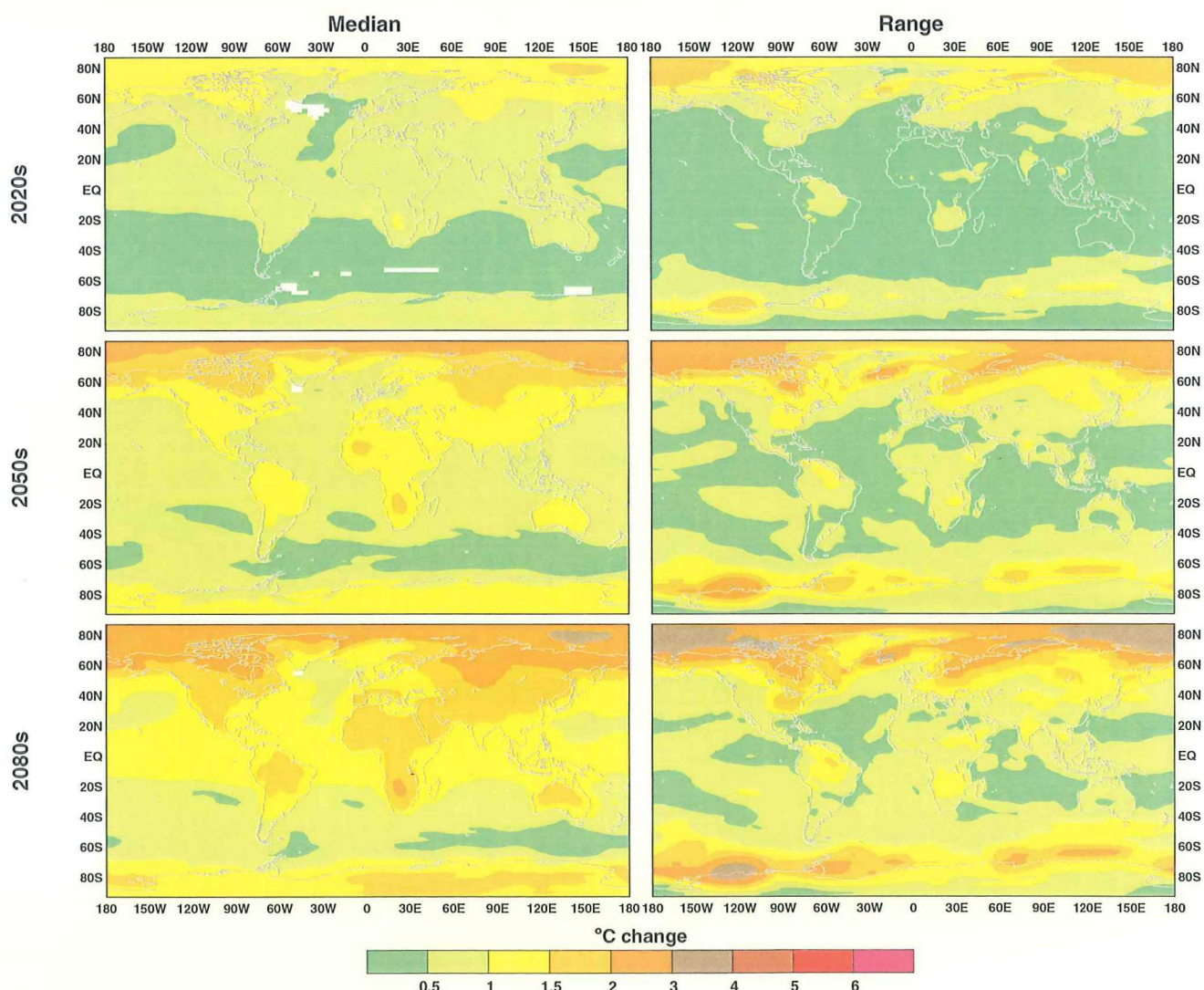
B1-low, DJF Temperature
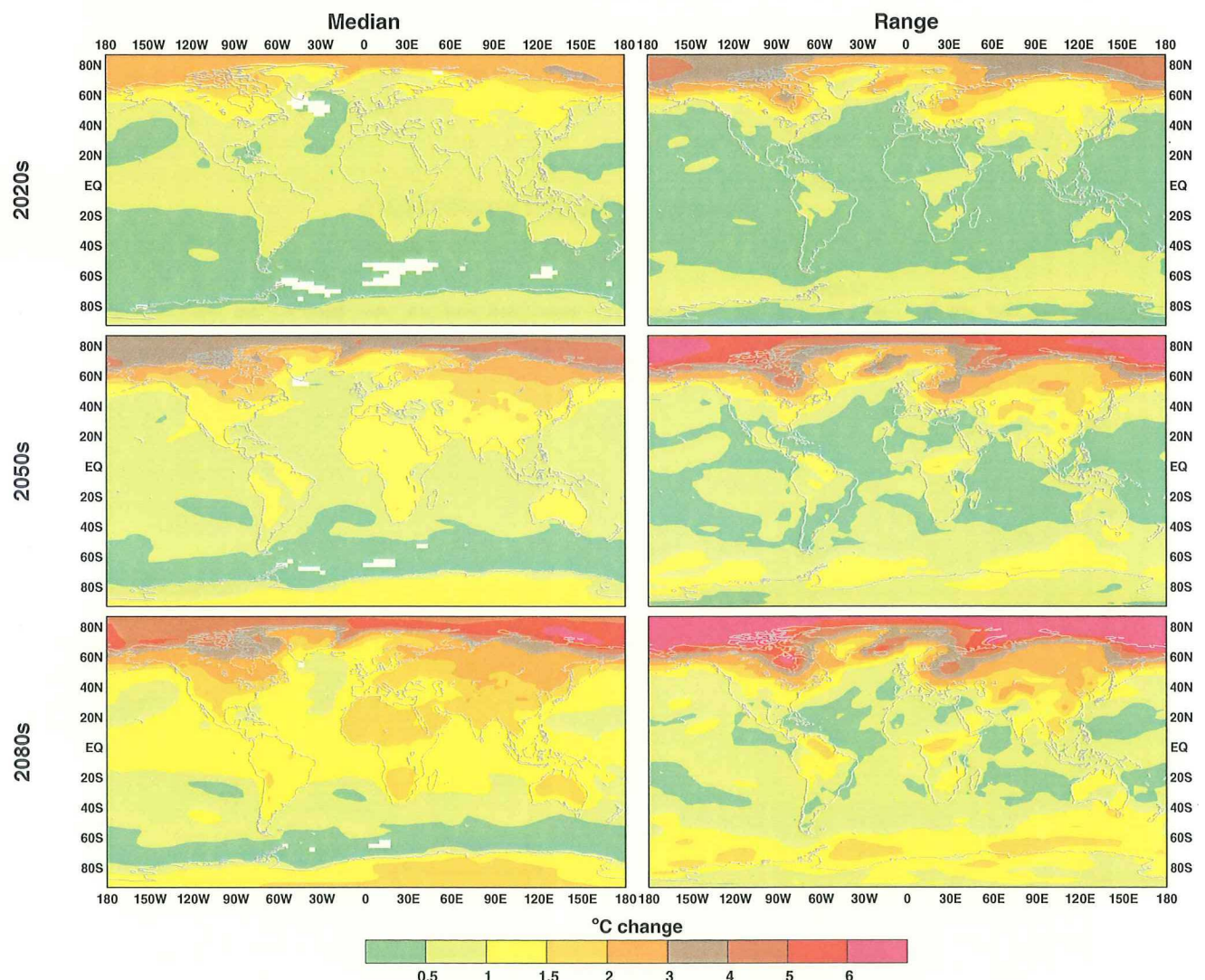
B1-low, MAM Temperature

Median · Range · °C change
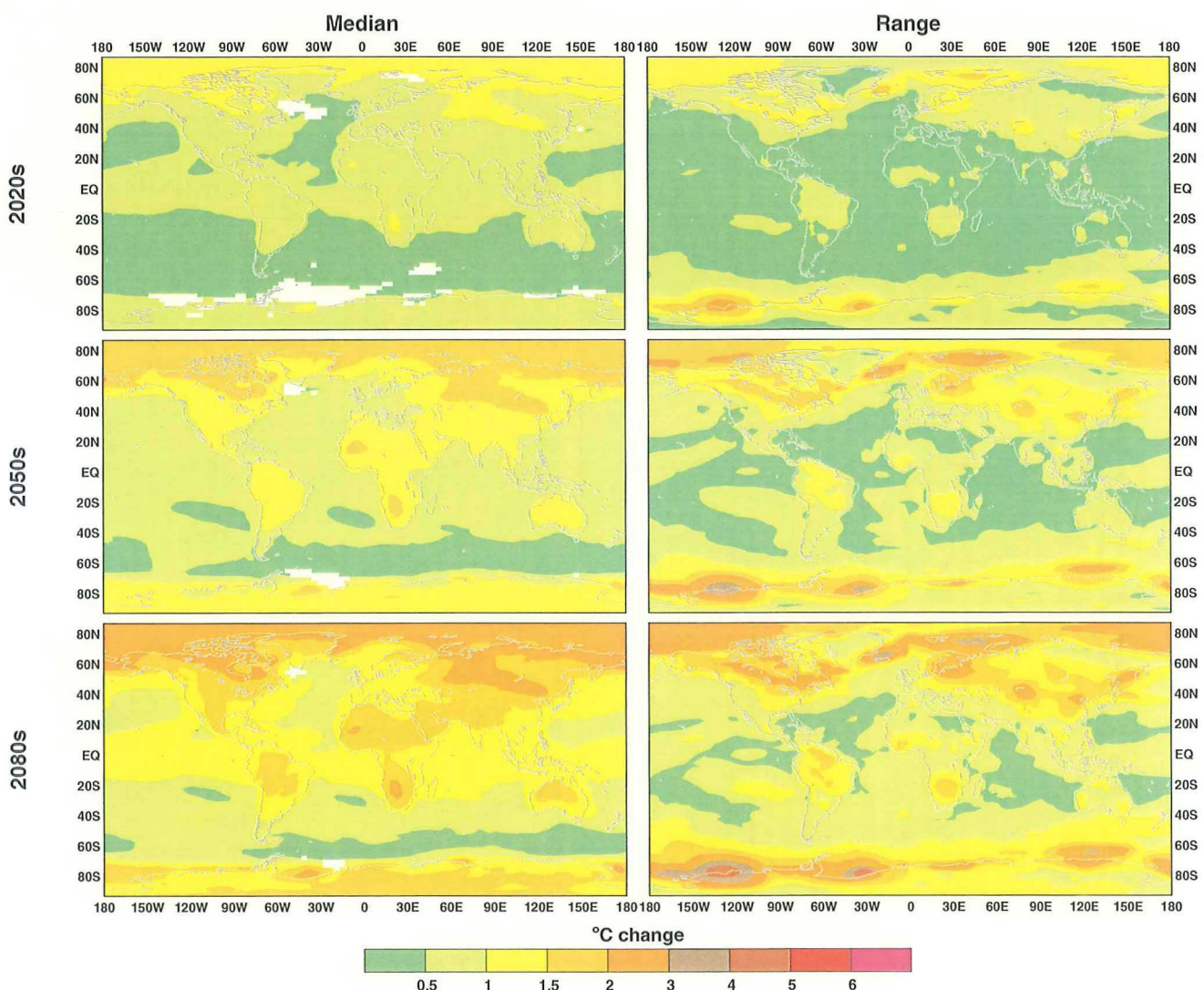
B1-low, JJA Temperature
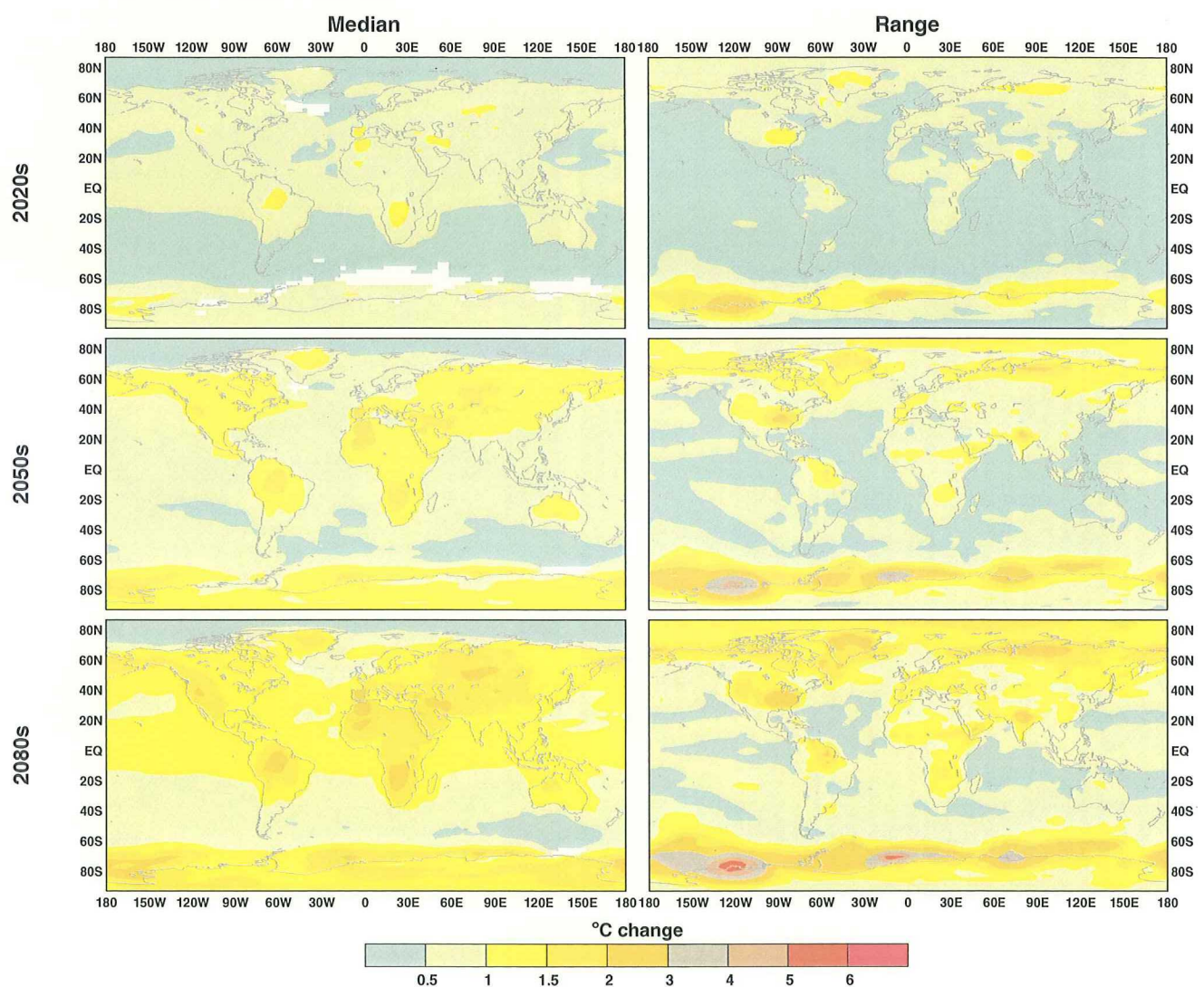
°C change

B1-low, SON Temperature
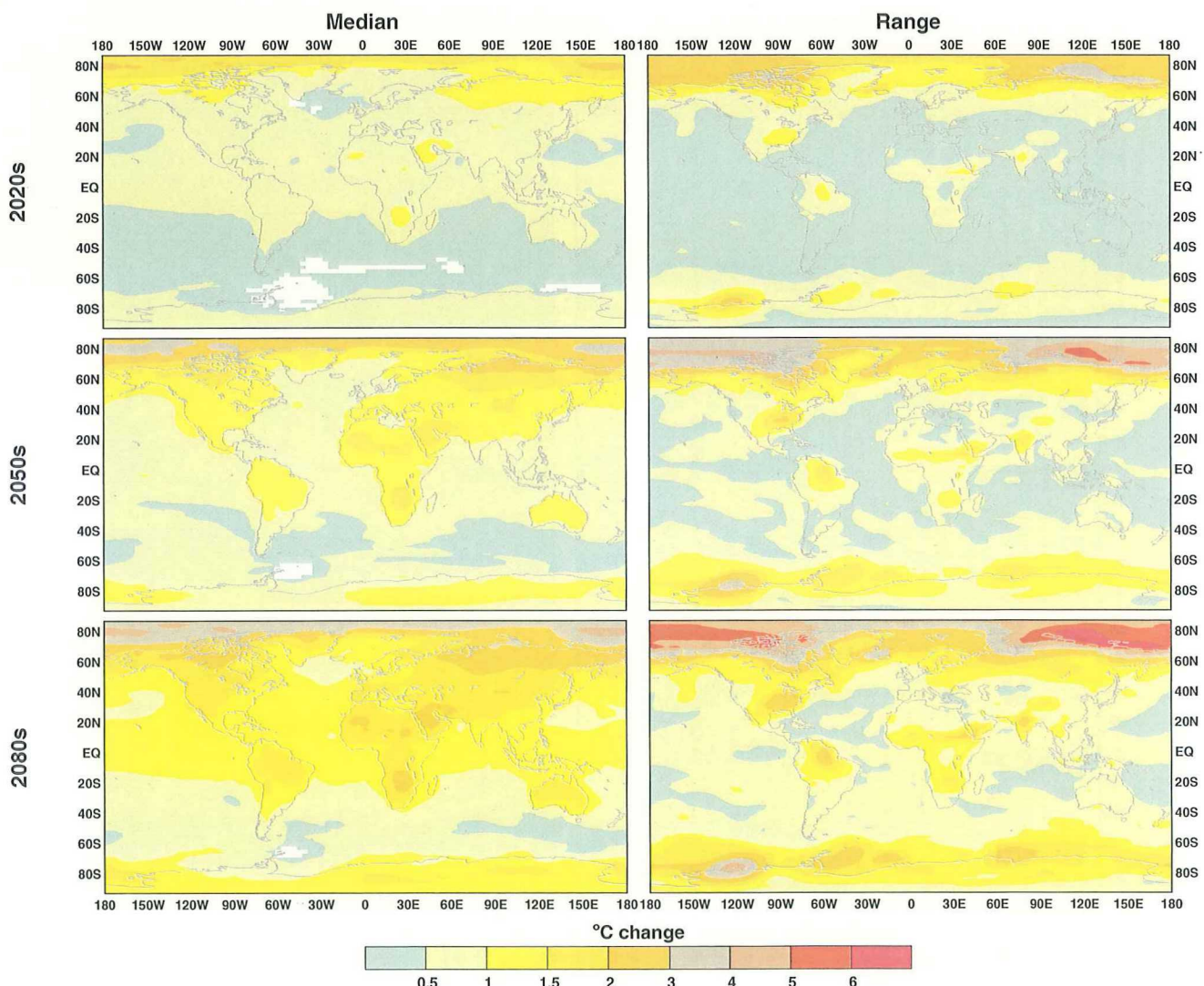
B1-low, Annual Precipitation

B1-low, DJF Precipitation

Median **Range**

2020s 2050s 2080s

Median of % changes

-50 -30 -20 -10 0 10 20 30 50

Range of % changes

10 20 30 40 50 75 100

B1-low, MAM Precipitation

Median

Range

2020s

2050s

2080s

Median of % changes

-50 -30 -20 -10 0 10 20 30 50

Range of % changes

10 20 30 40 50 75 100

B1-low, JJA Precipitation

Median

Range

2020s

2050s

2080s

Median of % changes

-50 -30 -20 -10 0 10 20 30 50

Range of % changes

10 20 30 40 50 75 100

B1-low, SON Precipitation

Median   **Range**

2020s   2050s   2080s

Median of % changes

-50 -30 -20 -10 0 10 20 30 50

Range of % changes

10 20 30 40 50 75 100

Figures A11-A20. The B2-mid characterization of temperature and precipitation change relative to 1961-1990. Each figure shows maps for the 2020s (top), 2050s (middle) and 2080s (bottom). The left hand panel shows median changes from 10 GCM simulations. The right hand panel shows the range of GCM results. Temperature changes (°C) are shown in Figures A11-A15; precipitation changes (percent) in Figures A16-A20. Consecutive figures show annual and seasonal (December-February, March-May, June-August and September- November) mean changes.

B2-mid, Annual Temperature

B2-mid, DJF Temperature

Median   **Range**

°C change

0.5   1   1.5   2   3   4   5   6

B2-mid, MAM Temperature

°C change

| 0.5 | 1 | 1.5 | 2 | 3 | 4 | 5 | 6 |
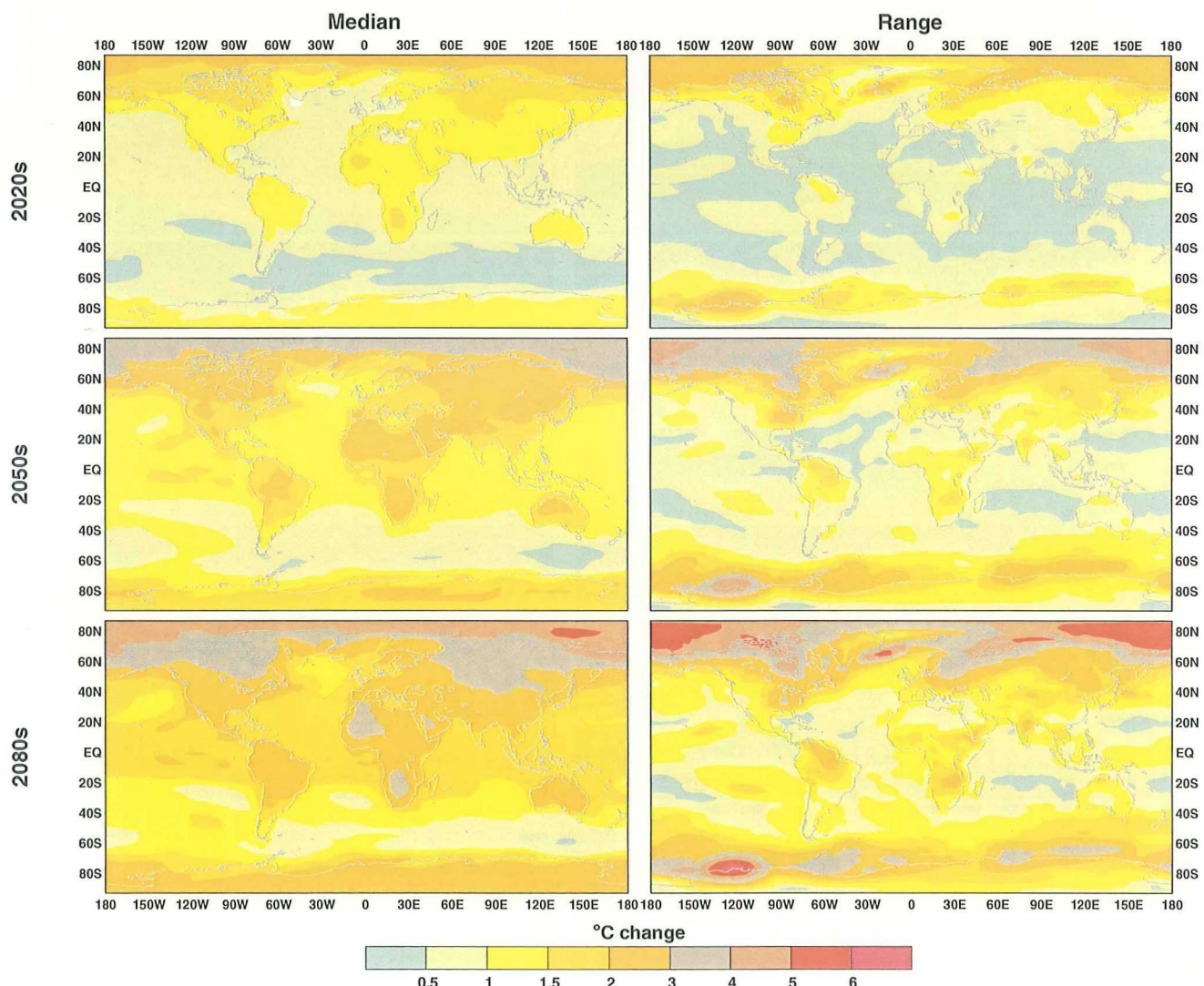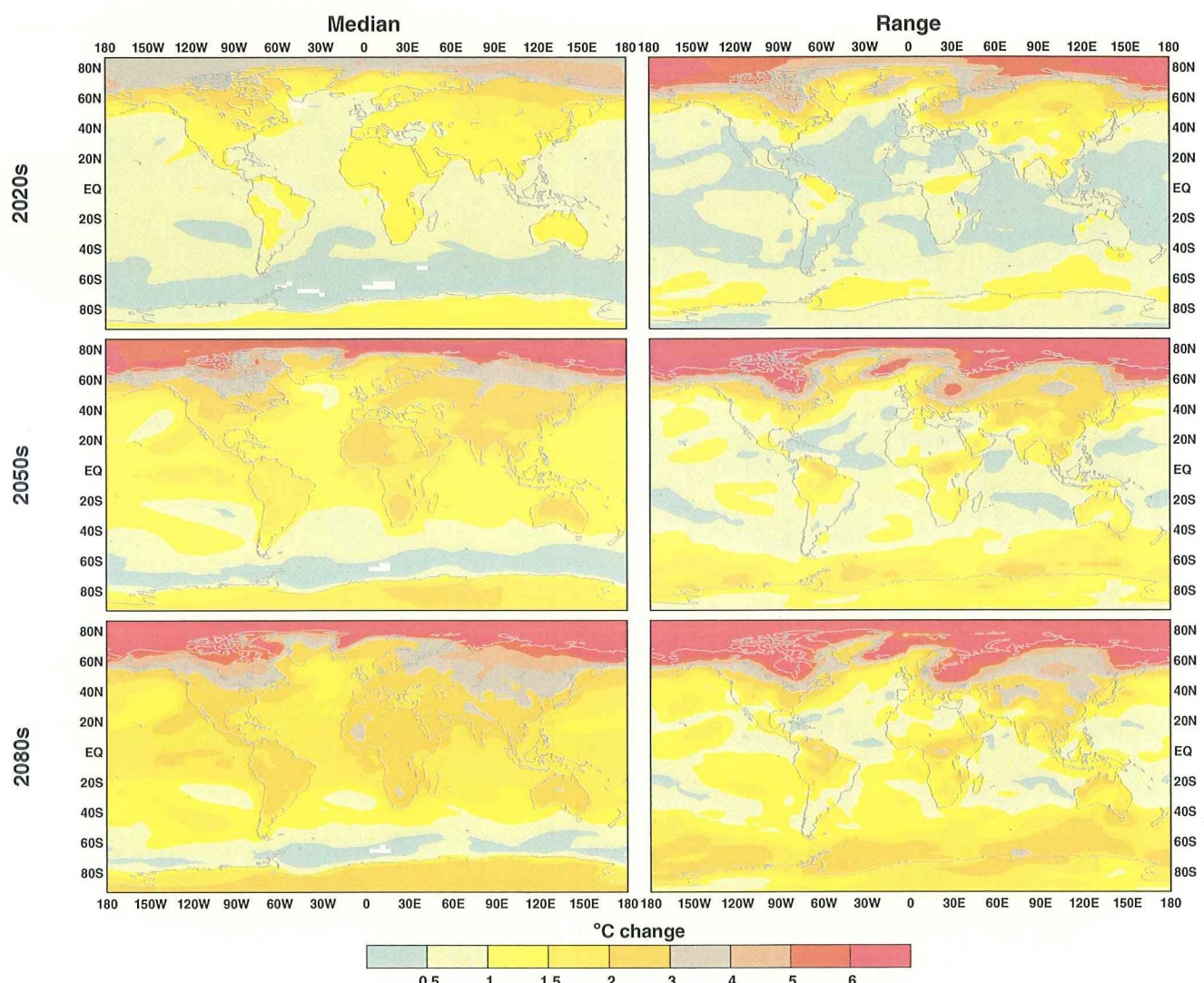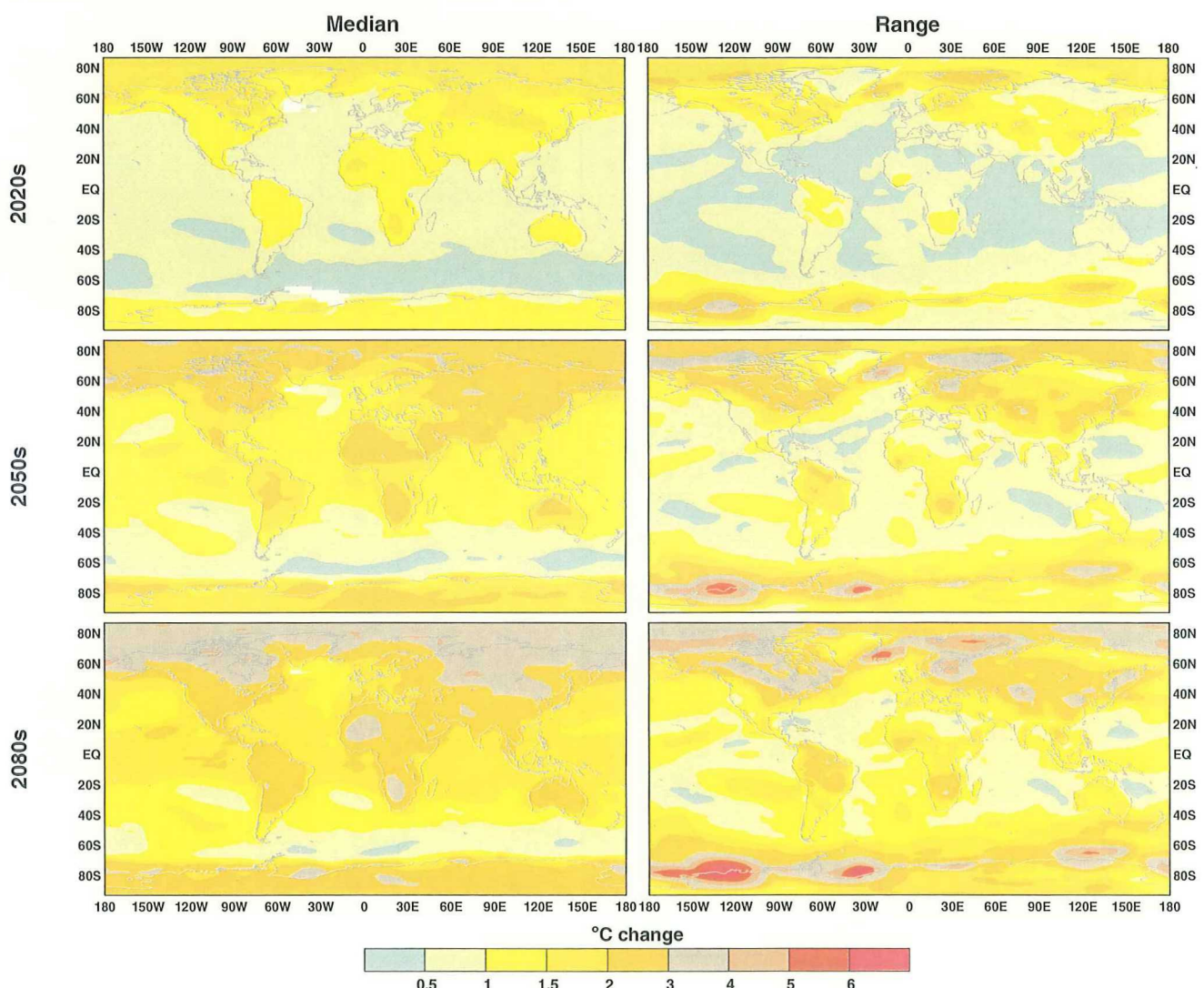
B2-mid, JJA Temperature
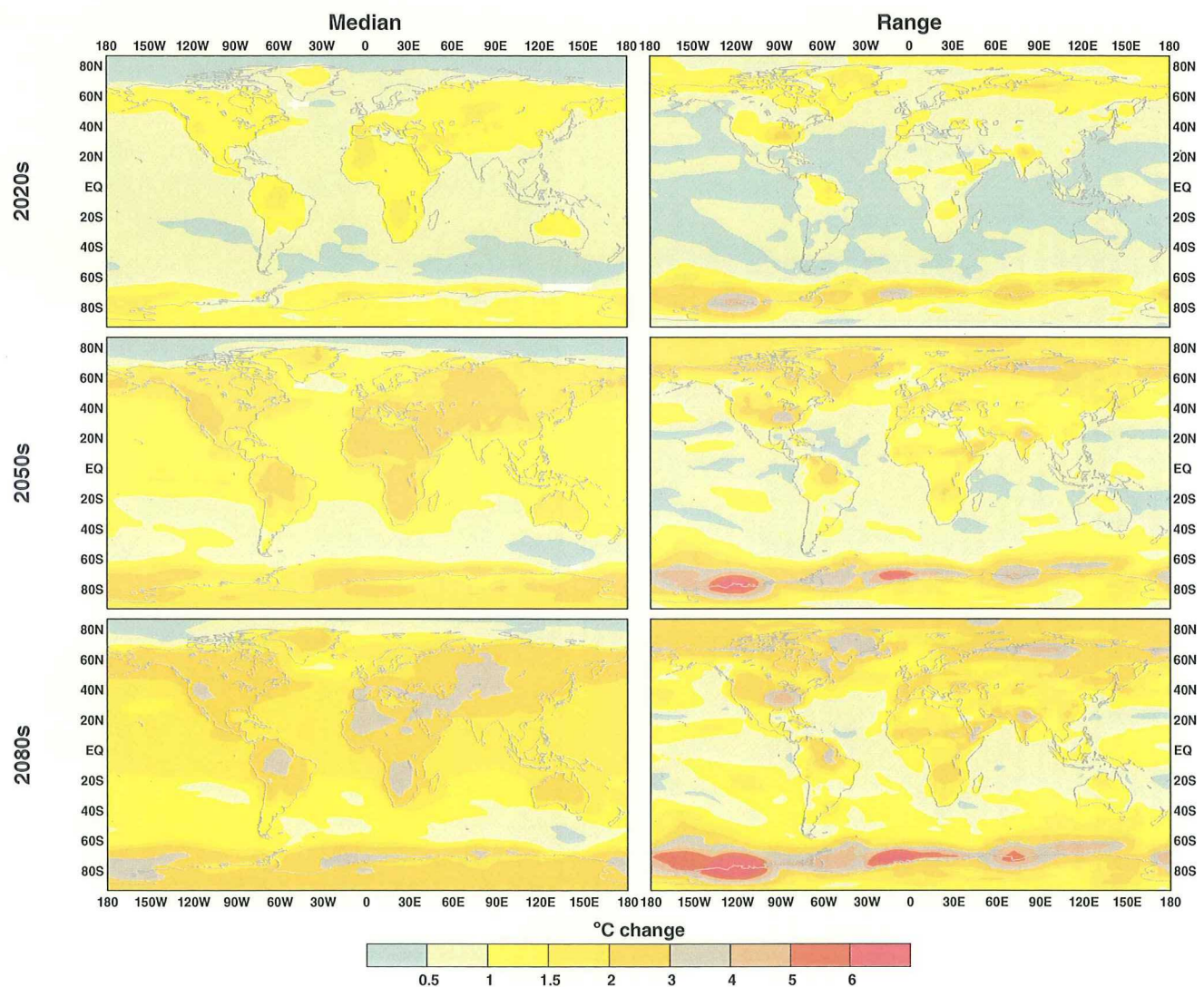
°C change

B2-mid, SON Temperature
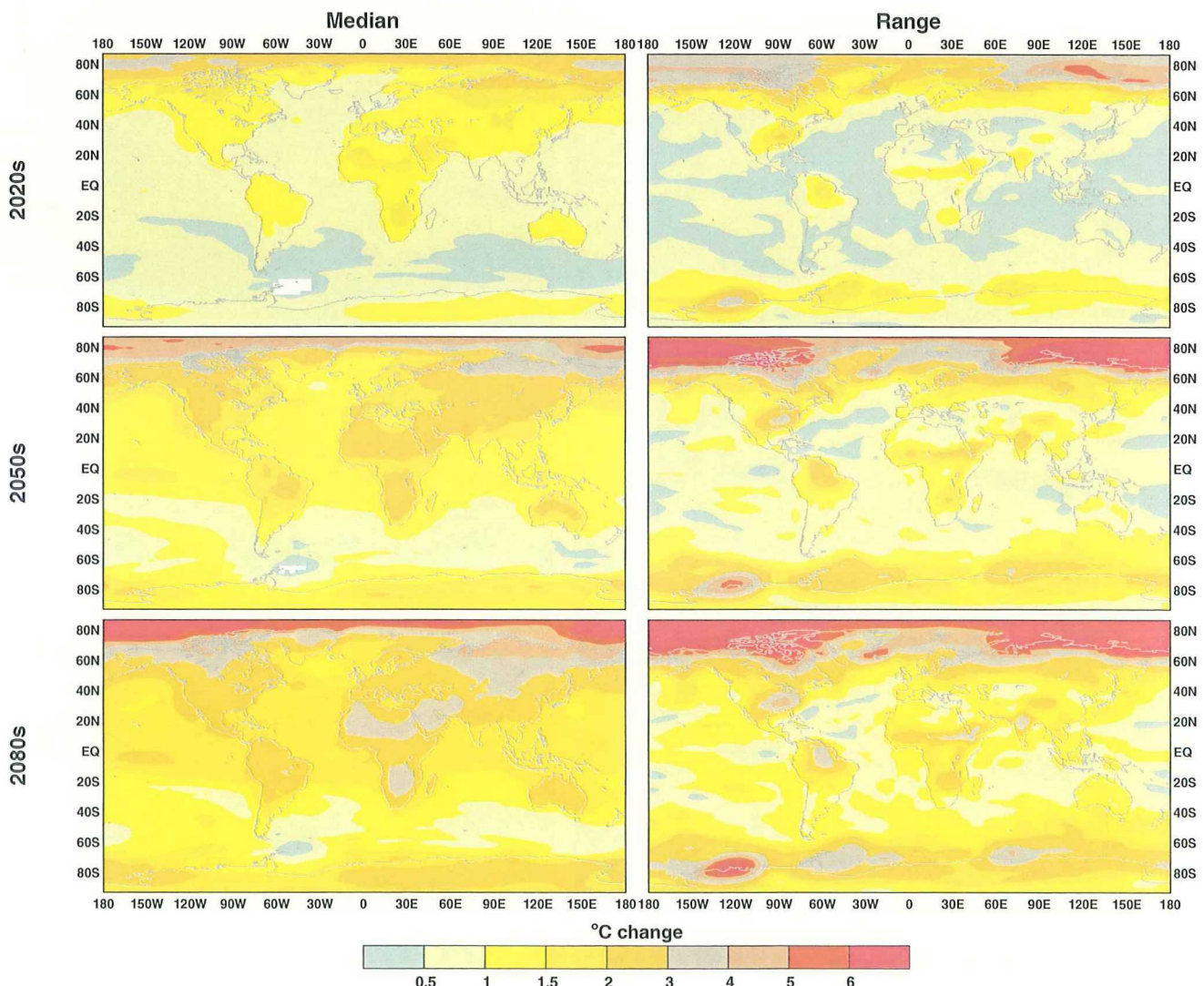
B2-mid, Annual Precipitation
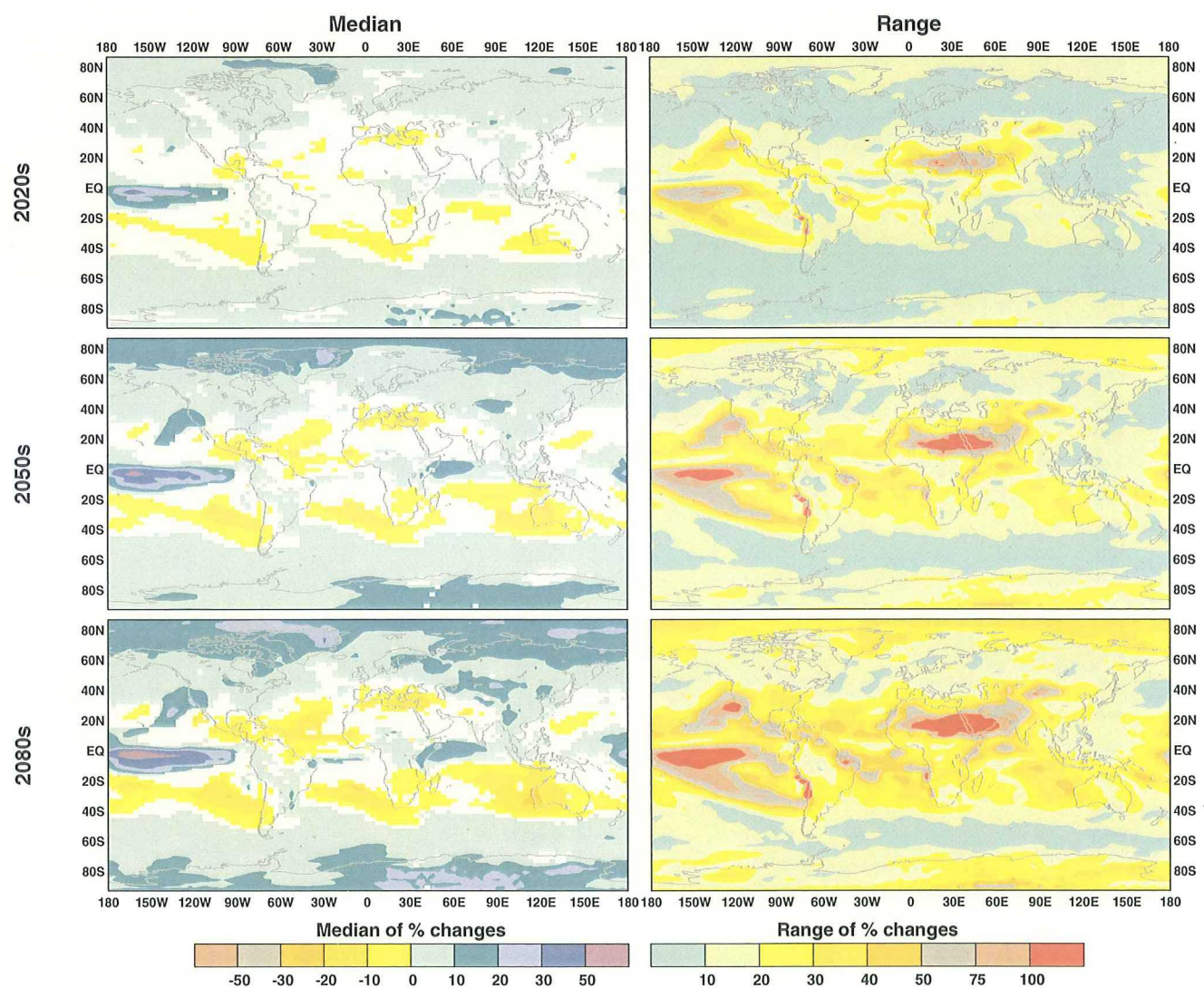
B2-mid, DJF Precipitation
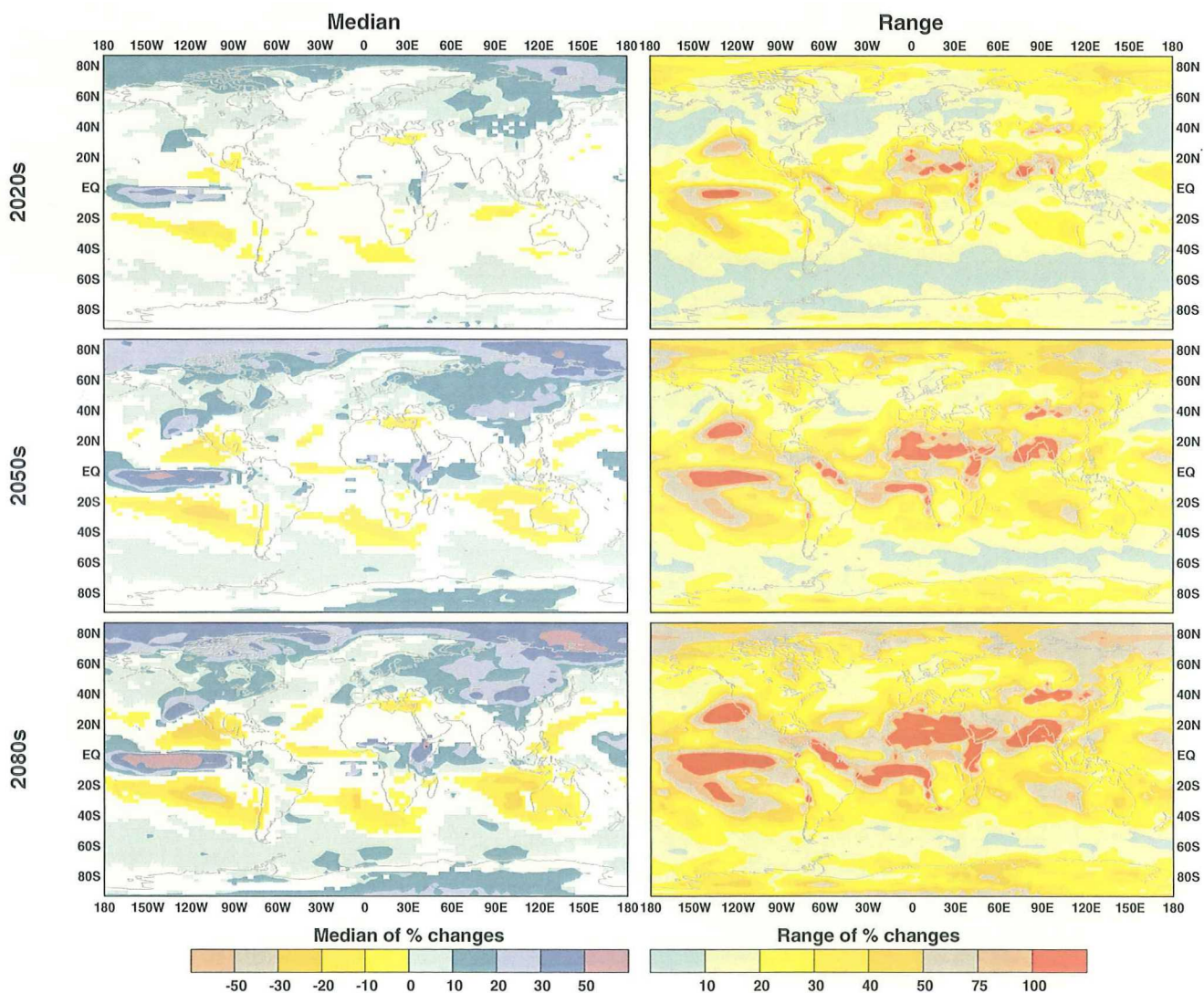
B2-mid, MAM Precipitation
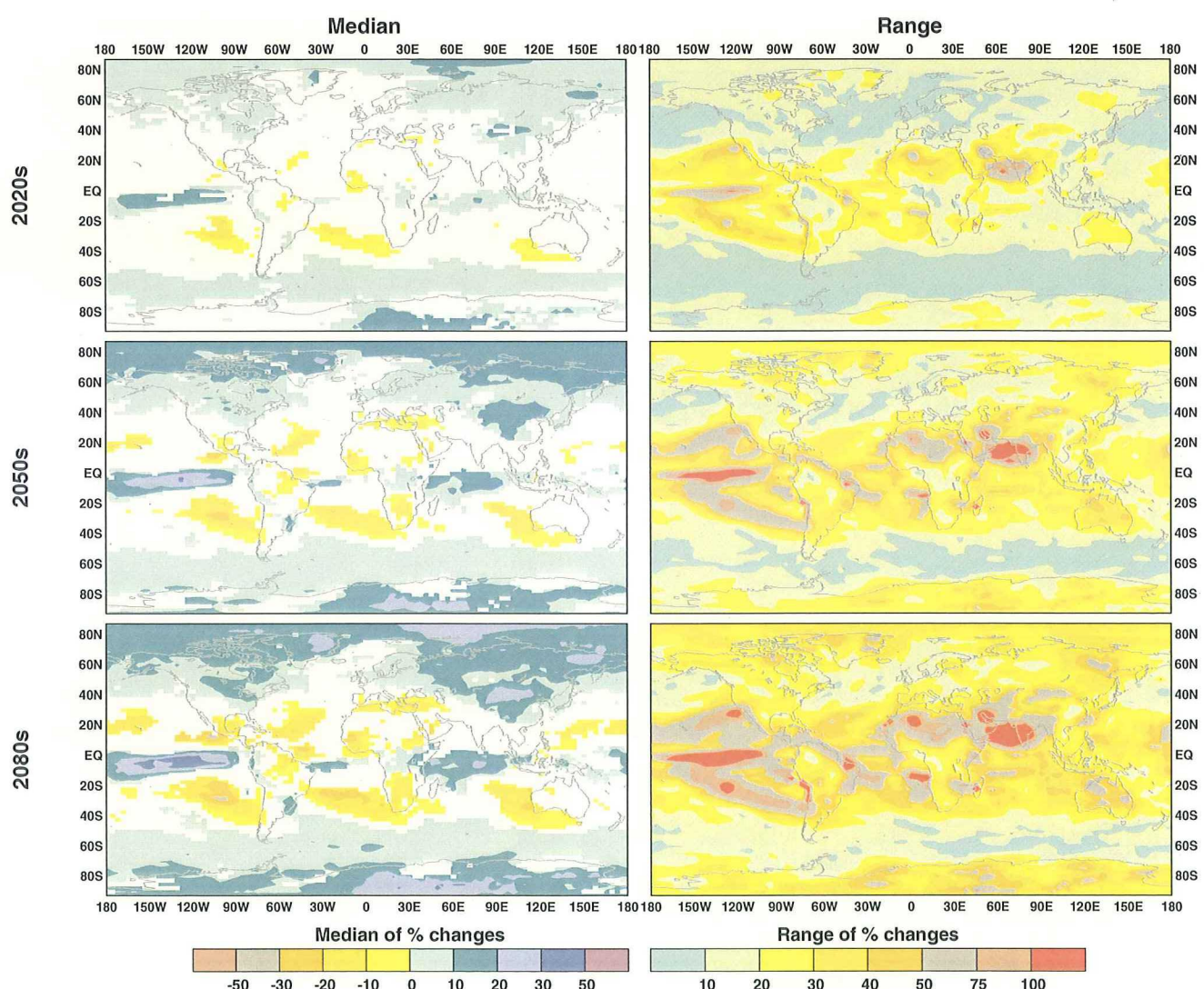
B2-mid, JJA Precipitation

B2-mid, SON Precipitation

Median of % changes

Range of % changes
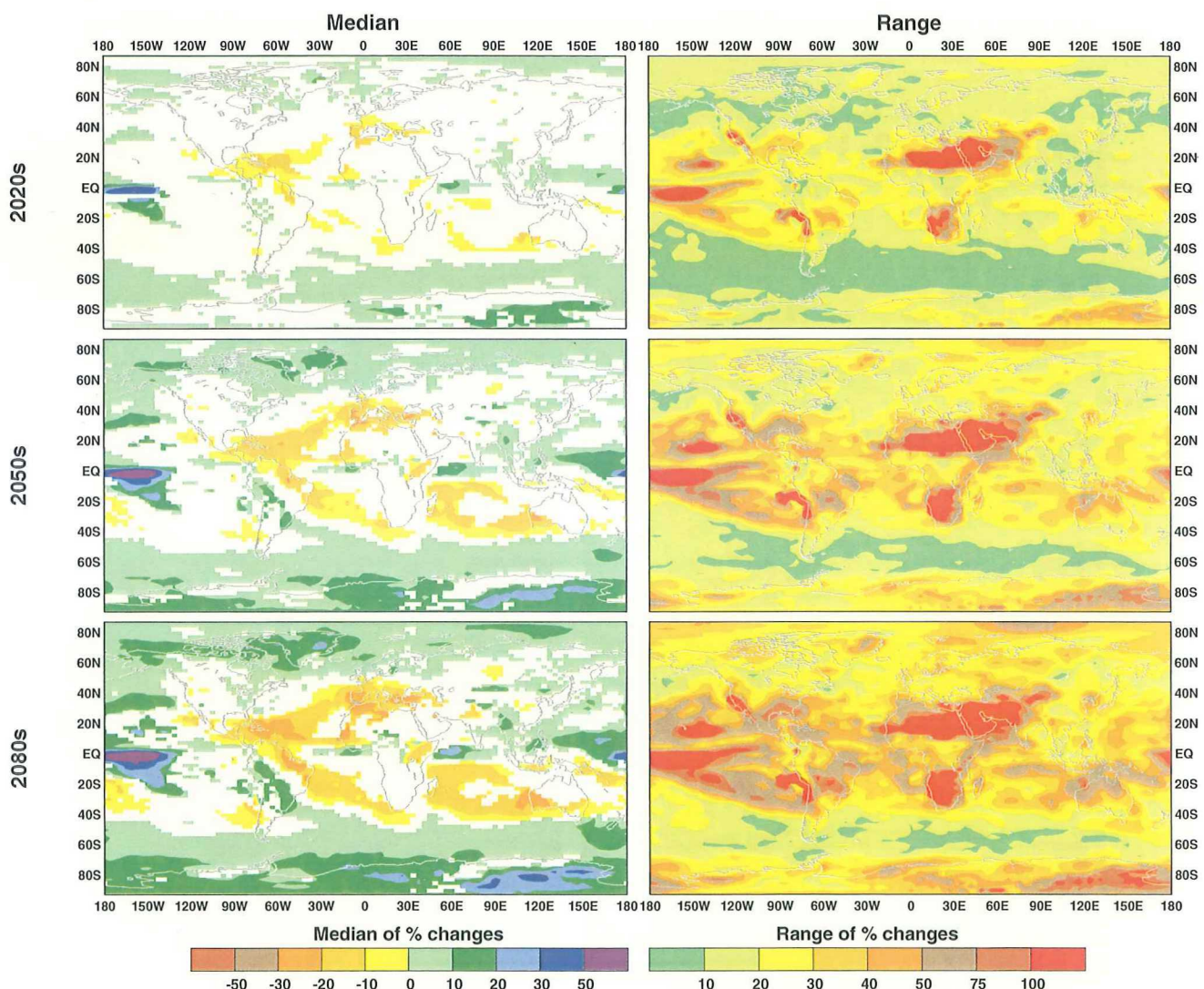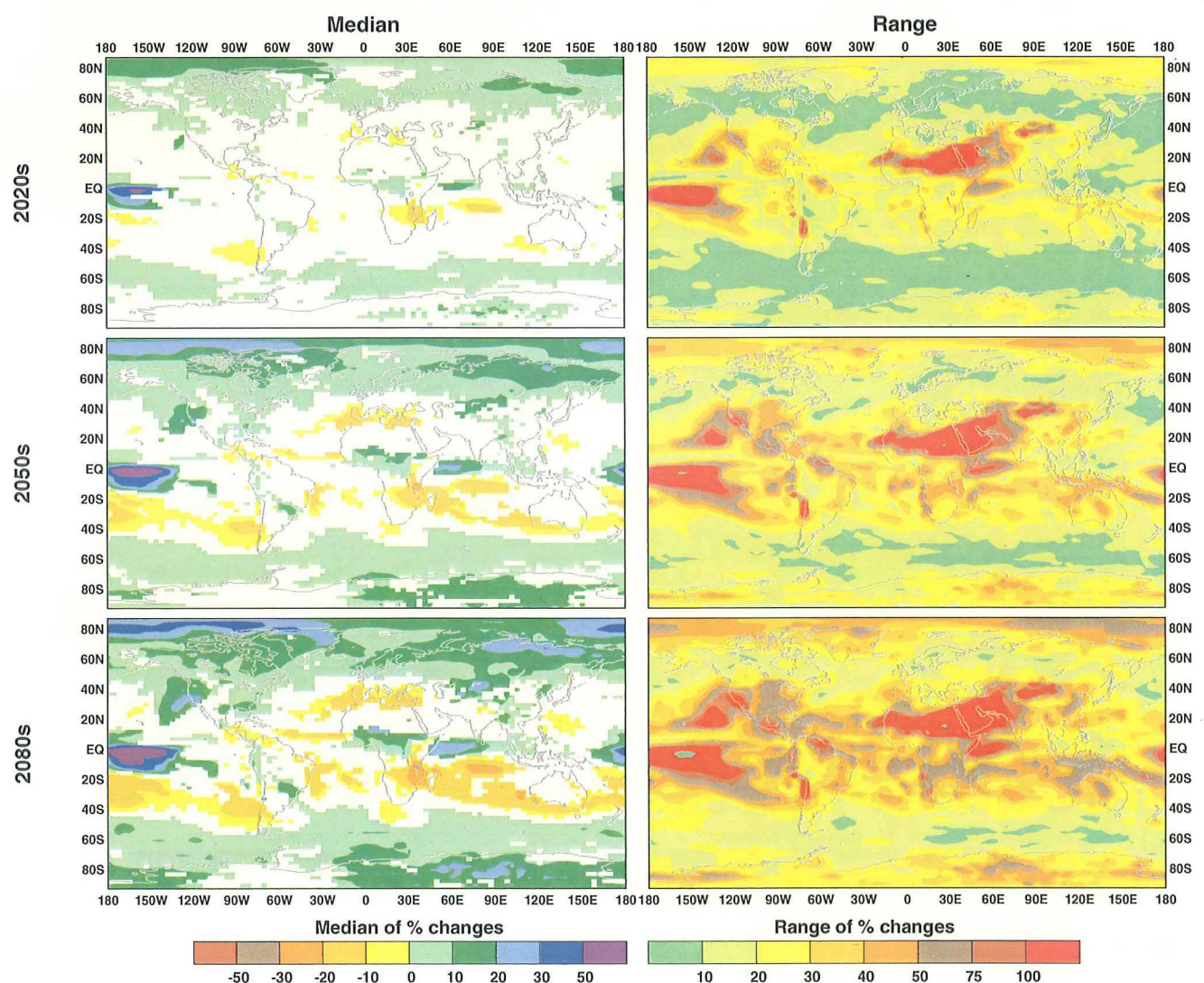
Figures A21-A30. The A1-mid characterization of temperature and precipitation change relative to 1961-1990. Each figure shows maps for the 2020s (top), 2050s (middle) and 2080s (bottom). The left hand panel shows median changes from 10 GCM simulations. The right hand panel shows the range of GCM results. Temperature changes (°C) are shown in Figures A21-A25; precipitation changes (percent) in Figures A26-A30. Consecutive figures show annual and seasonal (December-February, March-May, June-August and September-November) mean changes.

A1-mid, Annual Temperature

A1-mid, DJF Temperature

Median — **Range**

2020s — 2050s — 2080s

°C change

0.5 1 1.5 2 3 4 5 6
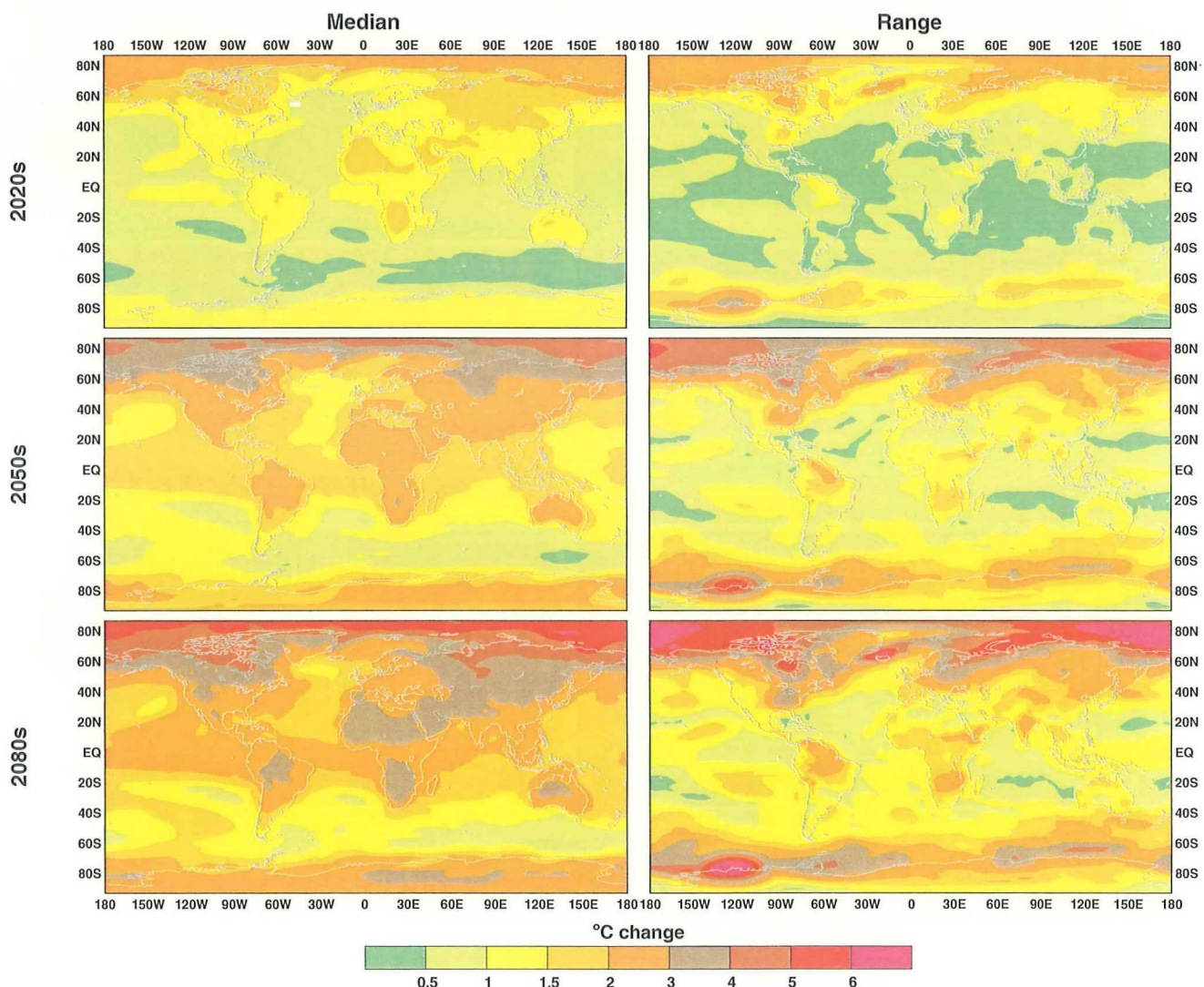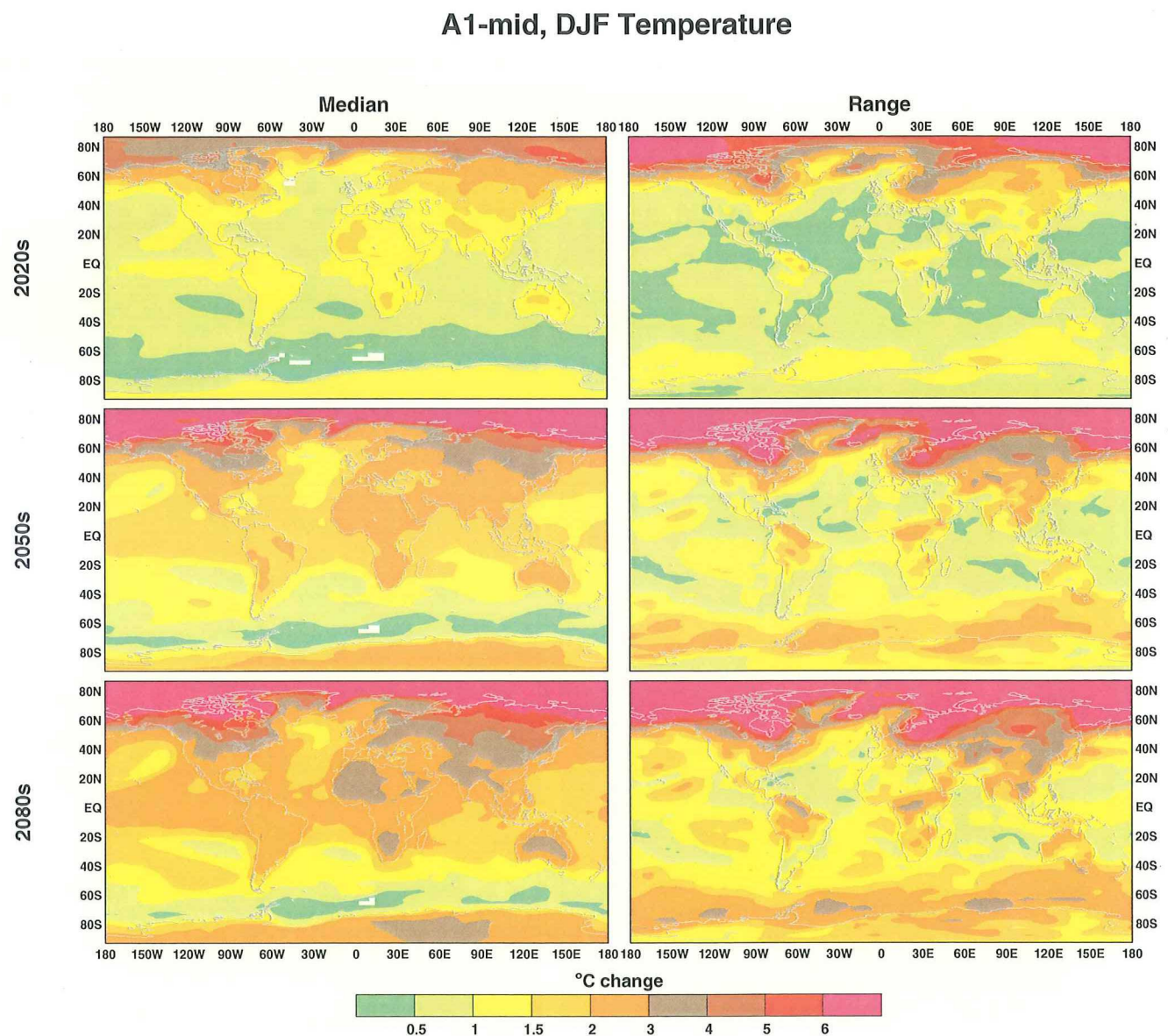
A1-mid, MAM Temperature

A1-mid, JJA Temperature

Median   **Range**

°C change

0.5   1   1.5   2   3   4   5   6

A1-mid, SON Temperature

Median   **Range**

°C change

| | 0.5 | 1 | 1.5 | 2 | 3 | 4 | 5 | 6 | |

A1-mid, Annual Precipitation

Median

Range

2020s

2050s

2080s

Median of % changes

-50 -30 -20 -10 0 10 20 30 50

Range of % changes

10 20 30 40 50 75 100
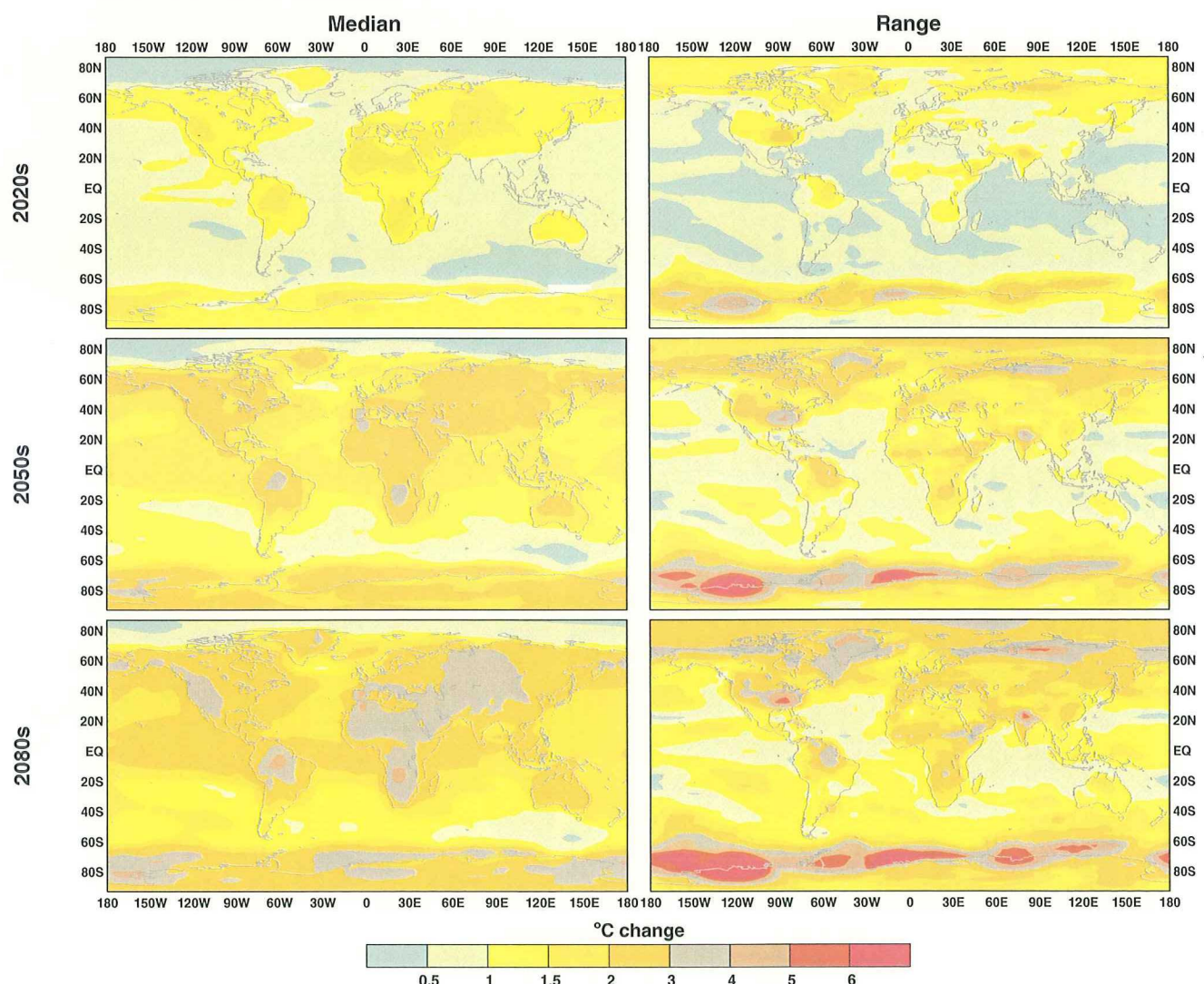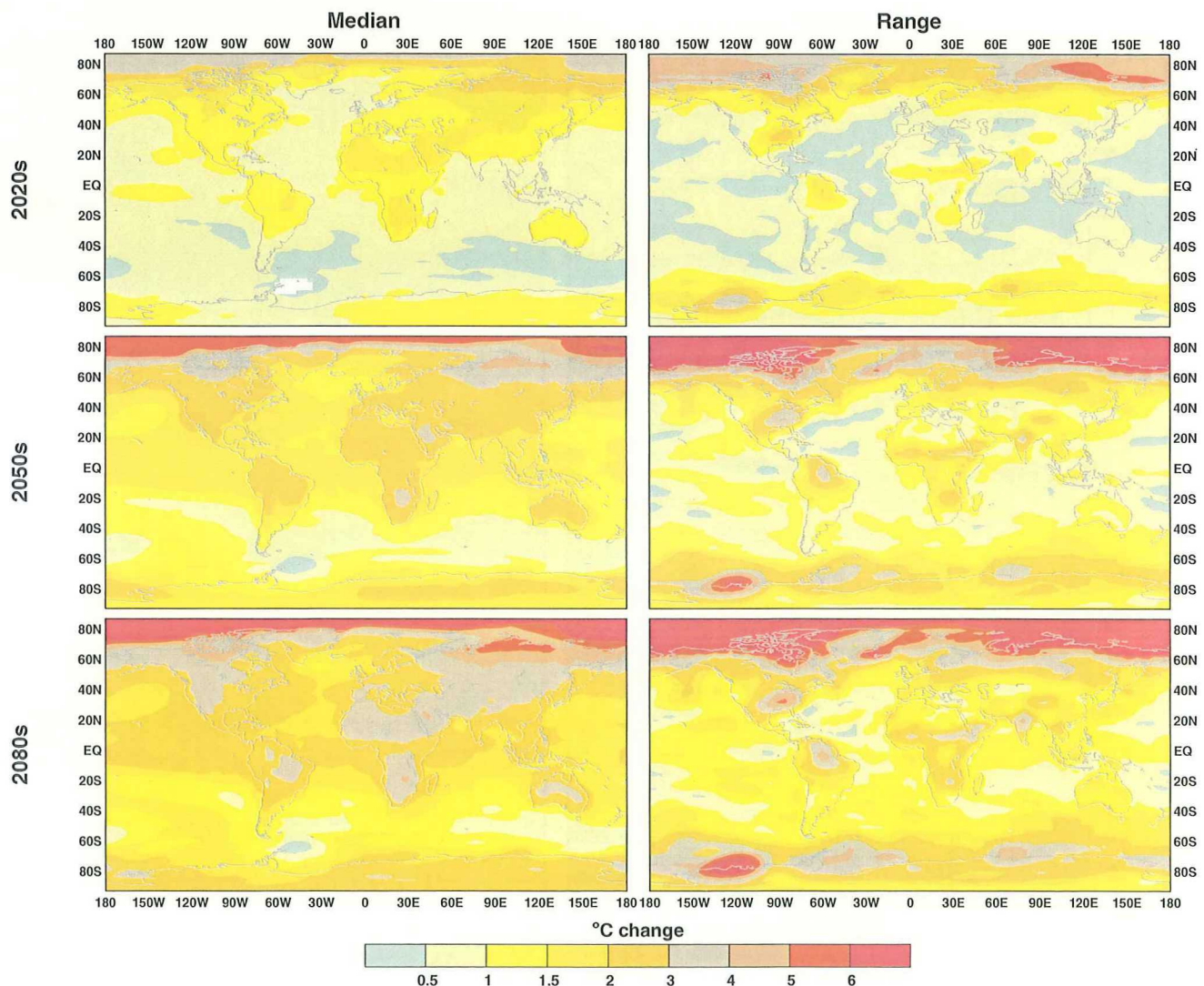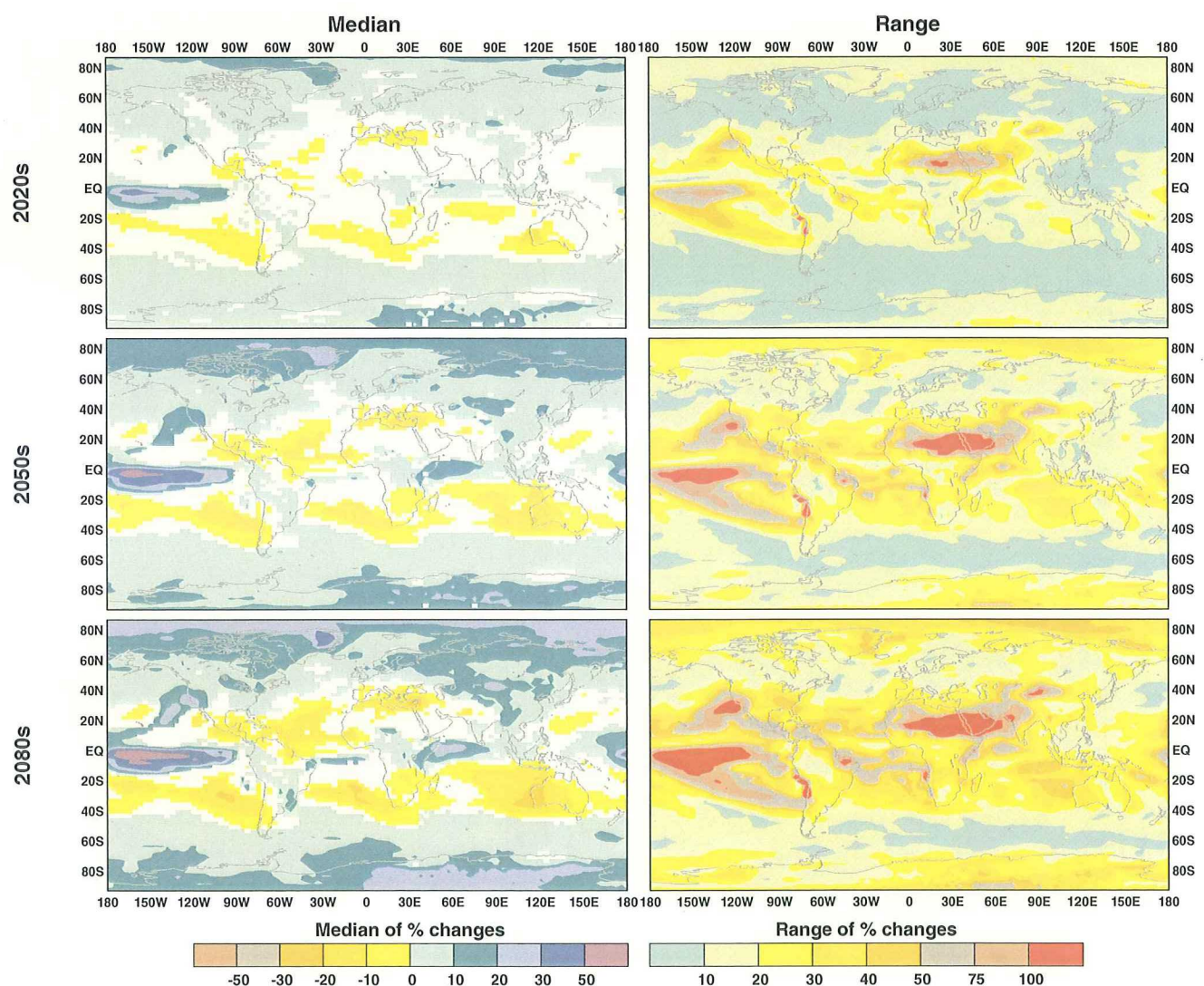
A1-mid, DJF Precipitation

A1-mid, MAM Precipitation

Median   **Range**

2020s

2050s

2080s

Median of % changes

-50   -30   -20   -10   0   10   20   30   50

Range of % changes

10   20   30   40   50   75   100

A1-mid, JJA Precipitation

Median

Range

2020s

2050s

2080s

Median of % changes

-50 -30 -20 -10 0 10 20 30 50

Range of % changes

10 20 30 40 50 75 100
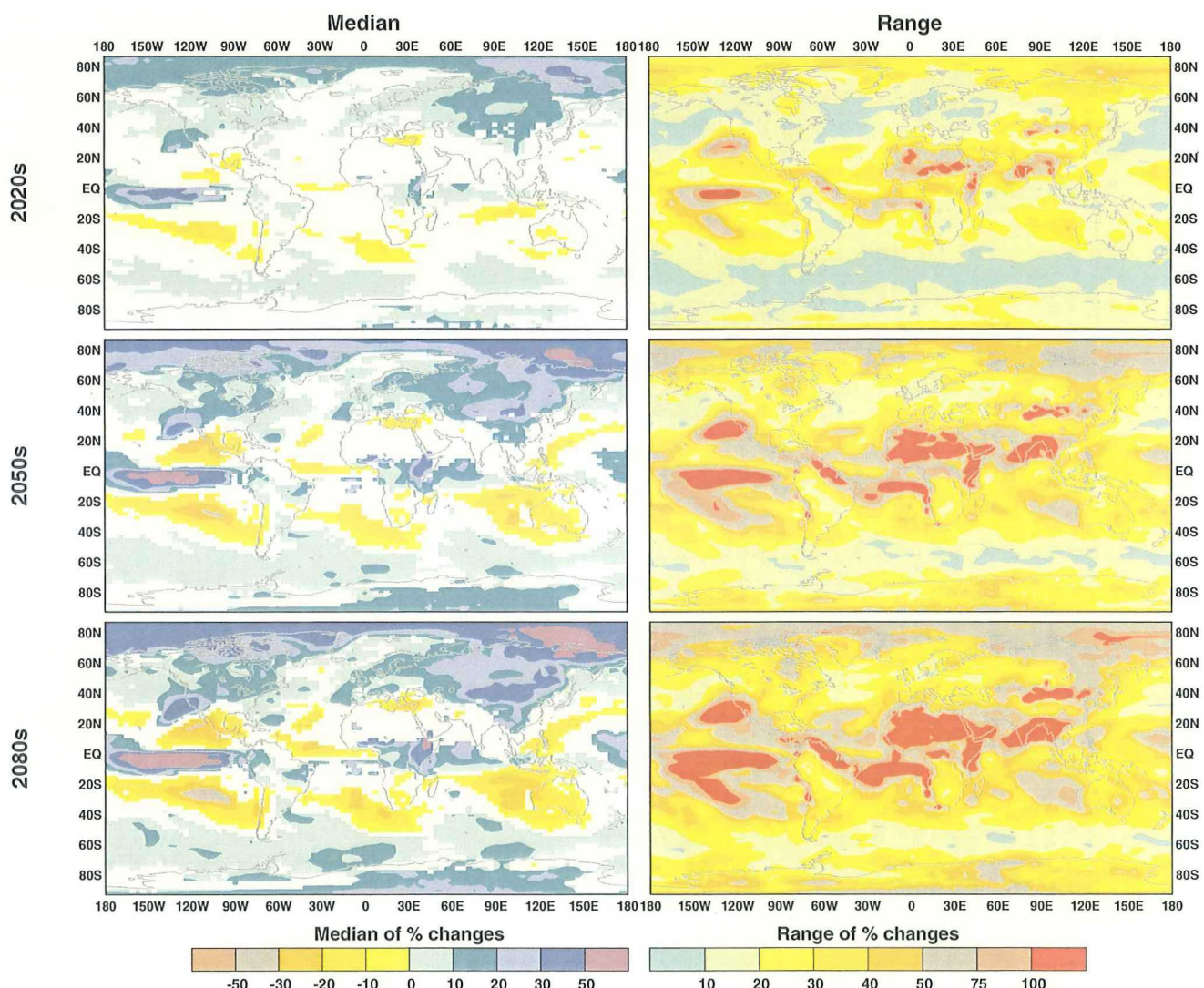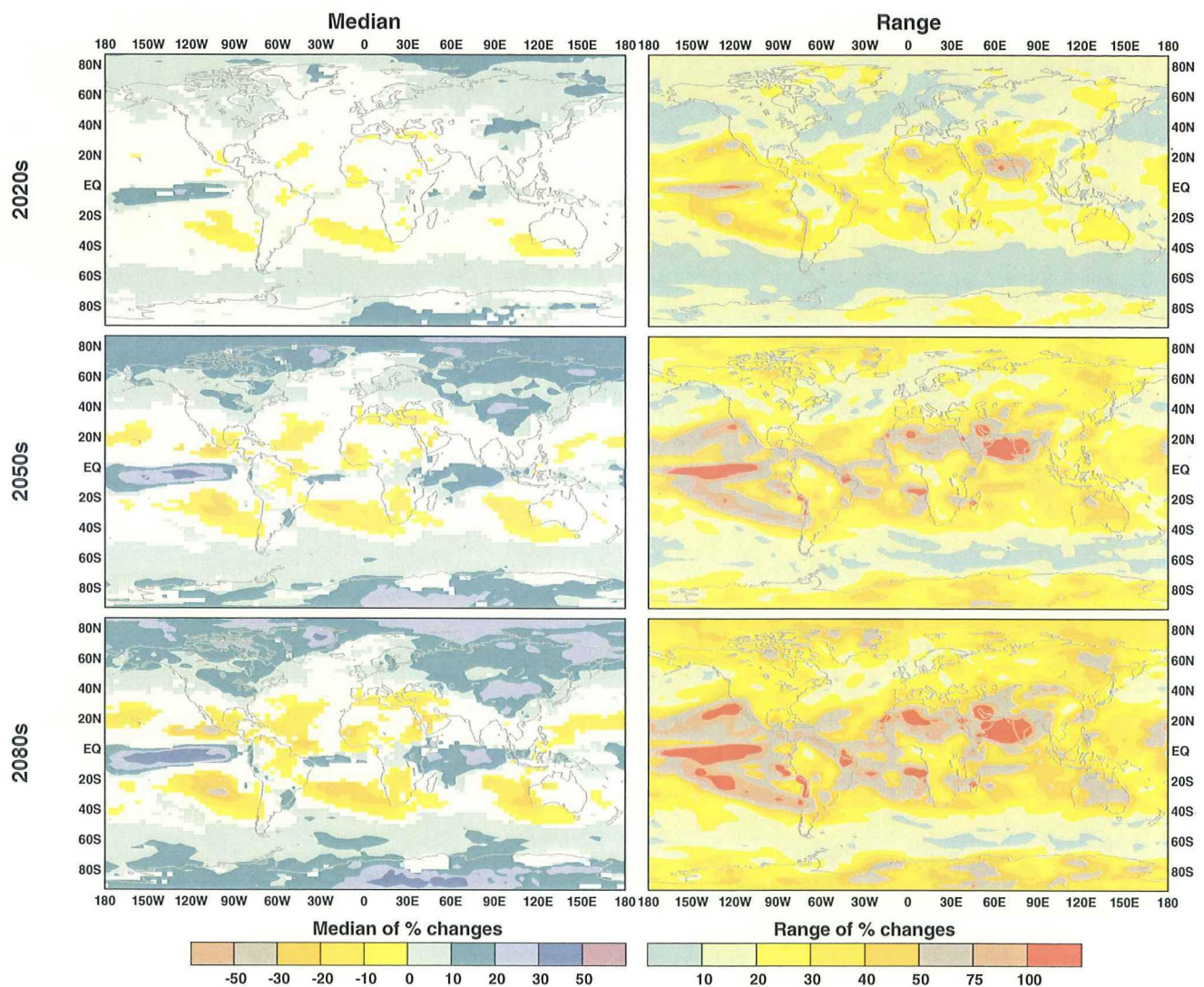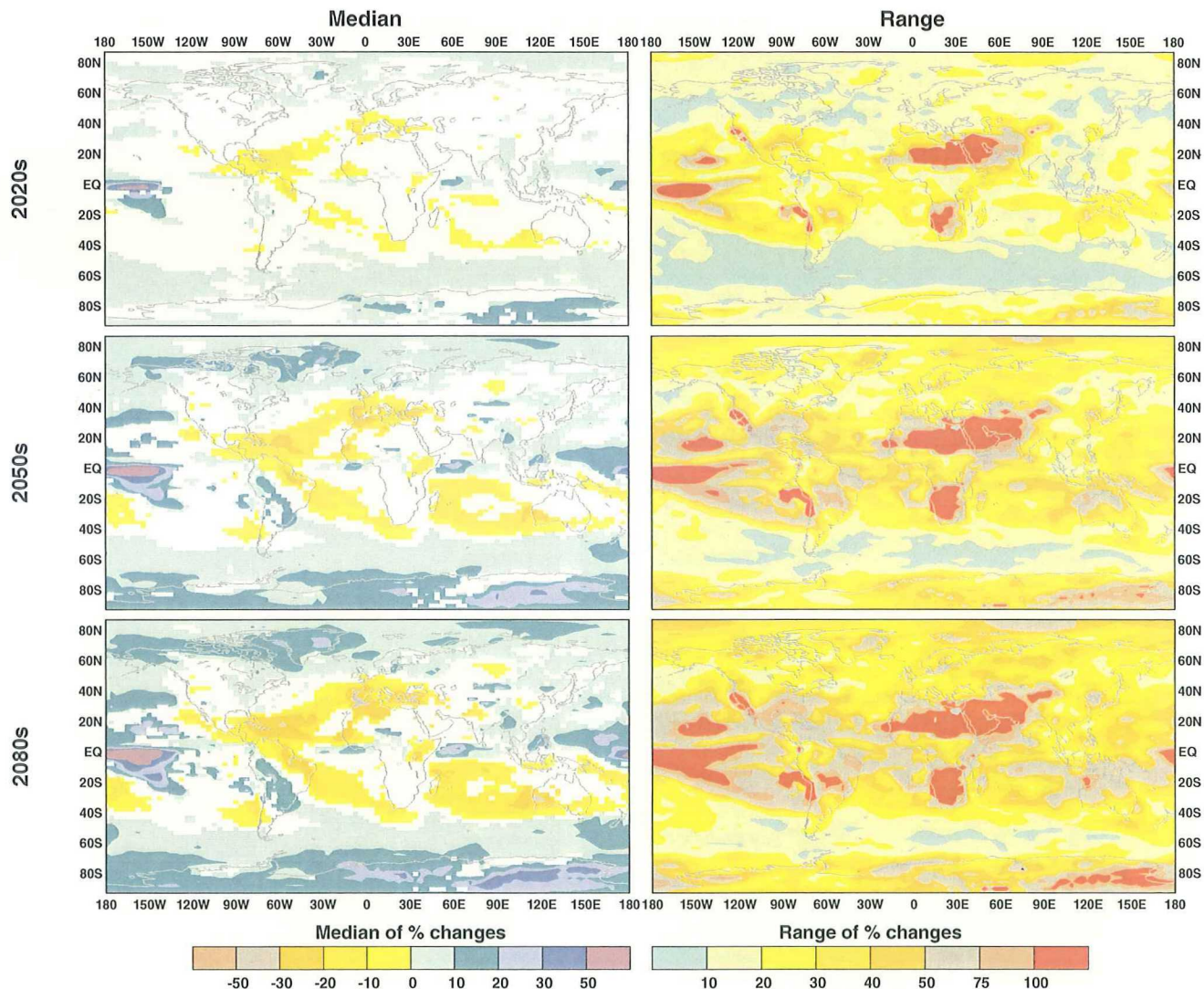
A1-mid, SON Precipitation
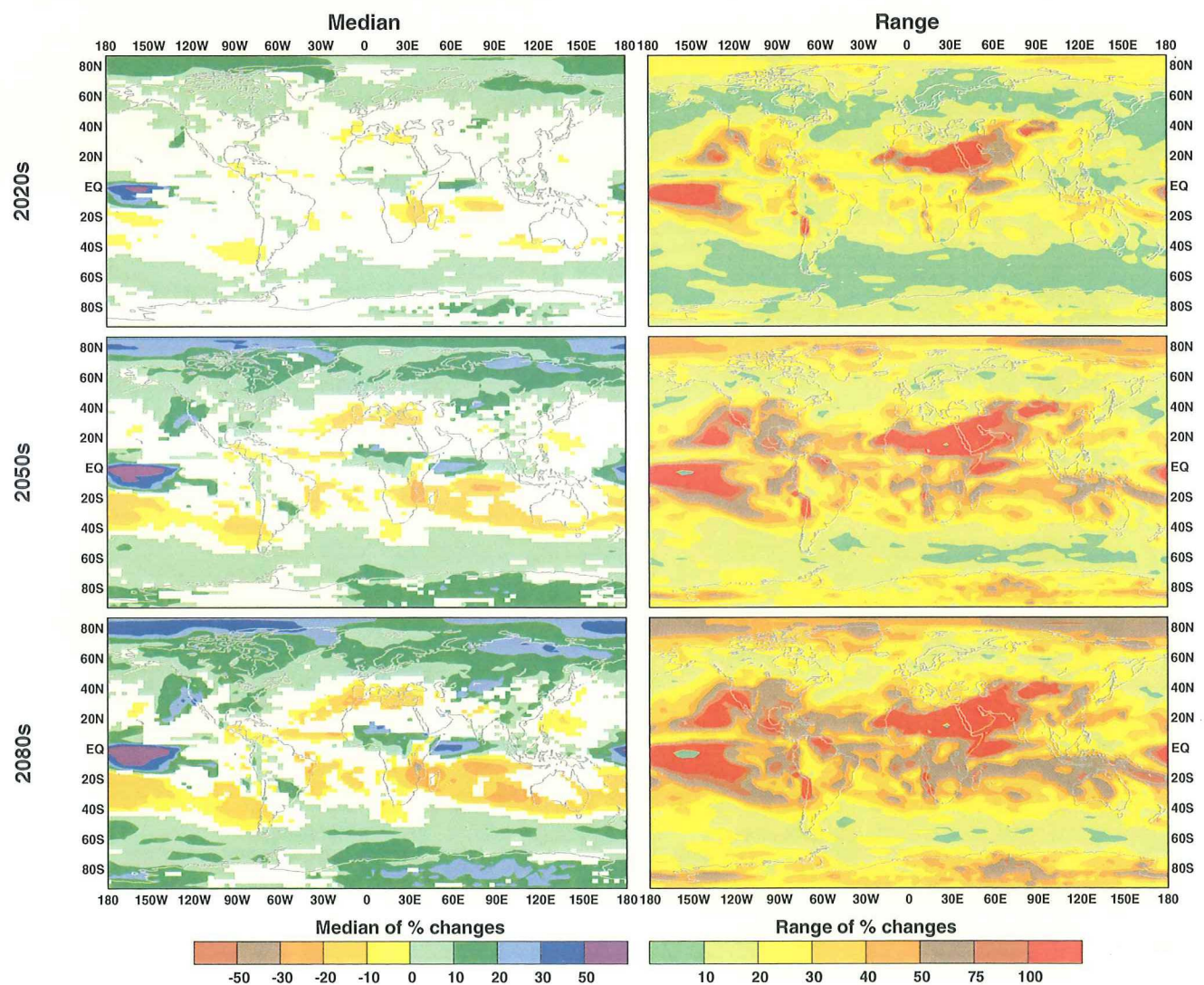
Figures A31-A40. The A2-high characterization of temperature and precipitation change relative to 1961-1990. Each figure shows maps for the 2020s (top), 2050s (middle) and 2080s (bottom). The left hand panel shows median changes from 10 GCM simulations. The right hand panel shows the range of GCM results. Temperature changes (°C) are shown in Figures A31-A35; precipitation changes (percent) in Figures A36-A40. Consecutive figures show annual and seasonal (December-February, March-May, June-August and September-November) mean changes.

A2-high, Annual Temperature
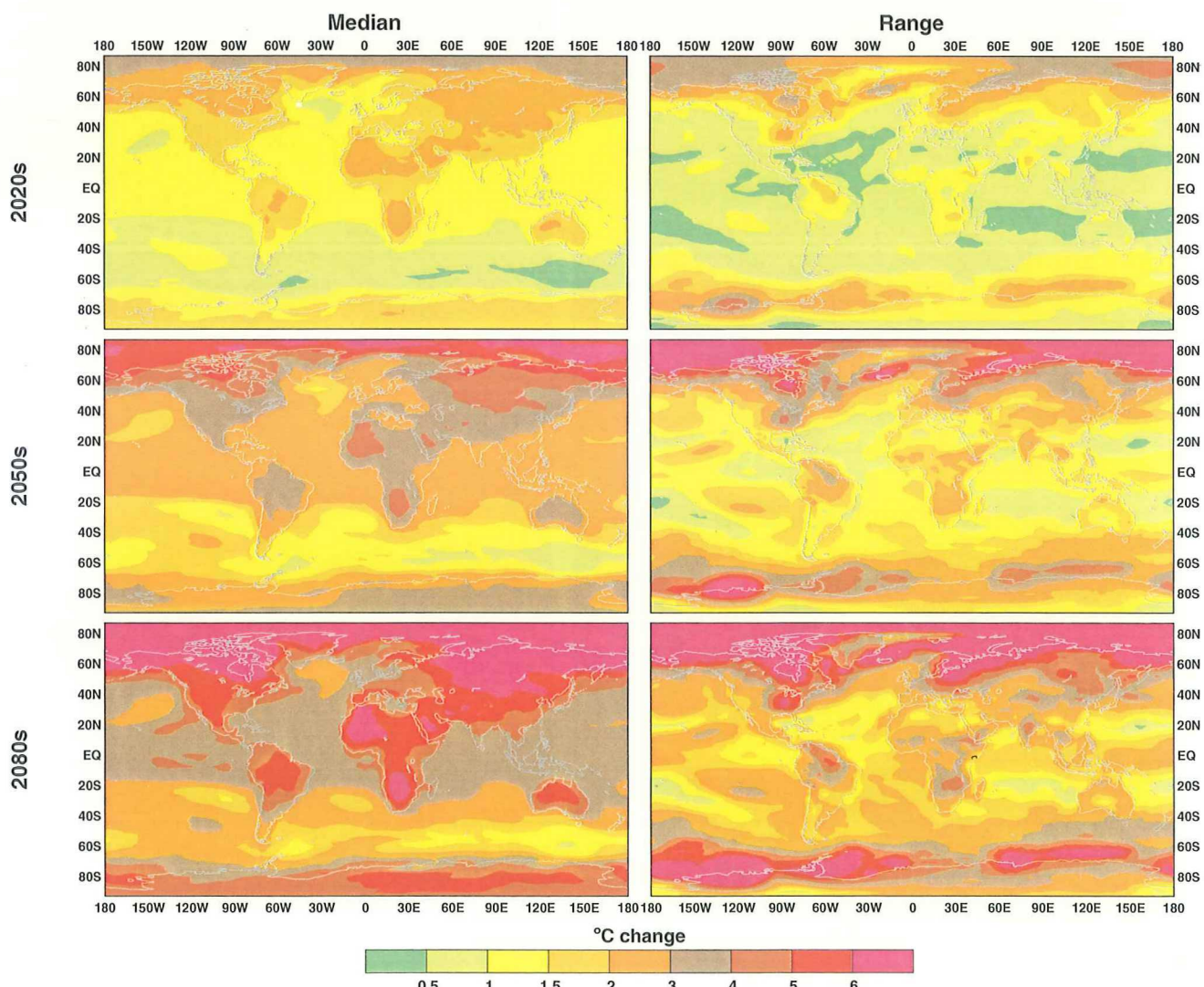
A2-high, DJF Temperature

°C change

| | 0.5 | 1 | 1.5 | 2 | 3 | 4 | 5 | 6 |

A2-high, MAM Temperature

Median   Range

°C change

0.5   1   1.5   2   3   4   5   6

A2-high, JJA Temperature

Median Range

2020s
2050s
2080s

°C change

0.5 1 1.5 2 3 4 5 6
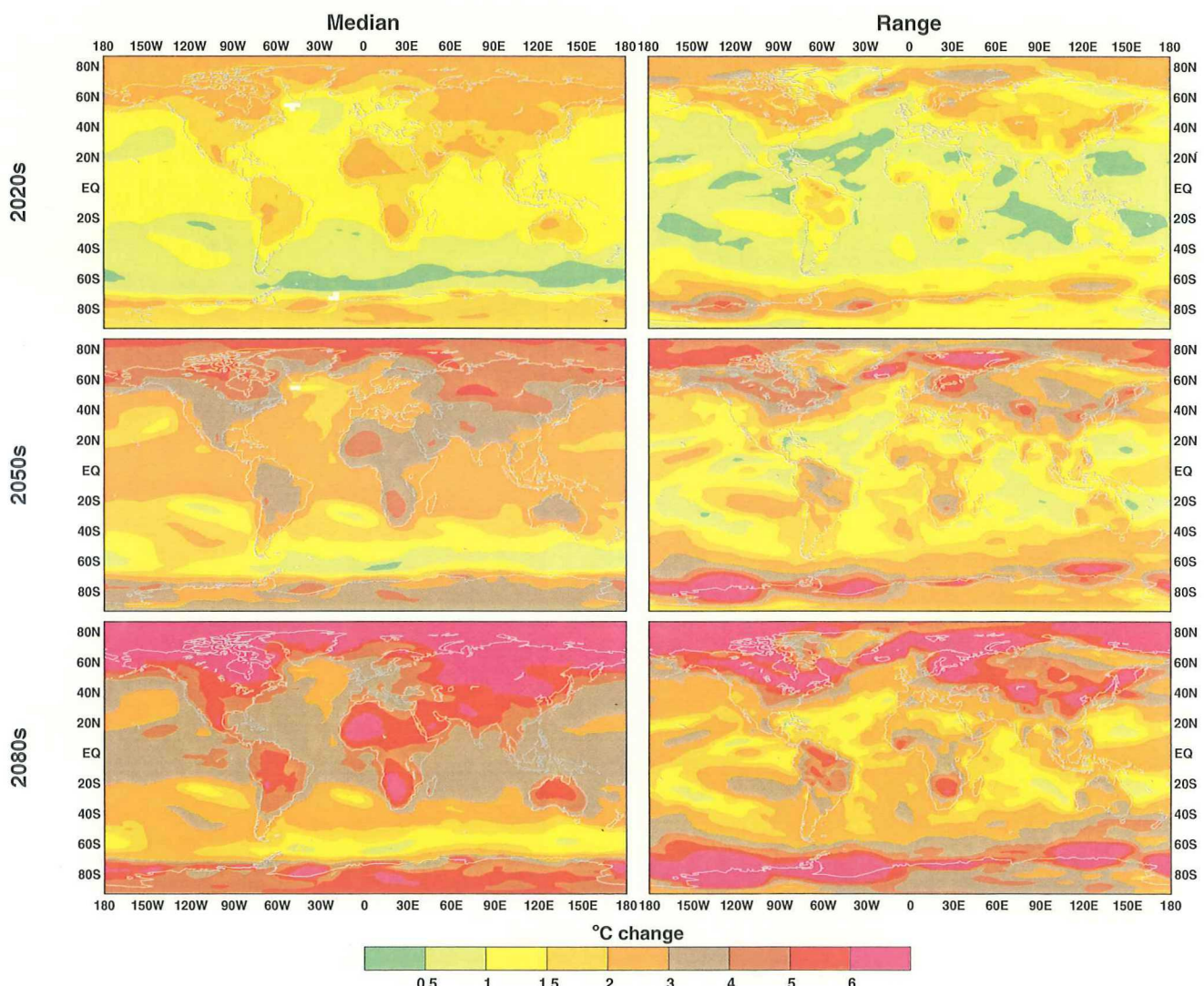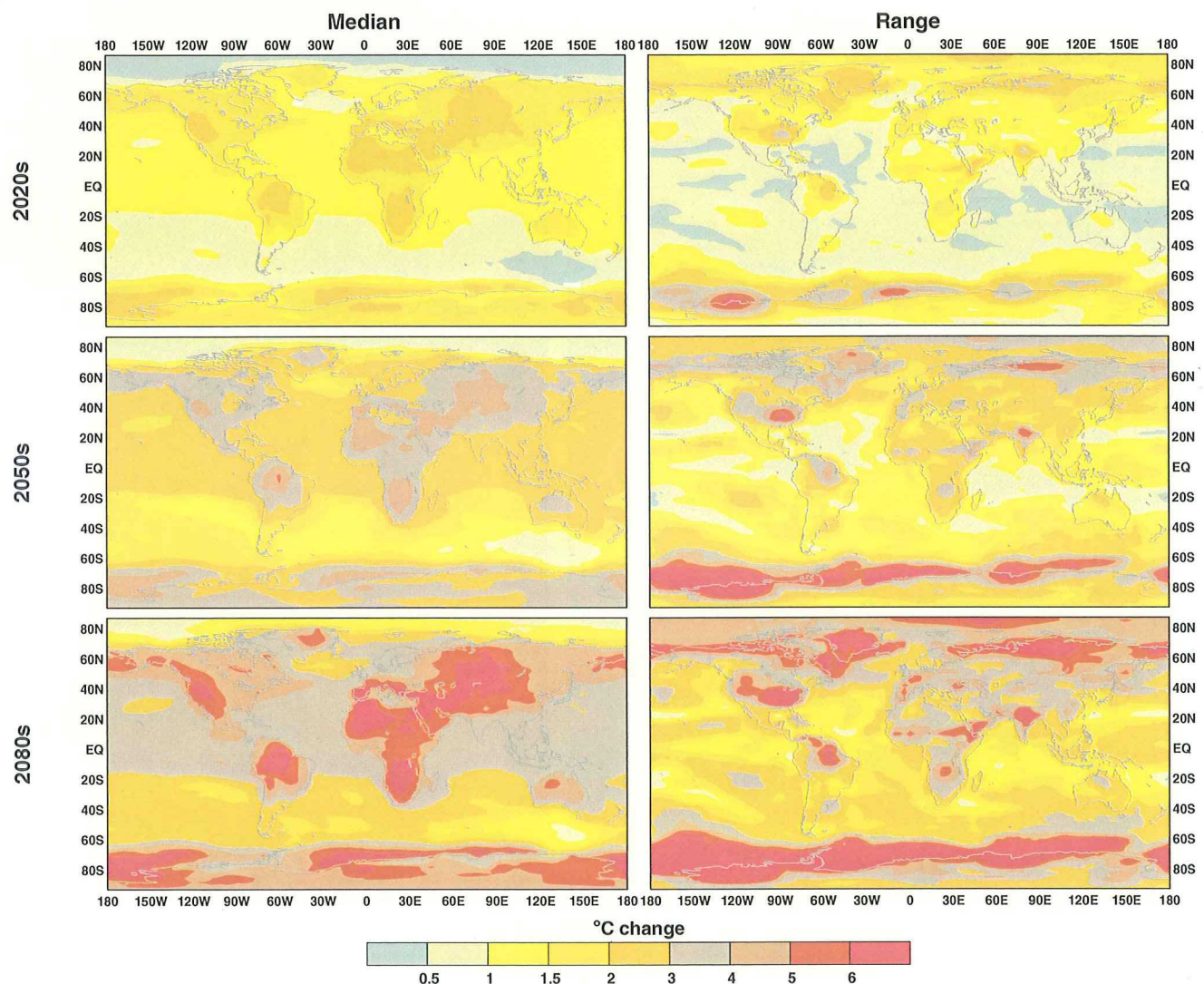
A2-high, SON Temperature

°C change

| | 0.5 | 1 | 1.5 | 2 | 3 | 4 | 5 | 6 | |
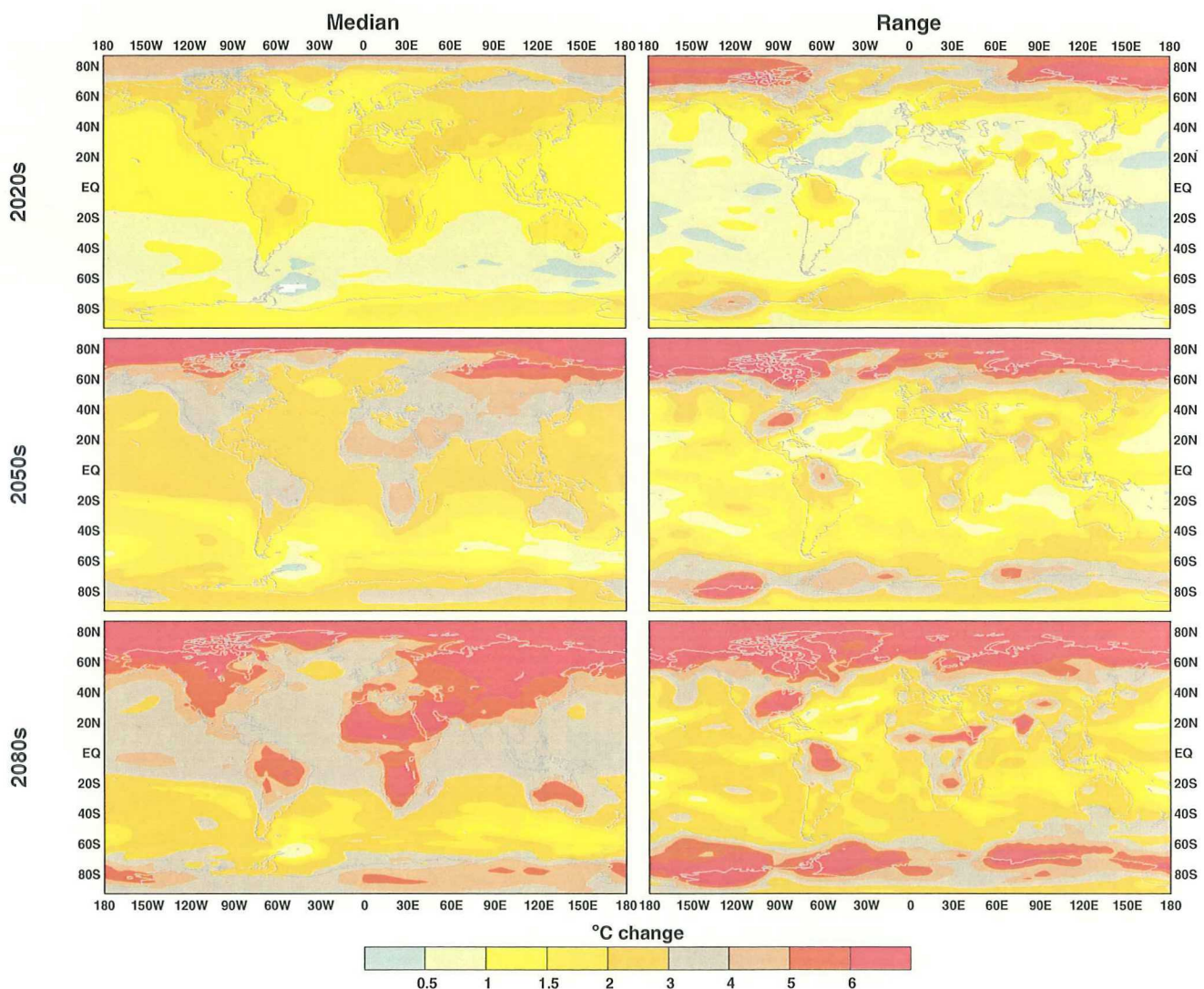
A2-high, Annual Precipitation

Median

Range

2020s

2050s

2080s

Median of % changes

-50 -30 -20 -10 0 10 20 30 50

Range of % changes

10 20 30 40 50 75 100
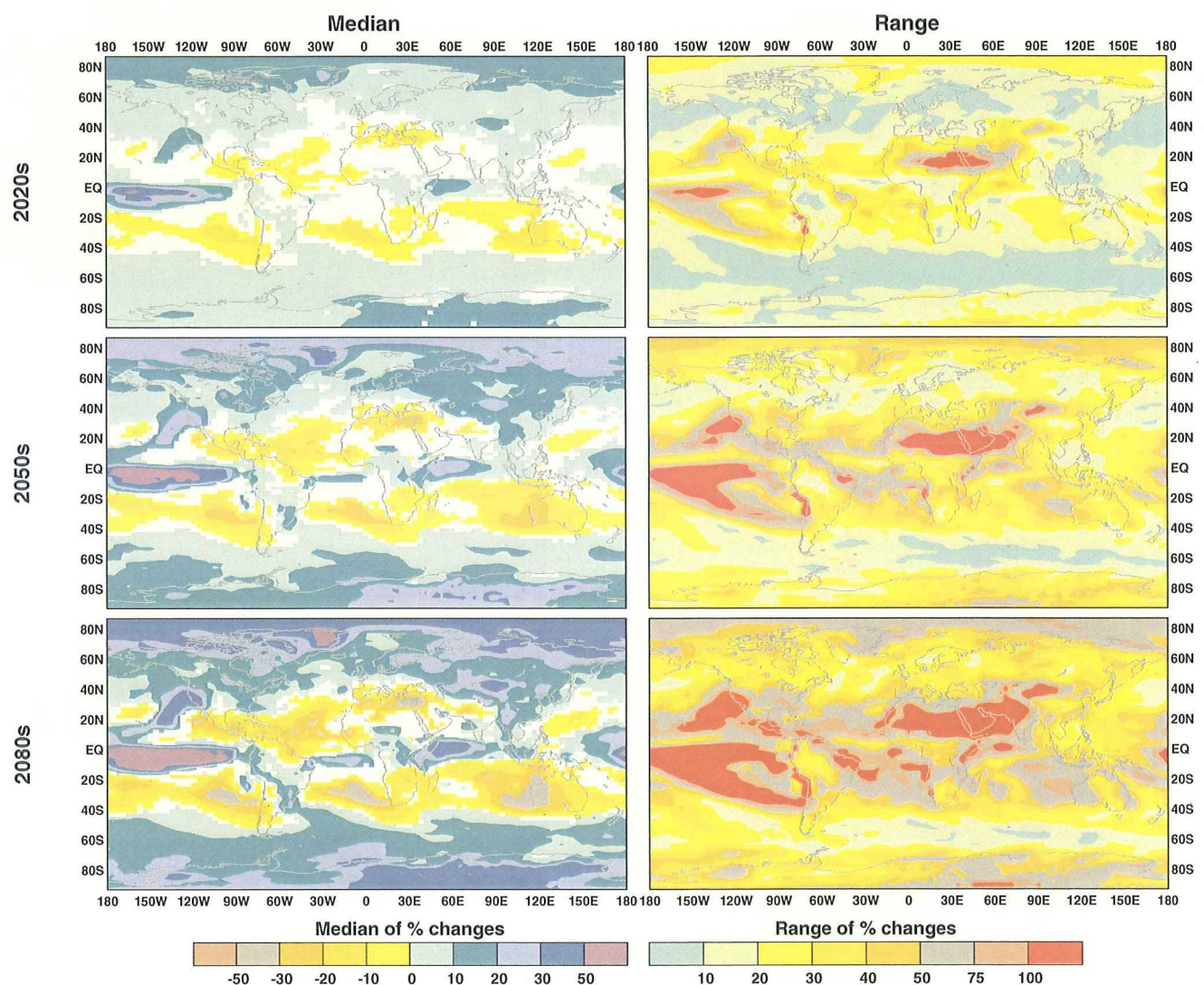
A2-high, DJF Precipitation

Median · Range

2020s · 2050s · 2080s

Median of % changes

-50 -30 -20 -10 0 10 20 30 50

Range of % changes

10 20 30 40 50 75 100
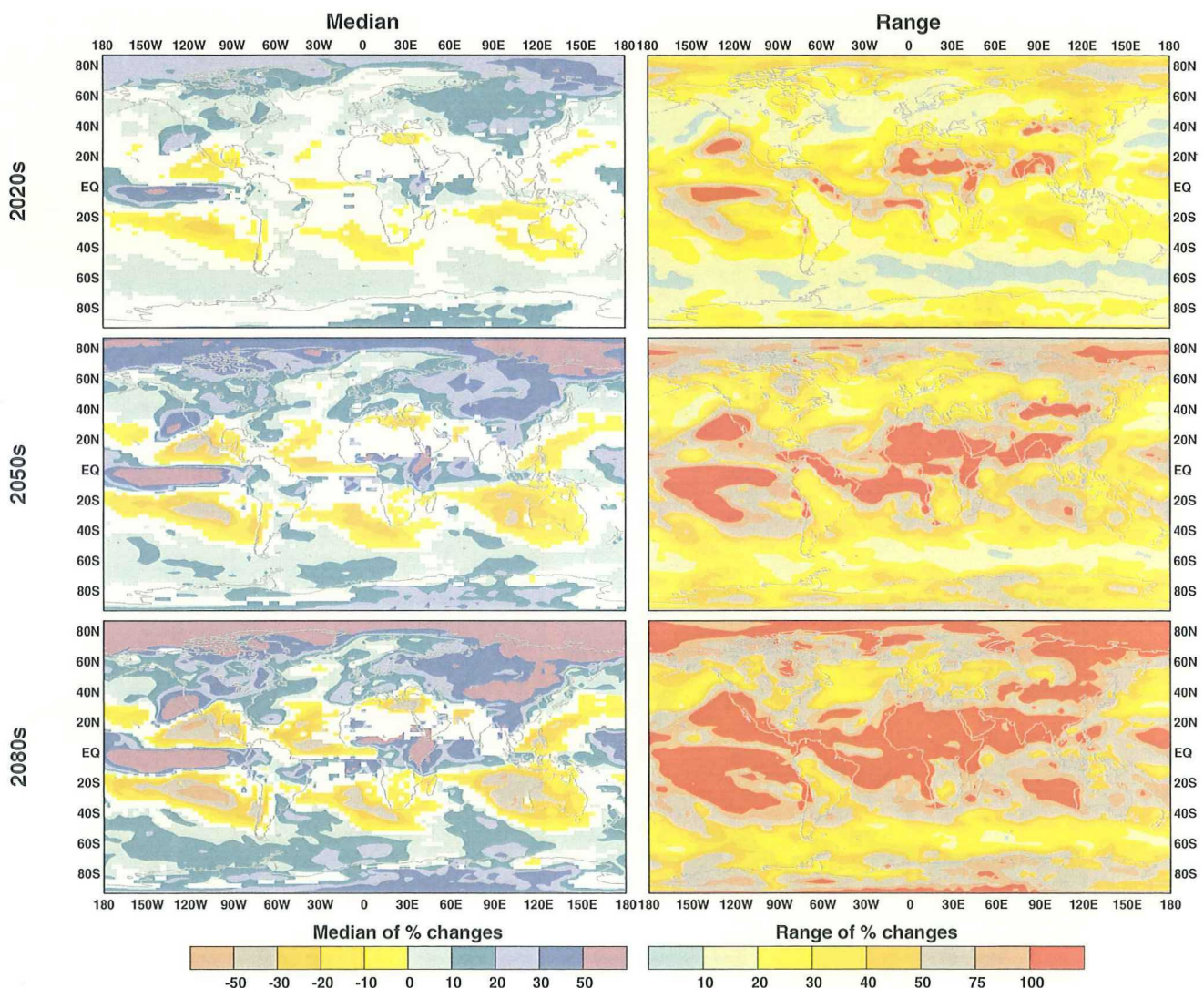
A2-high, MAM Precipitation

Median

Range

2020s

2050s

2080s

Median of % changes

-50 -30 -20 -10 0 10 20 30 50

Range of % changes

10 20 30 40 50 75 100
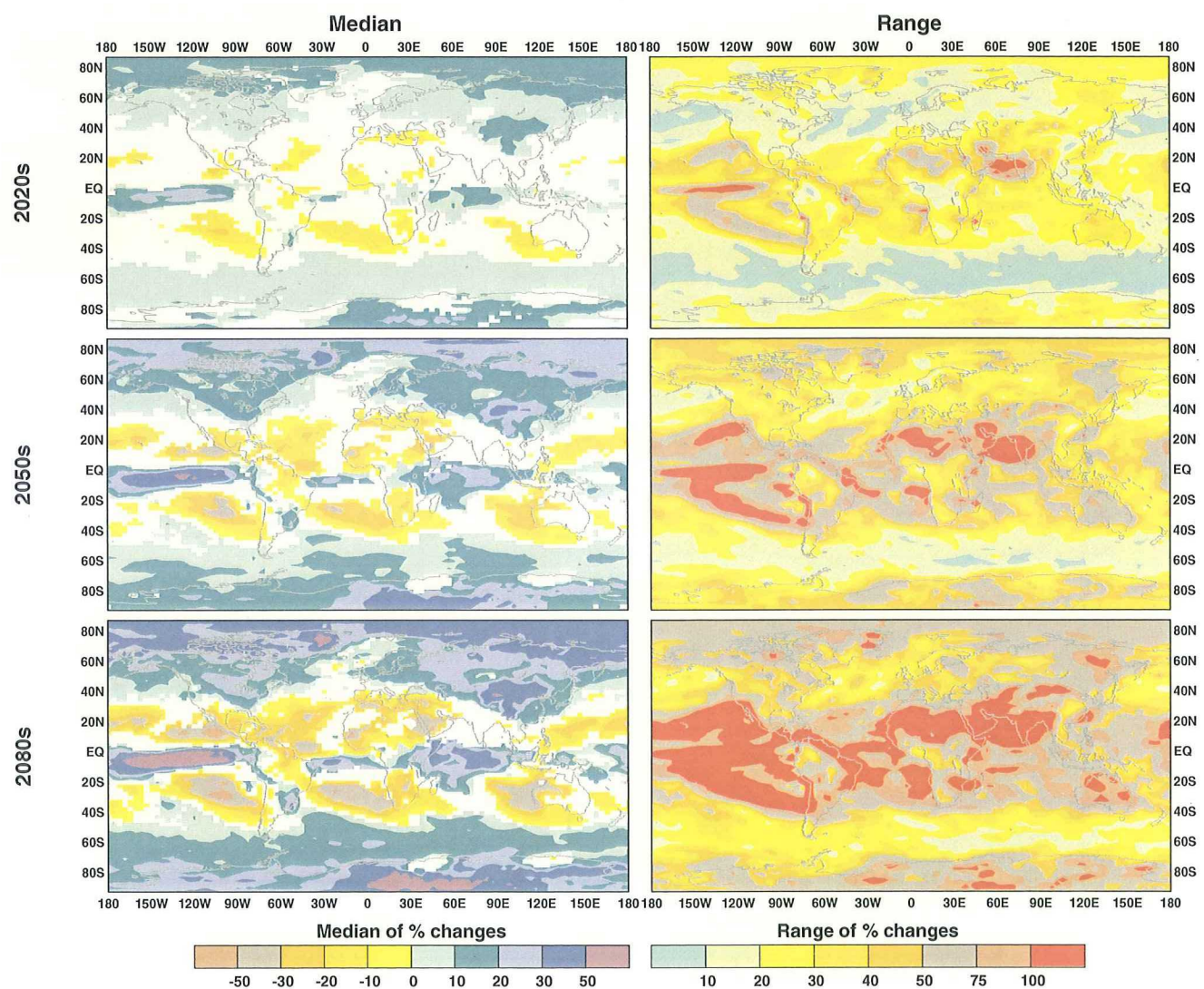
A2-high, JJA Precipitation

Median

Range

2020s

2050s

2080s

Median of % changes

-50 -30 -20 -10 0 10 20 30 50

Range of % changes

10 20 30 40 50 75 100
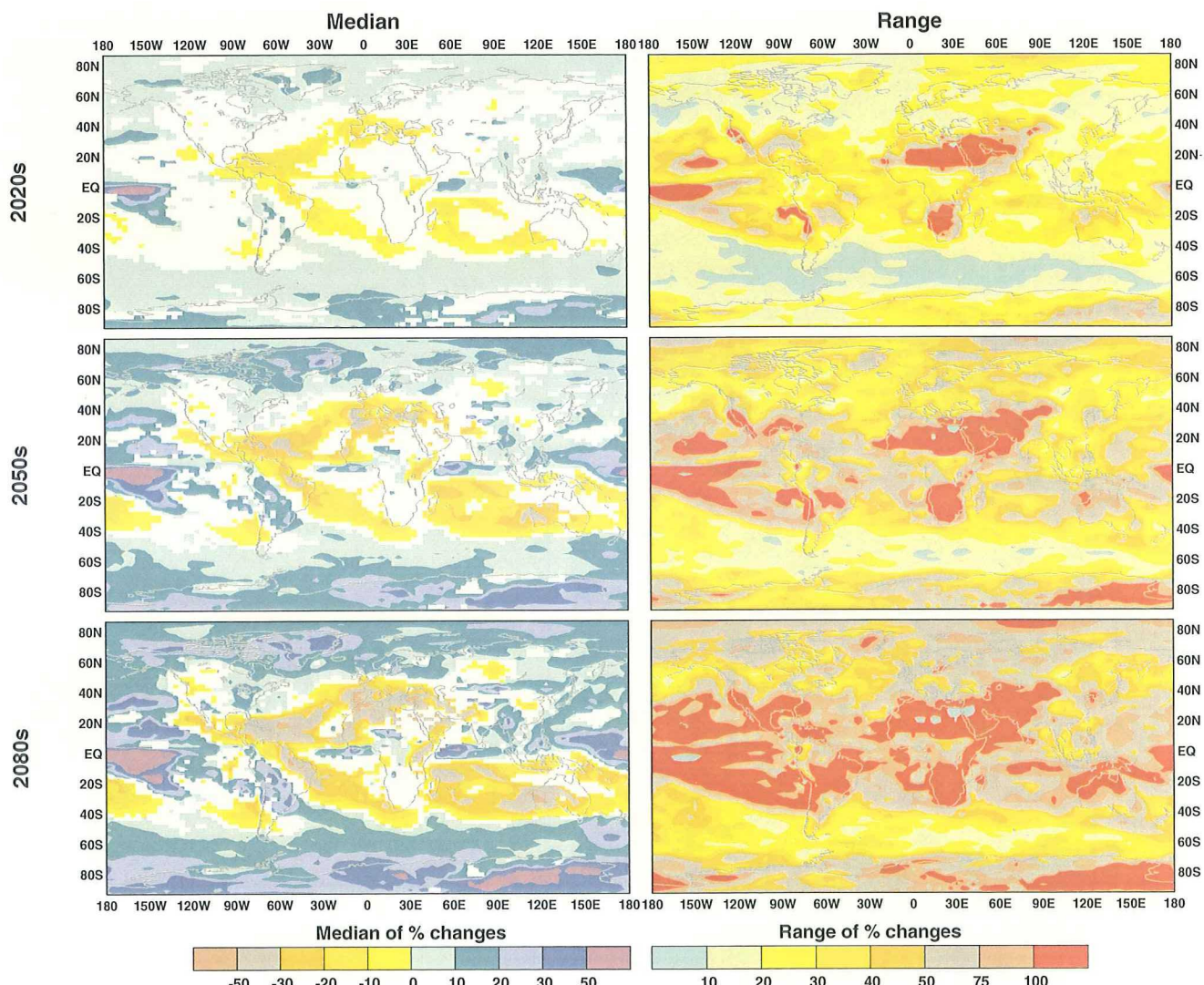
A2-high, SON Precipitation

Median   **Range**

2020s

2050s

2080s

Median of % changes

-50 -30 -20 -10 0 10 20 30 50

Range of % changes

10 20 30 40 50 75 100
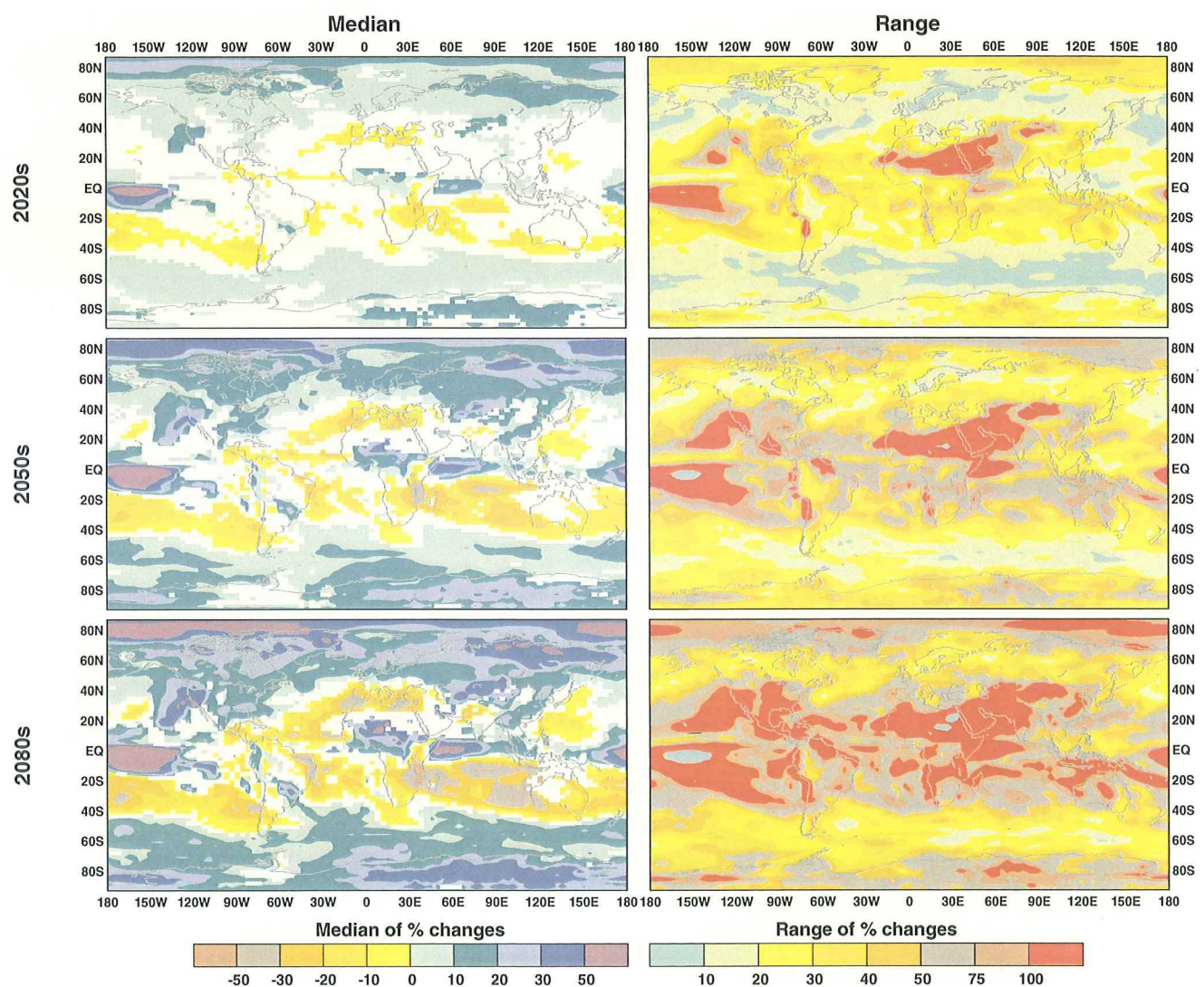
Appendix B: Regional Scatter Plots of Seasonal Temperature and Precipitation Change under the Four SRES-Based Scenarios

Scatter plots for the thirty two world regions listed in Table 10 are shown in Figures B1-B32. Characterizations are presented for three 30-year time periods in the future relative to the 1961-1990 baseline centred on 2025, 2055 and 2085. Each scatter plot depicts scaled outputs of mean seasonal temperature and precipitation change over the grid boxes representing a region from each of the ten GCM simulations (grid boxes differ between models). These simulations are described further in Section 4. For a given time period, lines connect four points for each GCM simulation. These are the standardized regional changes in climate from the GCM, linearly scaled according to the global warming from each of the four SRES-based scenarios (see Figure Bi). Note that the order of the points along a line is the same for all plots. Moreover, since linear scaling has been applied to the same pattern of change for all time periods, the relative positions of different lines remain invariant, extending outwards from the origin through time.
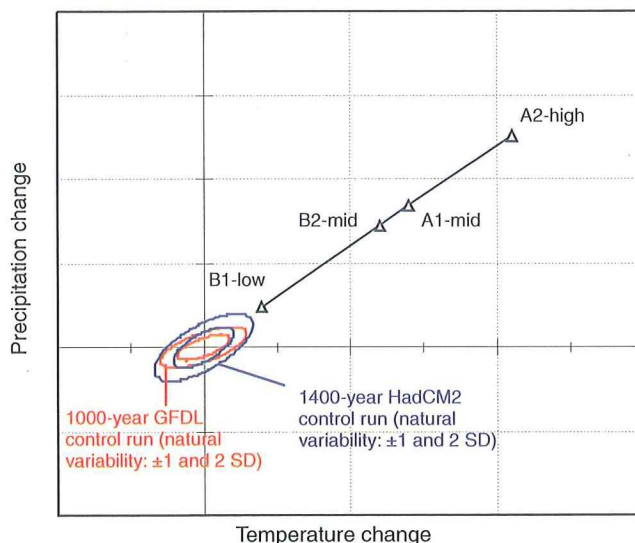
Figure Bi. Main features of the scatter plots

Also plotted are the ±1 and ±2 standard deviation (denoted as std in the Figures) limits of overlapping 30-year mean anomalies[5] relative to the long-term mean from two unforced simulations: the 1400-year HadCM2 and the 1000-year GFDL unforced simulations. These are plotted as ellipses (explained below) and are used to indicate natural multi-decadal variability (MDV) unforced by greenhouse gas concentration changes or any other forcing factor external to the climate system. The significance of the scenario changes in climate can be interpreted relative to these model-based limits, if we assume that they provide a reasonable representation of natural climate variability. Recent comparisons between the HadCM2 unforced simulation and palaeoclimatic reconstructions of climatic variability during the past millennium (Jones *et al.*, 1998; Hulme *et al.*, 1999) provide some support for this assumption.

---

[5] Note that results are similar when using non-overlapping 30-year anomalies

The length of the lines indicates the range of uncertainty in the magnitude of change brought about by the SRES-based scenario assumptions of different emissions trajectories and climate sensitivity. The spread of different lines on each plot indicates the extent of between-model (or intra-ensemble) disagreement across this sample of GCM outputs.

The ellipses have been calculated by assuming that the distributions of 30-year mean temperature and 30-year mean precipitation in the unforced simulations are normally distributed. In addition, recognising that modelled temperatures and precipitation are correlated in some seasons and regions, the ellipses are also elongated in the direction of the correlation. There is good agreement between the GFDL and HadCM2 ellipses in the majority of the regional plots presented in Figures B1-B32, although there are some regional cases that show large differences in magnitude in dry seasons (e.g. Figure B15: DJF, MAM and SON over the Sahara; Figure B25: MAM, JJA and SON over northern Australia) or differences in the sign of the correlation (e.g. Figure B16: DJF over West Africa).

Figure Bii illustrates the full elliptical distribution for the northern Asia region in winter based on the GFDL unforced simulation. The idealized joint normal distribution is shown as a three-dimensional surface. The individual 30-year mean modelled temperature and precipitation anomalies are plotted as points projected onto the idealized surface. In this case, the distribution of 30-year values is slightly skewed towards positive temperature and precipitation anomalies, with a longer tail towards negative anomalies. The orientation of the ellipse indicates a fairly strong positive correlation between modelled 30-year mean winter temperatures and precipitation under unforced conditions in this region, which is consistent with the observation that warmer winters tend to be associated with higher precipitation.
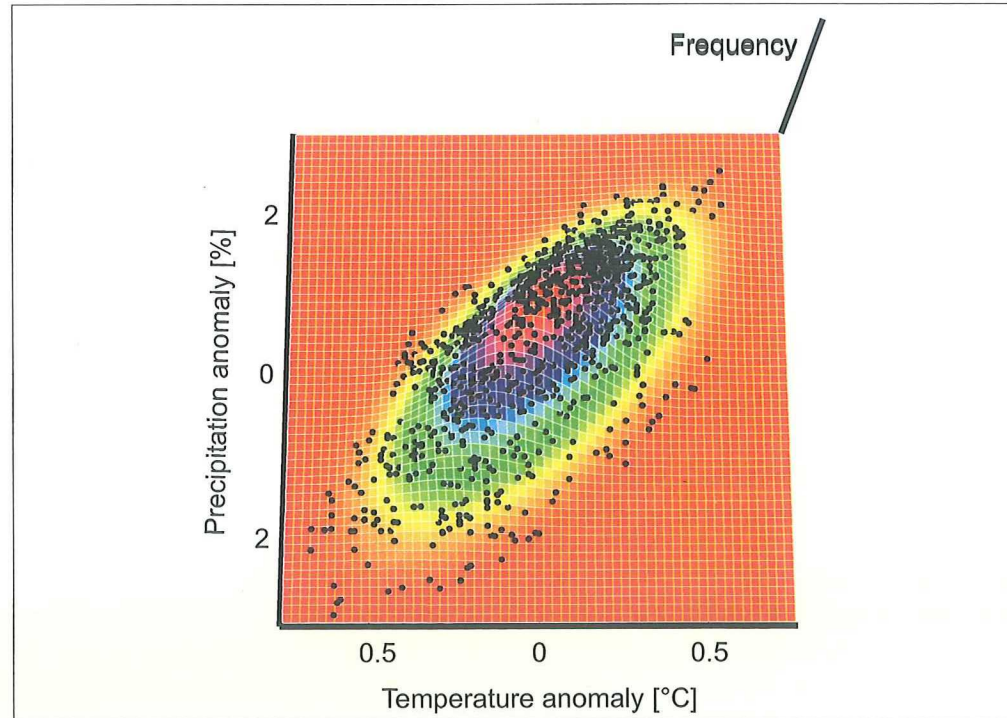
Figure Bii. Modelled multi-decadal variability of winter (DJF) temperature and precipitation in northern Asia using the GFDL 1000-year unforced simulation. The surface is an idealized joint normal distribution fitted to overlapping 30-year mean temperature and precipitation anomalies relative to the 1000-year mean. Original data points are shown as dots projected onto the idealized surface. The ellipse is orientated in the direction of the correlation between temperature and precipitation.

Figures B1-B32. Scatter plots showing seasonal temperature and precipitation change by the 2020s (top), 2050s (middle) and 2080s (bottom) relative to 1961-1990 under the four SRES-based scenarios for 32 world regions (cf. Table 10 and Figure 6). Also shown (as ellipses) is "natural" multi-decadal variability as simulated by the GFDL and HadCM2 GCMs. There are two pages of graphs per Figure and region and three graphs per season: December to February (first page, left), March-May (first page, right), June-August (second page, left) and September-November (second page, right).
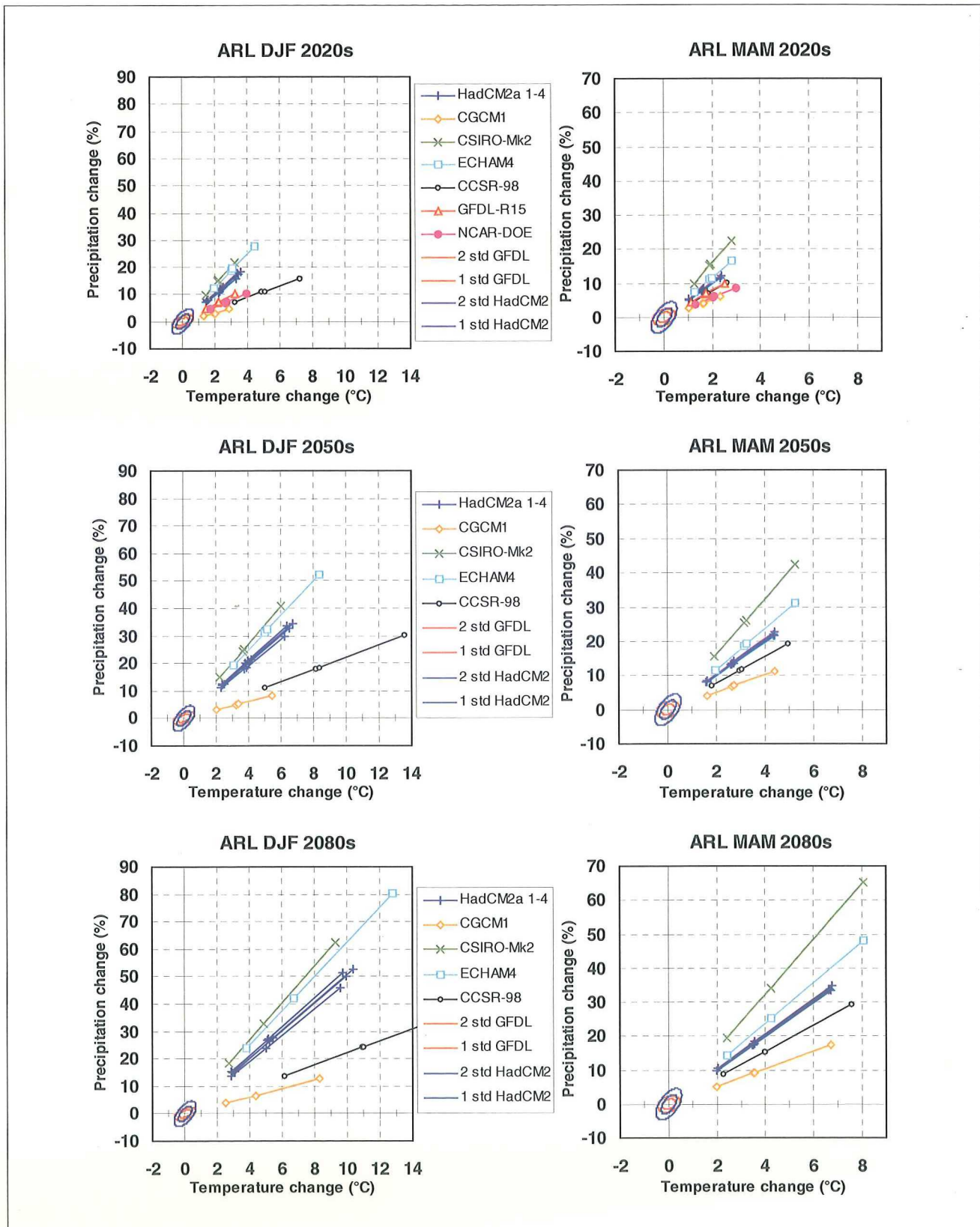
Figure BI. Arctic/land - December-February and March-May
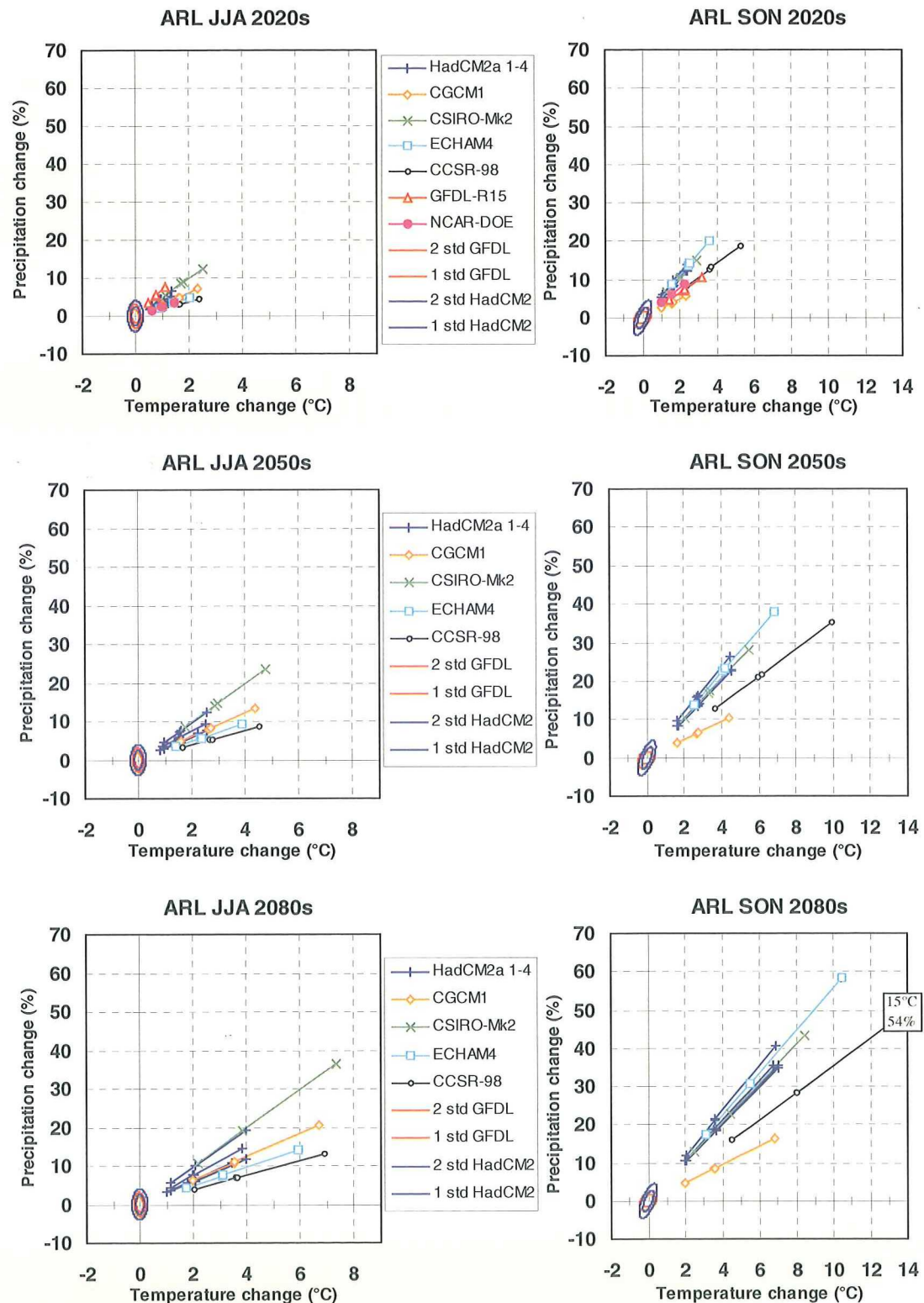
Figure B1. Arctic/land - June-August and September-November
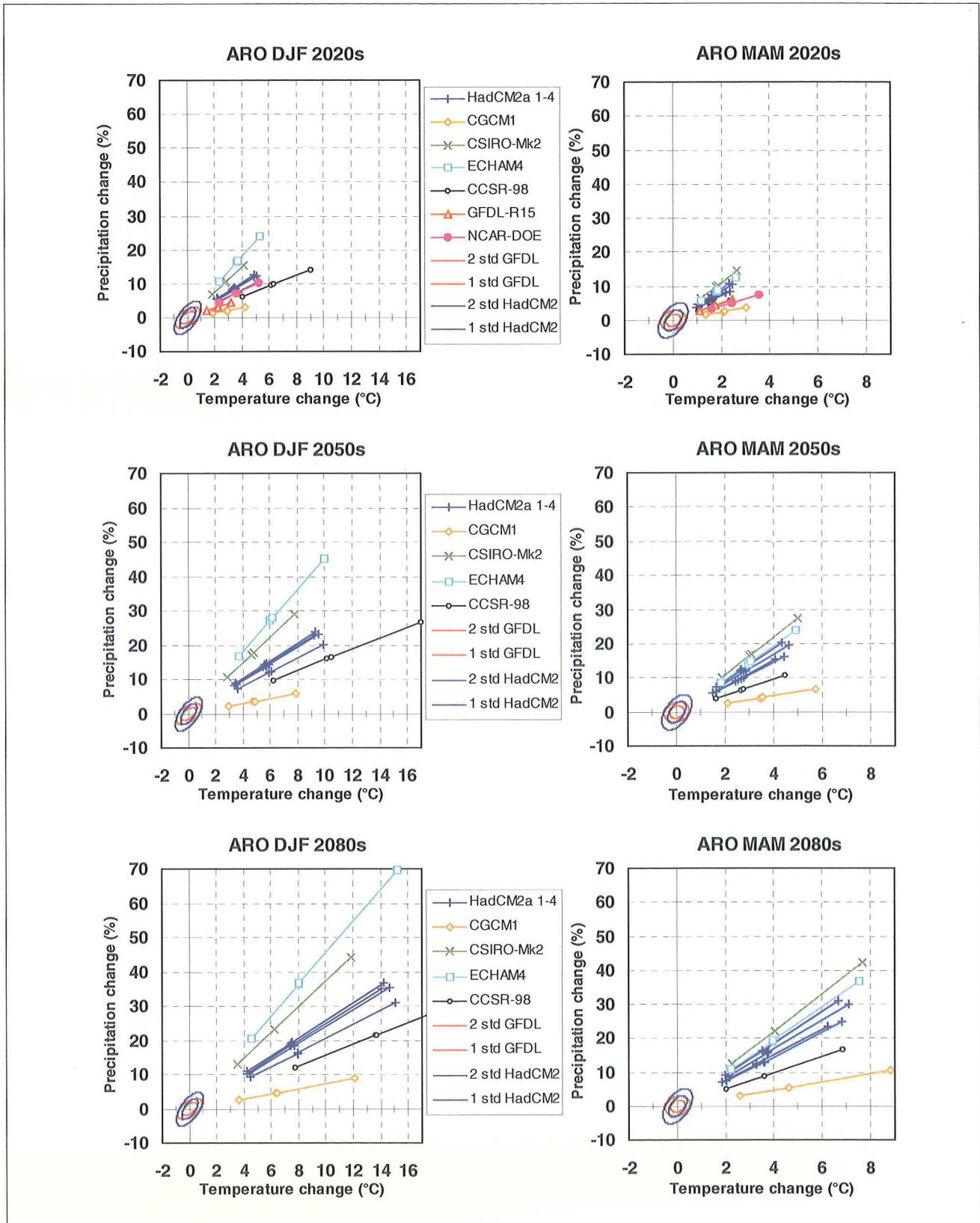
Figure B2. Arctic/ocean - December-February and March-May
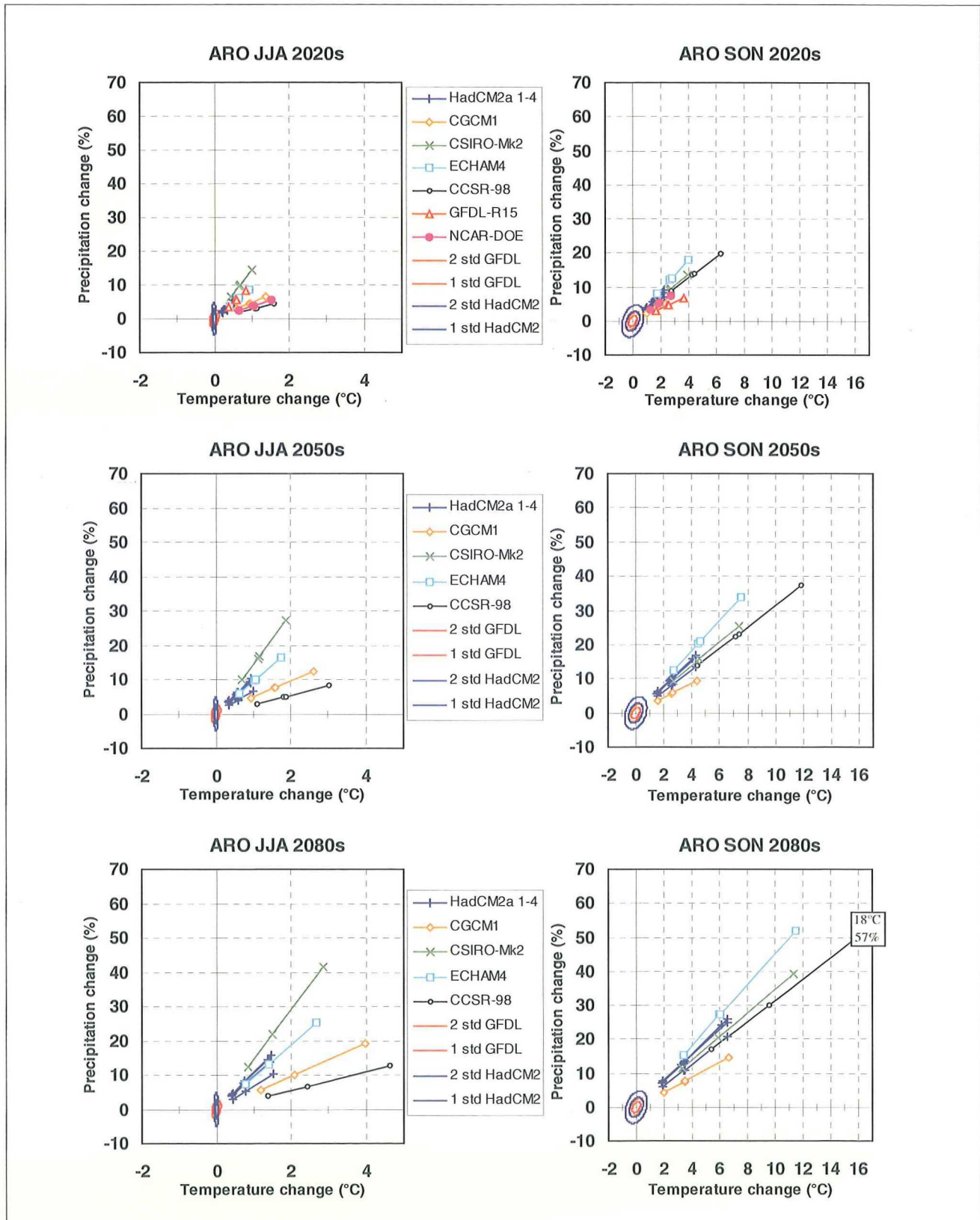
Figure B2. Arctic/ocean - June-August and September-November
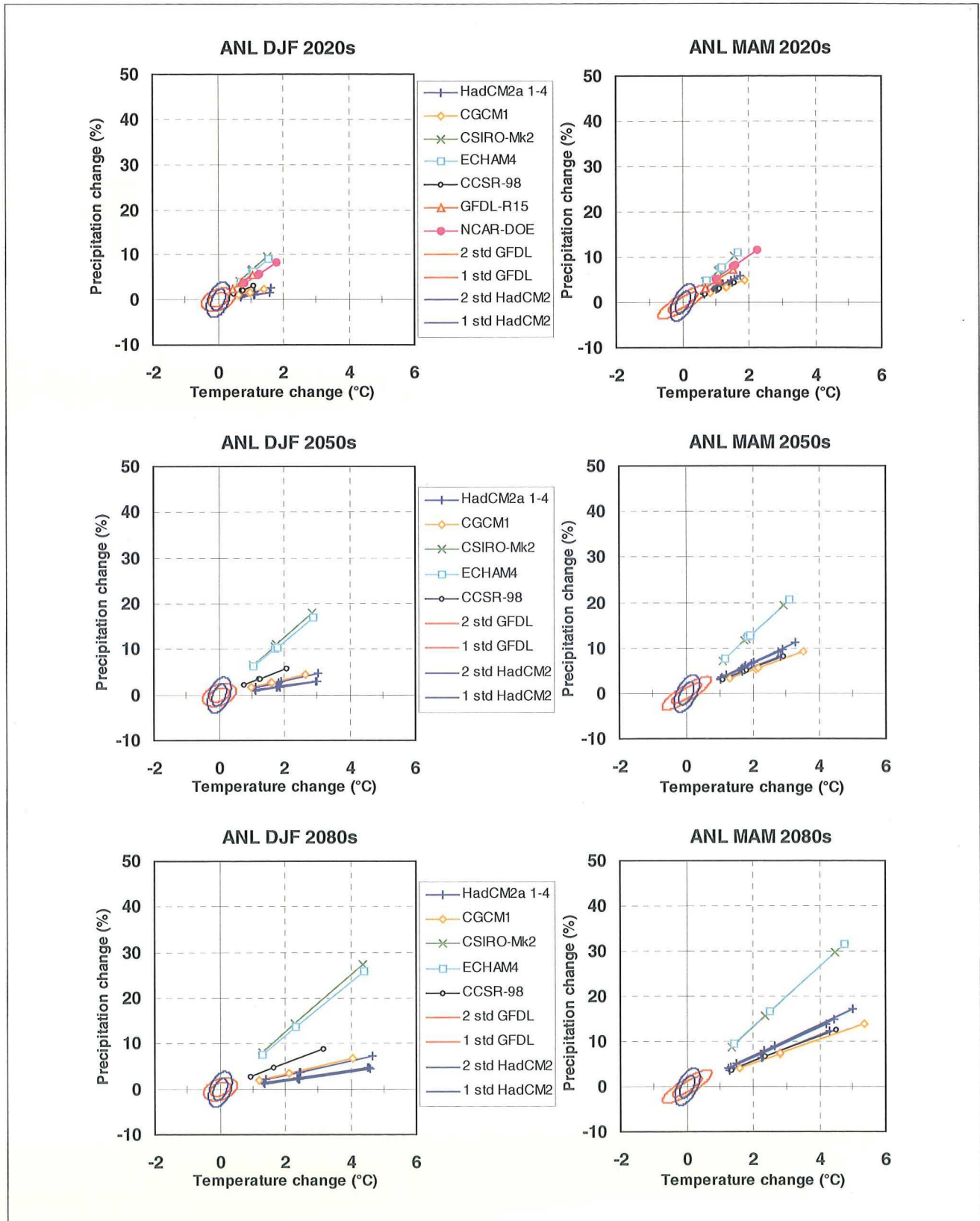
Figure B3. Antarctic/land - December-February and March-May
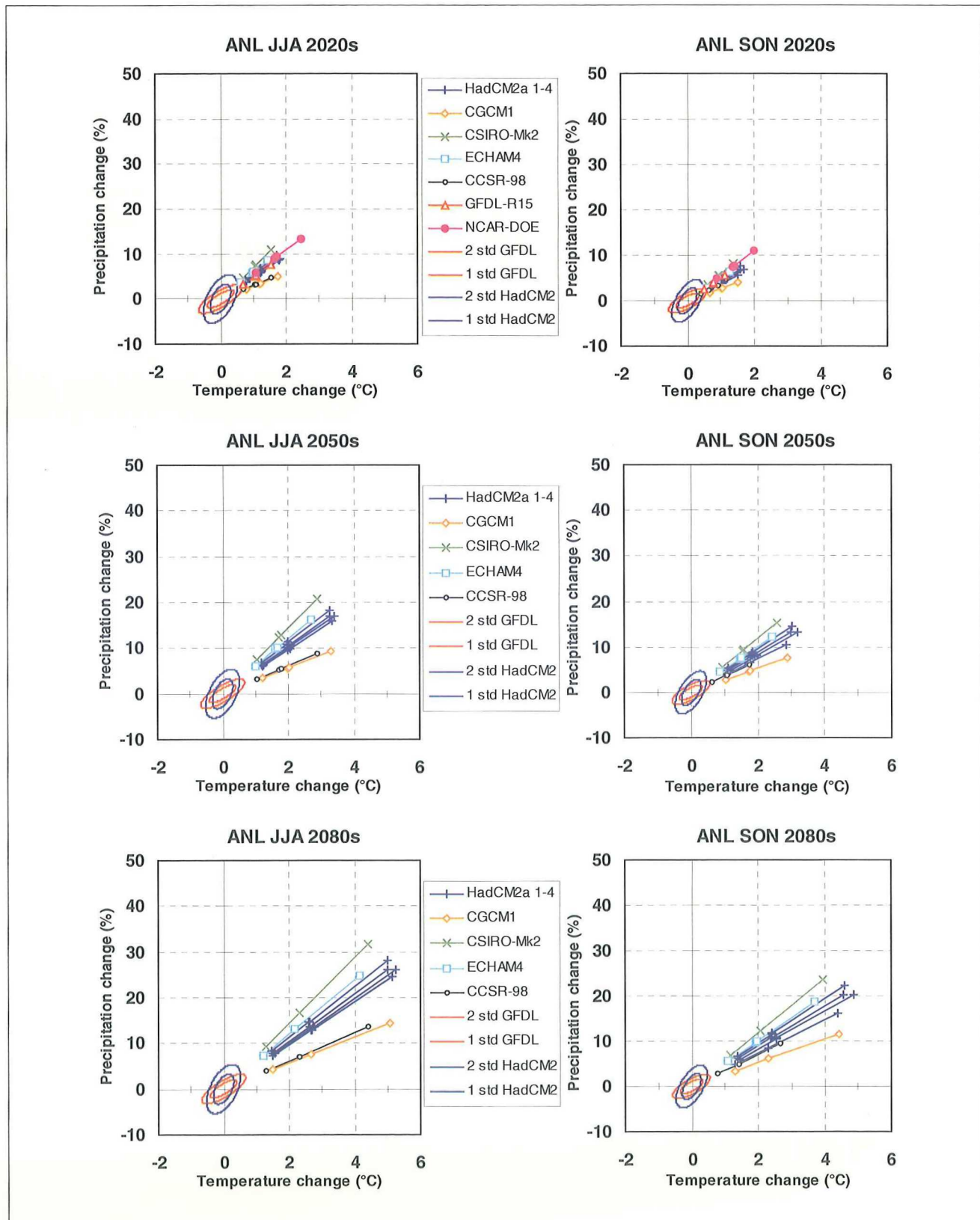
Figure B3. Antarctic/land - June-August and September-November
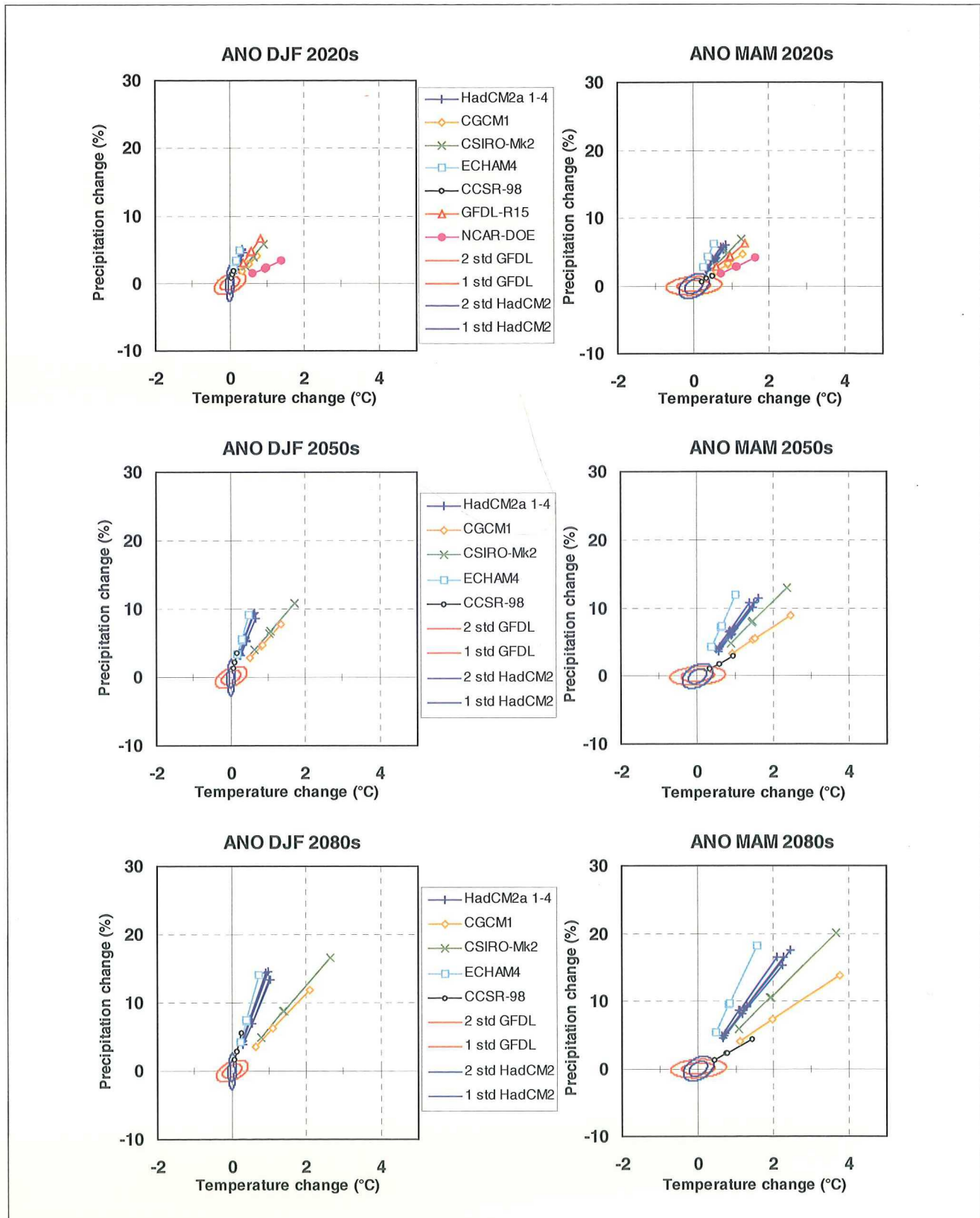
Figure B4. Antarctic/ocean - December-February and March-May
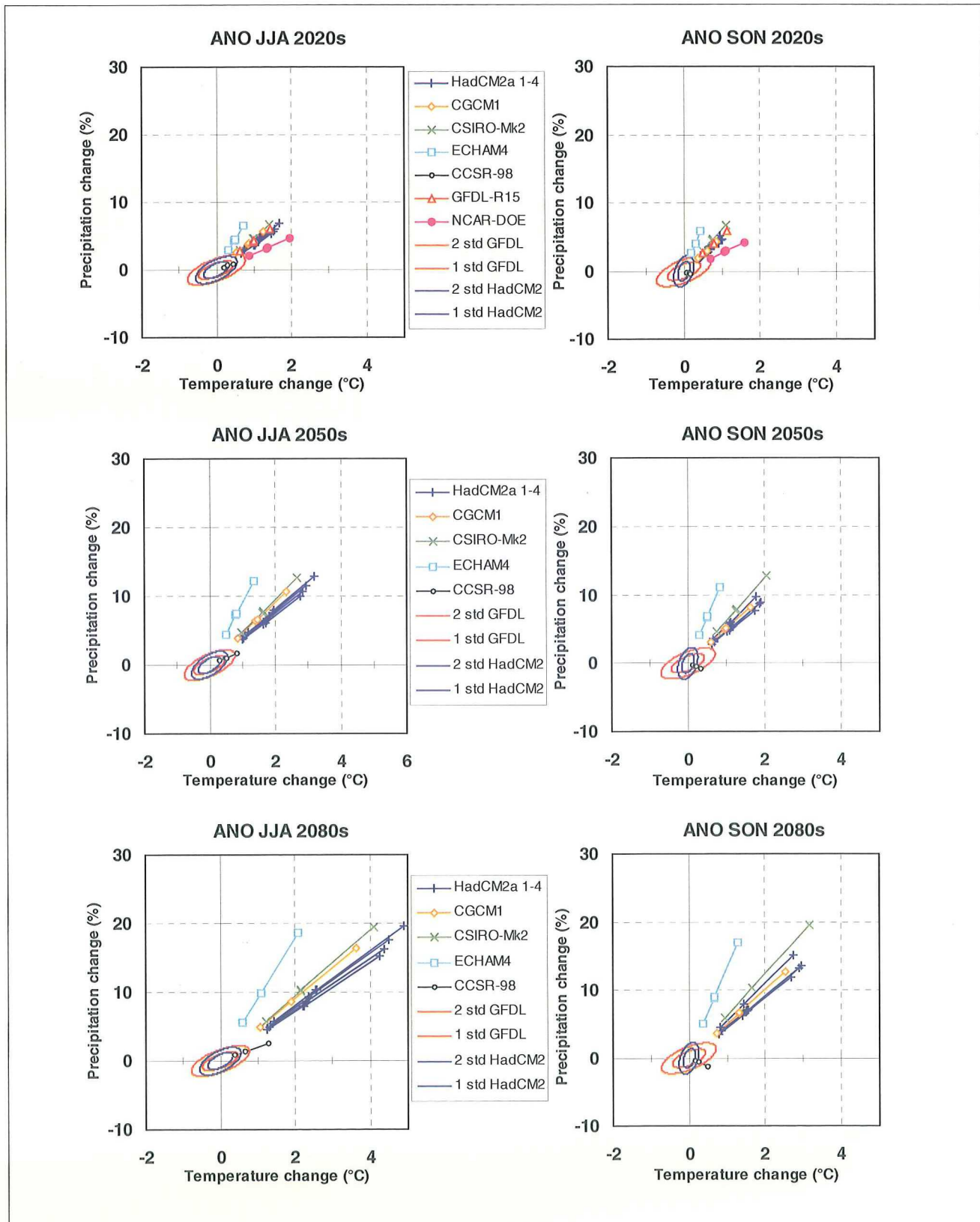
Figure B4. Antarctic/ocean - June-August and September-November
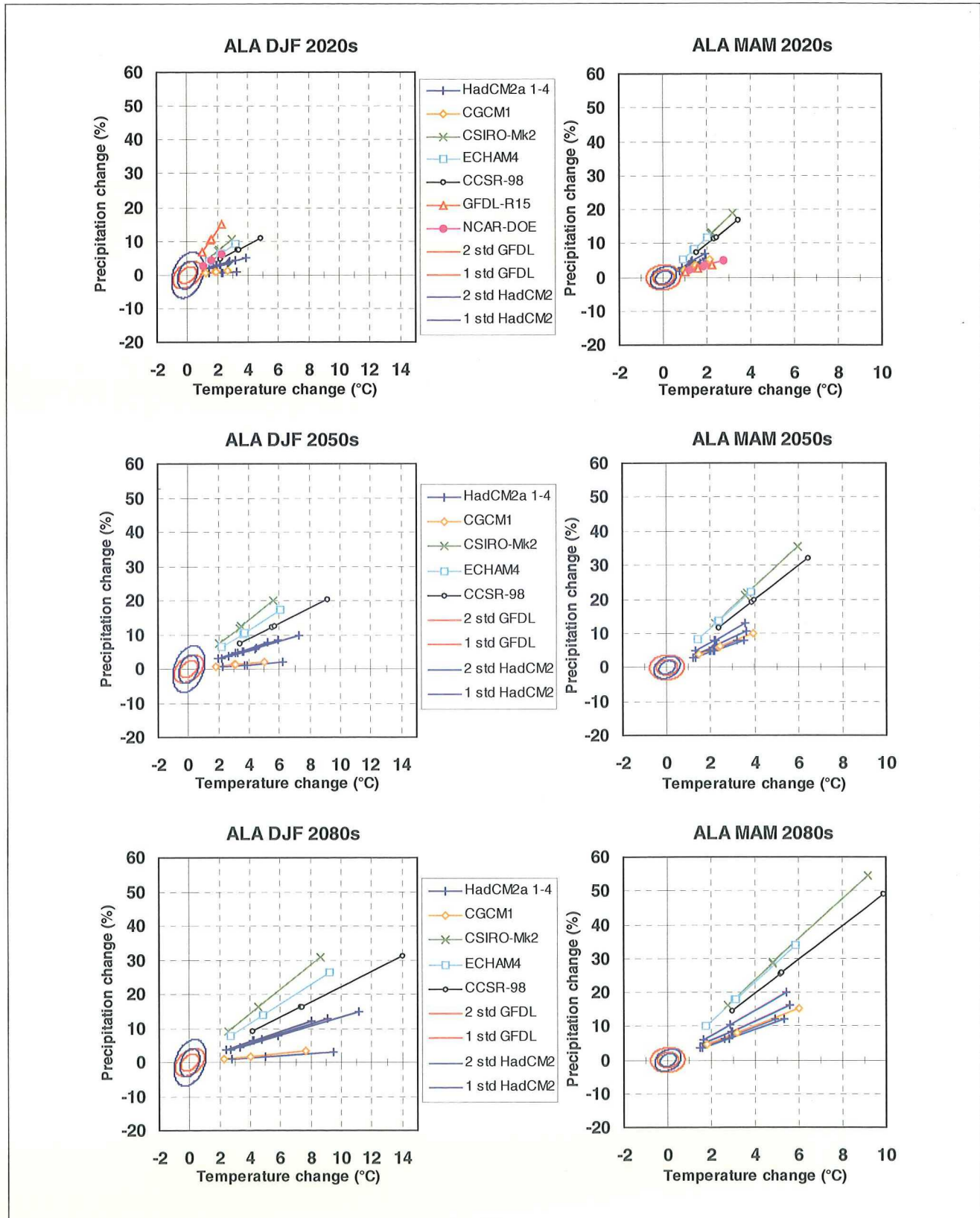
Figure B5. Alaska/NW Canada - December-February and March-May
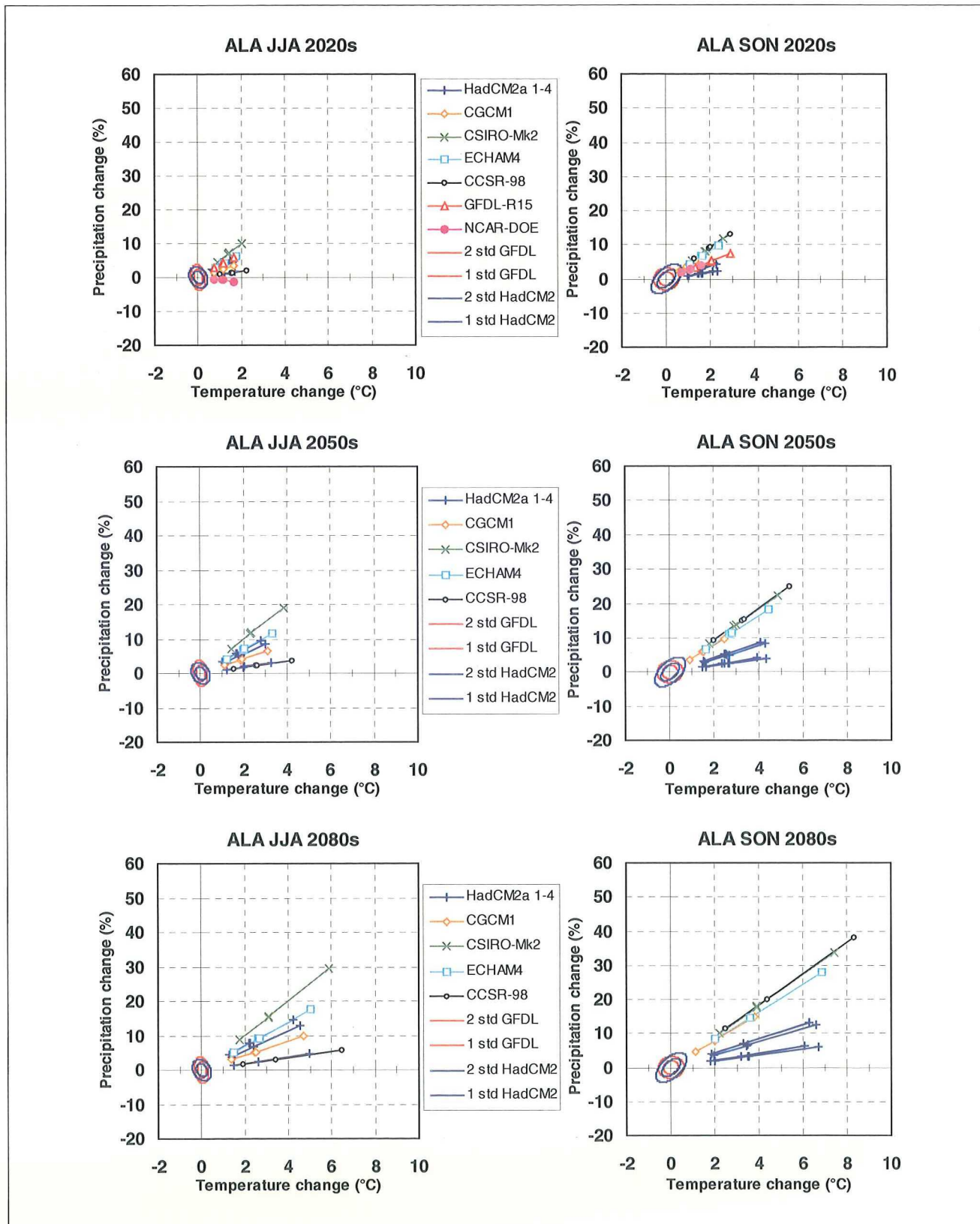
Figure B5. Alaska/NW Canada - June-August and September-November
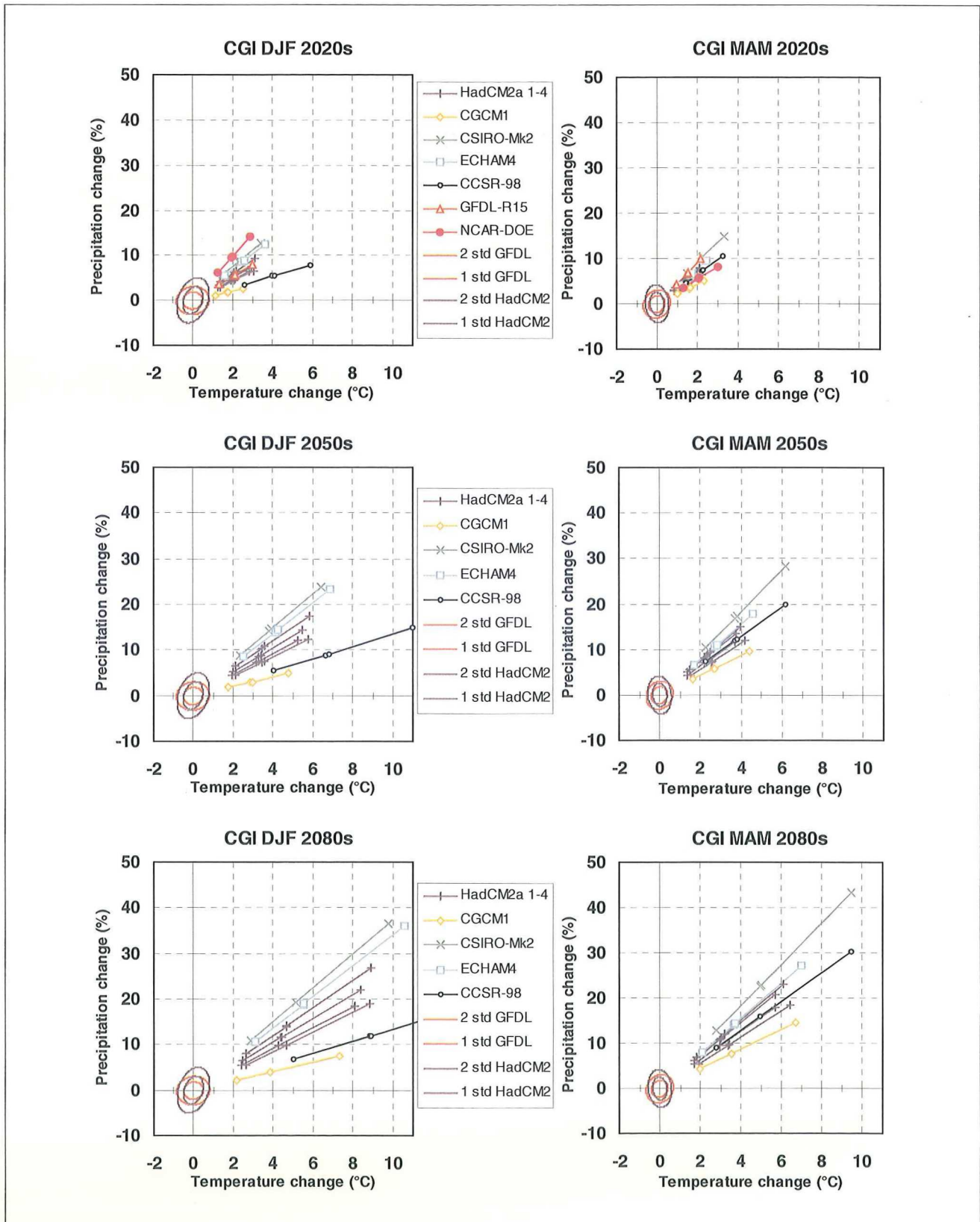
Figure B6. NE Canada/S Greenland/Iceland - December-February and March-May
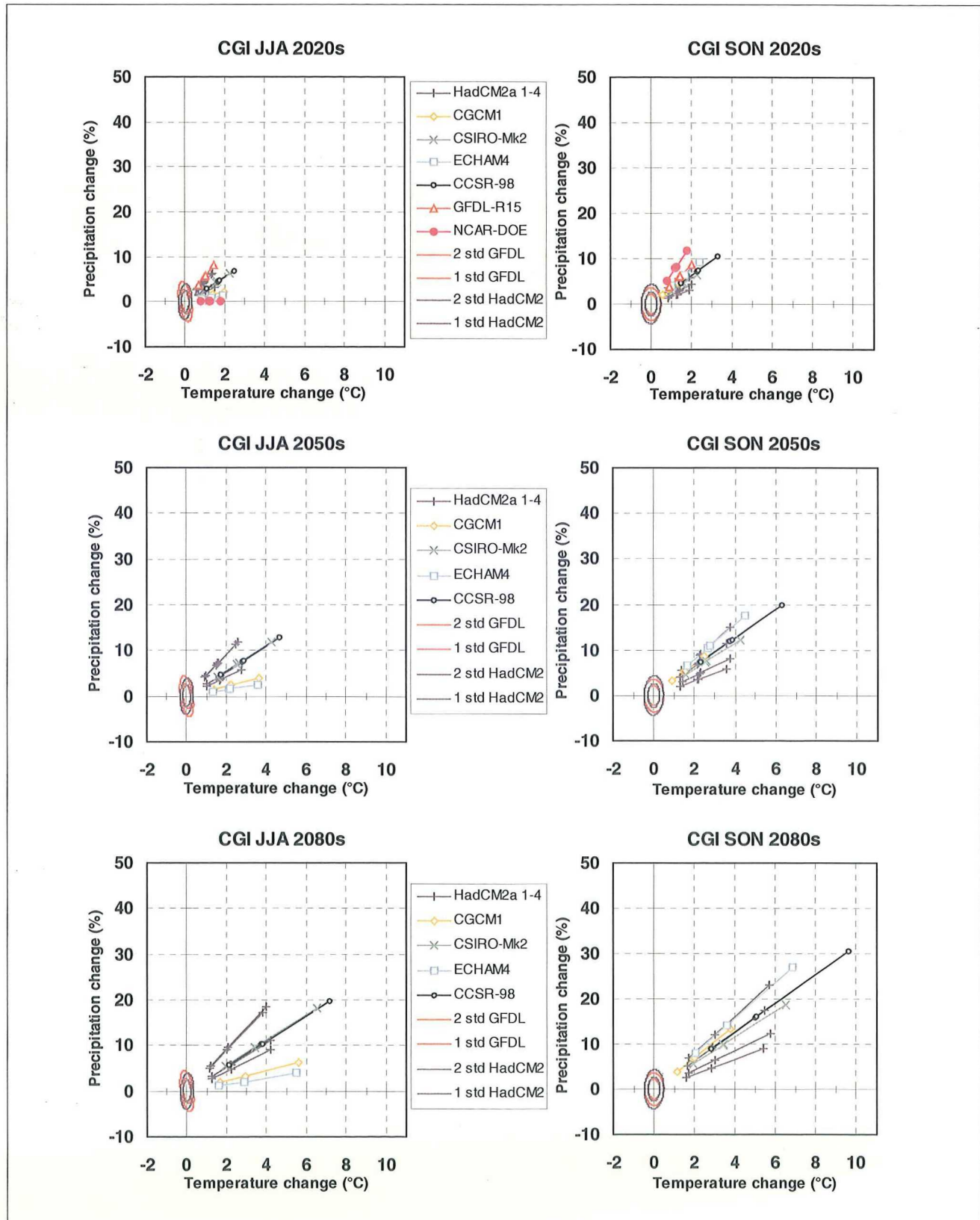
Figure B6. NE Canada/S Greenland/Iceland - June-August and September-November
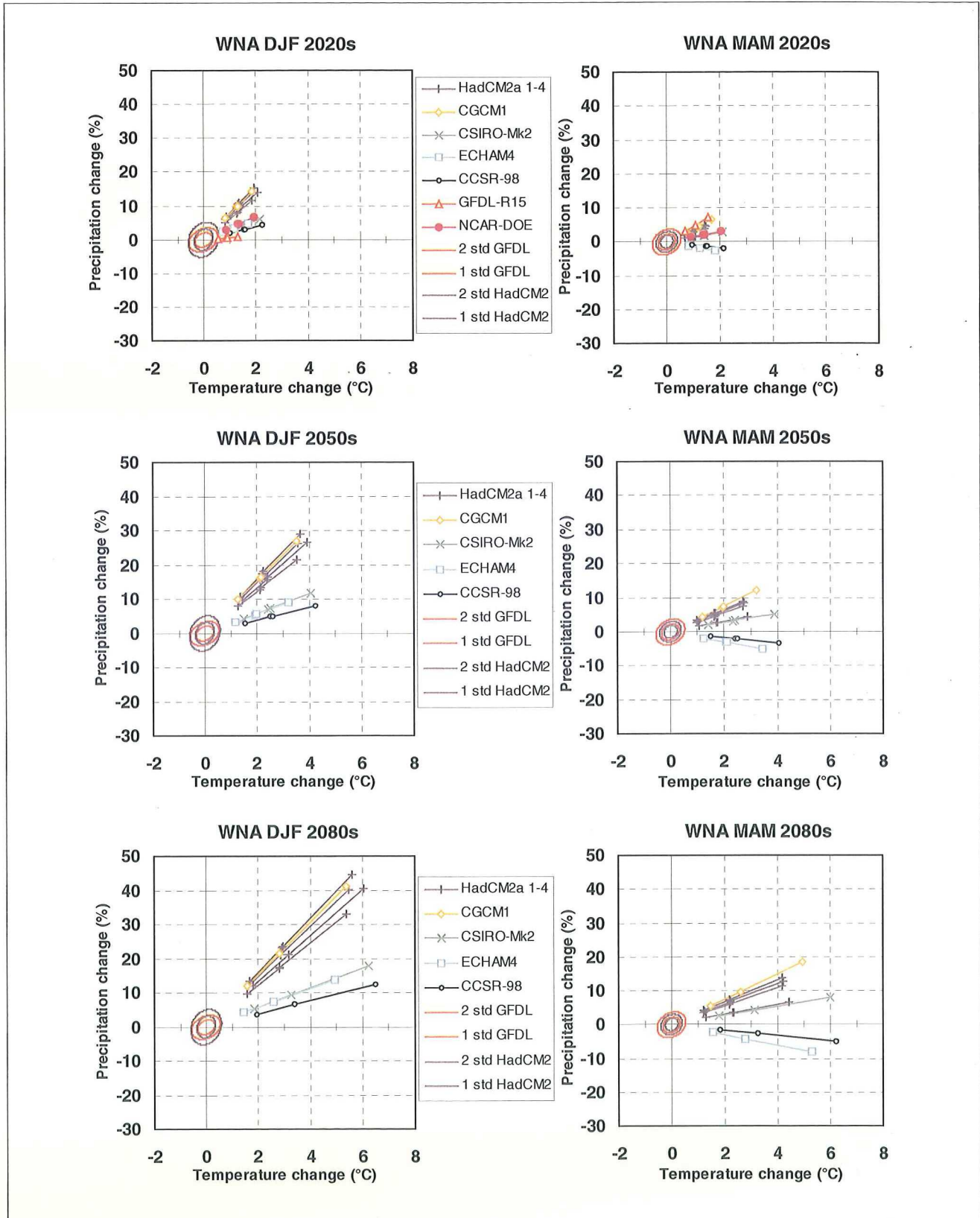
Figure B7. Western North America - December-February and March-May
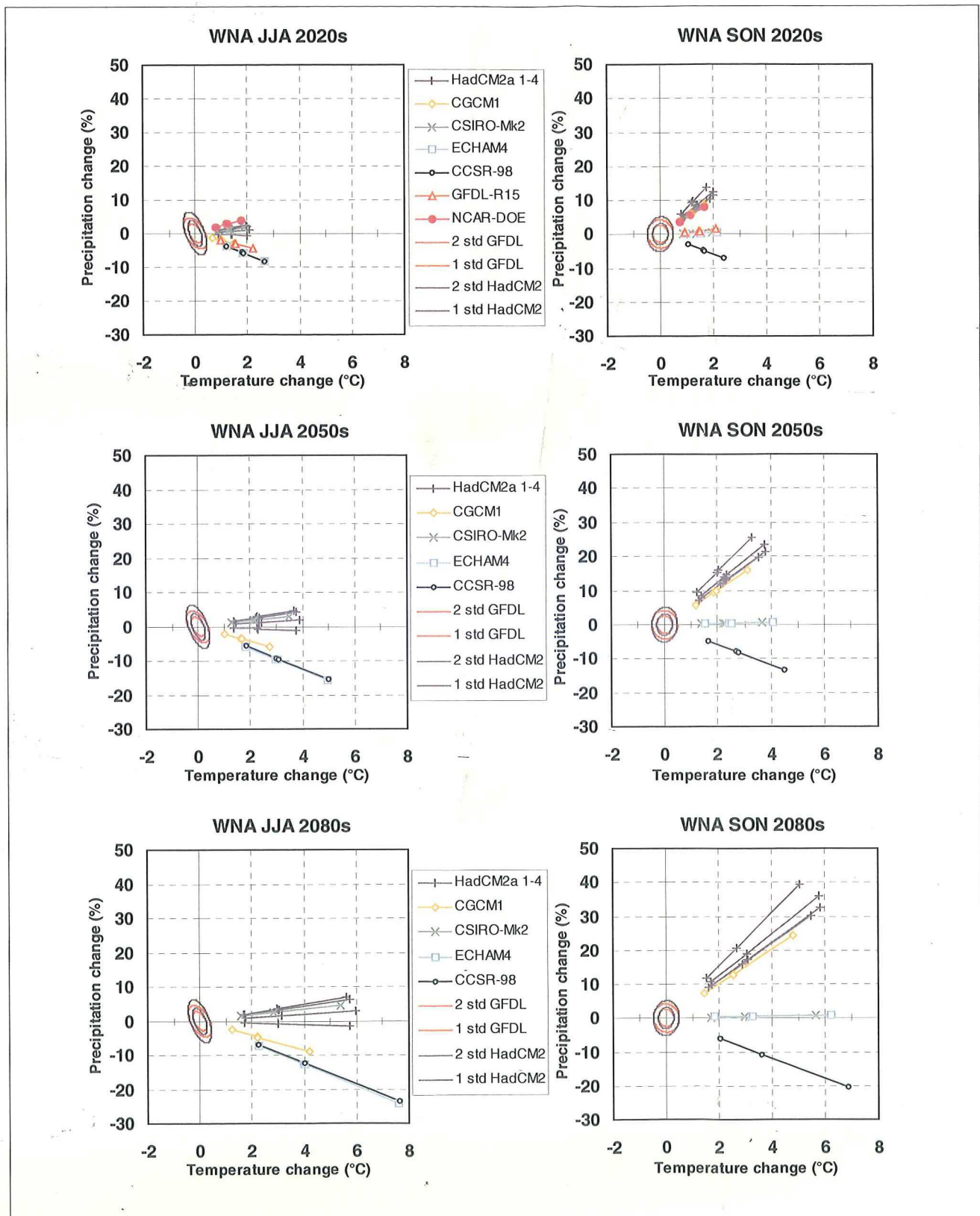
Figure B7. Western North America - June-August and September-November
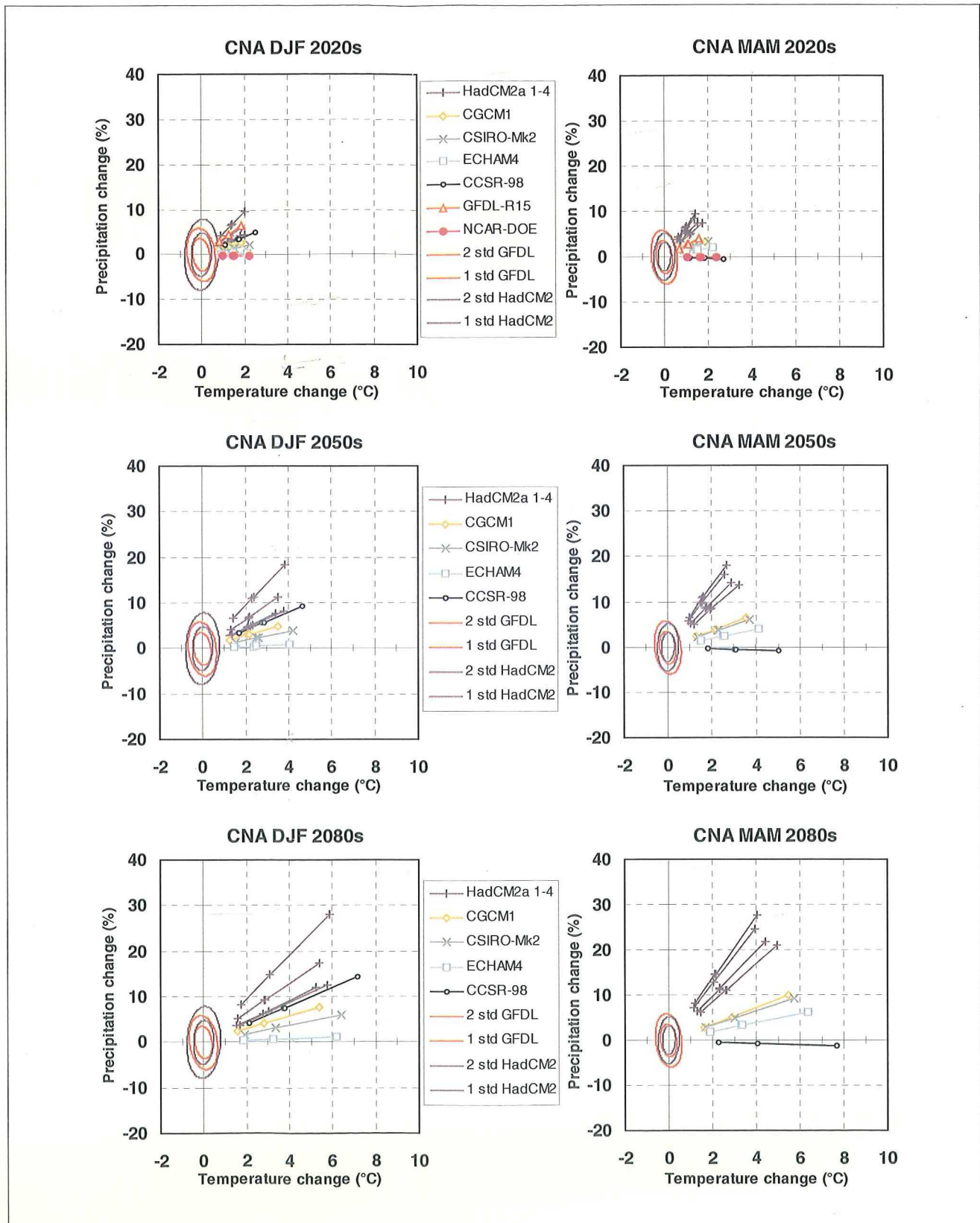
Figure B8. Central North America - December-February and March-May
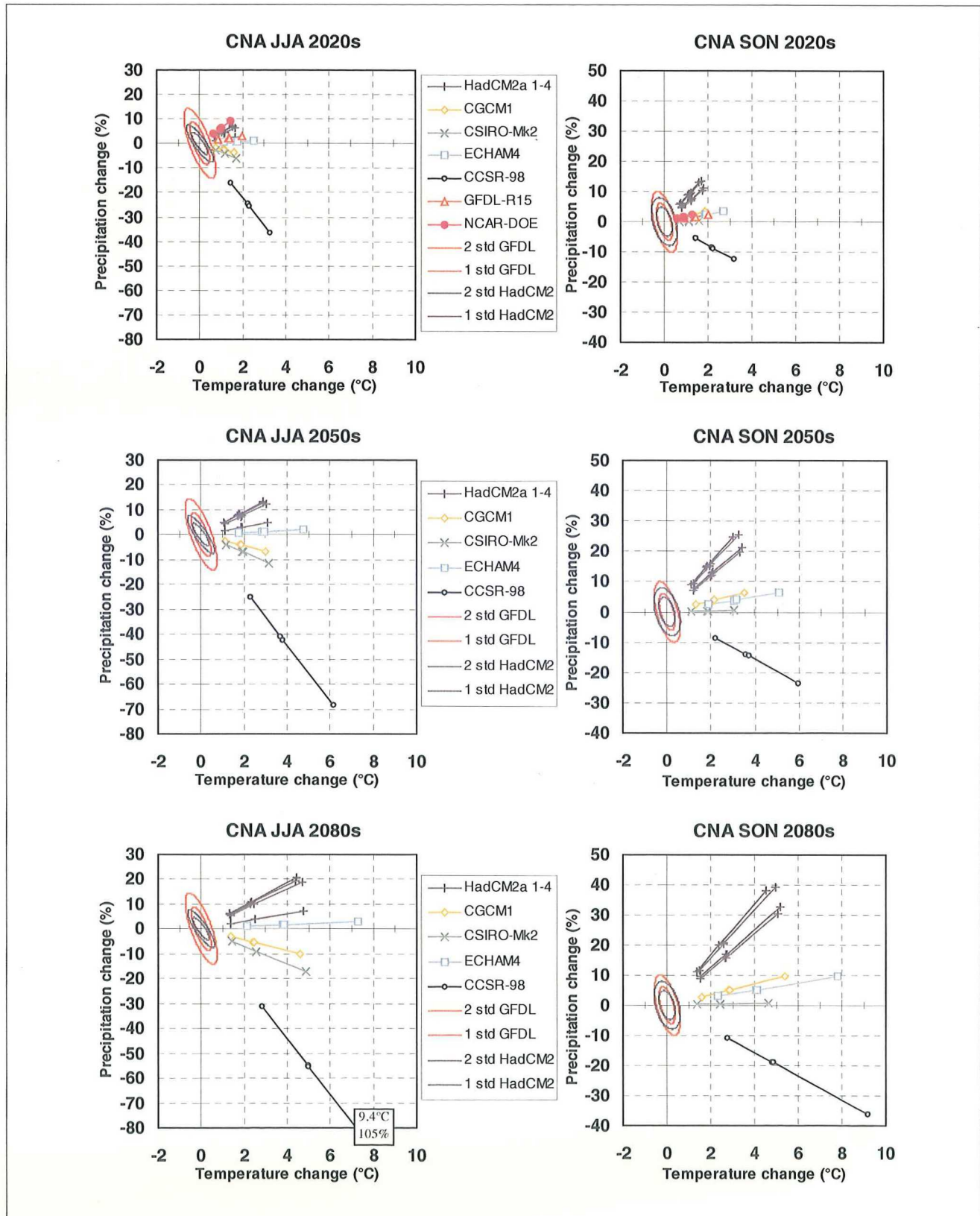
Figure B8. Central North America - June-August and September-November
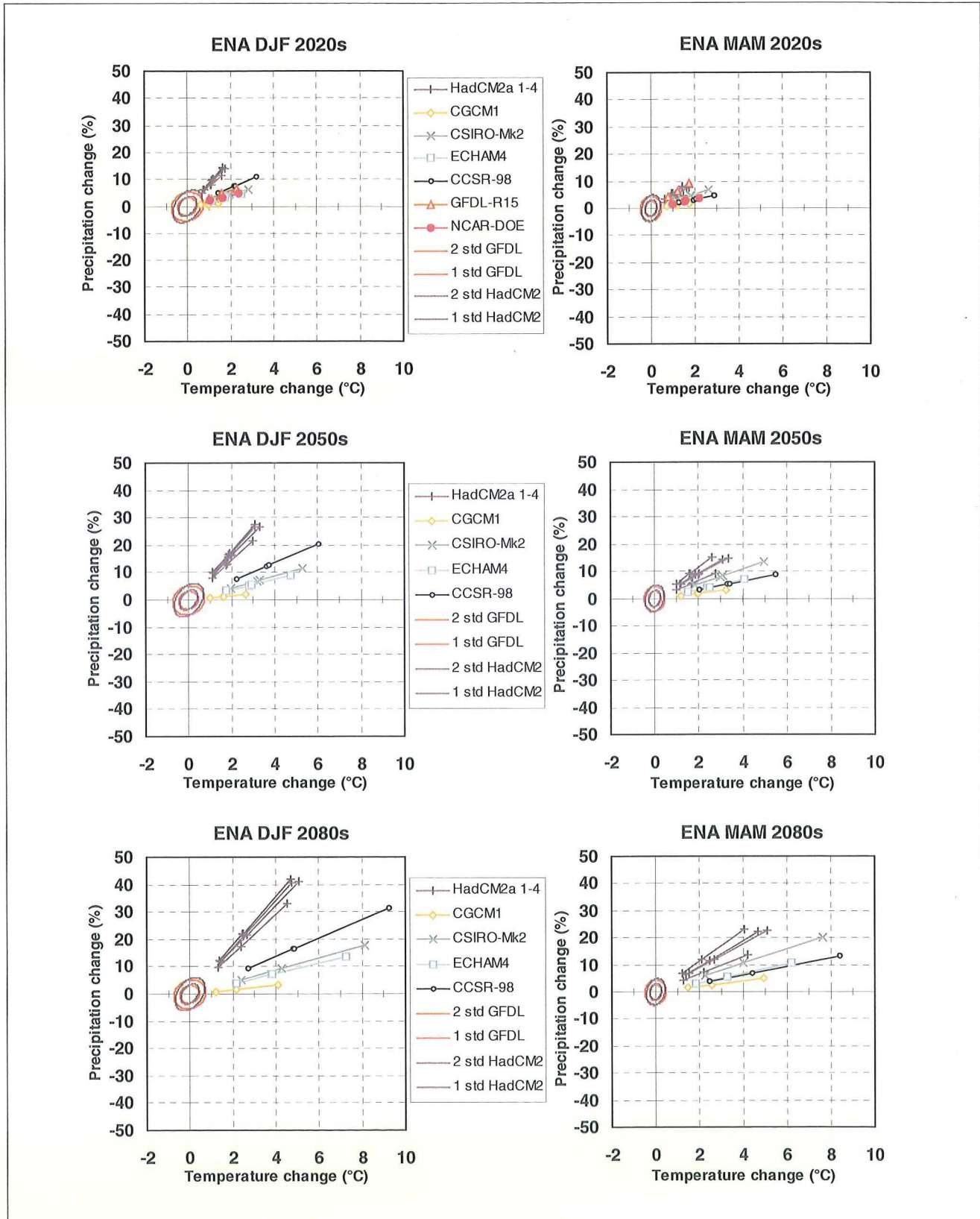
Figure B9. Eastern North America - December-February and March-May
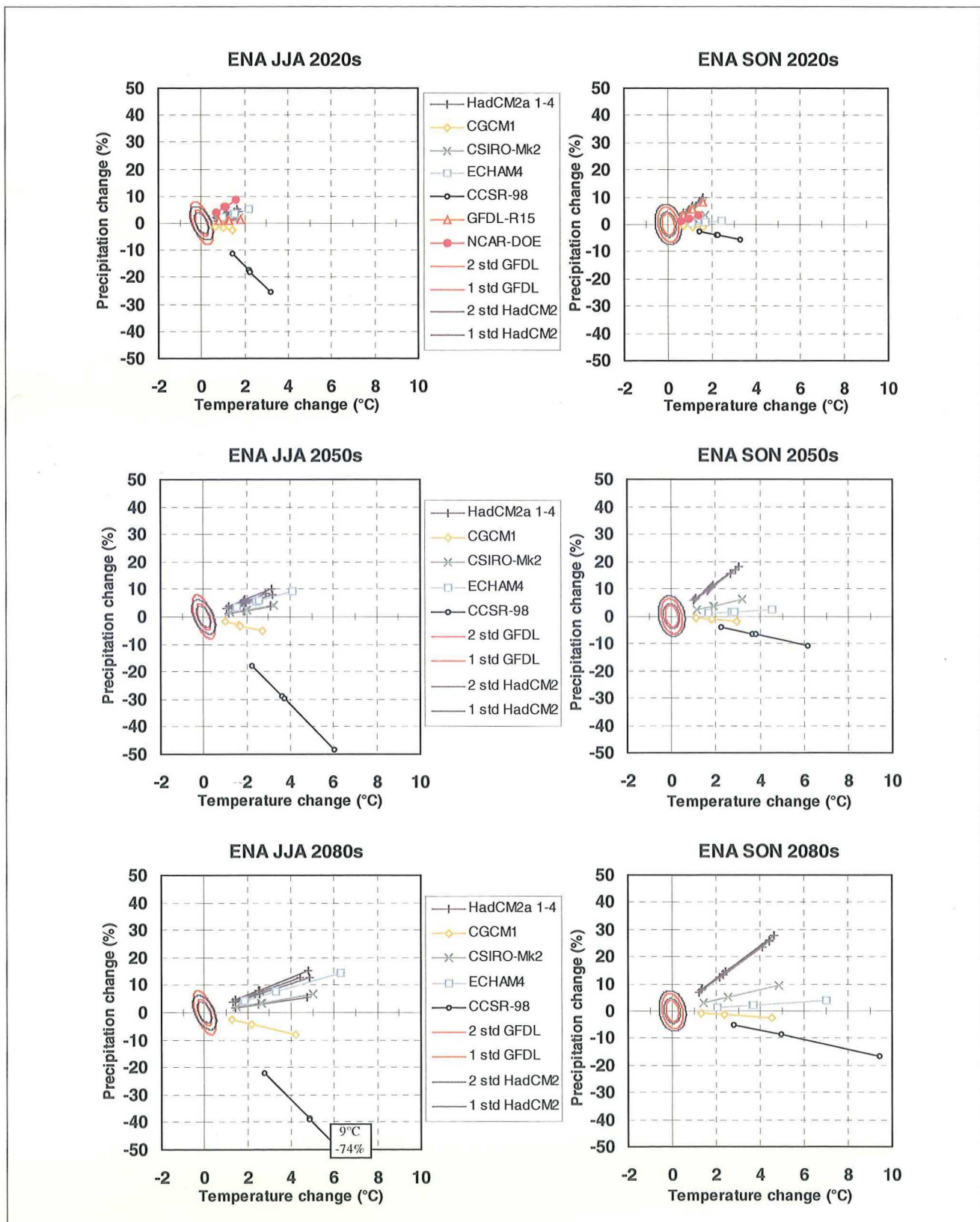
Figure B9. Eastern North America - June-August and September-November
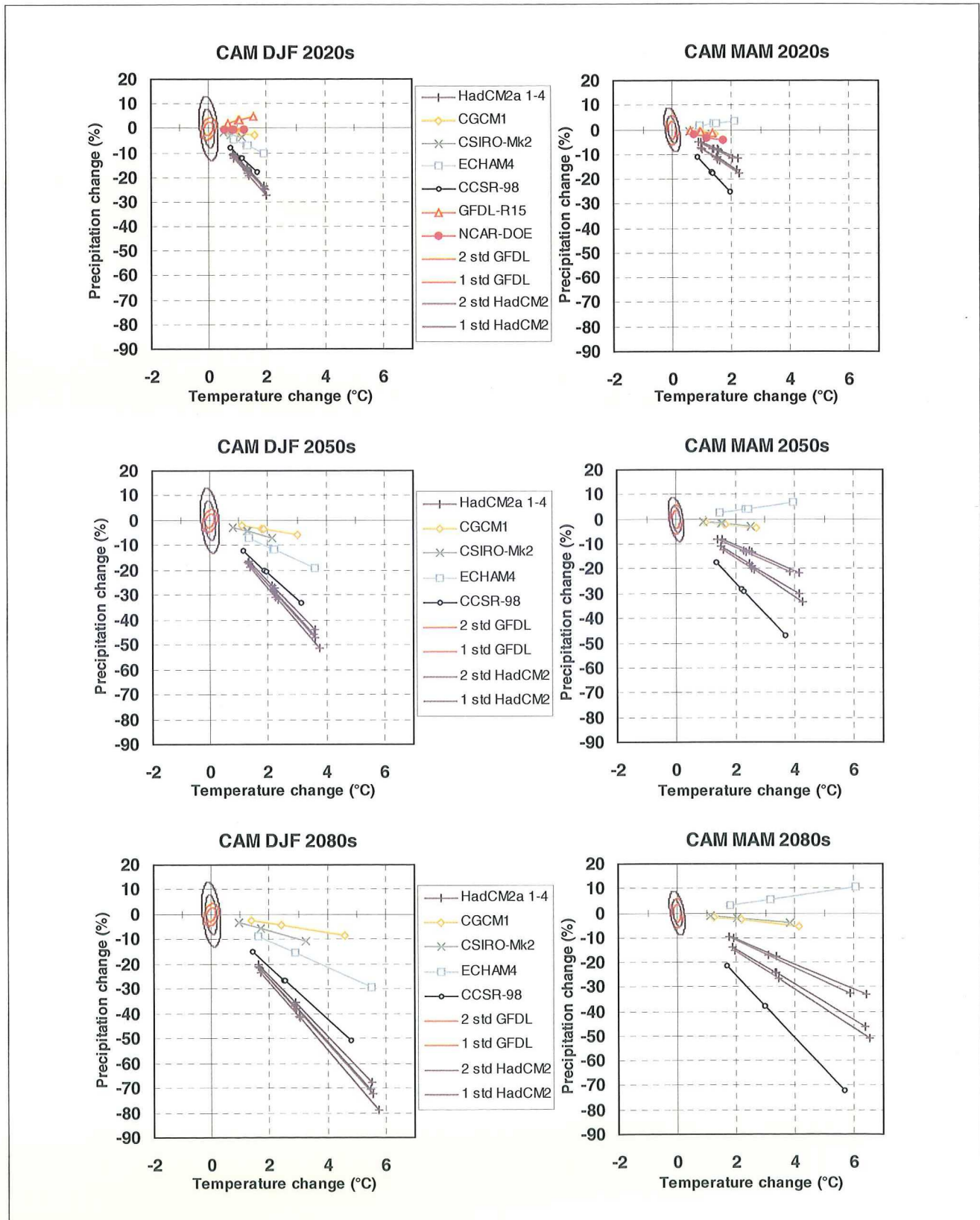
Figure B10. *Central America - December-February and March-May*
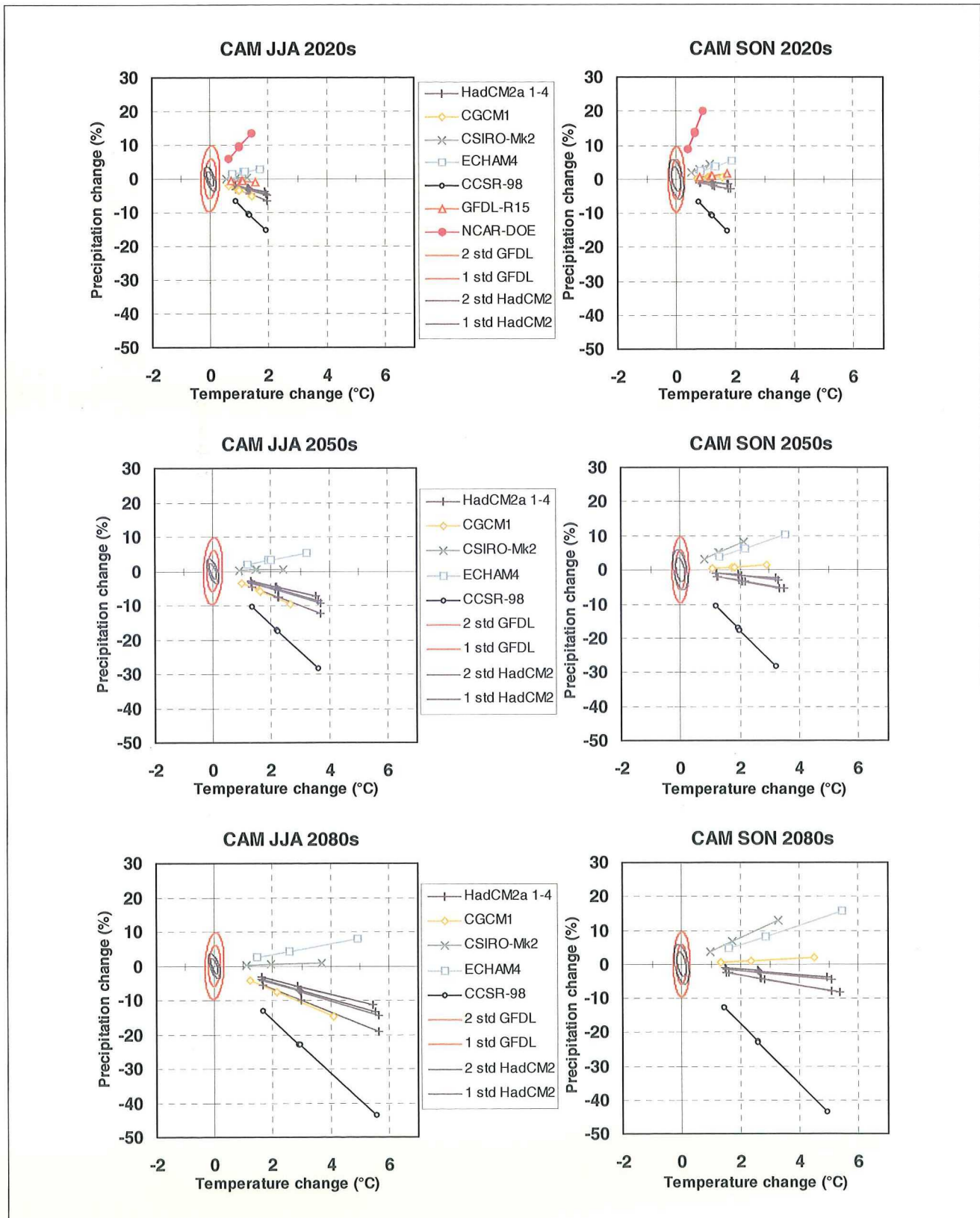
Figure B10. Central America - June-August and September-November
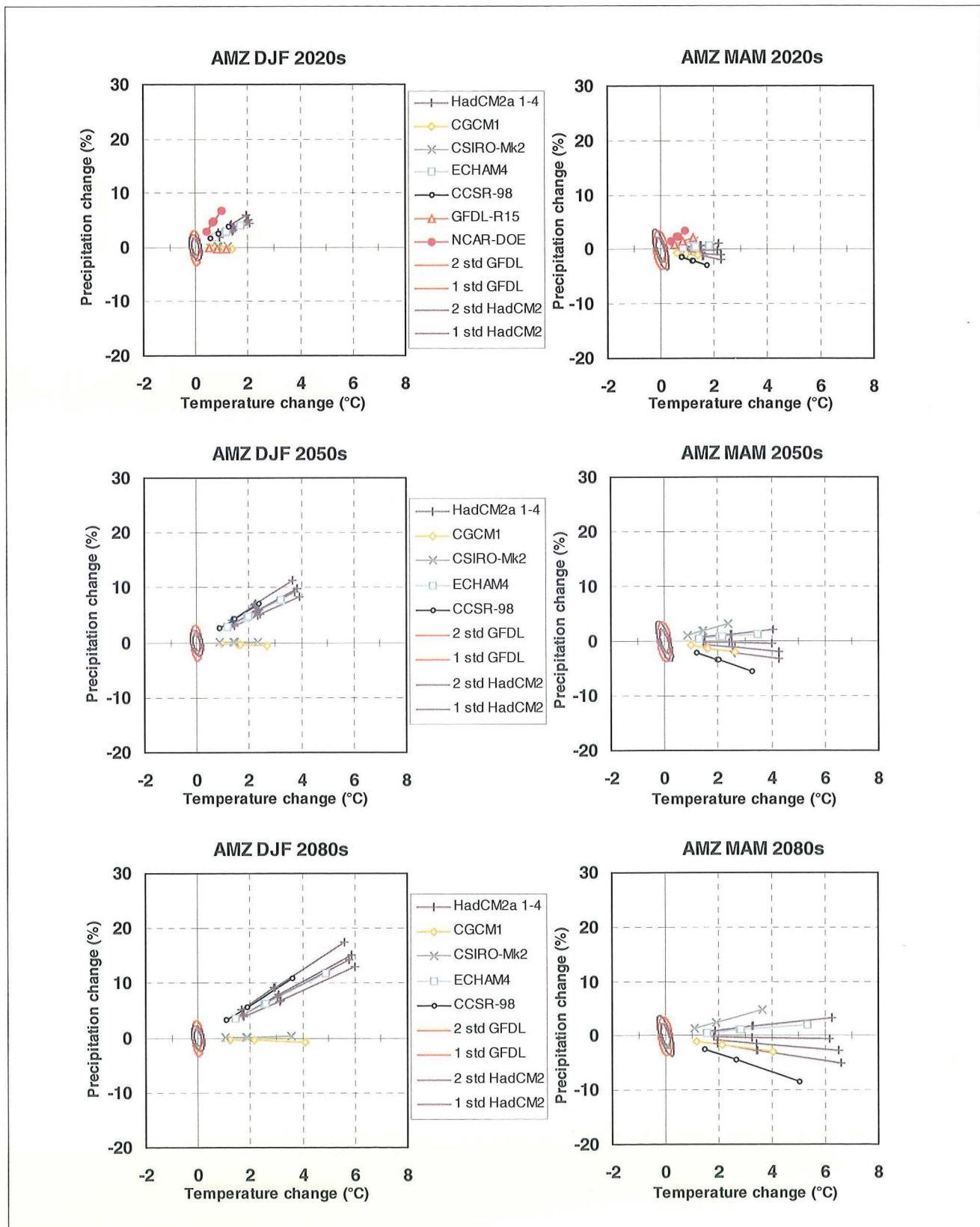
Figure B11. Amazonia - December-February and March-May
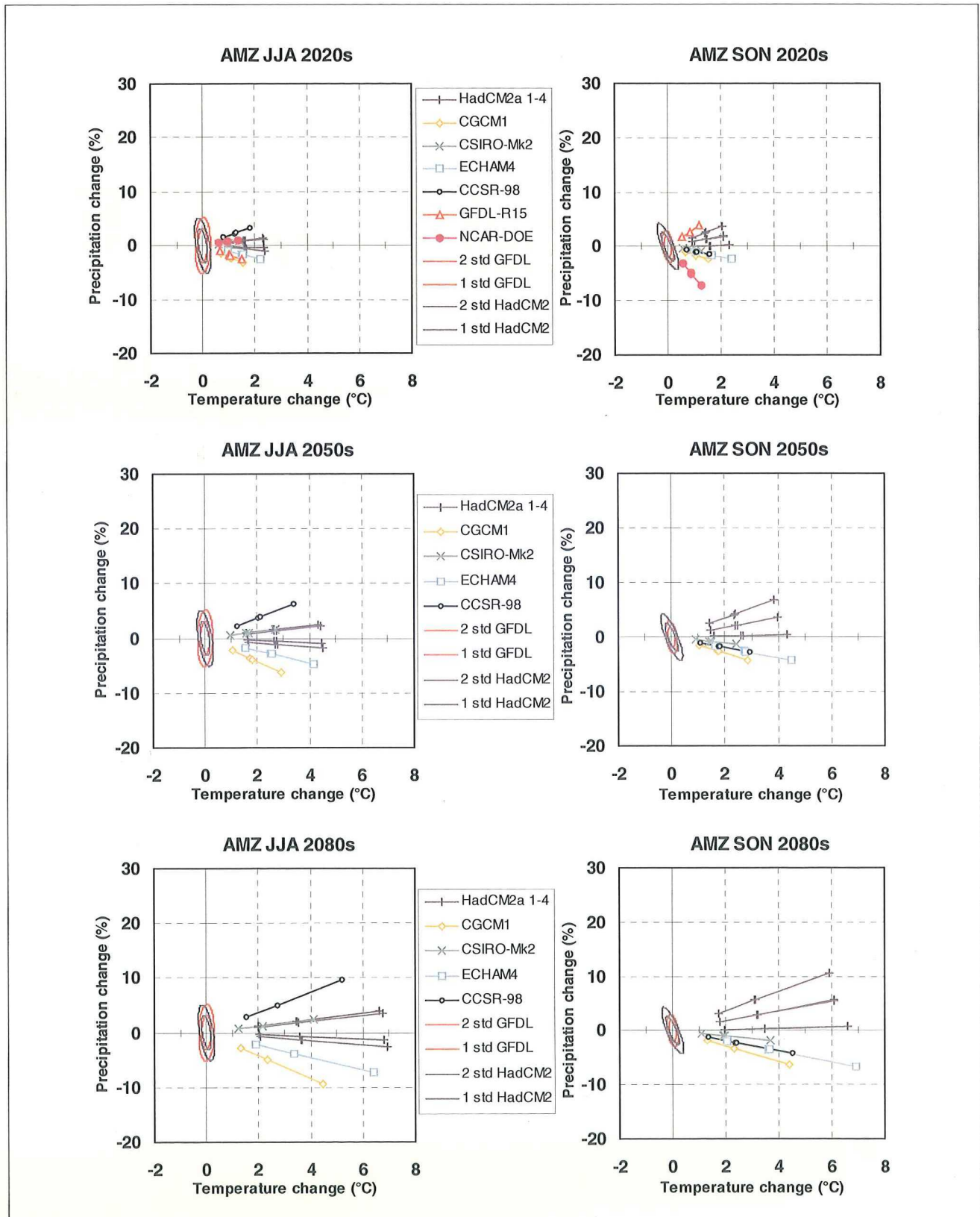
Figure B11. Amazonia - June-August and September-November
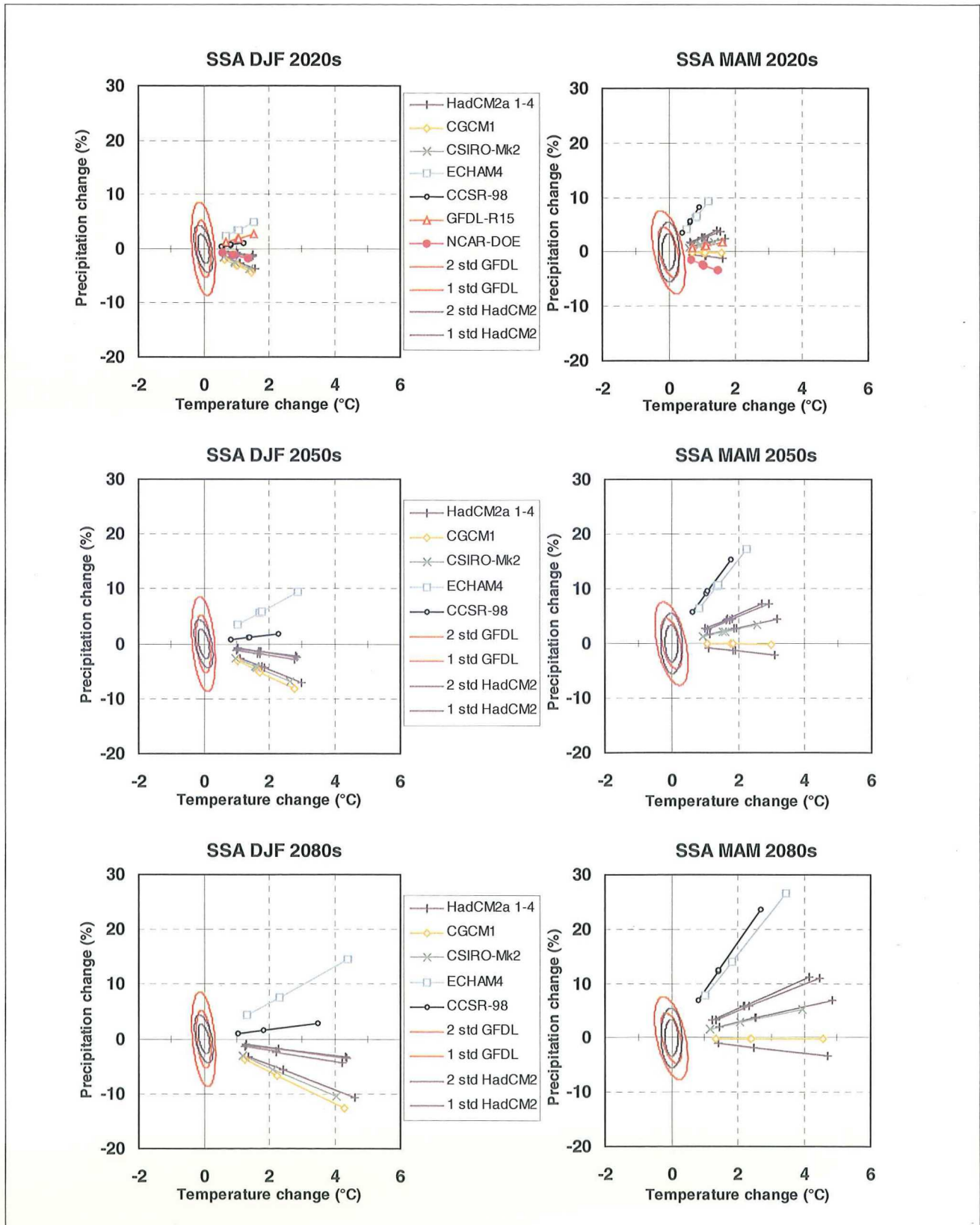
*Figure B12. Southern South America - December-February and March-May*
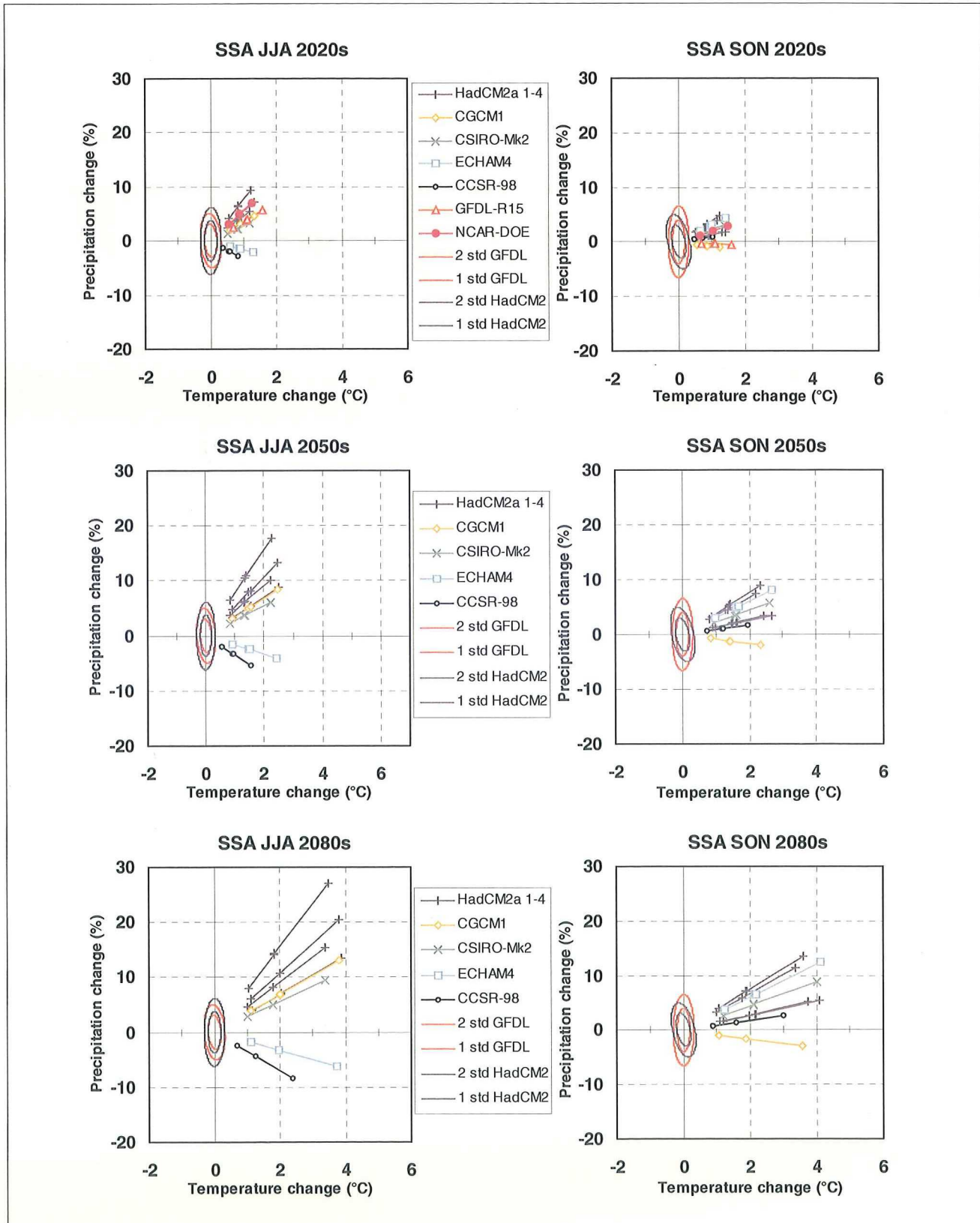
Figure B12. Southern South America - June-August and September-November
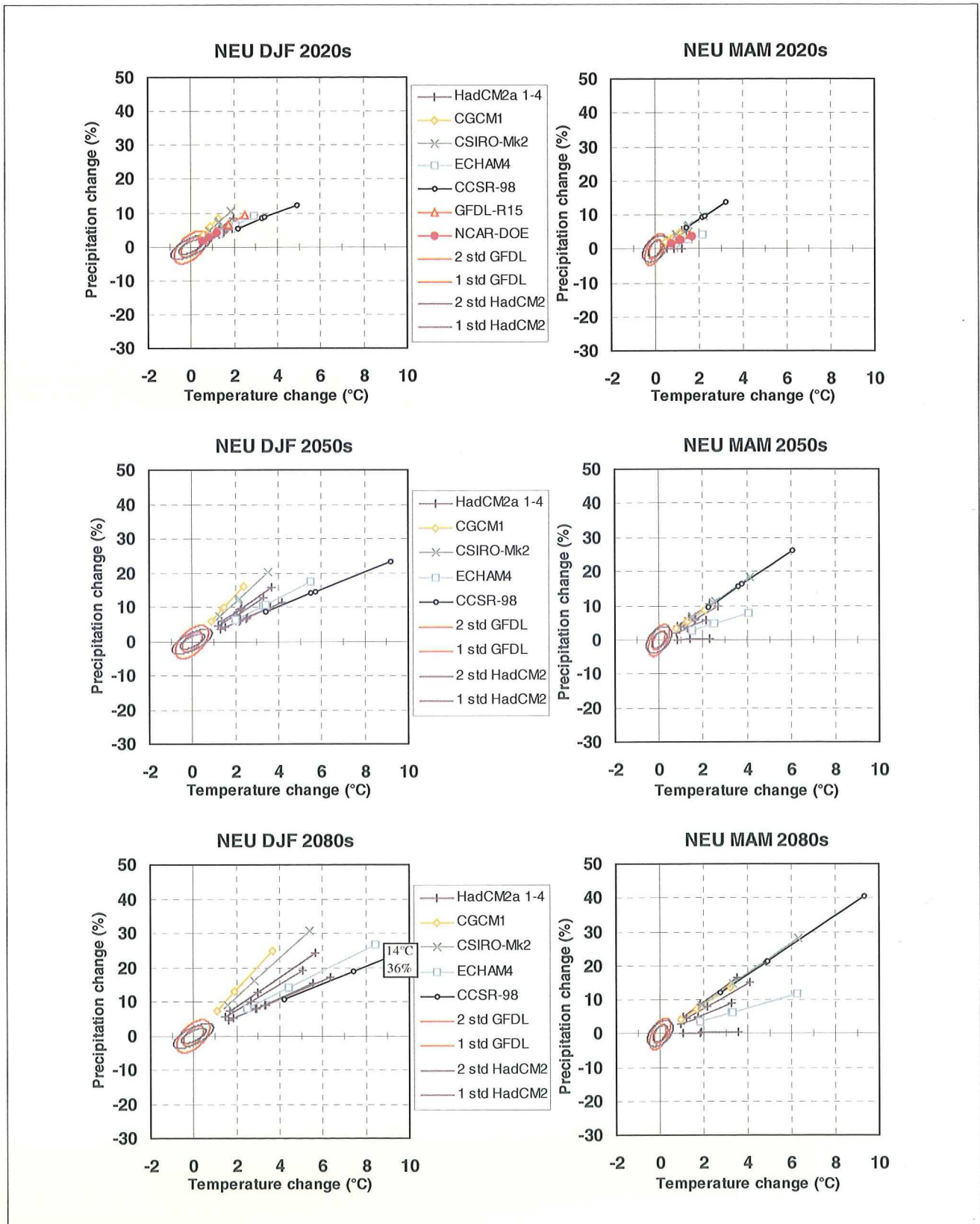
Figure B13. Northern Europe - December-February and March-May

NEU JJA 2020s

NEU SON 2020s

NEU JJA 2050s

NEU SON 2050s

NEU JJA 2080s

NEU SON 2080s
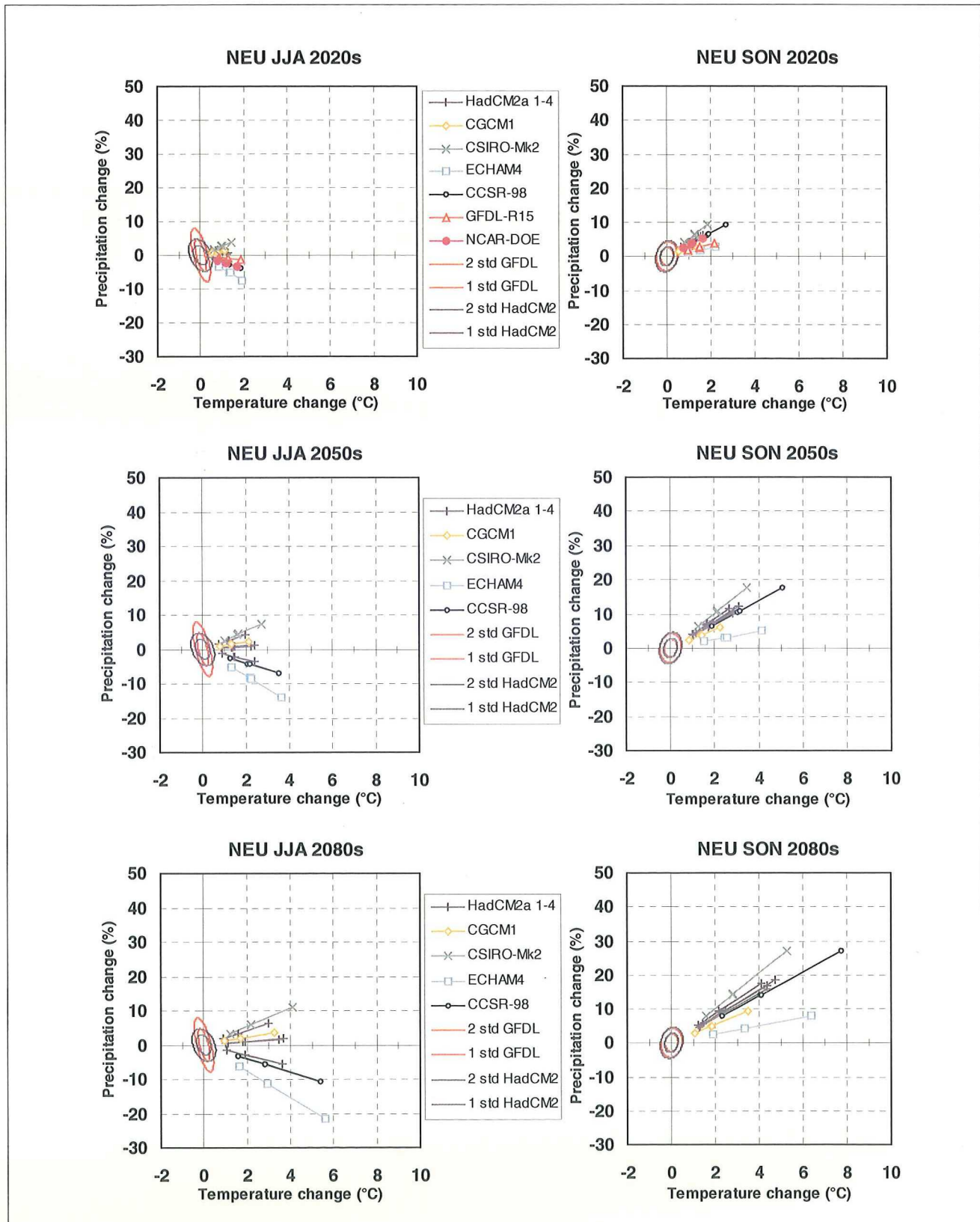
Figure B13. Northern Europe - June-August and September-November
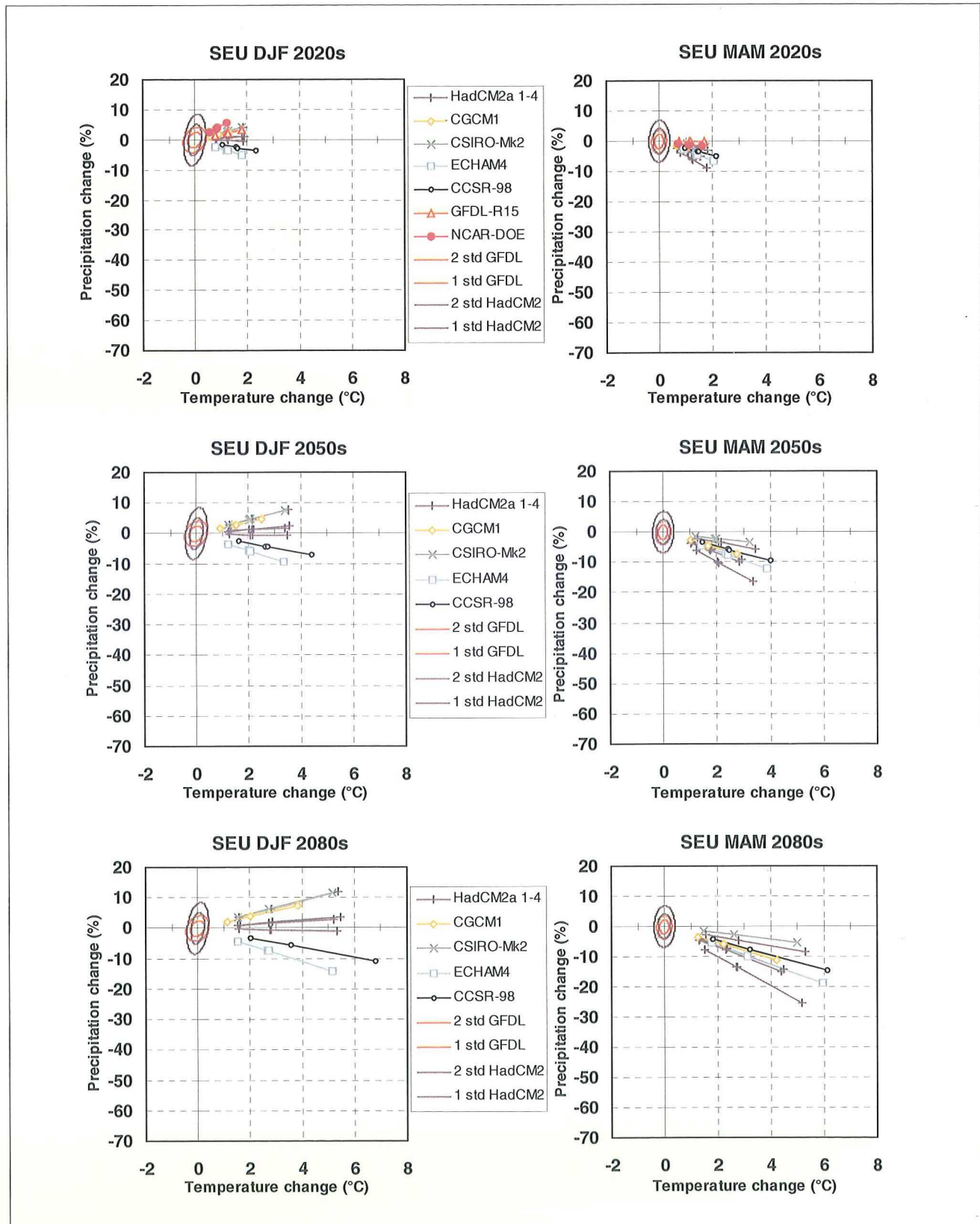
Figure B14. Southern Europe/North Africa - December-February and March-May
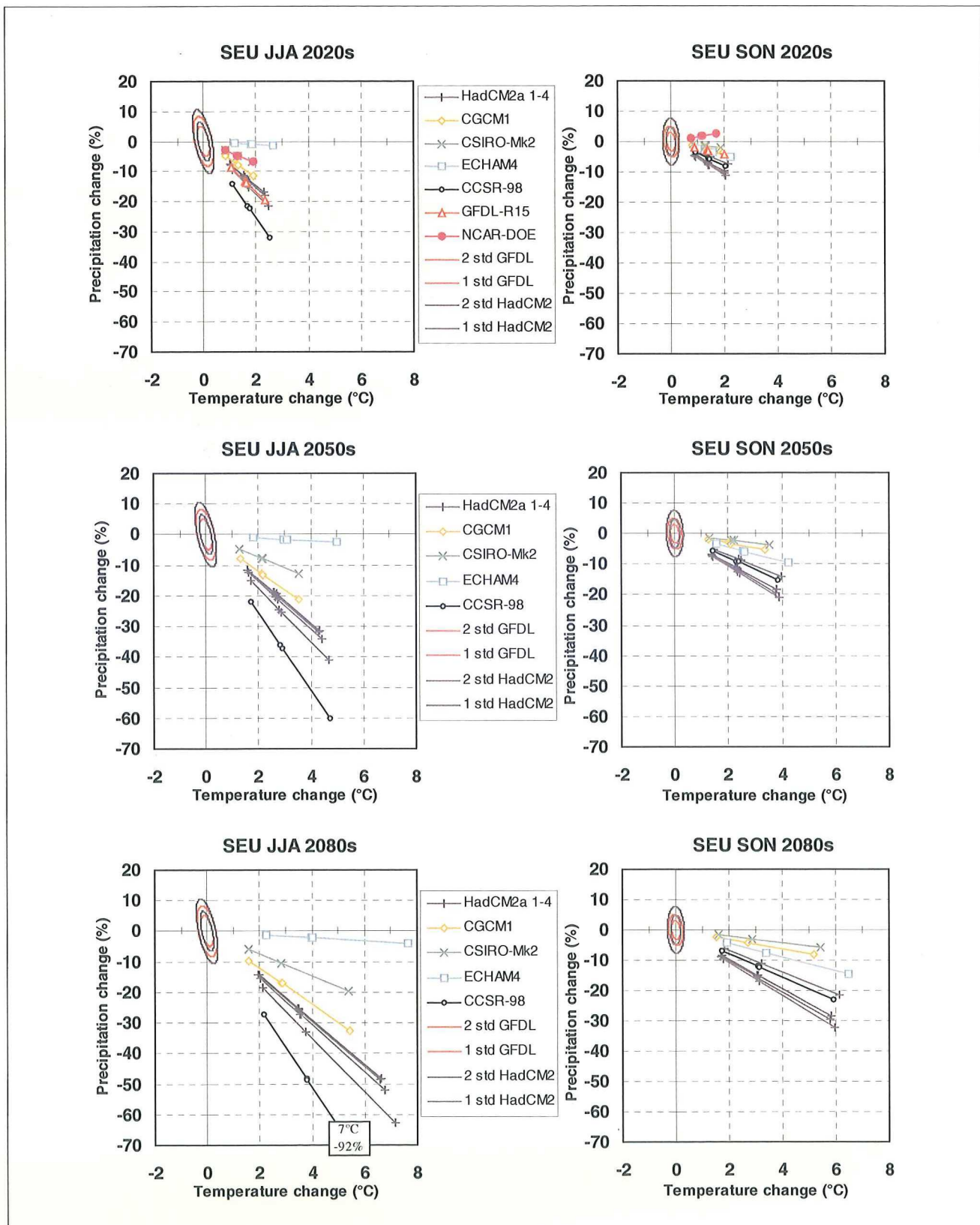
Figure B14. Southern Europe/North Africa - June-August and September-November
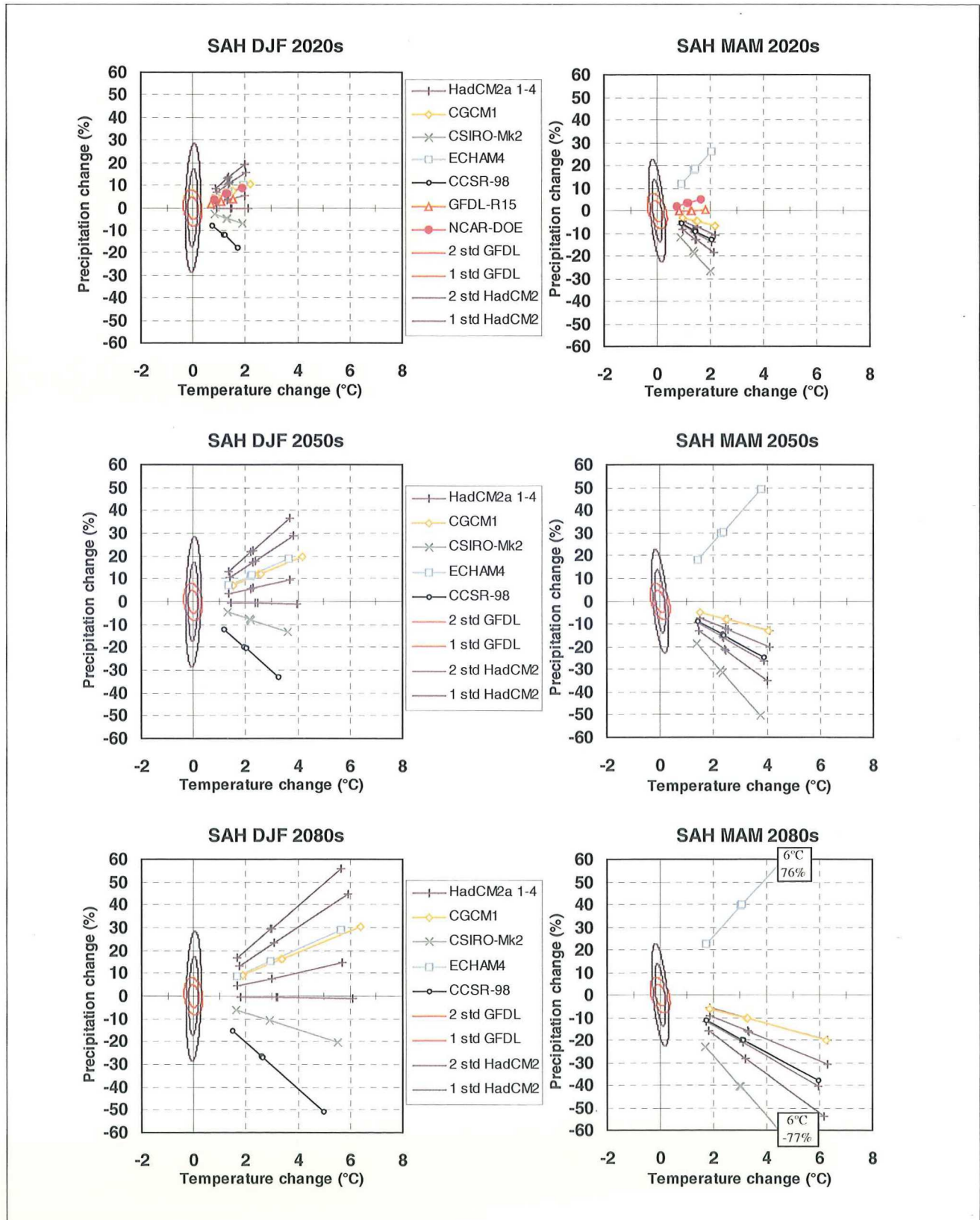
Figure B15. Sahara - December-February and March-May
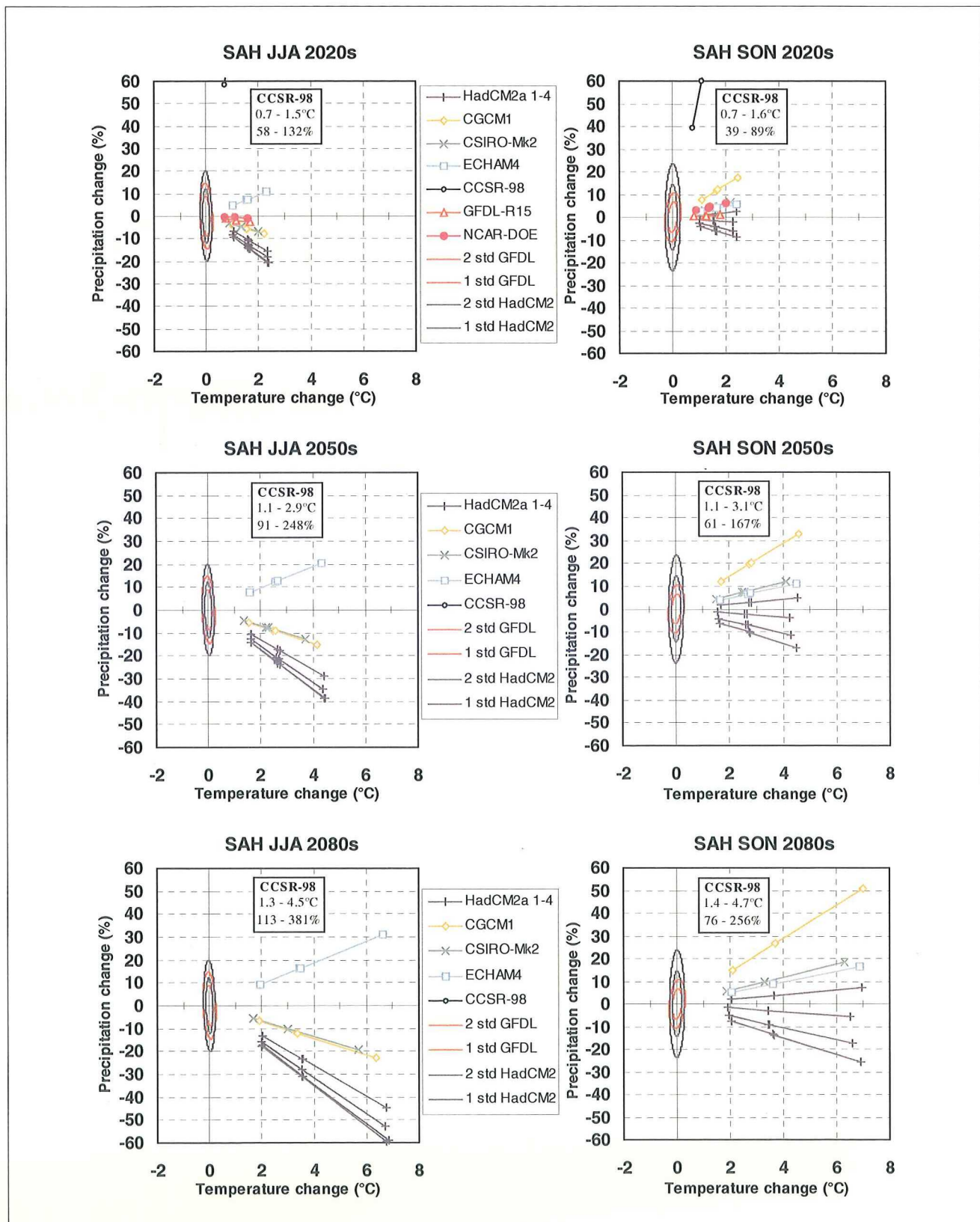
Figure B15. Sahara - June-August and September-November
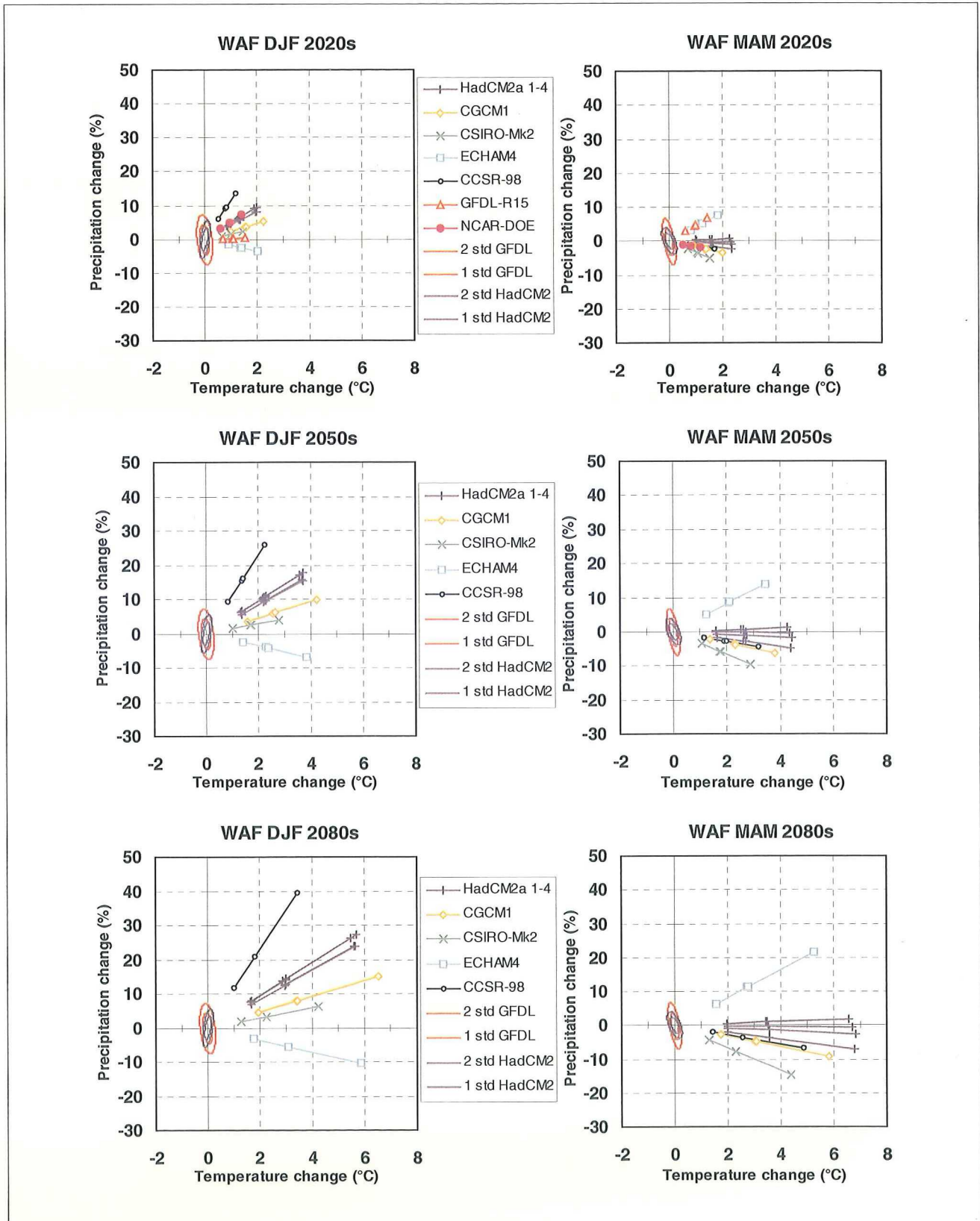
Figure B16. West Africa - December-February and March-May
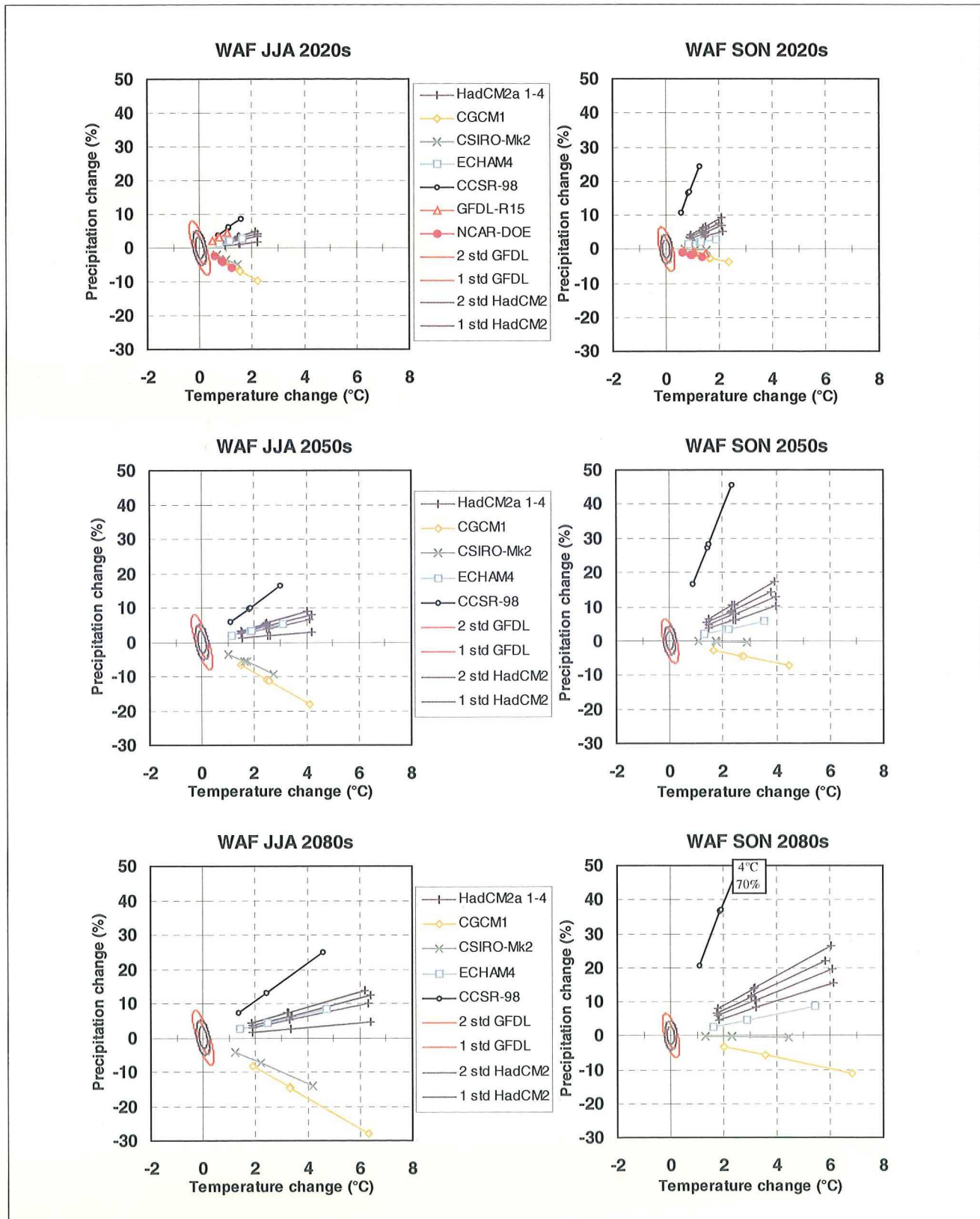
Figure B16. West Africa - June-August and September-November
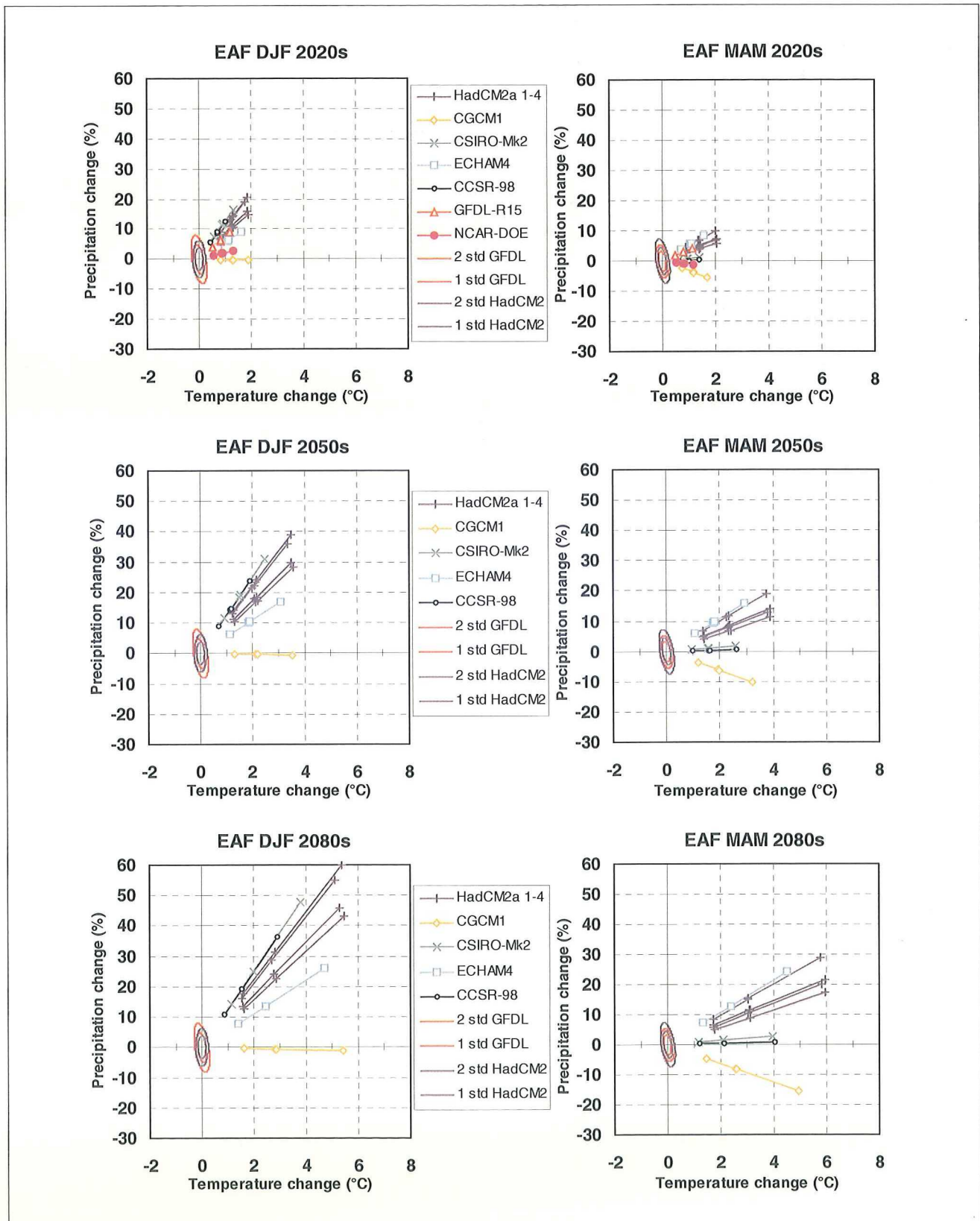
Figure B17. East Africa - December-February and March-May
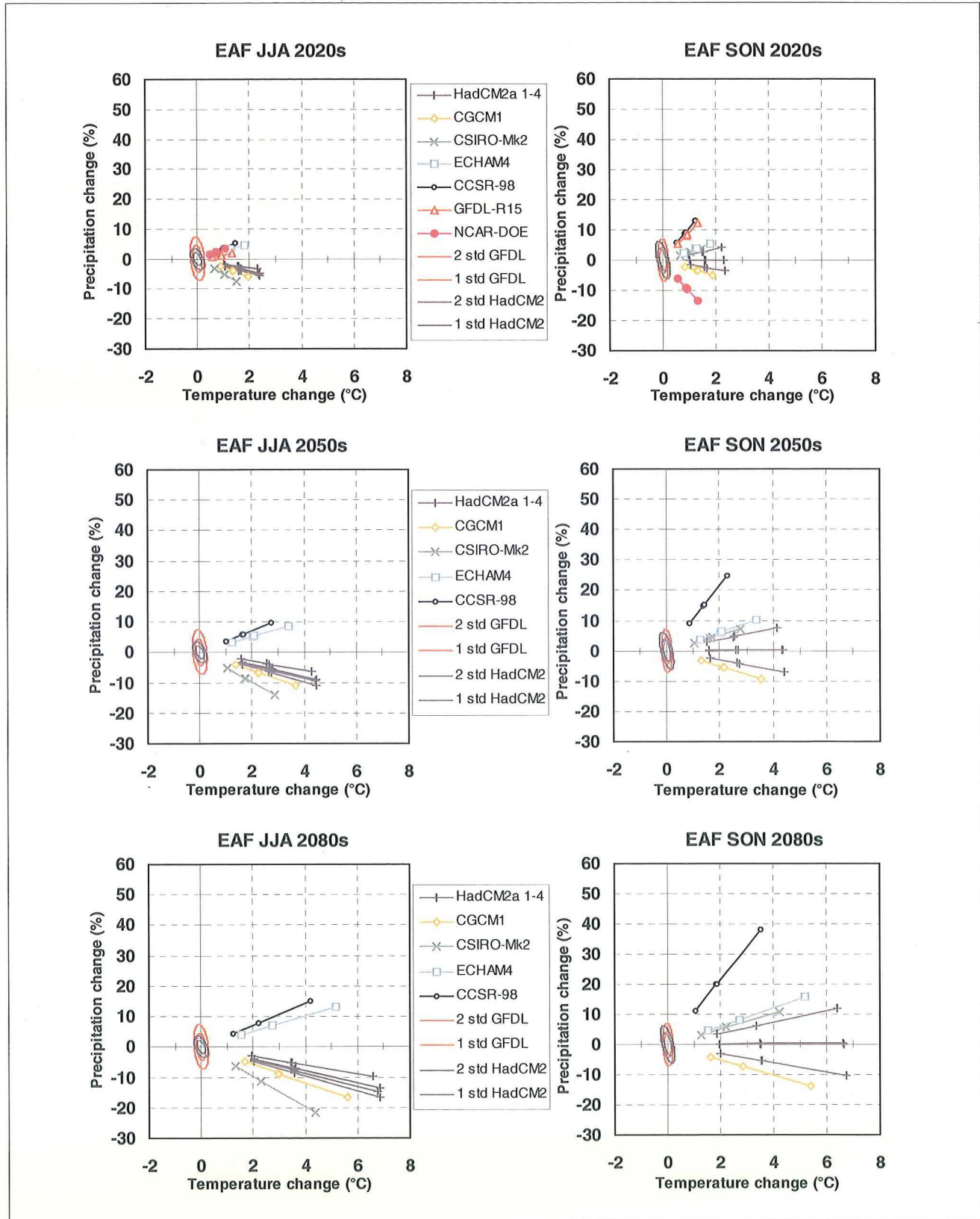
Figure B17. East Africa - June-August and September-November
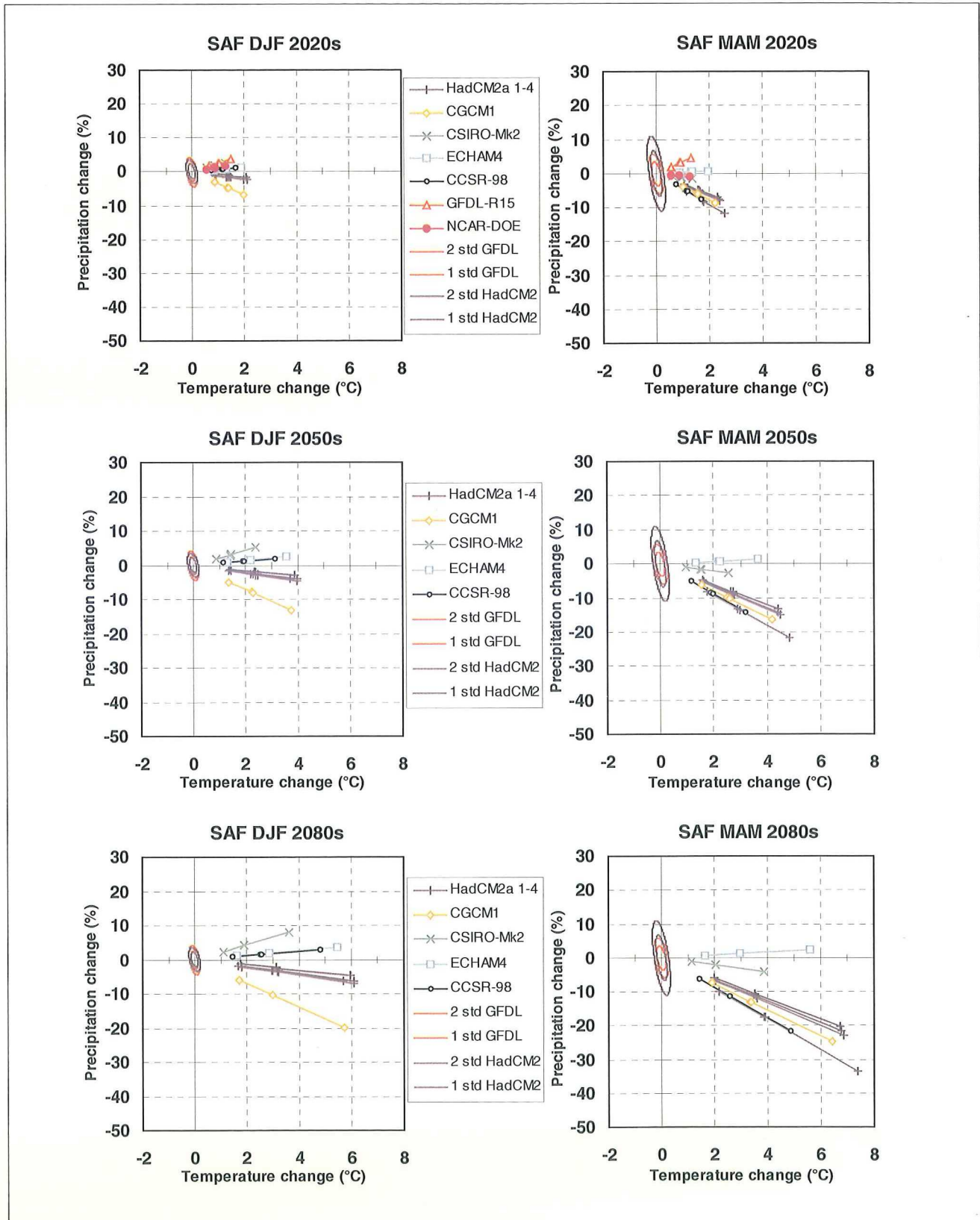
Figure B18. Southern Africa - December-February and March-May
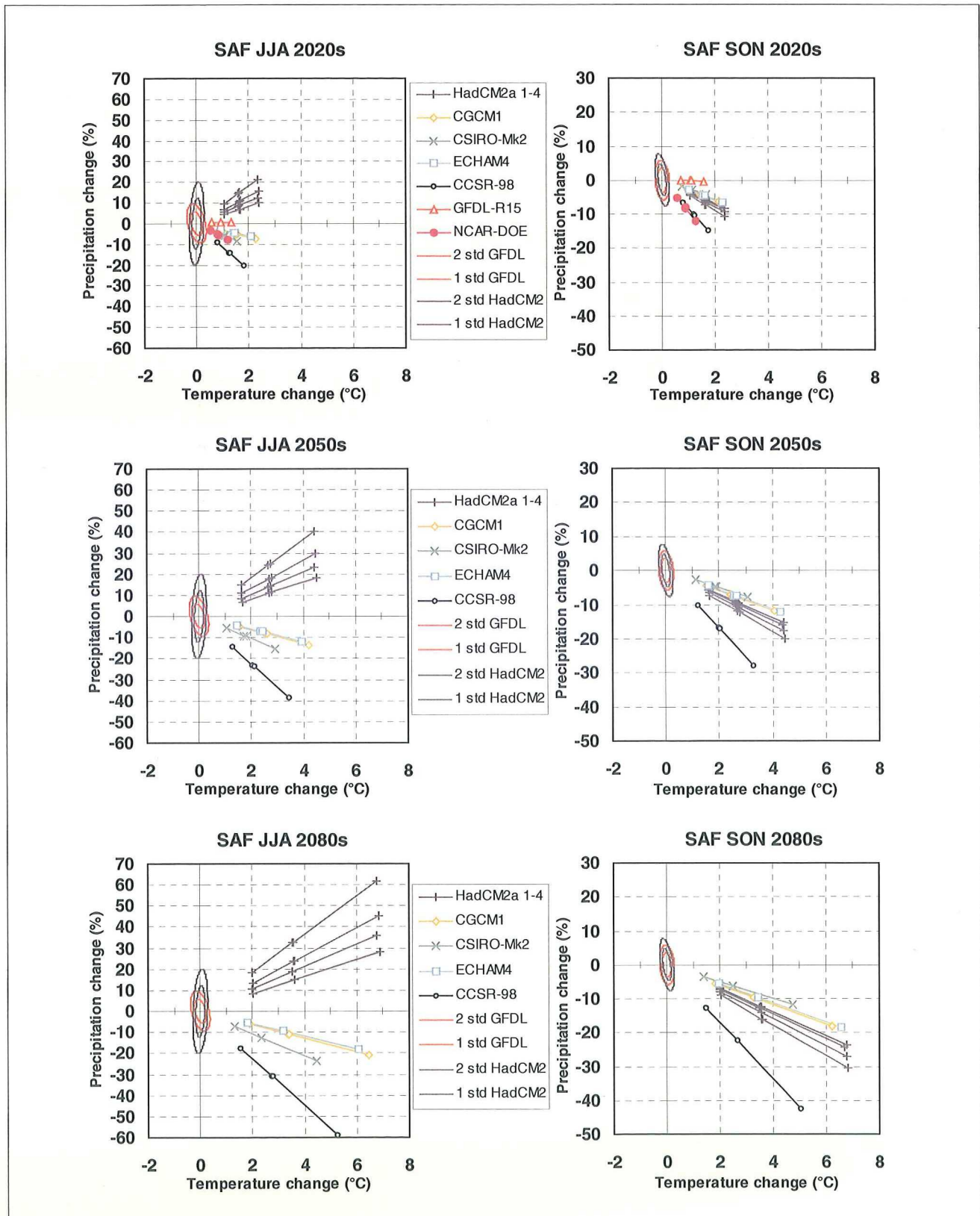
Figure B18. Southern Africa - June-August and September-November
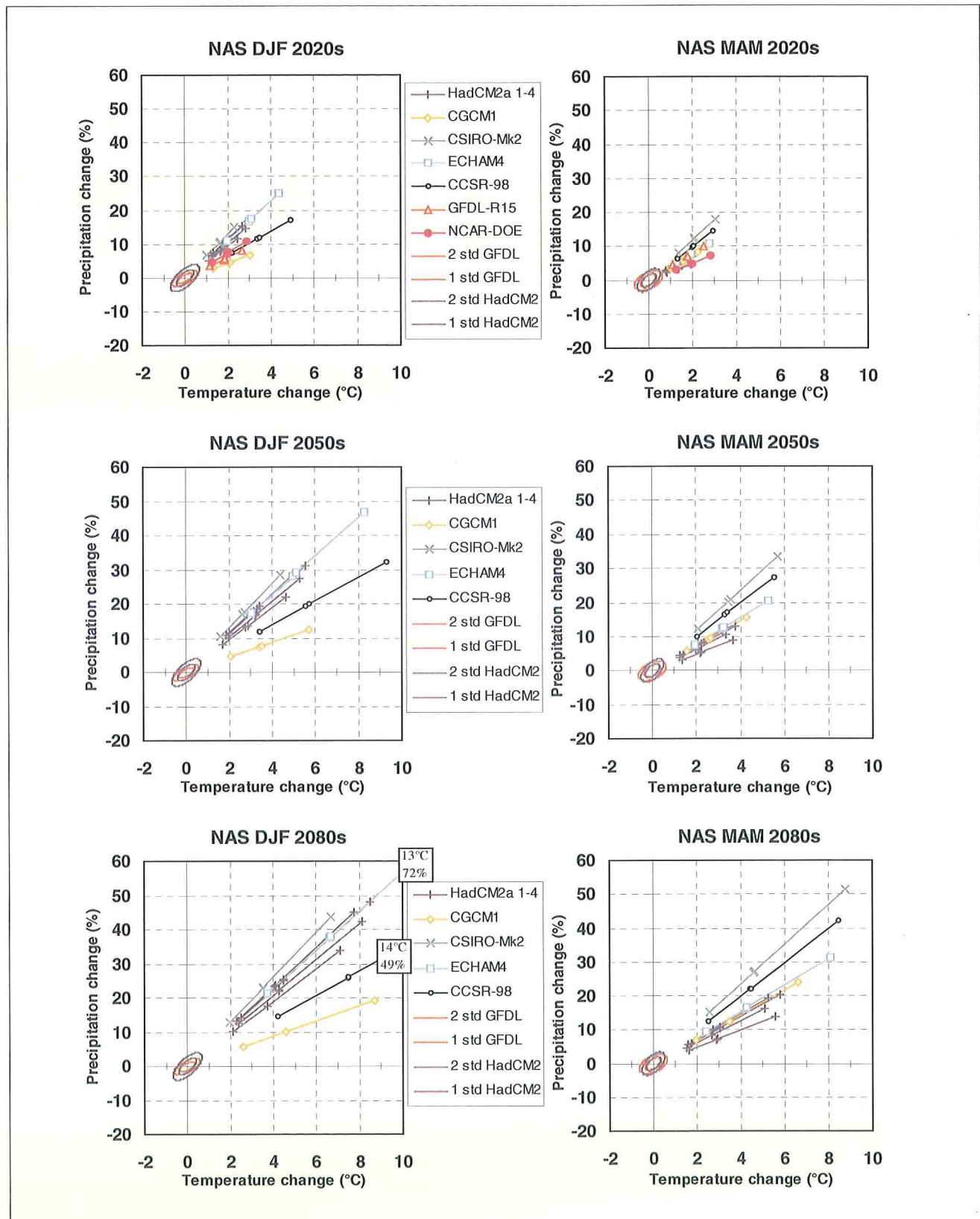
Figure B19. Northern Asia - December-February and March-May
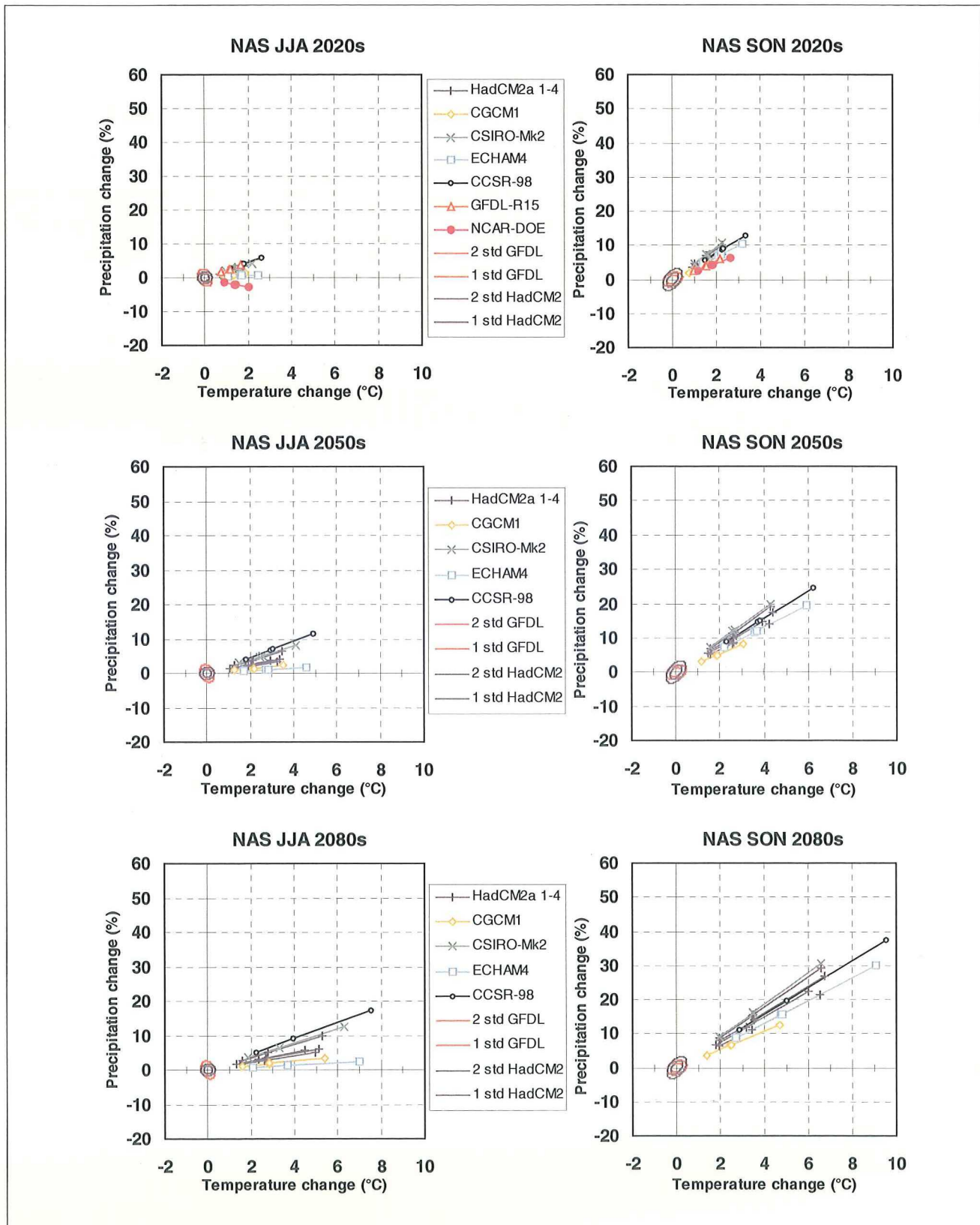
Figure B19. Northern Asia - June-August and September-November
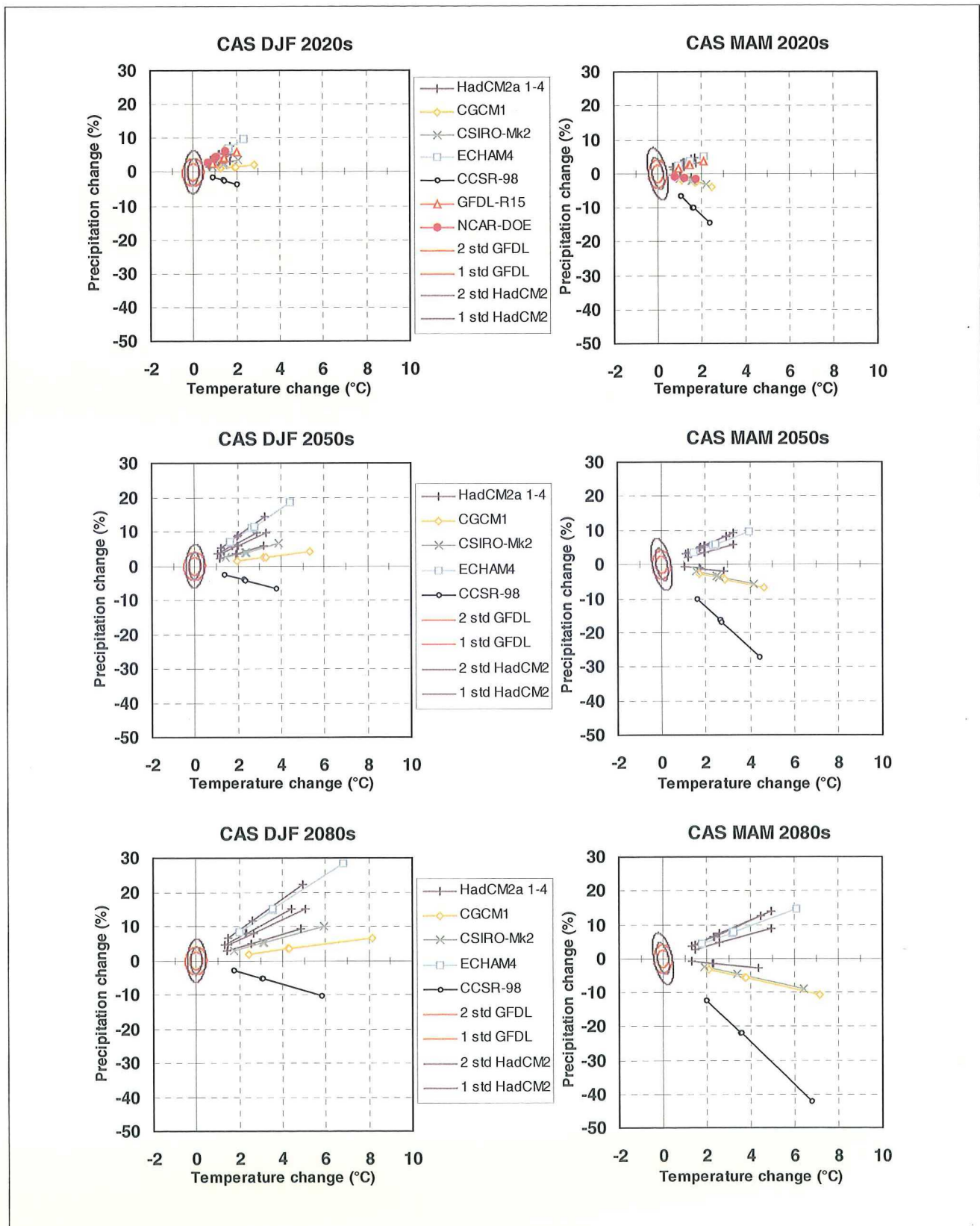
Figure B20. Central Asia - December-February and March-May
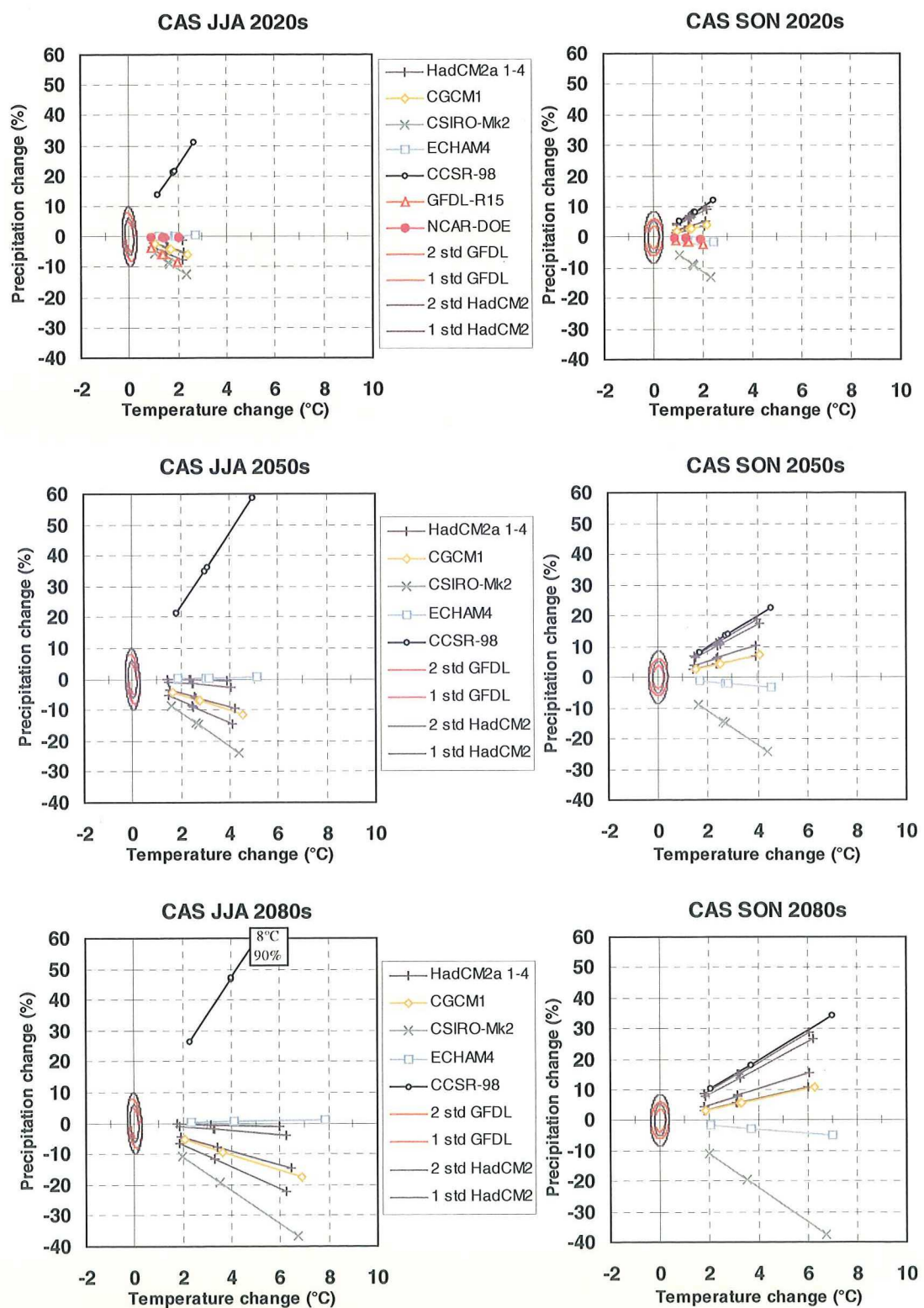
Figure B20. Central Asia - June-August and September-November
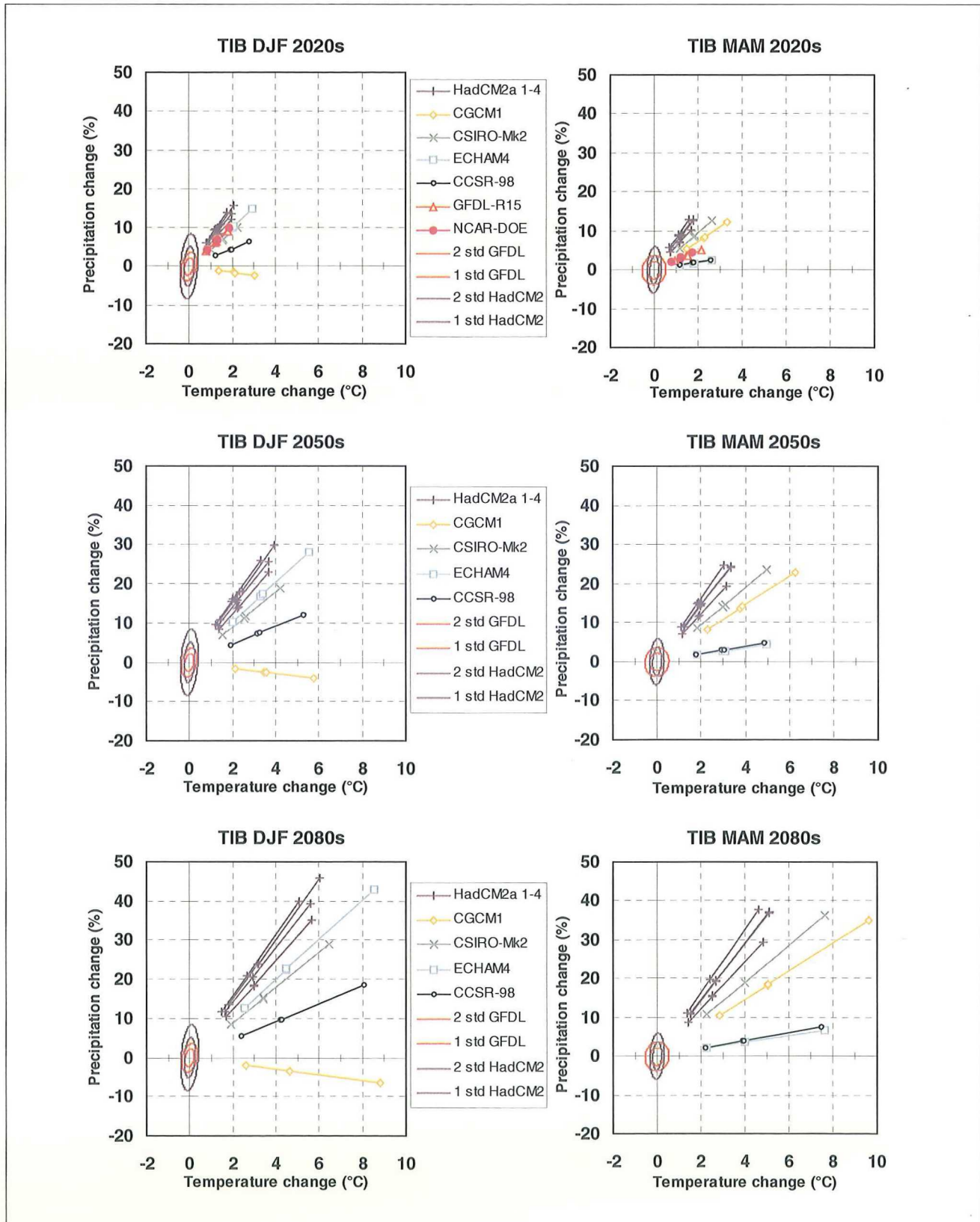
Figure B21. Tibetan Plateau - December-February and March-May
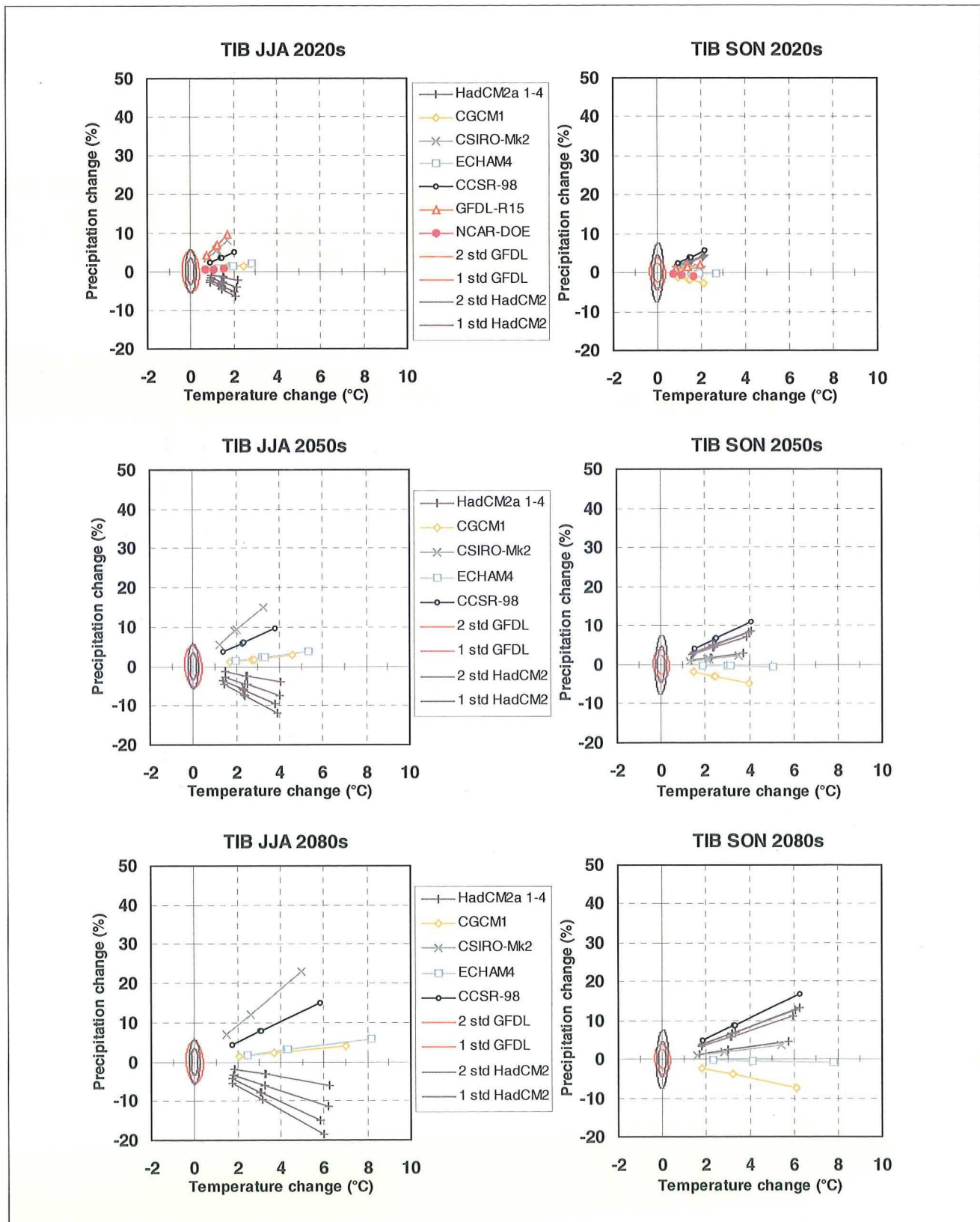
Figure B21. Tibetan Plateau - June-August and September-November
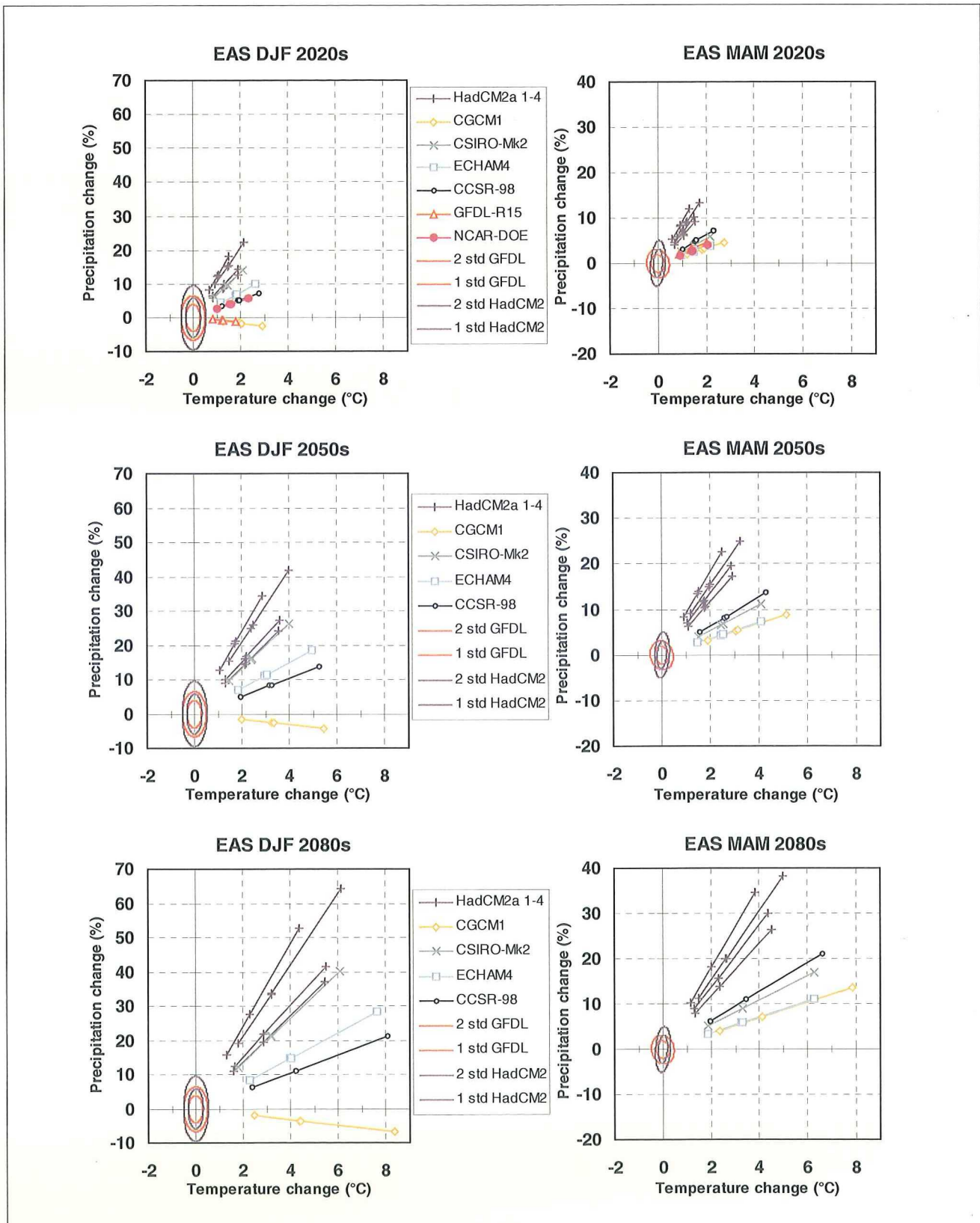
Figure B22. East Asia - December-February and March-May
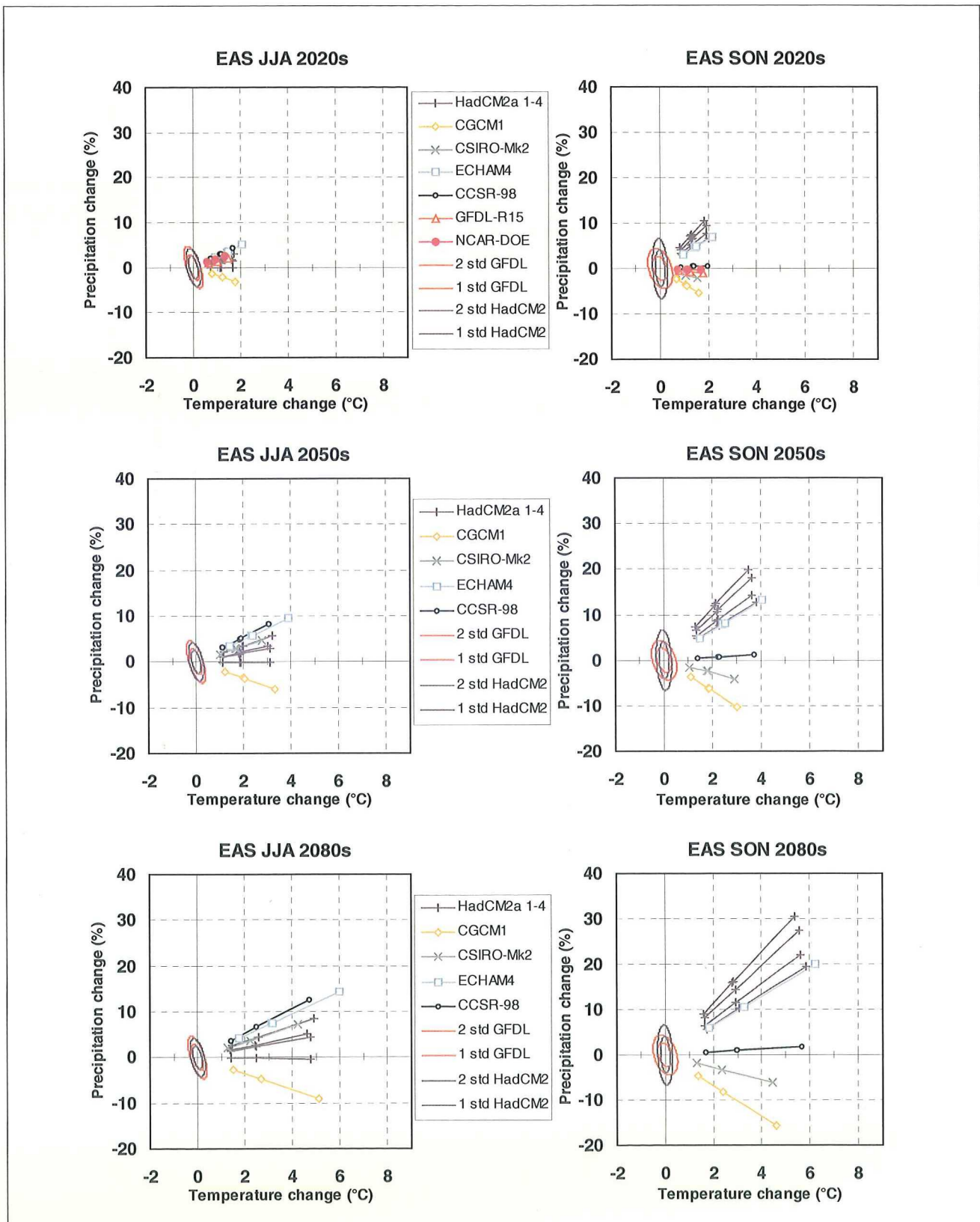
Figure B22. East Asia - June-August and September-November
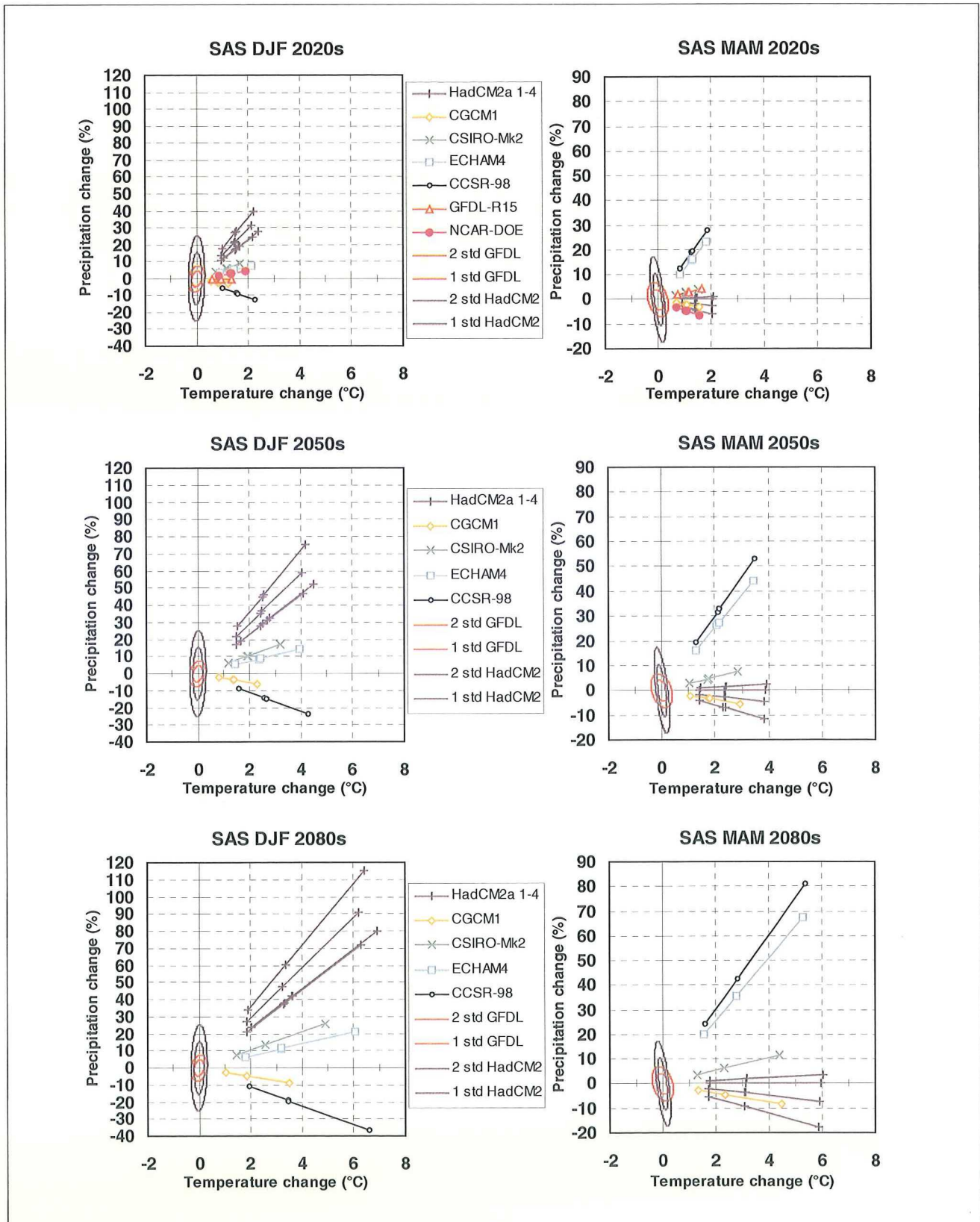
Figure B23. South Asia - December-February and March-May
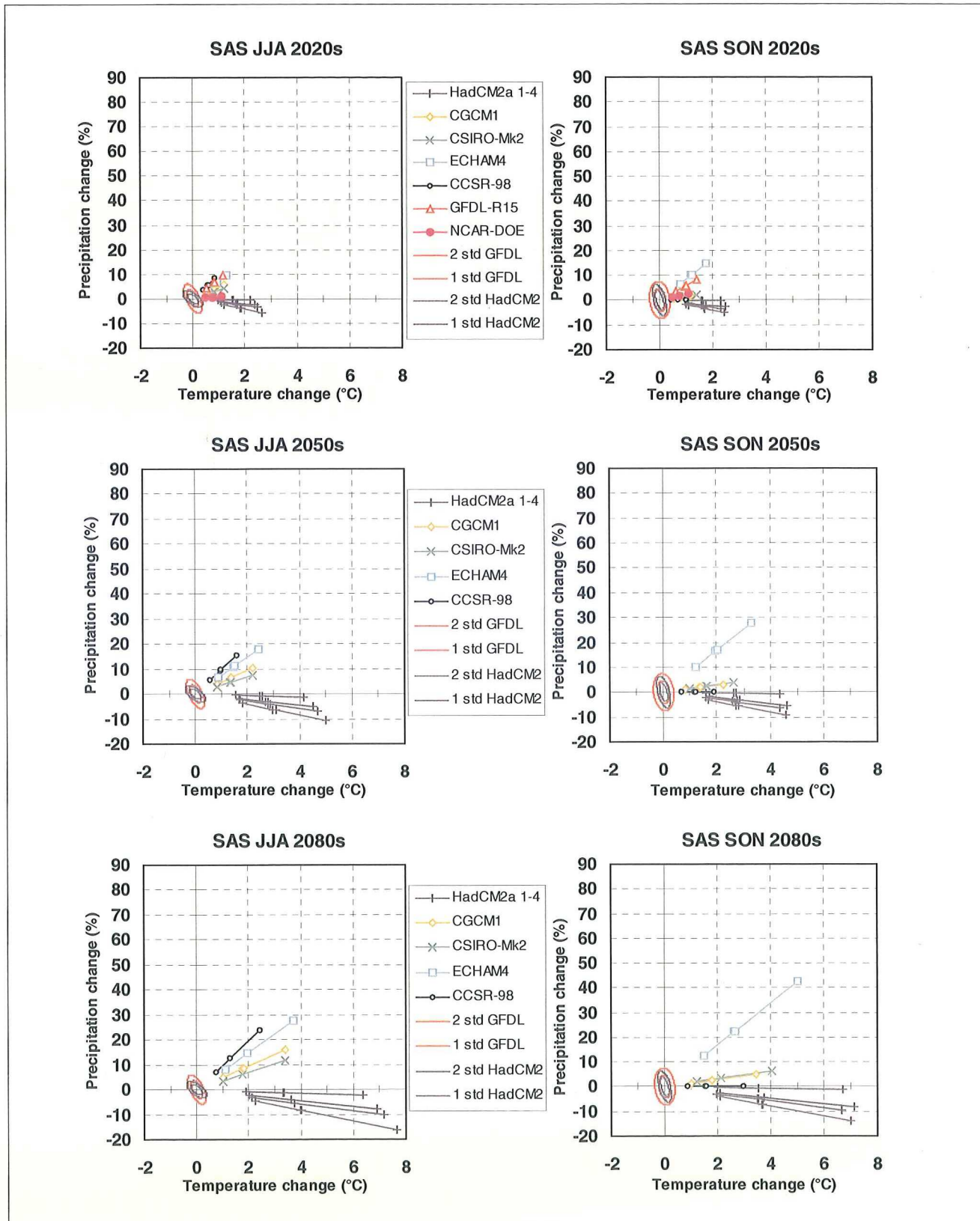
Figure B23. South Asia - June-August and September-November
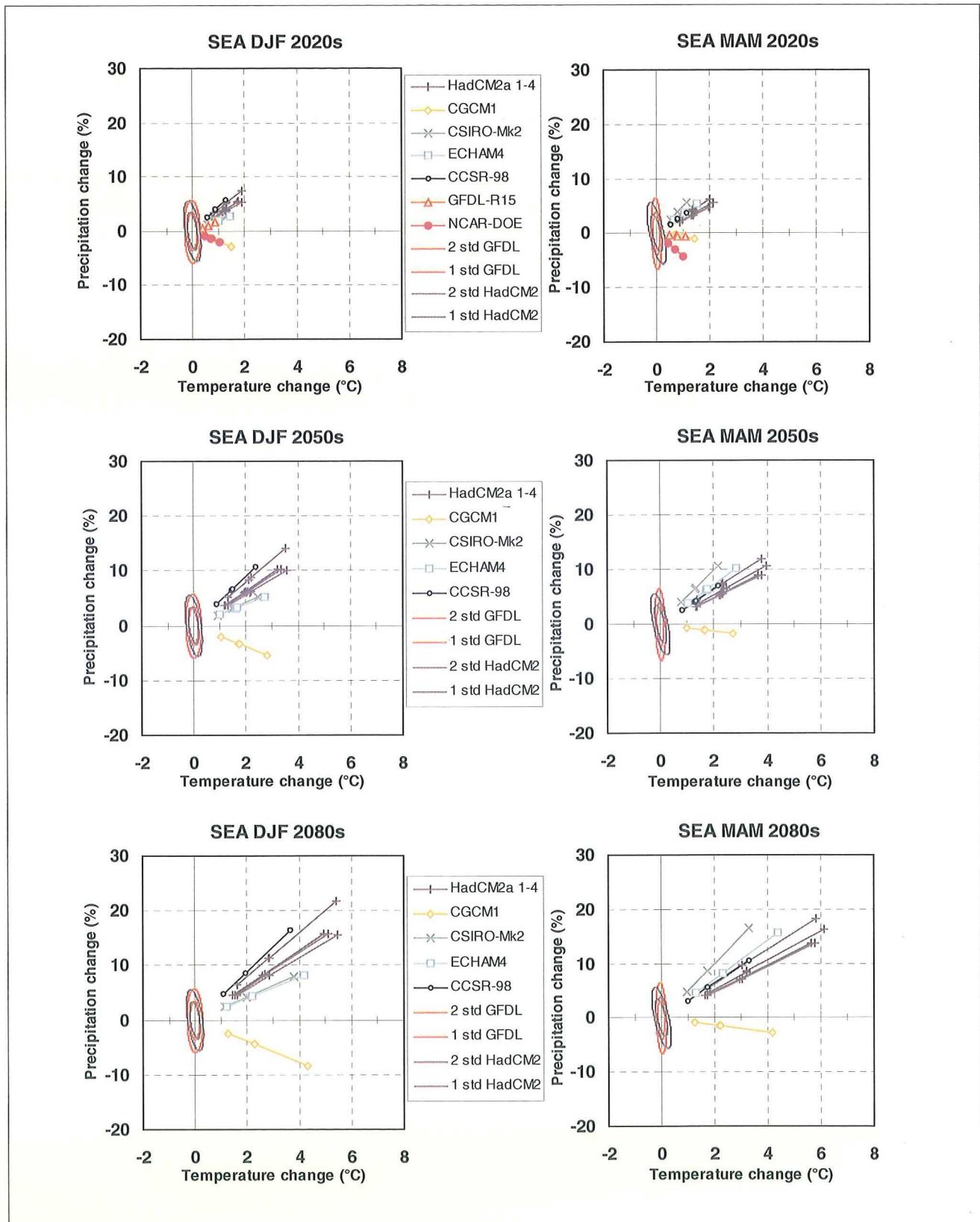
Figure B24. Southeast Asia - December-February and March-May
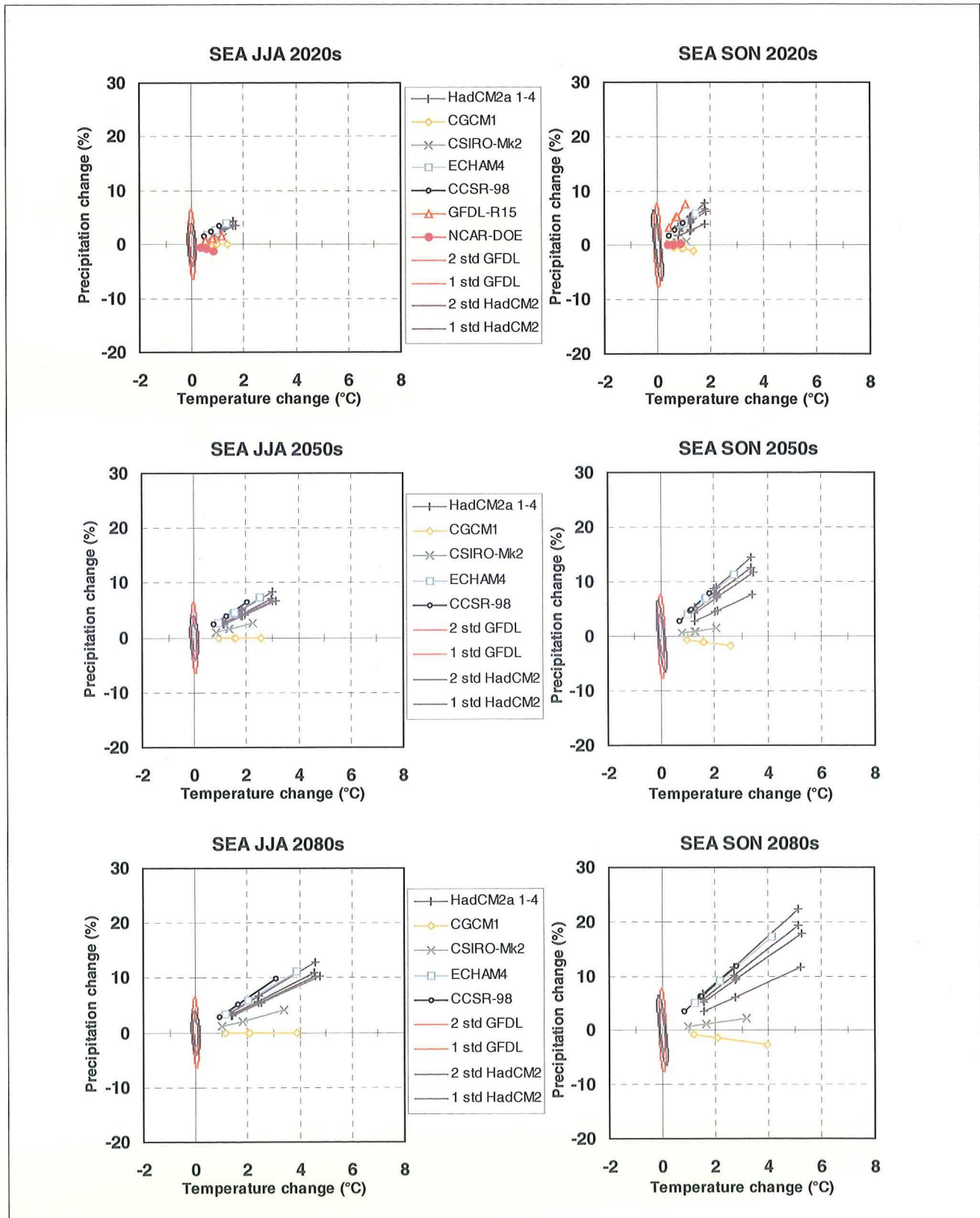
Figure B24. Southeast Asia - June-August and September-November
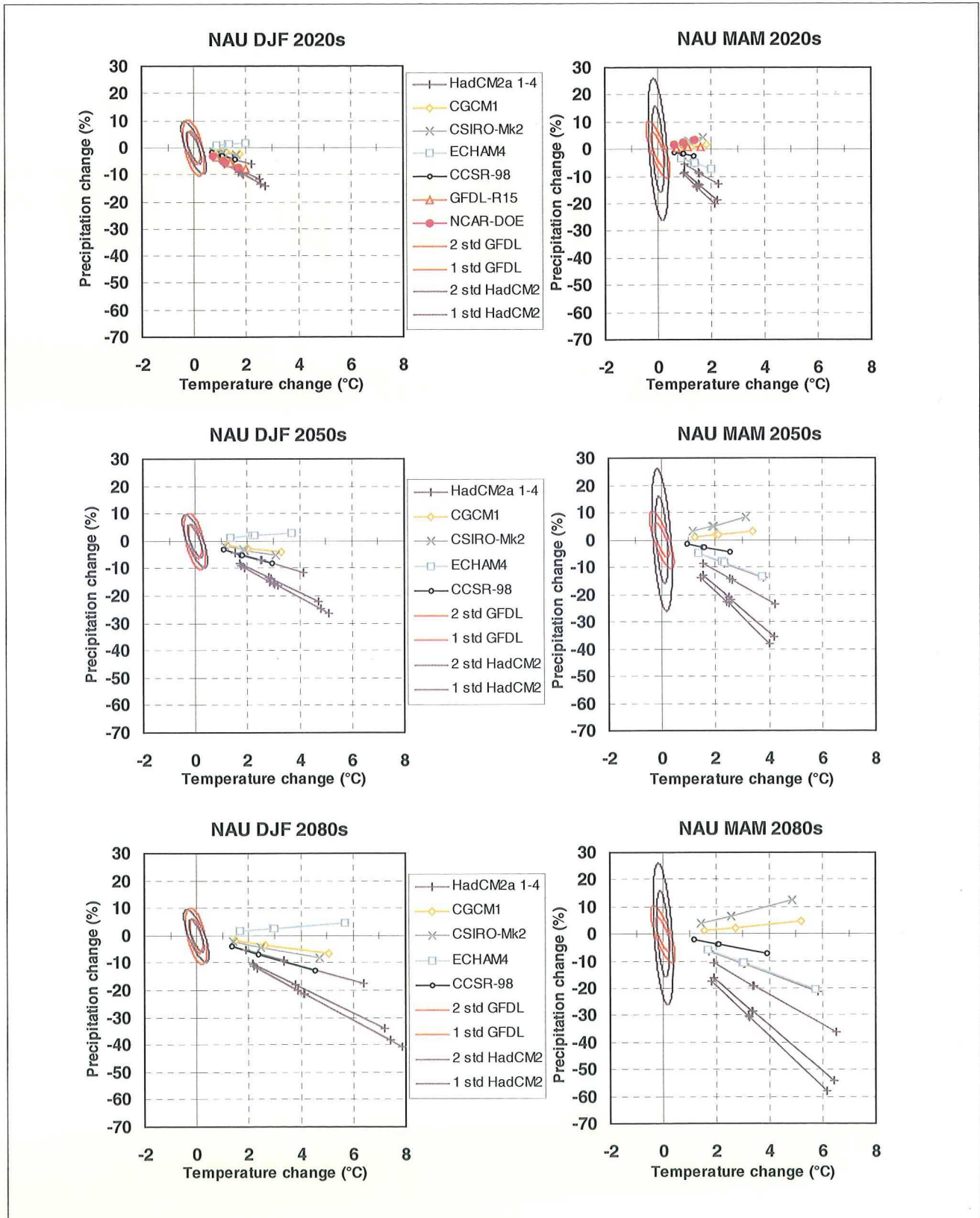
Figure B25. Northern Australia - December-February and March-May
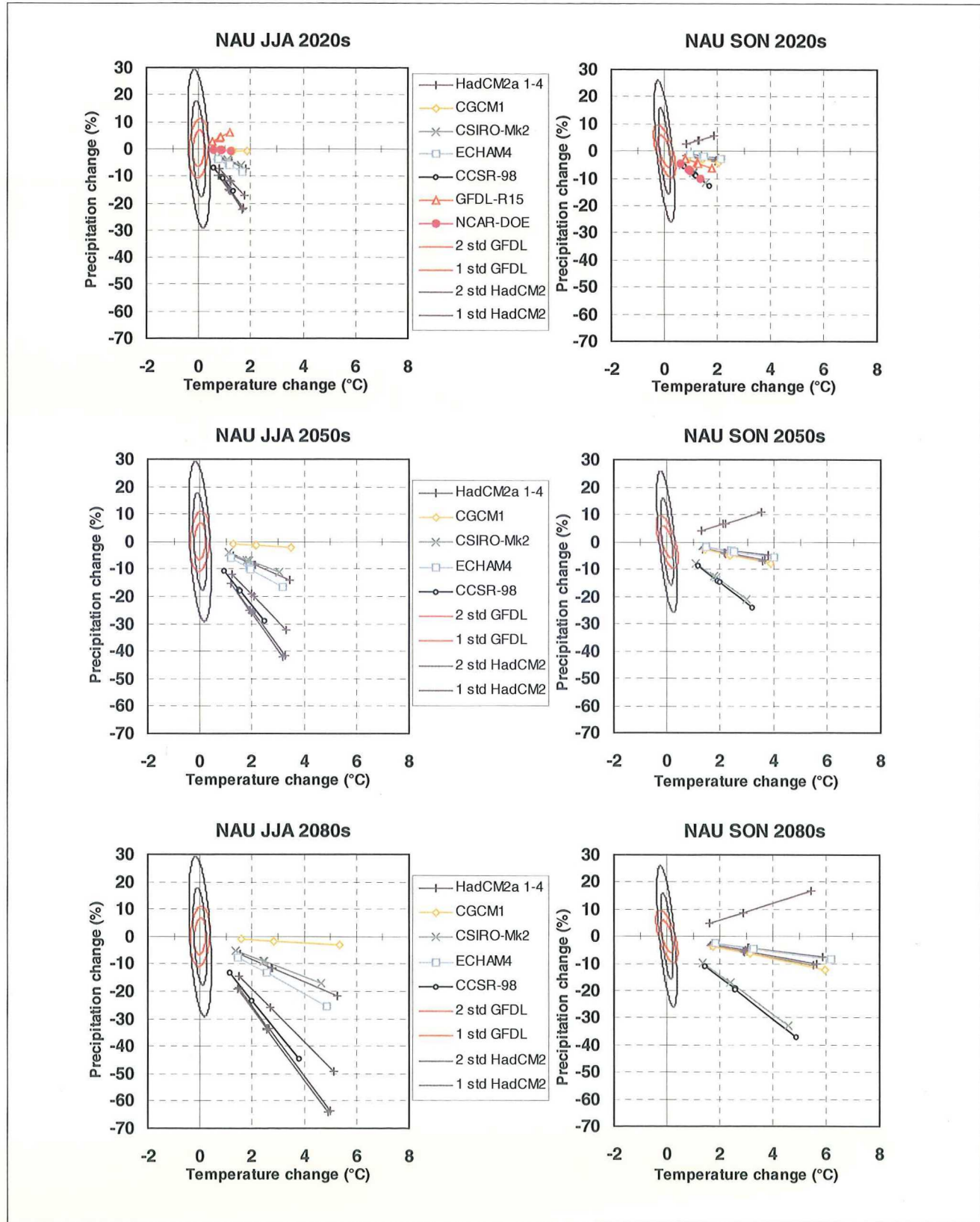
Figure B25. Northern Australia - June-August and September-November
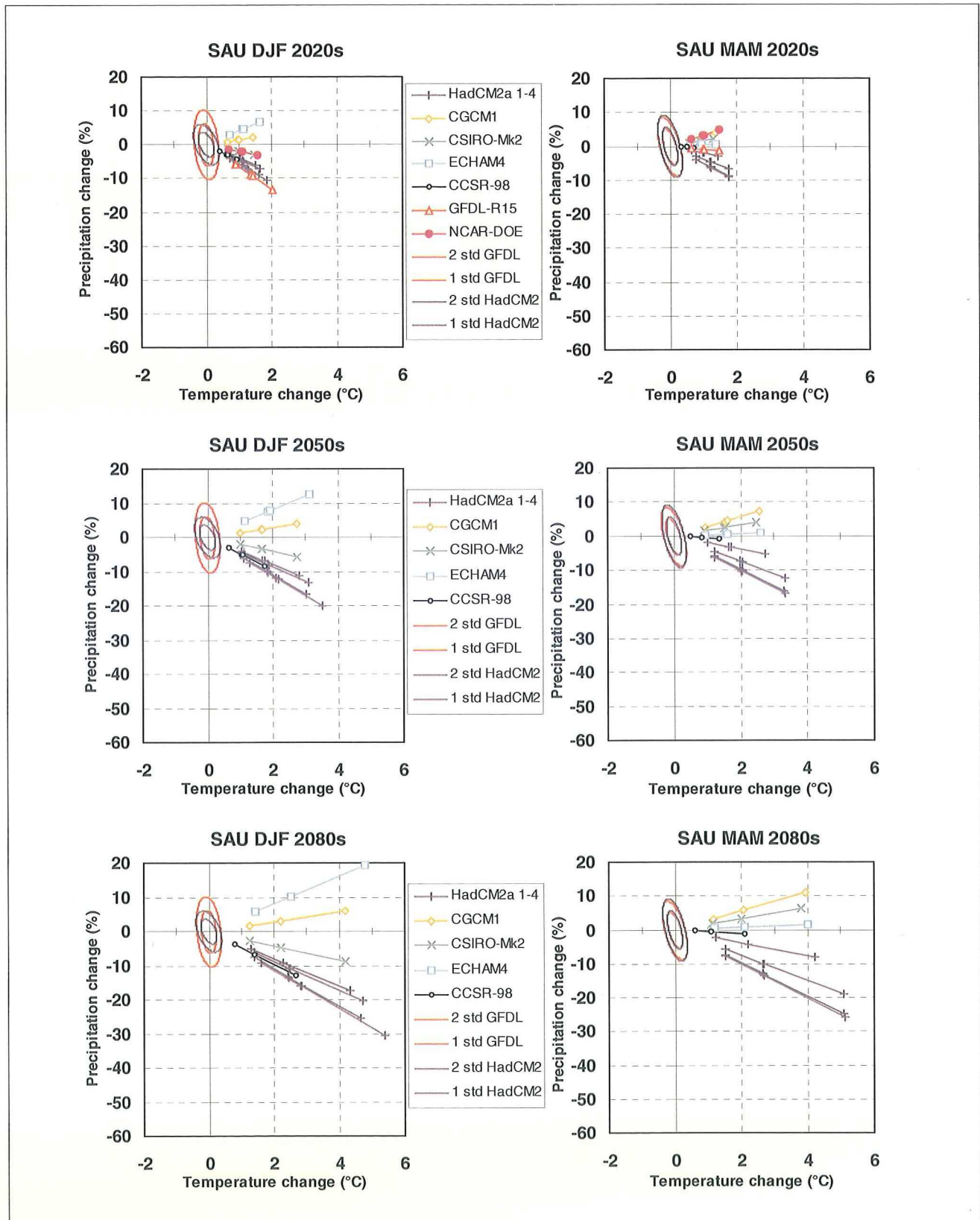
Figure B26. Southern Australia/New Zealand - December-February and March-May
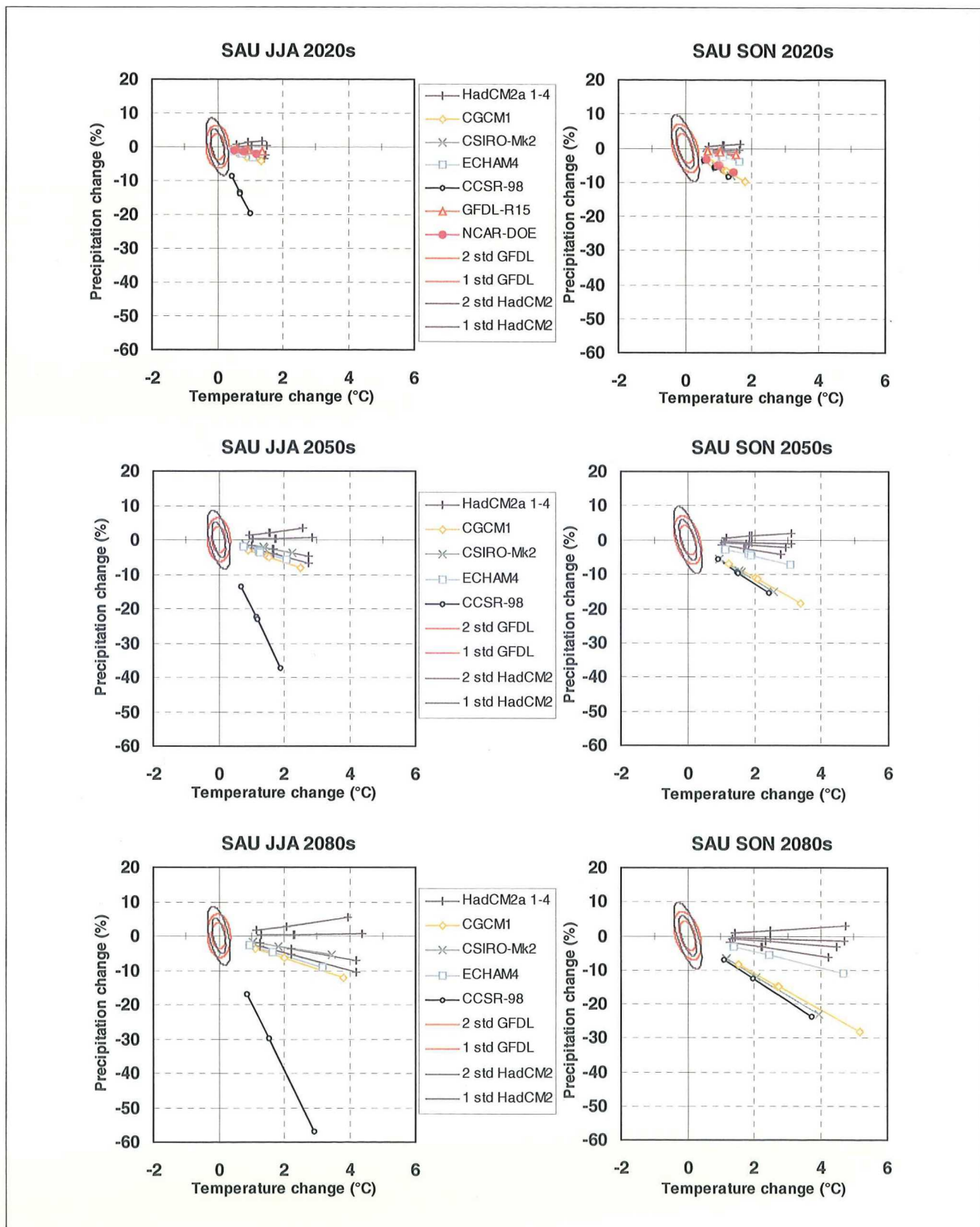
Figure B26. Southern Australia/New Zealand - June-August and September-November
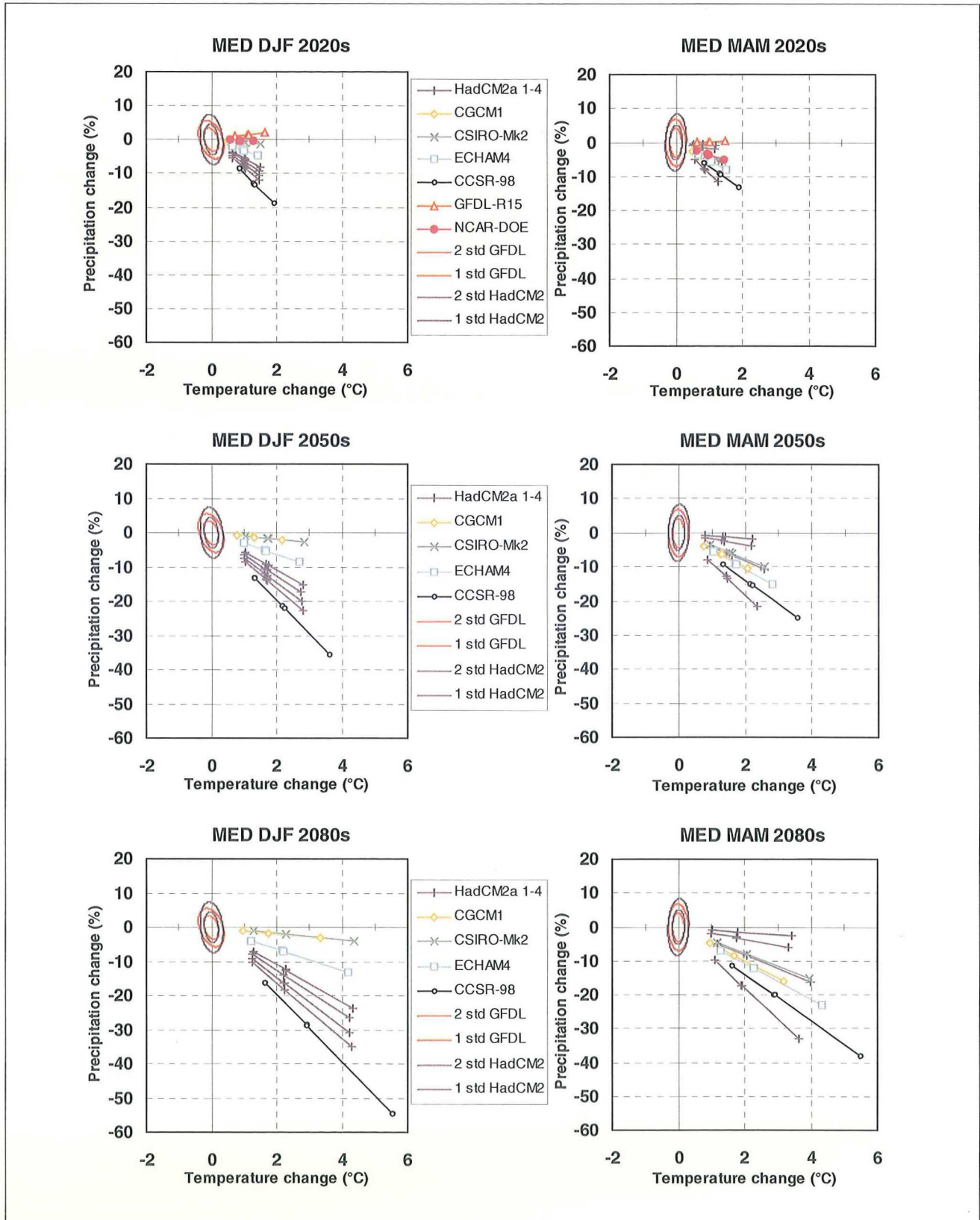
Figure B27. Mediterranean - December-February and March-May
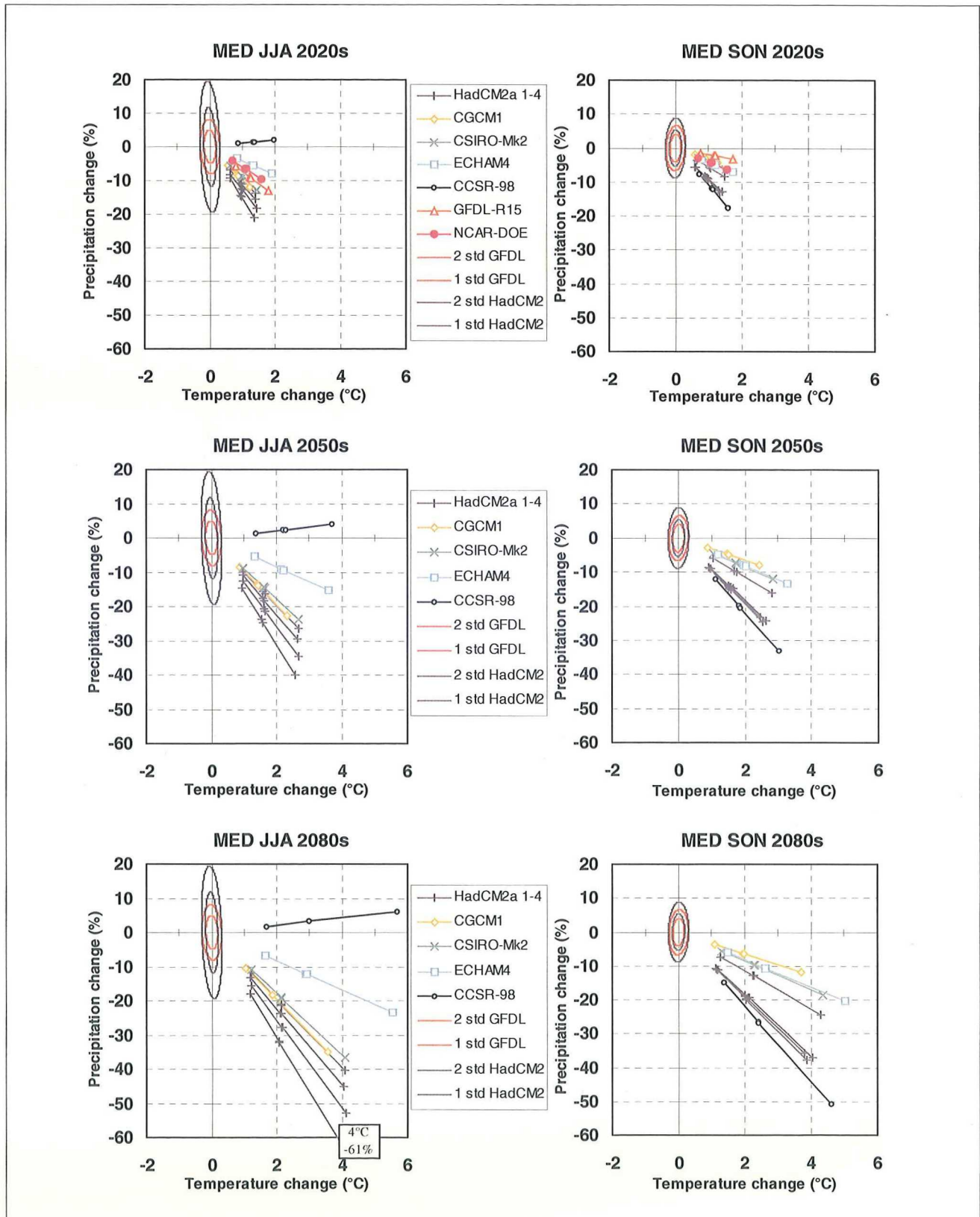
Figure B27. Mediterranean - June-August and September-November
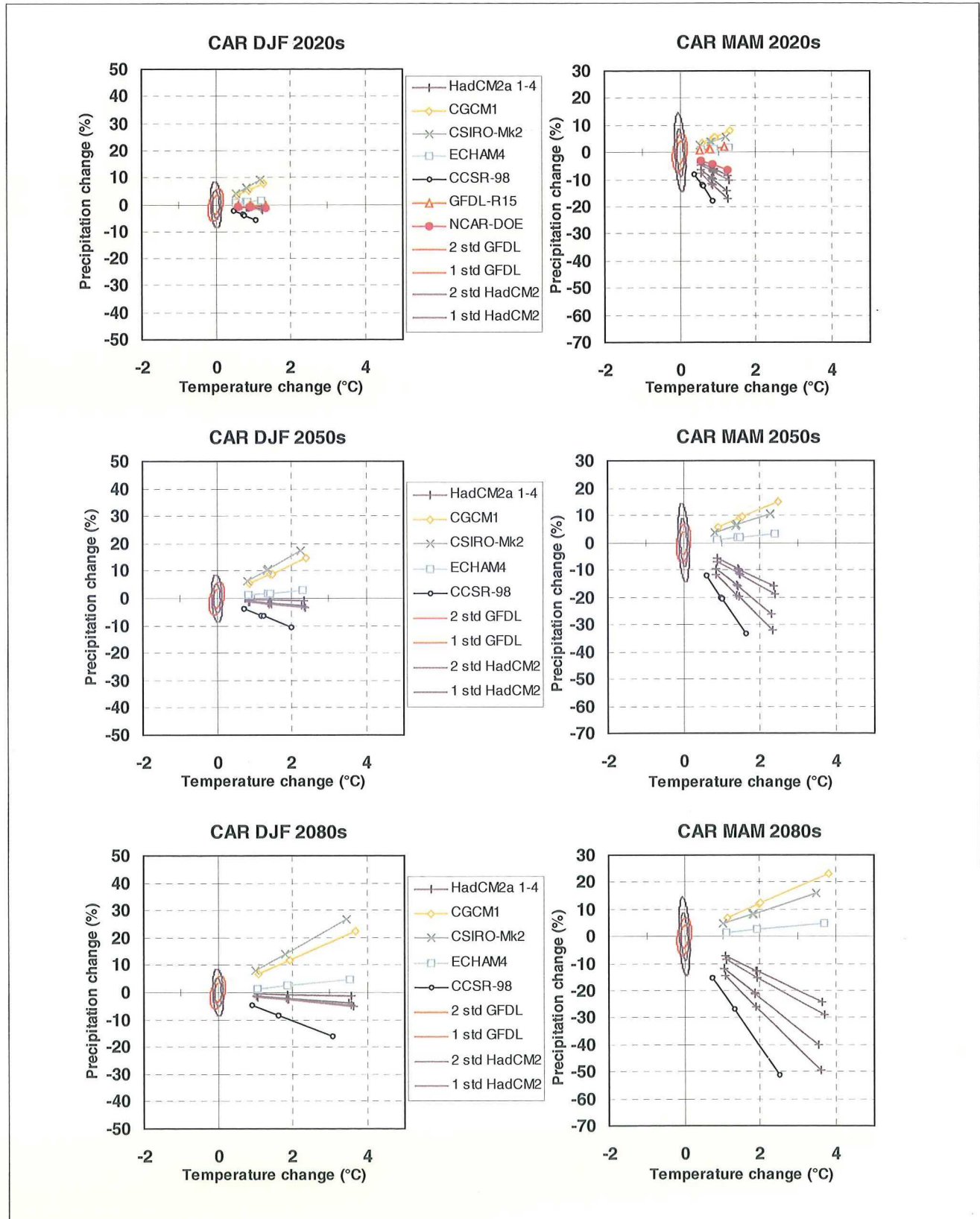
Figure B28. Caribbean - December-February and March-May
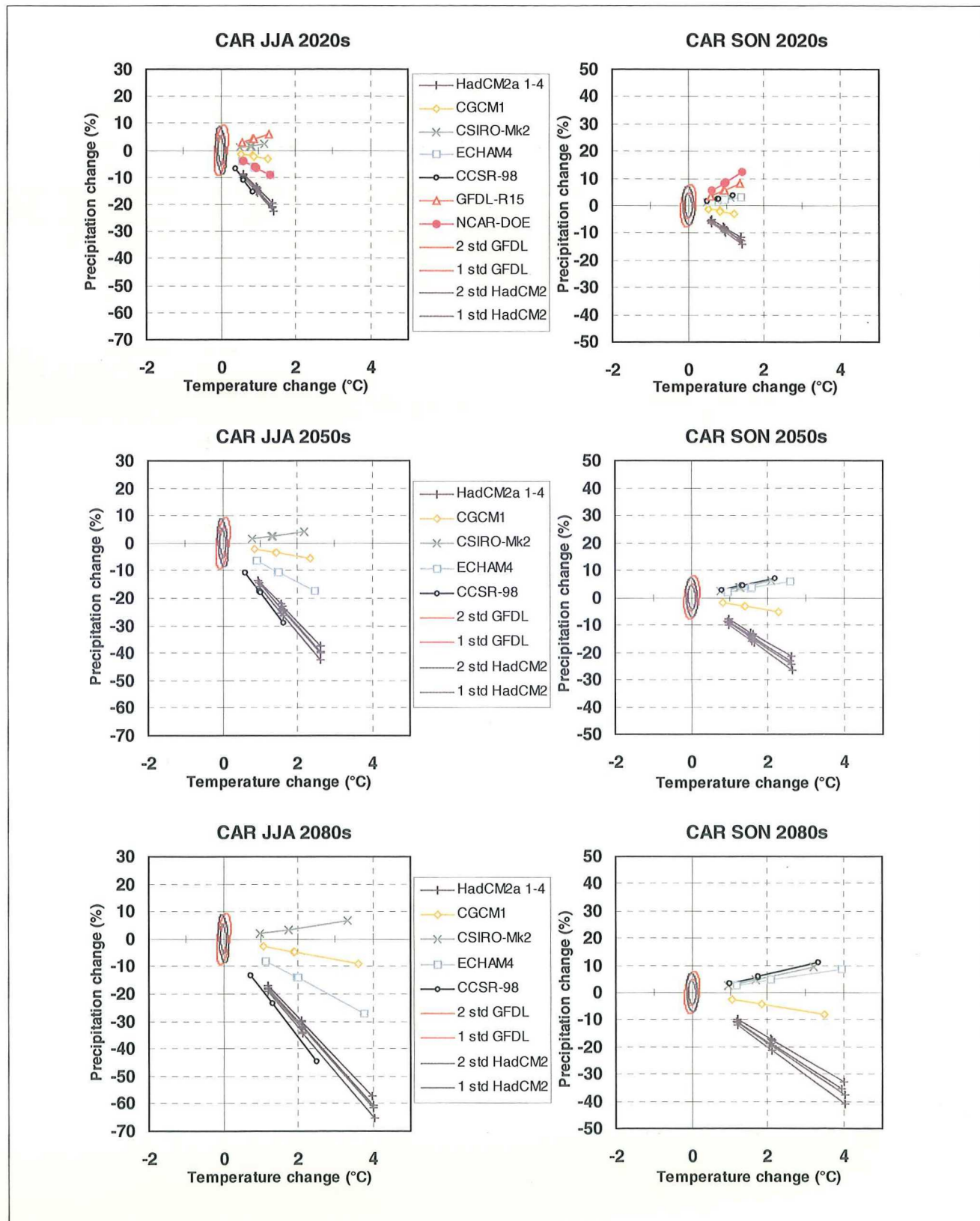
Figure B28. Caribbean - June-August and September-November
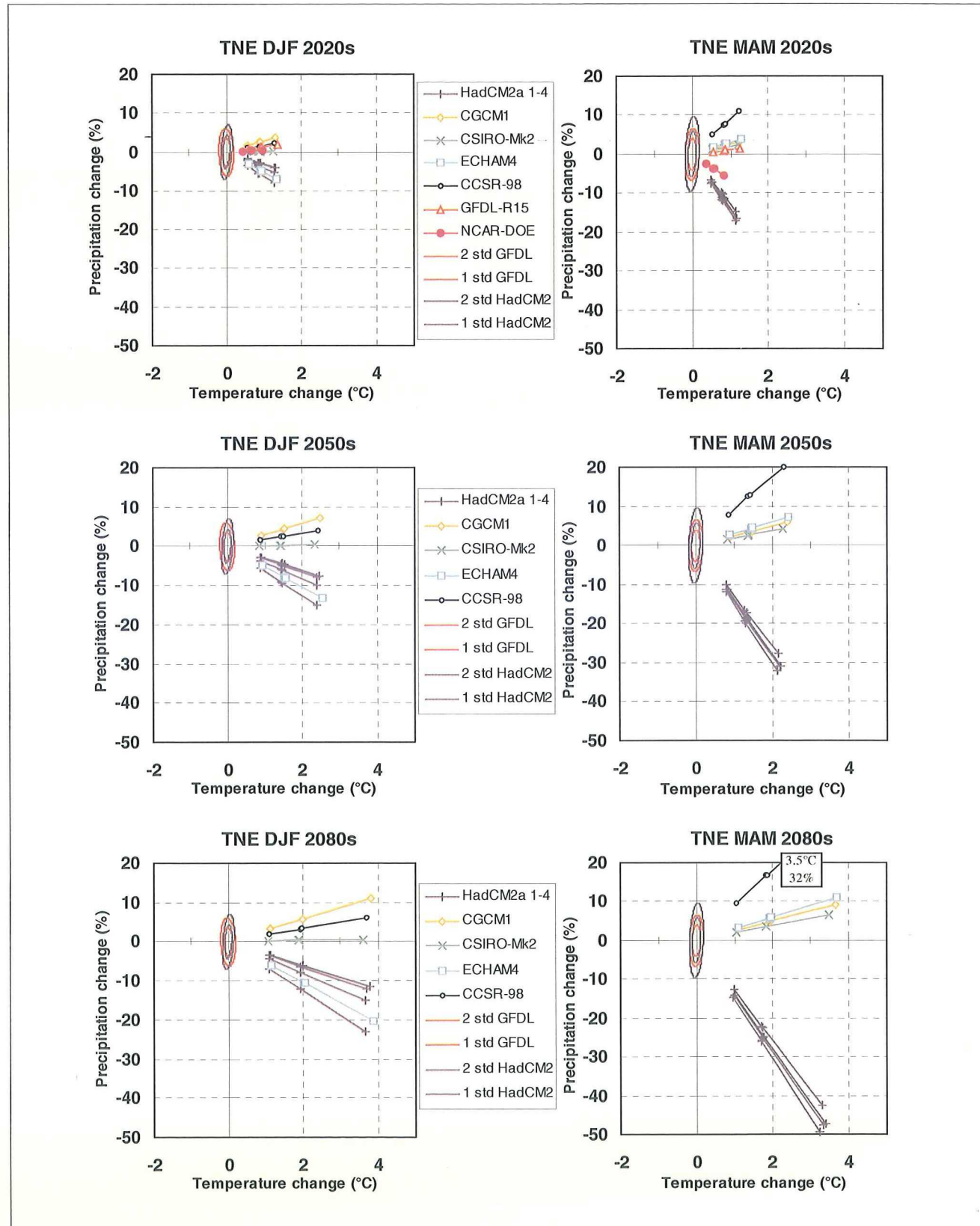
Figure B29. Tropical NE Atlantic - December-February and March-May
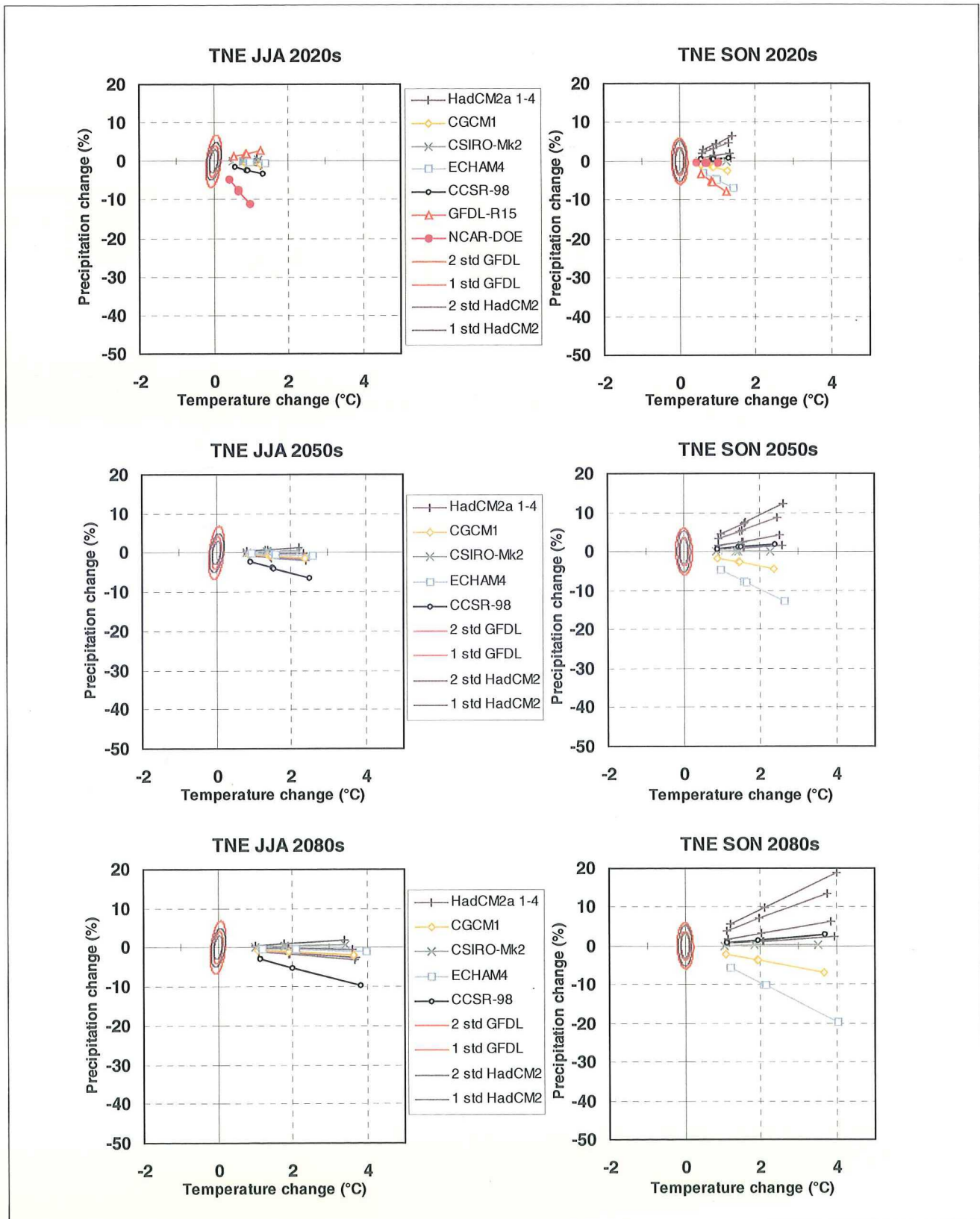
Figure B29. Tropical NE Atlantic - June-August and September-November
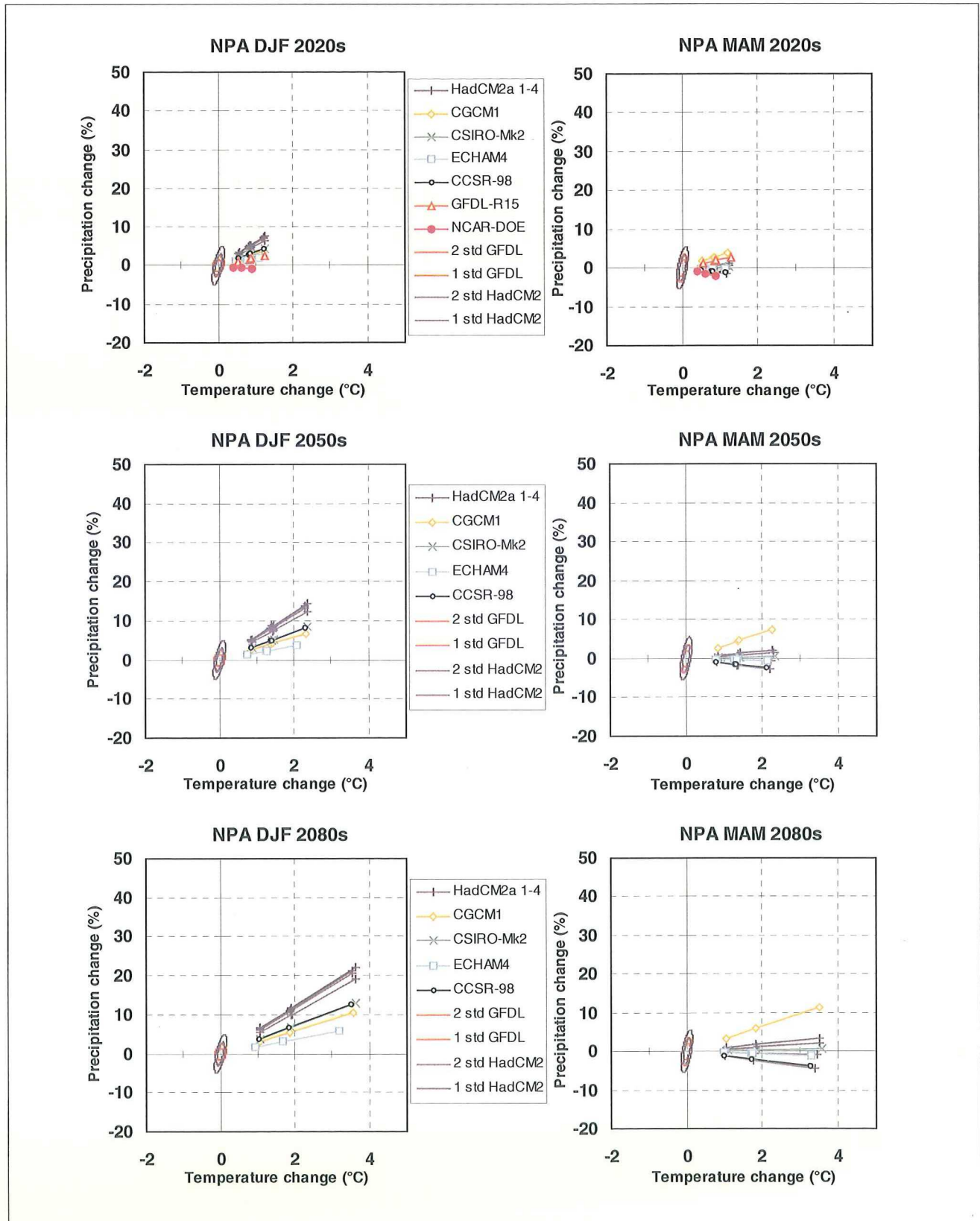
Figure B30. North Pacific - December-February and March-May
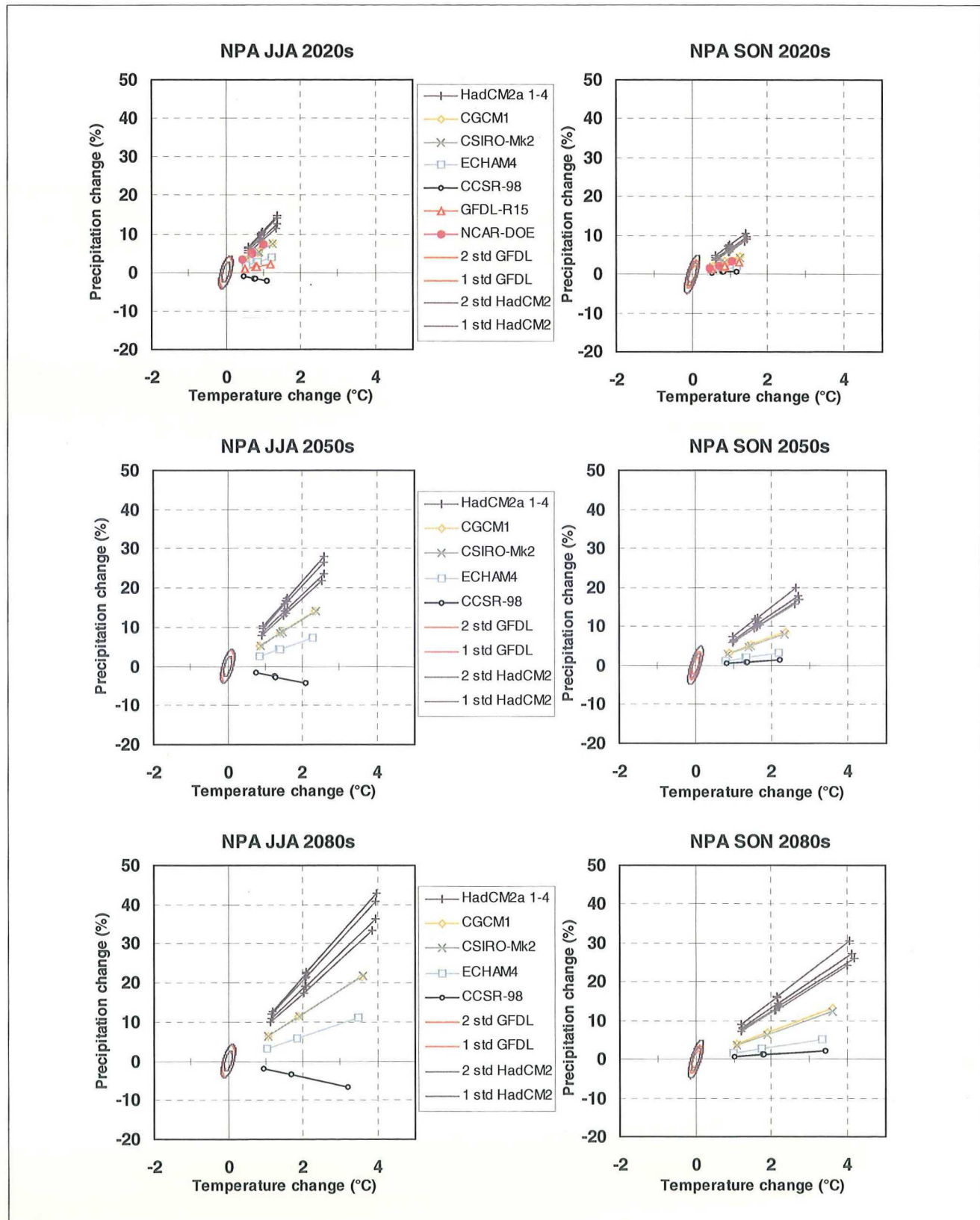
Figure B30. North Pacific - June-August and September-November
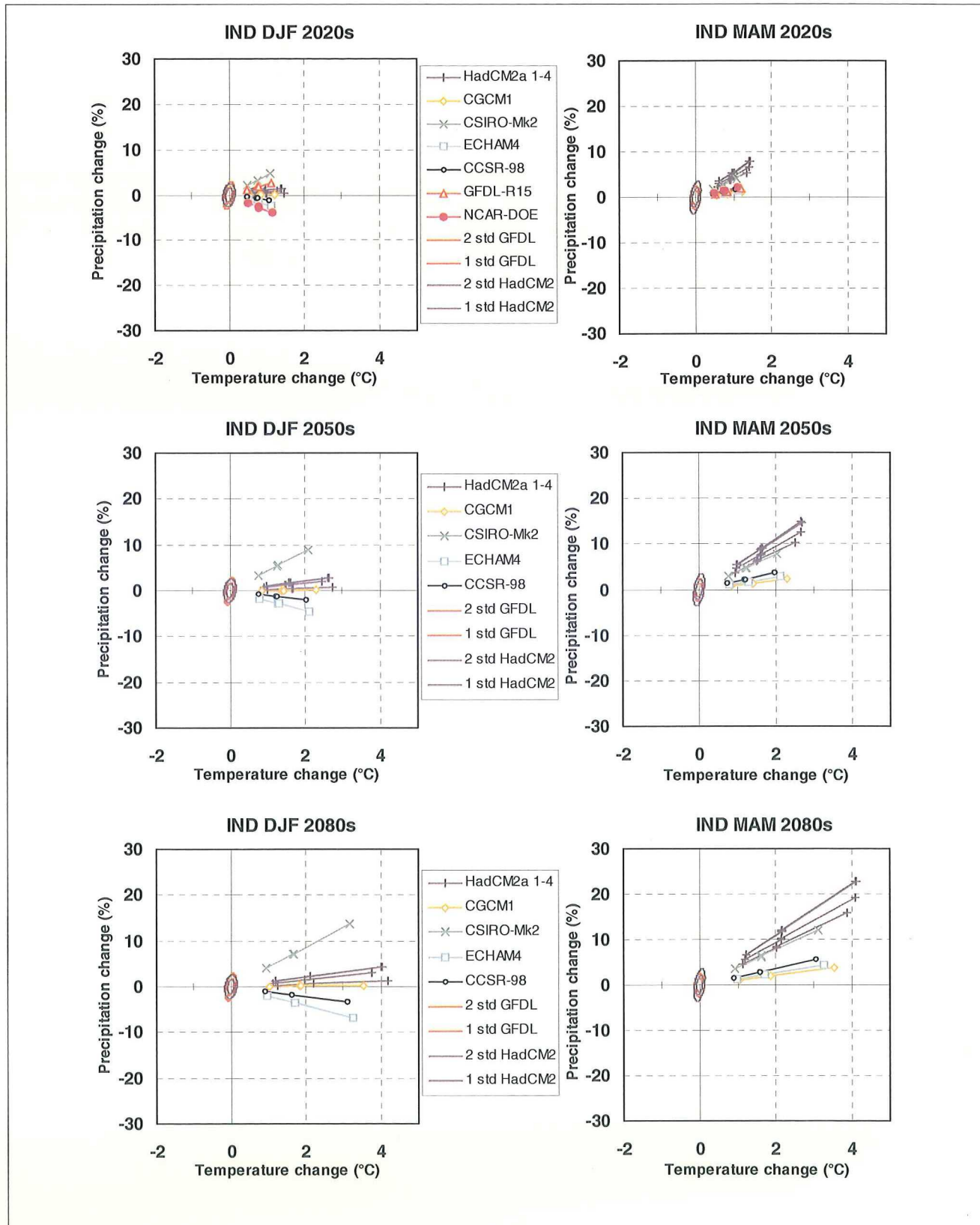
Figure B31. Indian Ocean - December-February and March-May
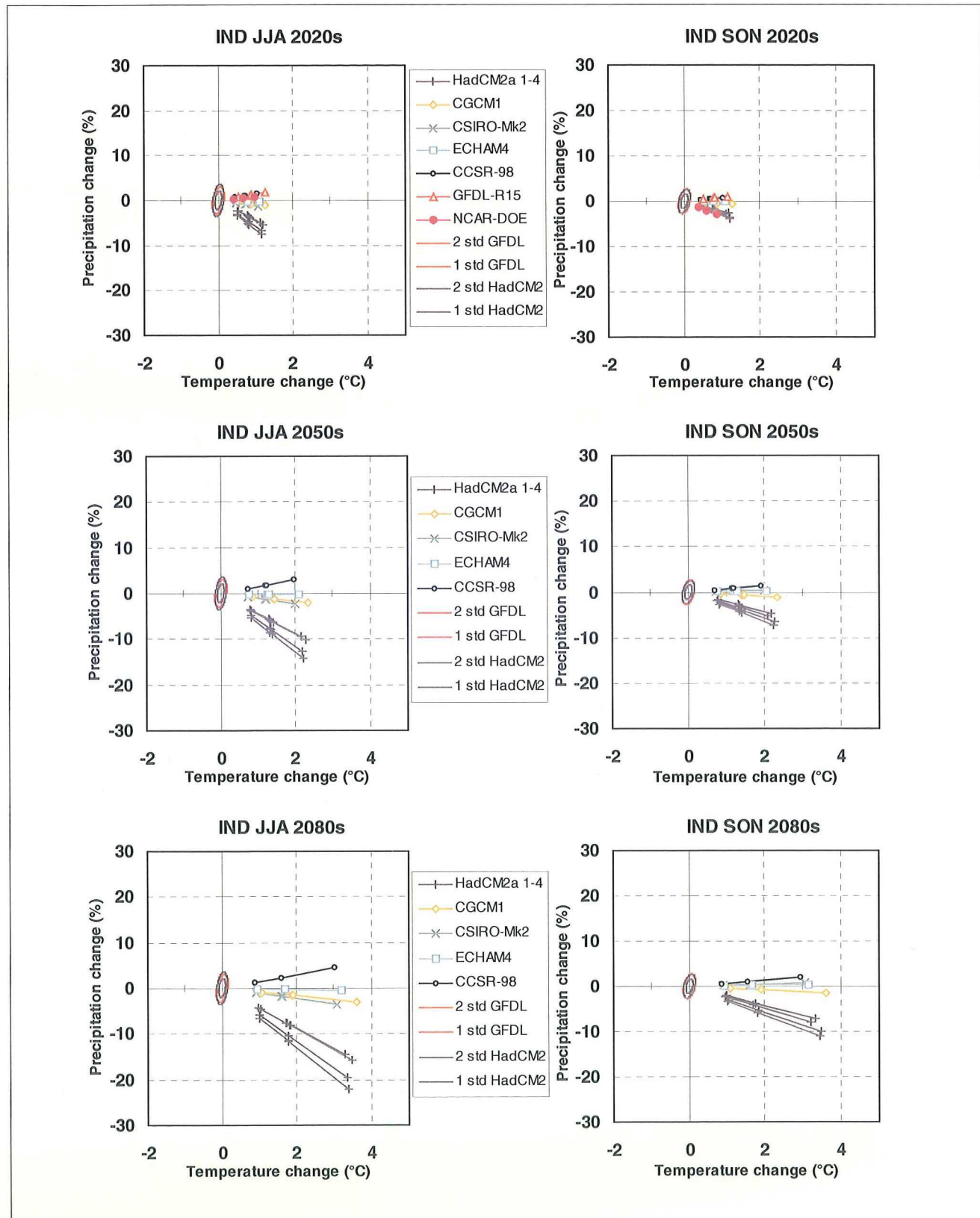
Figure B31. Indian Ocean - June-August and September-November
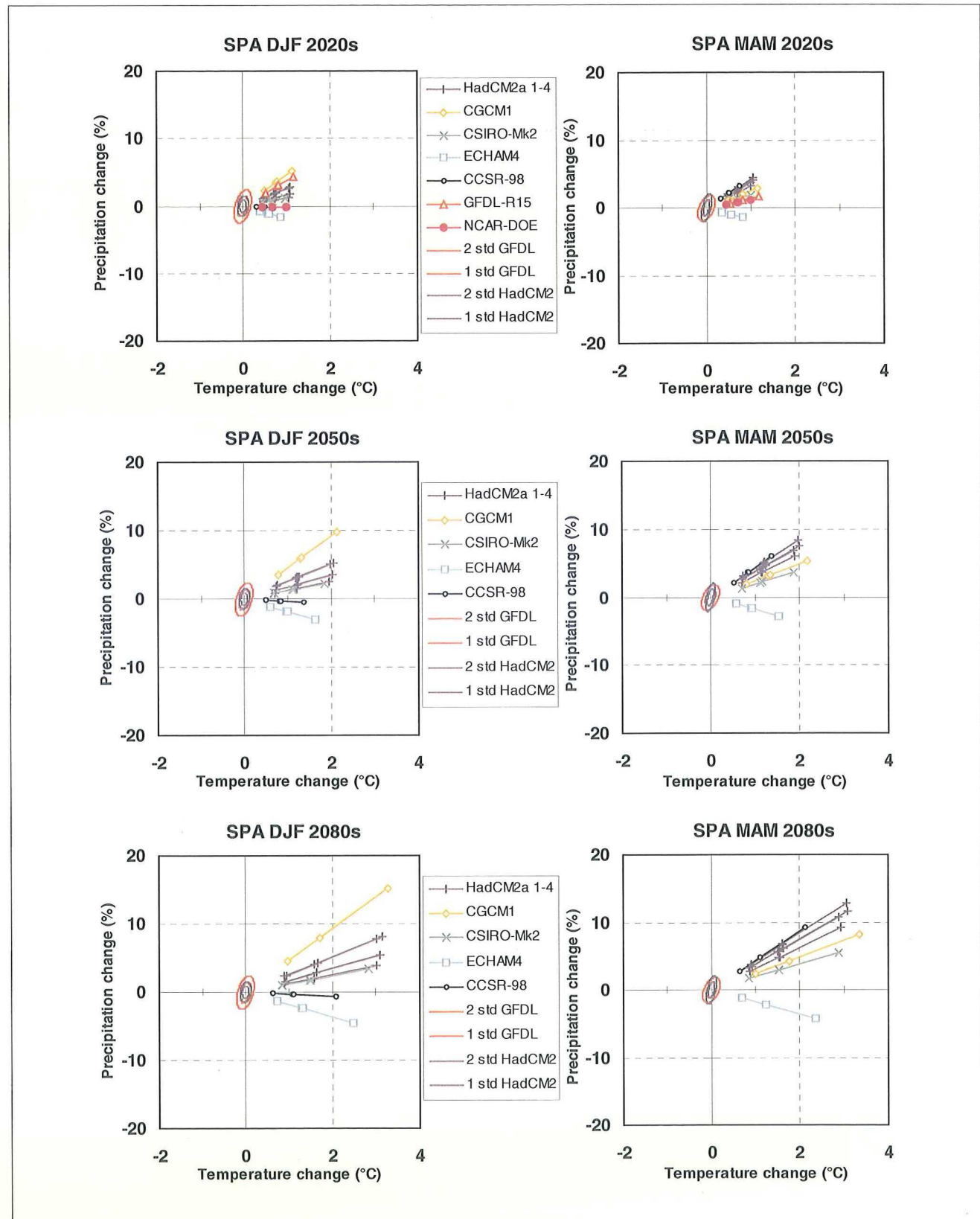
Figure B32. South Pacific - December-February and March-May
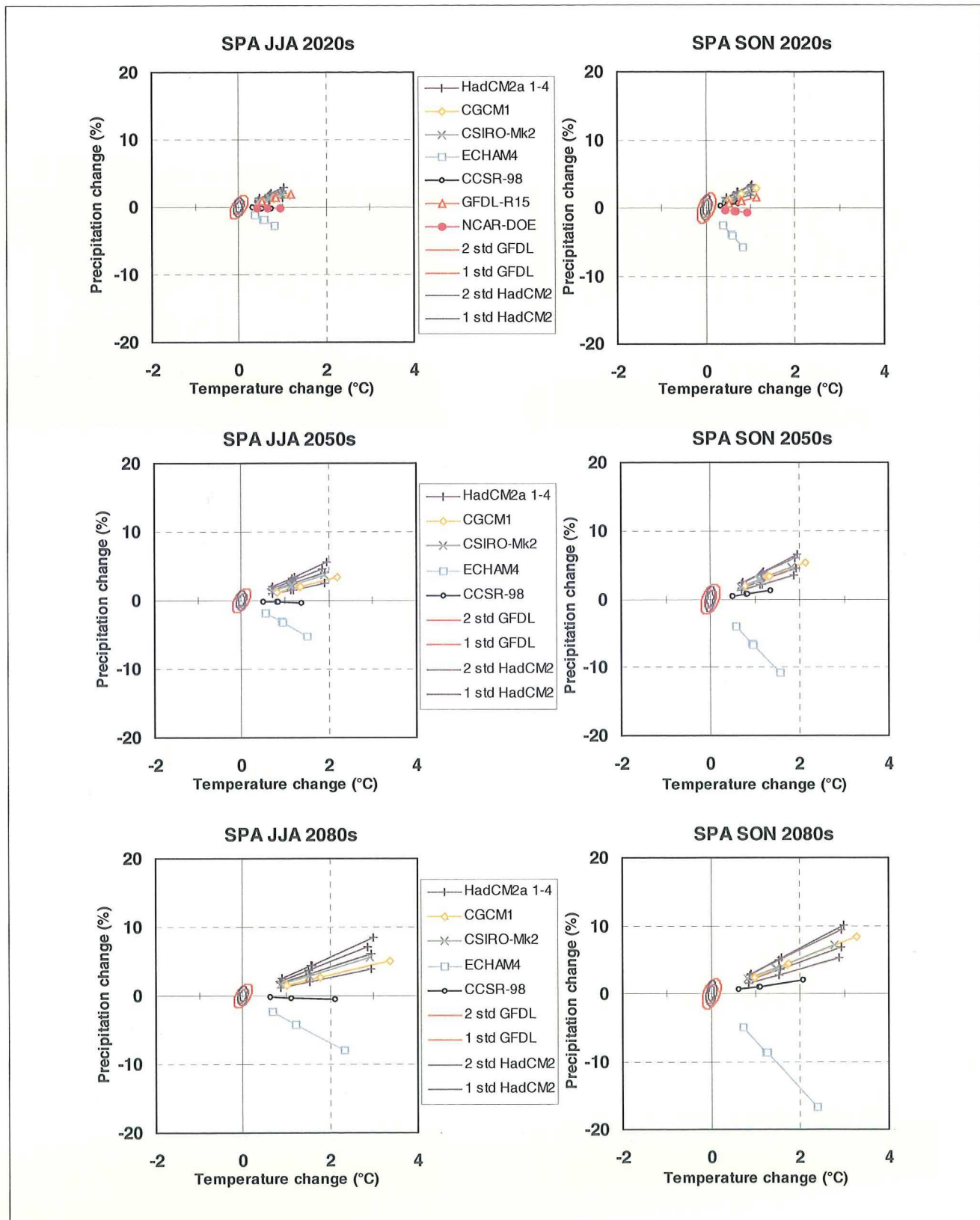
Figure B32. South Pacific - June-August and September-November

# Appendix C: Regional Climatic Effects Of Sulphate Aerosols
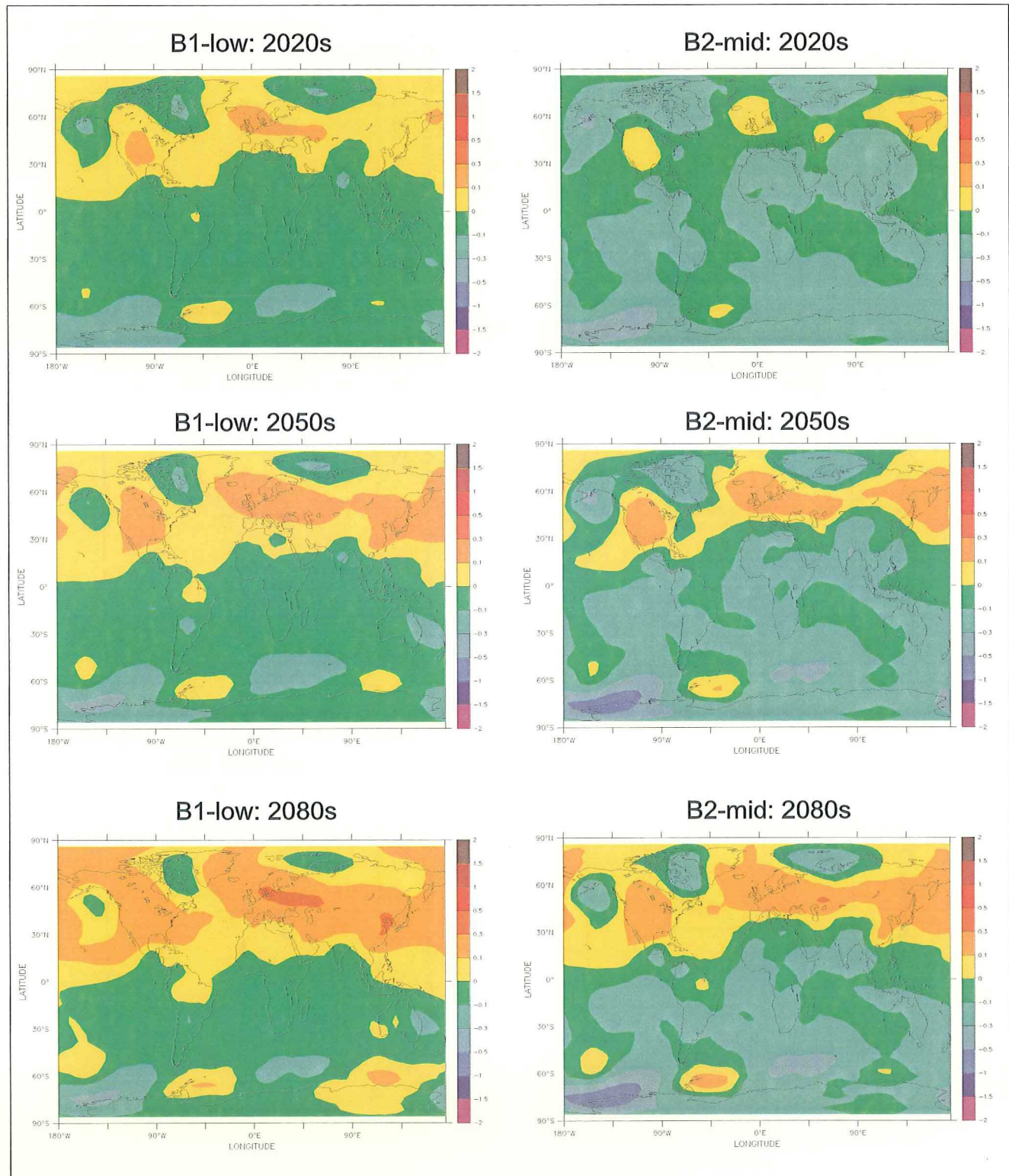
Figure C1. Modelled mean annual temperature response to sulphate aerosols (direct effect, °C) relative to 1961–1990 under the preliminary SRES B1 marker scenario assuming a 1.5°C climate sensitivity (B1-low – left panel) and the preliminary SRES B2 marker scenario with a 2.5°C climate sensitivity (B2-mid – right panel). GCM patterns are scaled regionally using the method described by Schlesinger et al. (1999).
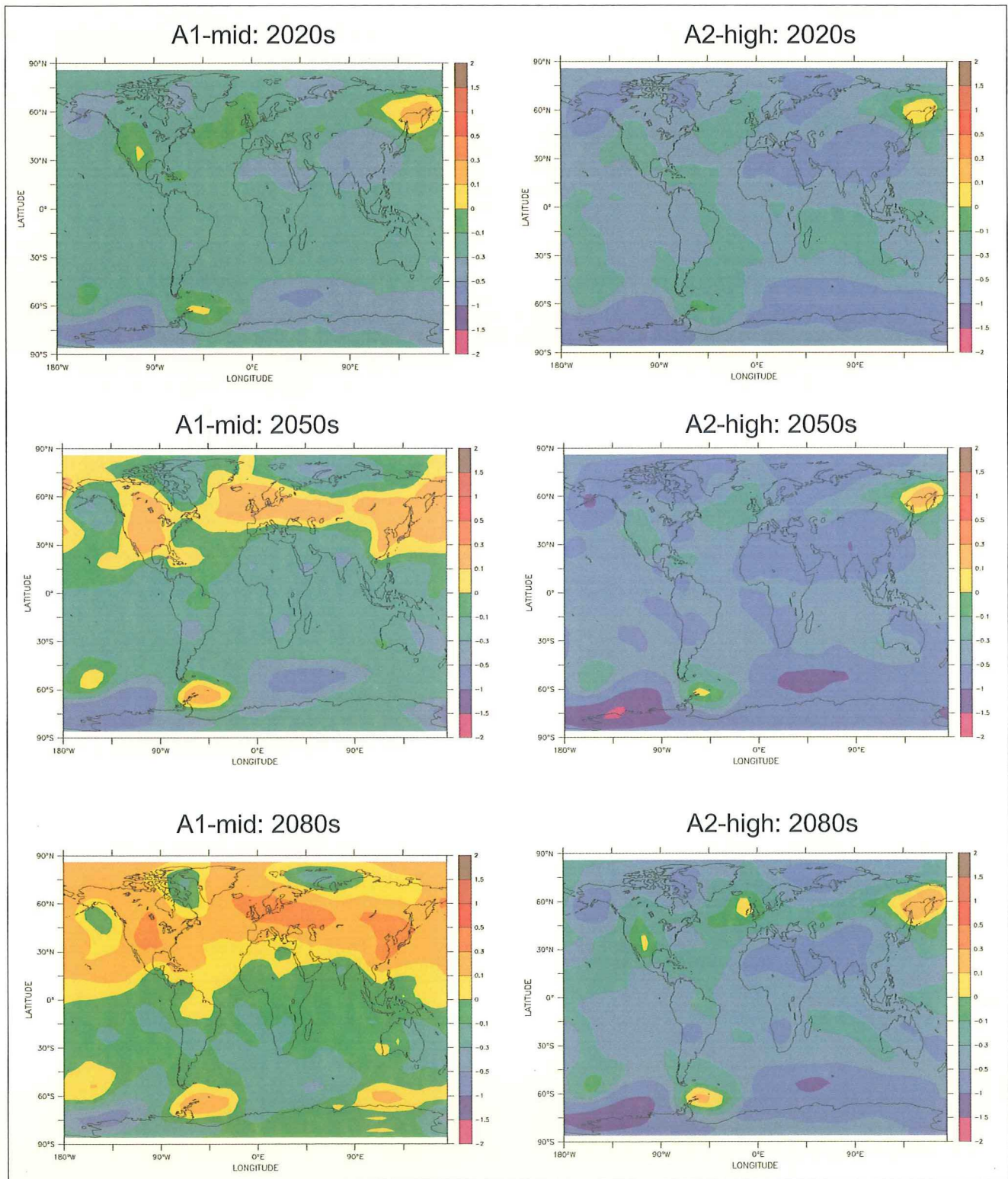
Figure C2. Modelled mean annual temperature response to sulphate aerosols (direct effect, °C) relative to 1961-1990 under the preliminary SRES A1 marker scenario assuming a 2.5°C climate sensitivity (A1-mid - left panel) and the preliminary SRES A2 marker scenario with a 4.5°C climate sensitivity (A2-high - right panel). GCM patterns are scaled regionally using the method described by Schlesinger et al. (1999).

Documentation page

Publisher	Finnish Environment Institute	Date November 2000

Author(s)	Timothy R. Carter, Mike Hulme, Jennifer F. Crossley, Sergey Malyshev, Mark G. New, Michael E. Schlesinger and Heikki Tuomenvirta

Title of publication	Climate Change in the 21st Century: Interim Characterizations based on the New IPCC Emissions Scenarios

Abstract

Emissions of greenhouse gases and aerosols into the atmosphere are believed to be changing the Earth's climate. In order to study the possible impacts of such changes on natural and human systems, plausible scenarios of future climate are required that represent the range of uncertainty in projections. These scenarios should also be consistent with other scenarios of concurrent socio-economic and environmental changes.

The Intergovernmental Panel on Climate Change (IPCC) has recently developed a new set of emissions scenarios for the Special Report on Emissions Scenarios (SRES). The scenarios span a wide range of uncertainties in future emissions arising from different assumptions of socio-economic development during the 21st century. Their effects on climate are currently being estimated using coupled atmosphere-ocean general circulation models (AOGCMs), but a representative set of AOGCM results spanning the SRES range of emissions is not yet available for use in impact assessment.

In the interim, this report presents an alternative method of characterizing the implications of the SRES emissions scenarios for regional climate. The method combines estimates of the global mean climate response to the SRES scenarios, using a simple climate model, with estimates of the regional pattern of climate response from AOGCM simulations assuming earlier emissions scenarios. Projected changes in mean seasonal temperature and precipitation are portrayed for the 2020s, 2050s and 2080s relative to 1961-1990 on global maps and on graphs for thirty-two world regions. Uncertainties in both the magnitude and direction of future regional climate change are depicted, based on a range of SRES scenarios and patterns from ten AOGCM simulations.

In addition, information is presented on the demographic and socio-economic driving factors underlying the SRES scenarios, the atmospheric carbon dioxide concentrations implied by the scenarios, and model estimates of global sea-level rise induced by projected temperature changes. All of these factors may also be important for determining future vulnerability to a changing climate.

Keywords	climate change, regional scenarios, impacts, SRES emissions scenarios, climate models, uncertainty, greenhouse gases, aerosols, atmospheric concentrations, stabilization

Publication series and number	The Finnish Environment 433

Theme of publication	International Cooperation

Project name and number, if any	Global change scenarios (XVB170)

Financier/ commissioner	Ministry of the Environment

Project organization	Finnish Environment Institute, University of East Anglia / UK, University of Illinois / USA, University of Oxford / UK, Finnish Meteorological Institute

ISSN 1238-7312	ISBN 952-11-0781-2
No. of page 148	Language English
Restrictions public	Price 213 FIM

For sale at/ distributor	Edita Ltd, tel. +358 9 566 0266, Oy Edita Ab, Asiakaspalvelu, Pl 800, 00043 Edita e-mail: asiakaspalvelu@edita.fi www-server: http://www.edita.fi/netmarket

Financier of publication	Finnish Environment Institute, P.O. Box 140, FIN-00251 Helsinki, Finland Ministry of the Environment, P.O. Box 380, FIN-00131 Helsinki, Finland

Printing place and year	Tummavuoren Kirjapaino, Vantaa 2000

Kuvailulehti

Julkaisija	Suomen ympäristökeskus	Julkaisuaika Marraskuu 2000
Tekijä(t)	Timothy R. Carter, Mike Hulme, Jennifer F. Crossley, Sergey Malyshev, Mark G. New, Michael E. Schlesinger ja Heikki Tuomenvirta	
Julkaisun nimi	Climate Change in the 21st Century: Interim Characterizations based on the New IPCC Emissions Scenarios	

Tiivistelmä		

Ilmakehään päästöinä joutuvien kasvihuonekaasujen ja aerosolien uskotaan jo alkaneen muuttaa maapallon ilmastoa. Jotta muutoksen vaikutuksia luontoon ja yhteiskuntaan voitaisiin tutkia, tarvitaan ilmastoskenaarioita, jotka kuvaavat kattavasti ilmaston mahdollisia kehitysvaihtoehtoja ja hahmottavat niiden epävarmuuksia. Skenaarioiden tulisi olla sopusoinnussa samanaikaisten yhteiskunnallisten, taloudellisten ja ympäristömuutosten kanssa.

Hallitustenvälinen ilmastonmuutospaneeli on hiljattain julkaissut Päästöskenaarioiden erityisraportin (SRES), jossa esitetään uudet skenaariot päästöjen kehitykselle. Ne kattavat laajasti päästöjen mahdolliset kehitystrendit, jotka ovat johdettavissa erilaisista yhteiskunnan ja talouden kehitystä koskevista oletuksista ja niihin liittyvistä epävarmuustekijöistä. Käynnissä olevissa tutkimuksissa päästöskenaarioita käytetään pakotteina ilmaston muutosta ennustavissa yleisen kiertoliikkeen malleissa, jotka kytkevät toisiinsa ilmakehän ja valtameret (AOGCM). Uusiin SRES:n päästöskenaarioihin perustuvia ilmastoskenaarioita ei kuitenkaan vielä ole käytettävissä ilmaston muutoksen vaikutusten tutkimuksissa.

Tässä raportissa esitetään välivaiheen vaihtoehtoinen menetelmä kuvata päästöskenaarioiden vaikutuksia alueelliseen ilmastoon. Menetelmässä arvioidaan yksinkertaisen mallin avulla kunkin SRES-skenaarion aiheuttama maapallon keskimääräisen ilmaston muutos ja johdetaan siitä alueelliset muutokset käyttäen aiempiin päästöskenaarioihin perustuvia AOGCM-simulointeja. Vuodenaikojen keskilämpötilojen ja sademäärien muutokset nykyilmastosta (jaksosta 1961-1990) 2020-, 2050- ja 2080-luvulle esitetään maapallon ilmastokarttoina ja erikseen 32 alueelle. Usean SRES-skenaarion ja 10 AOGCM-simuloinnin perusteella hahmotellaan alueellisen ilmastonmuutoksen suunnan ja suuruuden epävarmuutta.

Lisäksi esitetään tietoa SRES-skenaarioiden perustana olevista demografisista, yhteiskunnallisista ja taloudellisista tekijöistä, skenaarioista johdetuista hiilidioksidipitoisuuksista ja malleilla ennustetusta, lämpötilan muutoksen aiheuttamasta merenpinnan noususta. Nämä tekijät voivat olla merkittäviä määritettäessä ilmastonmuutokselle altistettujen järjestelmien haavoittuvuutta tulevaisuudessa.

Asiasanat	ilmastonmuutos, alueelliset skenaariot, vaikutukset, SRES päästöskenaariot, ilmastomallit, epävarmuus, kasvihuonekaasut, aerosolit, ilmakehän pitoisuudet, stabiloituminen
Julkaisusarjan nimi ja numero	Suomen ympäristö 433
Julkaisun teema	Kansainvälinen yhteistyö
Projektihankkeen nimi ja projektinumero	Globaalimuutosskenaariot (XVB170)
Rahoittaja/ toimeksiantaja	Ympäristöministeriö
Projektiryhmään kuuluvat organisaatiot	Suomen ympäristökeskus, East Anglian yliopisto / Englanti, Illinoisin yliopisto / USA, Oxfordin yliopisto / Englanti, Ilmatieteen laitos

Julkaisun myynti/ jakaja	Oy Edita Ab, Asiakaspalvelu, Pl 800, 00043 Edita puh. (09) 566 0266, telefax (09) 566 0380, sähköpostiosoite: asiakaspalvelu@edita.fi www-palvelin: http://www.edita.fi/netmarket
Julkaisun kustantaja	Suomen ympäristökeskus, PL 140, FIN-00251 Helsinki Ympäristöministeriö, PL 380, FIN-00131 Helsinki
Painopaikka ja -aika	Tummavuoren Kirjapaino Oy, Vantaa 2000

Presentationsblad

Sammandrag	

Man antar att jordens klimat påverkas av utsläpp av växthusgaser och aerosoler. För att utvärdera de potentiella effekterna av sådana förändringar behövs scenarier för färändringar i klimatet. Dessa scenarier bör representera osäkerheten i beräkningarna. Scenarierna bör också vara baserade på motsvarande antaganden som scenarier beträffande socio-ekonomiska och miljöförändringar.

Den internationella "Intergovernmental Panel on Climate Change (IPCC)" har nyligen utvecklat nya scenarier för rapporten "Special Report on Emissions Scenarios (SRES)". Dessa scenarier inkluderar osäkerheten i de framtida utsläppen baserade på olika antaganden beträffande den socio-ekonomiska utvecklingen under det 21 århundrandet. Effekterna på klimatet utvärderas med kopplade cirkulationsmodeller (AOGCMs), men representativa scenarier för alla SRES utsläppscenarier är ännu inte tillgängliga för utvärdering av effekter.

I väntan på dessa resultat presenteras i denna rapport en alternativ metod för att utvärdera effekterna av SRES utsläppsscenarierna på regionala klimatförändringar. Denna metod kombinerar beräkningar med simplare klimatmodeller av förändringar i det globala klimatet med beräkningar gjorda med AOGCM-modeller beträffande regionala förändringar för tidigare SRES scenarier.
Beräknade förändringar i medeltemperatur och nederbörd under de olika årstiderna för årtiondena 2020, 2050 och 2080, jämfört med 1961-1990, visas som globala kartor samt för 32 olika regioner. Osäkerheten i både storleken och riktningen av de beräknade regionala klimatförändringarna har uppskattats, baserat på SRES scenarierna och resultaten från 10 AOGCM simuleringar.

I rapporten presenteras också information om de demografiska och socio-ekonomiska faktorer som ligger bakom SRES scenarierna, halten av koldioxid för scenarierna, samt modellberäkningar av förändringar i den globala havsnivån orsakad av de beräknade temperaturförändringarna. Alla dessa faktorer kan också vara viktiga för att utvärdera känsligheten för klimatförändringar i framtiden

INTERNATIONAL COOPERATION

Climate Change in the 21st Century
- Interim Characterizations based on the New IPCC Emissions Scenarios

The Intergovernmental Panel on Climate Change (IPCC) has recently developed a new set of scenarios of greenhouse gas and aerosol emissions. The scenarios span a wide range of uncertainties in future emissions arising from different assumptions of socio-economic development during the 21st century. This report presents a method of characterizing the implications of these emissions scenarios for regional climate. The method combines estimates of the global mean climate response to emissions, using a simple climate model, with estimates of the regional pattern of climate response from atmosphere-ocean general circulation model simulations. Projected changes in mean seasonal temperature and precipitation are portrayed for the 2020s, 2050s and 2080s relative to 1961-1990 on global maps and on graphs for thirty-two world regions. Uncertainties in both the magnitude and direction of future regional climate change are depicted. It is hoped that this information may assist researchers wishing to select climate scenarios for new impact assessments. In addition, information is presented on the demographic and socio-economic driving factors underlying the emissions scenarios, on the atmospheric carbon dioxide concentrations implied by the scenarios, and on model estimates of global sea-level rise induced by projected temperature changes. All of these factors may be important for determining future vulnerability to a changing climate.

9 789521 107818